DOCTOR OF PHILOSOPHY

A screen for phosphatidylinositol 3,4-bisphosphate and other 3-phosphoinositide effector proteins

Dixon, Miles

Award date:
2010

DOCTOR OF PHILOSOPHY

A screen for phosphatidylinositol 3,4-bisphosphate and other 3-phosphoinositide effector proteins

Miles Dixon

2010

University of Dundee

A Screen for Phosphatidylinositol 3,4-bisphosphate and Other 3-Phosphoinositide Effector Proteins.

Miles J. Dixon

A Thesis Submitted for the Degree of Ph.D.

The Division of Molecular Physiology
University of Dundee

September 2010

Table of Contents

Abbreviations

Agonists and Reagents

EGF	epidermal growth factor
PDGF	platelet derived growth factor
NGF	nerve growth factor
bpV(phen)	potassium bisperoxo(1,10-phenanthroline)oxovandadium (V)
FBS	foetal bovine serum
TX-100	triton X-100
EGTA	ethylene glycol tetraacetic acid
EDTA	ethylenediaminetetraacetic acid
PMSF	phenylmethylsulfonyl fluoride
TBST	tris-buffered saline with Tween-20
DMSO	dimethyl sulfoxide
IPTG	isopropyl β-D-thiogalactoside
PVDF	polyvinylidine fluoride
DMEM	Dulbecco's modified Eagles medium

Domains

PH	pleckstrin homology
FYVE domain	Fab1p, YOTB, Vac1 and EEA1
FERM	band 4.1, ezrin, radixin, moesin
ENTH	epsin NH2-terminal homology
SH2	Src homology 2
SH3	Src homology 3

PX	Phox homology
IQ	isoleucine and glutamine calmodulin-binding motif
PDZ	postsynaptic density 95, discs large, zonula occludens-1
CH	calponin homology
UIM	ubiqutin interacting motif
SAM	sterile alpha motif

Inositol Phosphates

$Ins(1,4,5)P_3$	inositol 1,4,5-trisphosphate
$Ins(1,3,4)P_3$	inositol 1,3,4-trisphosphate
$Ins(1,3,4,5)P_4$	inositol 1,3,4,5-tetrakisphosphate

Lipids

DAG	sn-1,2-diacylglycerol
PtdOH	phosphatidic acid
PtdSer	phosphatidylserine
PtdCho	phosphatidylcholine
PtdEth	phosphatidylethanolamine
PI	phosphoinositide
3-PI	3-phosphoinositide
PtdIns	phosphatidylinositol
PtdIns3P	phosphatidylinositol 3 phosphate
PtdIns4P	phosphatidylinositol 4 phosphate
PtdIns5P	phosphatidylinositol 5 phosphate
$PtdIns(3,4)P_2$	phosphatidylinositol 3,4-bisphosphate

PtdIns(3,5)P_2	phosphatidylinositol 3,5-bisphosphate
PtdIns(4,5)P_2	phosphatidylinositol 4,5-bisphosphate
PtdIns(3,4,5)P_3	phosphatidylinositol 3,4,5-trisphosphate

Proteins

Btk	Bruton's tyrosine kinase
PDK1	3-phosphoinositide-dependent protein kinase 1
PI 3-kinase	phosphoinositide 3-kinase
PtdIns 4-kinase	phosphatidylinositol 4-kinase
PtdIns4P 5-kinase	phosphatidylinositol 4-phospahate 5-kinase
PIPP	Proline rich inositol polyphosphate 5-phosphatase
PTEN	Phosphatase and tensin homology deleted on chromosome 10
SKIP	Skeletal muscle and kidney enriched 5-inositol phosphatase
SHIP1/2	Src homology 2 domain containing inositol polyphosphate 5-phosphatase 1/2
PKA	protein kinase A
PKB	protein kinase B
PKC	protein kinase C
Grp1	general receptor for phosphoinositides
DAPP1	dual adaptor for phosphotyrosine and 3-phosphoinositides
MUPP1	multi-PDZ domain protein
PRD	peroxiredoxin
SWAP-70	switch-associated protein 70
GAP1	Ras GTPase-activating protein 3 (IP4BP)
DOCK180	dedicator of cytokinesis

ARNO	ARF nucleotide-binding site opener (cytohesin 2)
Gab1	GRB2-associated-binding protein 1
ARAP	Arf-GAP with Rho-GAP domain, ANK repeat and PH domain-containing protein
TAPP-1	pleckstrin homology domain containing, family A (phosphoinositide binding specific) member 1
PARIS-1	Prostate antigen recognized and identified by SEREX 1
IQGAP1	IQ motif containing GTPase activating protein 1
CLIC1	Chloride intracellular channel protein 1
mTORC2	mammalian target of rapamycin complex 2
Src	sarcoma
Abl	Abelson murine leukemia viral oncogene homolog 1
EEA1	early endosome antigen 1
PLC	phospholipase C

Techniques/Instruments

SDS-PAGE	SDS polyacrylamide gel electrophoresis
MS	mass spectrometry
SILAC	stable isotope labelling with amino acids in cell culture
MALDI	matrix-assisted laser desorption/ionization
ESI	electrospray ionization
TOF	time of flight
LC	liquid chromatography
SPR	surface plasmon resonance
ITC	isothermal calorimetry

FTICR	Fourier transform ion cyclotron resonance
CID	collision induced dissociation

Other

ATP	adenosine triphosphate
CNS	central nervous system
PCR	polymerase chain reaction
RT	room temperature
Ca^{2+}	calcium
Na^{+}	sodium
K^{+}	potassium
cAMP	cyclic adenosyl monophosphate
GDP	guanosine diphosphate
GTP	guanosine triphosphate
DNA	deoxyribonucleic acid
EST	expressed sequence tag
SA chip	streptavidin-dextrose chip
CO_2	carbon dioxide
SDS	sodium dodecyl sulfate
LDS	Lithium Dodecyl Sulfate
PEP	posterior error probability
AQ	anion exchange chromatography (Q-sepharose) eluate
CS	cation exchange chromatography (S-sepharose) eluate
F0	combined flow through (from both AQ and CS) fraction
GPCRs	G-protein coupled receptors

G-protein	GTP-binding protein
GEF	gunaosine nucleotide exchange factor
GAP	GTPase activating protein
NADPH	nicotinamide adenine dinucleotide phosphate
DSTT	Division of Signal Transduction Therapy
GST	glutathione-sepharose
PCR	polymerase chain reaction
MIL	membrane insertion loop
SNX	sorting nexins
PTP	protein tyrosine phosphatase
ROS	reactive oxygen species
CSF	colony-stimulating factor
PDB	protein data bank
RTK	receptor tyrosine kinase

Single Letter Amino Acid Code.

A	-	Alanine.
C	-	Cysteine.
D	-	Aspartic acid.
E	-	Glutamic acid.
F	-	Phenylalanine.
G	-	Glycine.
H	-	Histidine.
I	-	Isoleucine.
K	-	Lysine.
L	-	Leucine.
M	-	Methionine.
N	-	Asparagine.
P	-	Proline.
Q	-	Glutamine.
R	-	Arginine.
S	-	Serine.
T	-	Threonine.
V	-	Valine.
W	-	Tryptophan.
X	-	Any amino acid.
Y	-	Tyrosine.

List of Figures

Figure

List of Tables.

Table

Acknowledgements.

I am extremely grateful to Pete Downes for the opportunity to do my Ph.D. in his lab and beholden to Ian Batty for his day-to-day supervision and constant enthusiasm for this project. My thanks must also go to the rest of the Downes/Leslie lab, both past and present, who have contributed to this work directly or indirectly, and made my time in Dundee so enjoyable.

Finally, I am deeply indebted to my parents for their unwavering encouragement and support without which my studies would not have been possible.

Declaration.

I herby declare that the following thesis is based on the results of investigations conducted by myself and that this thesis is of my own composition. Work other than my own is clearly indicated in the text by reference to the relevant researchers or their publications. This dissertation has not in whole, or in part, been previously presented for a higher degree.

Miles J. Dixon

I certify that Miles Dixon has spent the equivalent of at least nine terms in research work in the Department of Molecular Physiology, University of Dundee and that he has fulfilled the conditions of Ordinance General No. 14 of the University of Dundee and is qualified to submit the accompanying thesis in application for the degree of Doctor of Philosophy.

C. Peter Downes, OBE, FRSE

Professor of Biochemistry

Publications arising wholly or in part from this work:

Batty IH, van der Kaay J, Gray A, Telfer JF, Dixon MJ, Downes CP.

The control of phosphatidylinositol 3,4-bisphosphate concentrations by activation of the Src homology 2 domain containing inositol polyphosphate 5-phosphatase 2, SHIP2. Biochem J. 2007 Oct 15; 407 (2):255-66.

Miles J. Dixon, Alexander Gray, François-Michel Boisvert, Mark Agacan, Nicholas A. Morrice, Robert Gourlay, Nicholas R. Leslie, C. Peter Downes and Ian H. Batty.

A Screen for Phosphatidylinositol 3,4-bisphosphate and other 3-Phosphoinositide Effector Proteins. MCP submitted May 2010.

Summary.

Class I phosphoinositide (PI) 3-kinases exert profound effects on cell growth, division, motility and metabolism via their primary lipid product phosphatidylinositol 3,4,5-trisphosphate (PtdIns(3,4,5)P_3) and a metabolite of this, phosphatidylinositol 3,4-bisphosphate (PtdIns(3,4)P_2). Many effector proteins for PtdIns(3,4,5)P_3 are well recognised but by contrast, few molecular targets for PtdIns(3,4)P_2 have been identified. This study describes a screen to identify PI 3-kinase-responsive proteins that is selective particularly for these. The approach features a unique three-tier affinity approach and incorporates a primary recruitment of target proteins to membranes of intact cells, selectively enriched in PtdIns(3,4)P_2. In addition, this screen utilises stable isotope labelling with amino acids in cell culture (SILAC) to differentially label cells stimulated in the absence and presence of the PI 3-kinase inhibitor wortmannin. The integration of these techniques provides a ratio-metric readout, allowing authentically 3-phosphoinositide (3-PI) responsive components to be distinguished from the co-purifying background proteins. The identification of tandem pleckstrin homology domain containing protein-1 (TAPP-1) and protein kinase B (PKB) among a multitude of proteins expressing known lipid binding domains (LBDs) demonstrates the utility of this strategy. Analysis of other similarly, isotopically enriched candidate 3-PI interacting proteins yielded two novel lipid binding proteins, PARIS-1 (prostate antigen recognised and identified by SEREX 1) and IQGAP1 (IQ motif containing GAP1). The concentration dependent interaction of PARIS-1 and IQGAP1 with PtdIns(3,4,5)P_3 was confirmed by an *in vitro*, SPR based assay. Intriguingly, IQGAP1, a potential tumour promoter, lacks a currently established LBD and may therefore exemplify an entirely novel 3-PI selective binding domain.

Chapter 1.

General Introduction.

1. Introduction.

This thesis will describe the optimisation and implementation of a screen for potential molecular targets for a class of intracellular lipid signals known to execute vital roles in important cellular processes. The controlled synthesis and degradation of such lipid signals are vital for normal cell function but equally aberrations in either their metabolism or the proteins which respond to them are implicated in a variety of disease states from diabetes to cancer.

1.1 Cell Signalling.

Cells within all tissues need to communicate in order to regulate cell activity and elicit a concerted response, such as senescence or growth. Cell communication encompasses a wide range of events but essentially can be divided into three types; autocrine, paracrine and endocrine. Autocrine and paracrine signalling is undertaken by all cells and operates over short distances, whereas endocrine signalling is undertaken by more specialist cell types over larger distances. The term cell signalling broadly describes the many facets involved in translating the received communication, from transferring the signal across the outer plasma membrane to eliciting a measured and co-ordinated response.

1.1.1 Cell Membranes.

All cell membranes consist of lipids which have amphipathic properties, possessing both a hydrophilic headgroup and hydrophobic tail(s), the latter consisting of saturated and/or unsaturated hydrocarbons. These lipids consists of phospholipids (glycerophopholipids and sphingomyelin), which are a major component but also of cholesterol and glycolipids. The fluidity, thickness and function of a membrane vary

according to the lipid constituents. However, it is the inherent amphipathic characteristics of lipids which orientate them into a bilayer, resulting in a highly hydrophobic internal region between the internal and external lipid monolayers or leaflets. This provides a barrier, preventing the movement of molecules, very often retaining them against their concentration gradient, as with stores of energy and components for growth. Whilst this compartmentalisation is crucial, it poses a problem in transferring signals from one cell to another or across internal compartments and requires additional signalling machinery – membrane receptors.

1.1.2 Receptors.

Cell surface receptors provide a mechanism by which to transduce across membranes signals provided by non-cell penetrant or polar ligands such as growth factors and neurotransmitters. Notable exceptions to this requirement are provided by steroid hormones and nitric oxide which are small and hydrophobic enough to readily cross membranes and exert their effects directly. However, receptors transduce non-permeable signals by undergoing a chemical or conformational change on the intracellular face of the bilayer following extracellular ligand binding. The cell surface receptors can be divided into three classes based on their mechanism of action, ion-channel-linked receptors, G-protein coupled receptors and enzyme-linked receptors.

Ion-channel-linked receptors or ionotrophic receptors are transmembrane proteins which upon ligand binding undergo a conformational change, allowing the passage of ions, such as Na^+, K^+ and Cl^-, through an internal pore. An example of such an ionotrophic receptor is provided by the nicotinic acetycholine receptor in neurones which, following activation by acetycholine, allows passage of Na^+/K^+ ions down their

concentration gradients. The effect is to depolarise the electrical potential maintained courtesy of the Na^+-K^+ pump (intracellularly relatively negative, as three Na^+ ions are actively pumped out for every two K^+ ions pumped in) and initiate an action potential down the axon.

G-protein coupled receptors (GPCRs) are the largest family of receptors and are responsible for regulating a wide variety of processes including olfaction, sight, inflammation, neurotransmission, secretion, contraction, and electrochemical impulses from the nervous system. Indeed approximately 40% of all prescription pharmaceuticals target GPCRs [1]. Characteristically, GPCRs are serpentine proteins which cross the membrane seven times. Each of these transmembrane regions orientates itself to form a ring structure, creating a pore for ligand binding. Upon ligand binding, the GPCR undergoes a conformational change on the intracellular face of the membrane. This in turn, induces a change in the conformation of an internal membrane-bound transducer; a heterotrimeric GTP-binding protein (G-protein). There are several types of heterotrimeric G-proteins including, G_s, G_i and G_q, each of which is linked to a signalling outcome. The G-protein is comprised of three subunits, α, β and γ, of which the α-subunit exchanges guanosine diphosphate (GDP) for guanosine triphosphate (GTP) upon GPCR activation. Once GTP is bound the G-protein undergoes a further conformational change and separates into two components, the GTP bound α-subunit and a βγ complex, both of which are now capable of interacting with and activating/inhibiting effector proteins.

Enzyme-linked receptors, typically have only one transmembrane region and their cytosolic tail is either intrinsically capable of enzyme activity or associates directly with an effector possessing enzyme activity. Although most possess only a single

transmembrane pass, many require dimerisation either to facilitate ligand binding and/or to achieve activation following ligand binding. The most abundant enzyme-linked receptor class are the receptor tyrosine kinases (RTKs), activated by many growth factors and hormones including epidermal growth factor (EGF), platelet-derived growth factor (PDGF) and insulin. Following ligand binding and dimerisation, these receptors undergo trans-autophosphorylation, transferring a phosphate group from adenosine triphosphate (ATP) to a specific tyrosine residue(s) within cytoplasmic tail of the opposing RTK dimer. Phosphorylation of these tyrosine residues, if within the kinase region, increases the enzyme activity towards effector substrates. If the tyrosine phosphorylation is outside the kinase region, it usually creates a unique sequence of additional residues surrounding the phosphorylated tyrosine, known as a consensus sequence. The phosphotyrosine residue then usually represents a docking site within the appropriate consensus sequence, providing a target for the binding, recruitment or activation of specific effector proteins via modules or domains which recognise such sequences, often with high affinity (introduced in 1.4).

1.1.3 Second Messengers.

Second messengers are molecular intermediaries responsible for transferring the signalling output of ligand bound cell surface receptors to the intracellular environment. The concept of second messengers was first introduced by Earl Sutherland in 1958 following his studies on cyclic adenosine monophosphate (cAMP) [2]. He observed that, whilst adrenaline resulted in liver cells converting glycogen to glucose, this could not be achieved without the second messenger cAMP.

1.2 Phosphatidylinositol (PtdIns).

Prior to Earl Sutherland's seminal paper on cAMP [2], Mabel and Lowell Hokin reported an agonist-stimulated phosphatidylinositol (PtdIns) turnover [3]. Inositol lipids had already been observed within mycobacterium [4] and this was followed by similar observations of inositol phospholipids within animals and plants [5-8]. Several groups, notably C. Ballou, R. Dawson and D.M. Brown contributed to establishing the D-1 positional substitution of the myo-inositol ring to phosphatidic acid [9-11]. Later, the same groups, following up on Jordi Folch's observation of a polyphosphoinositide [6], determined that mono-, bis-, and tris- phosphate components of myo-inositol could be isolated [5,12-22]. Finally, these inositol derivatives from PtdIns, PtdIns4P and PtdIns(4,5)P_2 were suggested to be interconvertable by phosphorylation/dephosphorylation following studies measuring the radiolabelled incorporation of phosphate, myo-inositol and glycerol into tissue slices [13,14]. The structure of phosphoinositides (PIs) is shown in Figure 1 and highlighted are the positions at which the molecule is capable of modification by a variety of enzymes.

Figure 1.1 The structure of inositol phospholipids.

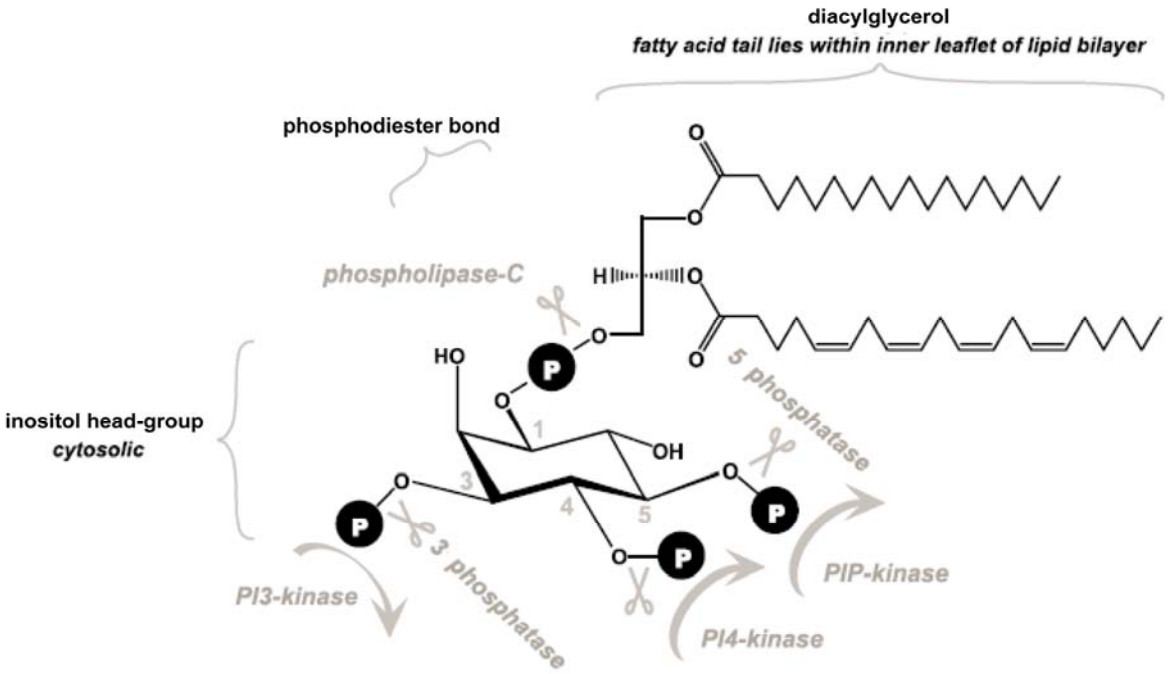

The inositol head-group, which can be reversibly phosphorylated on the 3-, 4- and 5- positions of the inositol ring by a variety of enzymes, is attached to diacylglycerol (typically stearyl/arachidonyl) via a phosphodiester bond. The stearic acid (sn-1 position of the glycerol moiety) and arachidonic acid (sn-2 position of the glycerol) are highly hydrophobic and consequently are inserted in the inner leaflet of the membrane, presenting the water-soluble inositol head-group to the cytosol. Figure adapted from [23].

1.2.1 The Abundance and Occurrence of Phosphoinositides (PIs).

Phospholipid components of cell membranes can be divided into two types, acidic phospholipids and non-acidic phospholipids. These two types can be subdivided, with non-acidic phospholipids including phosphatidylethanolamine (PtdEth), phosphatidylcholine (PtdCho) and sphingomyelin. Acidic phospholipids consist of three major types, phosphatidylserine (PtdSer), phosphatidic acid (PtdOH) and PI (PtdIns and its polyphosphate derivates). To put the abundance of these phospholipids in perspective, PtdSer is the most abundant of the acidic phospholipids followed by PtdOH and PI – which comprises ~1-5% of total cellular lipids [24,25]. The acidic phospholipids have several overlapping roles in signalling including; (i) facilitating binding to second messengers, seen with PtdSer/PtdOH and electrostatic interactions with FYVE (Fab1p, YOTB, Vac1 and EEA1) domains (see Chapter 5) [26]; (ii) acting as substrates in the production of second messengers, such as with PtdIns(4,5)P_2 and phospholipase-C (PLC) mediated synthesis of Ins(1,4,5)P_3 and diacylglycerol (DAG) [27]; and (iii) are second messengers themselves, such as PtdIns(3,4,5)P_3 and PtdIns(3,4)P_2 [28,29]. PIs in particular, play a crucial role in cell signalling, are generated by de-novo synthesis or recycling from other PI species and differ only in the chemical moiety (head-group) attached via the sn-3 carbon of diacylglycerol.

This interconversion of PI species is achieved by a considerable network of PI kinases and phosphatases. The concerted actions of these enzymes can result in the production of seven polyphosphoinositide derivatives, as reflected in Figure 1.2, but each with much lower abundance than PtdIns. Of the seven naturally occurring derivatives, PtdIns4P and PtdIns(4,5)P_2 are the most abundant with PtdIns(4,5)P_2 accounting for about 5% of the total PI [24,25]. The concentrations of PtdIns4P and PtdIns(4,5)P_2 are

maintained by appropriate kinases and phosphatases such as the PtdIns 4-kinase and the PtdIns4P 5-kinase respectively. However, despite such apparent scarcity, PtdIns and its metabolites have a disproportionately important role in cell signalling, with PtdIns(4,5)P_2 particularly important as a substrate for two separate "arms" of the PI signalling pathway.

Figure 1.2 The phosphoinositide cycle.

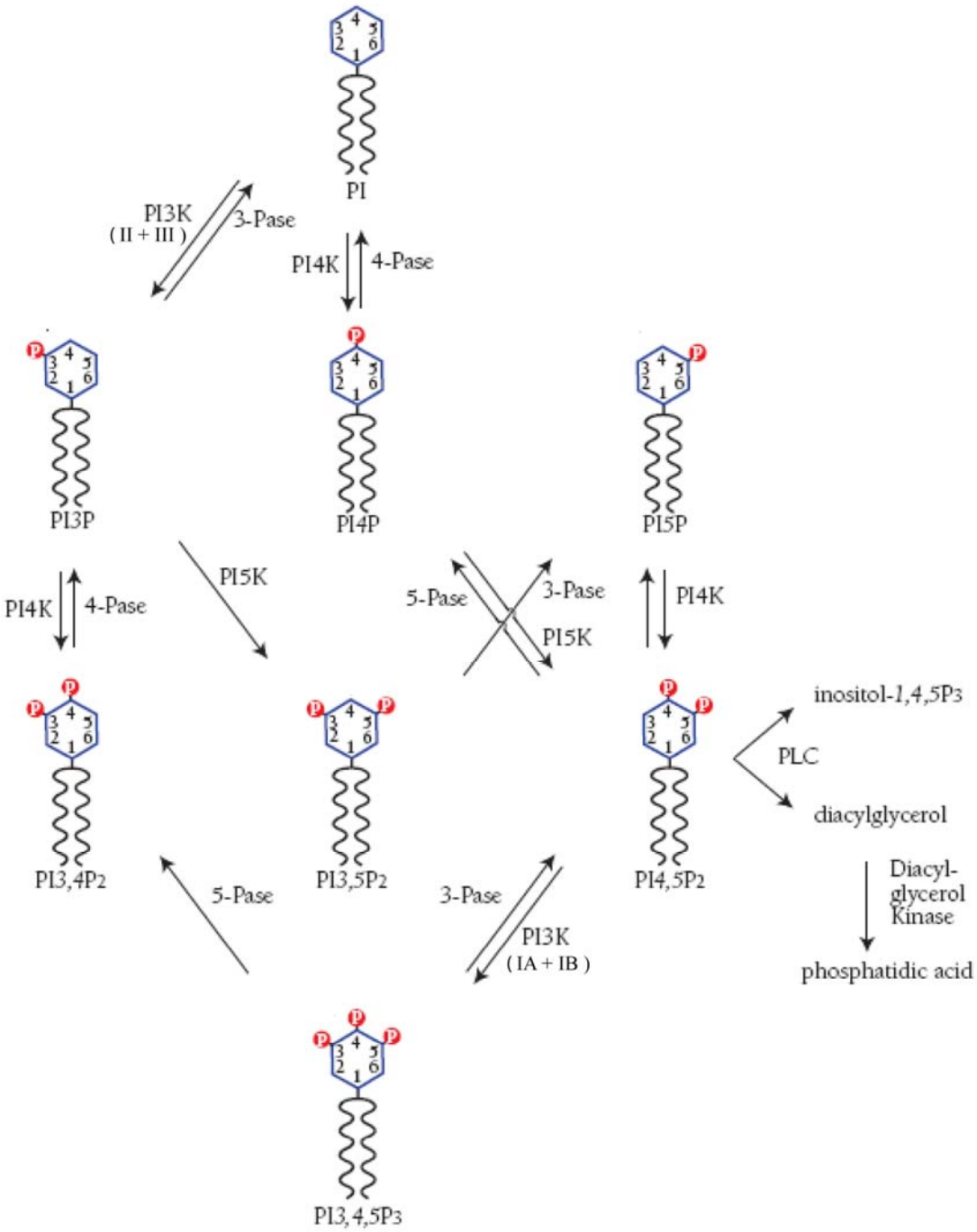

The synthesis and degradation of PIs is maintained by the constitutive or regulated activity of a number of lipid kinases and phosphatases. Key examples of the 3- and 4-phosphatases (Pase) as well as the substrate selectivities of the PI 3-kinase enzymes (PI3K) will be introduced individually in Chapter 1.3. Also indicated is the PLC mediated hydrolysis of PtdIns(4,5)P_2 into Ins(1,4,5)P_3 and DAG. Figure adapted from [30].

1.2.2 PtdIns(4,5)P_2 and PLC.

The first of these "arms" of the PI pathway was uncovered when a causal link between PI turnover and Ca^{2+} signalling was suggested by R. Michell [31]. The precise nature of the role that PI metabolites play in this context was subsequently shown by M. Berridge and colleagues [32]. Thus, Berridge *et al.* demonstrated that activation of receptors coupled to PI-PLC results in the hydrolysis of PtdIns(4,5)P_2, generating two second messengers, Ins(1,4,5)P_3 and DAG [27]. The soluble Ins(1,4,5)P_3 is able to freely diffuse through the cytosol and activates release of Ca^{2+} from intracellular stores via a specific Ins(1,4,5)P_3 receptor. Changes in intracellular Ca^{2+} levels then trigger many downstream responses, regulating a wide range of cellular processes including fertilisation, muscle contraction and cell motility [33]. Subsequently, numerous kinases and phosphatases are capable of metabolising Ins(1,4,5)P_3, its metabolites serving both to terminate Ca^{2+} signalling or perhaps, generate additional signalling molecules [i.e. Ins(1,3,4,5)P_4 production by Ins(1,4,5)P_3 3-kinase] and allow the recycling of inositol and PtdOH (derived from DAG) back to PtdIns [34-36].

1.3 The Enzymes responsible for 3-PI metabolism.

A second "arm" of the PI signalling pathway was to be discovered upon the observation of an enzyme capable of phosphorylating PI species at the D3 position of the inositol ring (PI 3-kinases) [37]. Two key PI metabolites phosphorylated on the D3 position include PtdIns(3,4,5)P_3 and PtdIns(3,4)P_2, both of which are approximately 1000 fold less abundant than PtdIns(4,5)P_2 [24,25] but are crucial second messengers required for normal cell function [38]. The enzymes responsible for their synthesis and degradation following PI 3-kinase activation determine the prevailing output of 3-PI signalling events and these are detailed within the signalling pathway illustrated in Figure 1.3. The capacity of these 3-PI metabolising enzymes to generate rapidly one lipid species either at expense of, or alongside another, is highlighted by the extremes of lipid concentrations achieved by specific stimuli such as growth factors, insulin or invasive pathogens [39-41].

Figure 1.3 The class IA PI 3-kinase signalling pathway.

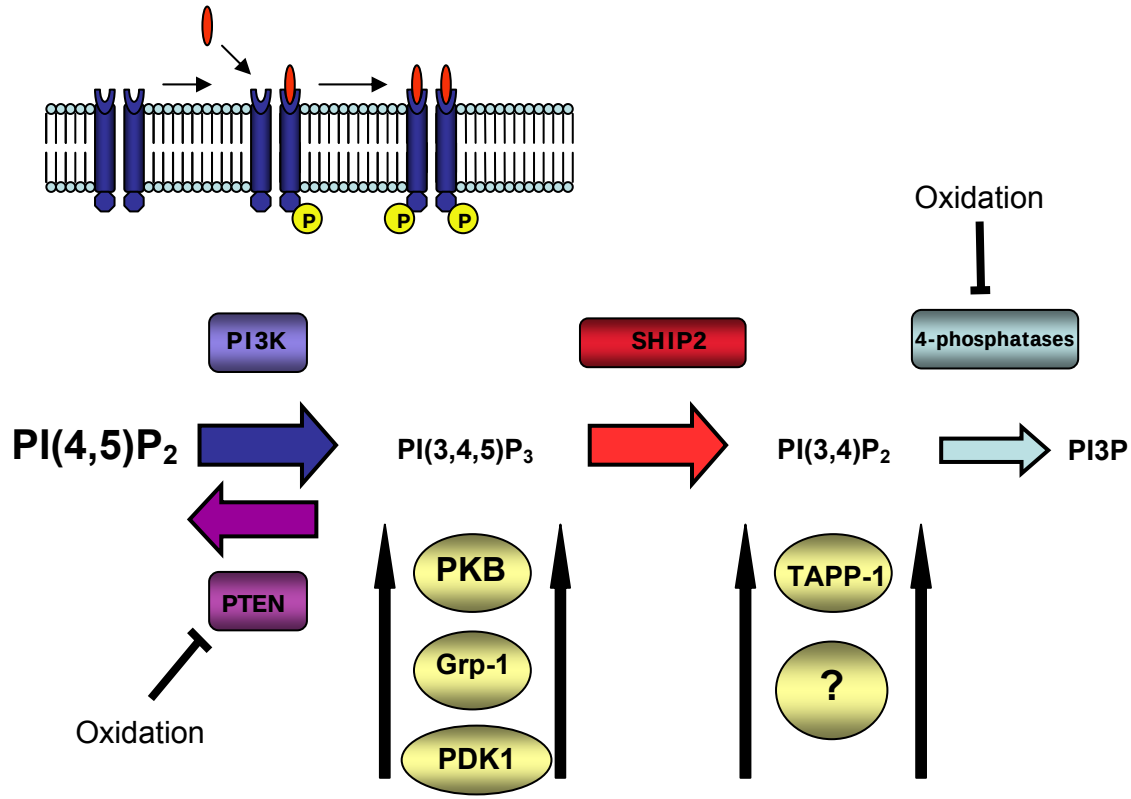

Following activation of class IA PI 3-kinases, downstream of activated RTKs (Chapter 1.1.2), the coordinated actions of lipid phosphatases such as PTEN, SHIP2 (5-phosphatases) and the 4-phosphatases can control the prevailing outcome of the 3-PI second messengers generated; either PtdIns(3,4)P_2 and/or PtdIns(3,4,5)P_3, and recruit effector proteins accordingly.

1.3.1 PI 3-Kinases.

PI 3-kinases (the most intensively studied PI kinase) were first observed unknowingly in 1984 as a minor inositol lipid kinase activity associated with the immunoprecipitated oncogene product Src [42]. They were reported shortly afterwards in 1985 associated with the Polyoma Middle T antigen and Abl [43], and later in activated growth factor receptor complexes such as those stimulated by PDGF [44] and CSF-1 [45]. Their novel ability to phosphorylate the D-3 position on the inositol ring was reported in 1988 [37] and dramatic and transient rises in PtdIns(3,4,5)P_3 as a response to physiological stimuli were observed in 1989 [39]. PI 3-kinases have since been shown to be integral to many physiological functions such as cell growth, proliferation, survival, intracellular trafficking, differentiation [46-50], migration [51], secretion [52], axonal guidance [53] and apoptosis [54], as well as the dysfunction of these processes implicated in diseases such as cancer and diabetes [55-57].

Eight different PI 3-kinase isoforms have now been identified and these are divided into three classes (class I [subclasses IA and IB], II and III). The three classes of PI 3-kinase are differentiated and defined by their structure and substrate specificity [47,50]. Although Class I PI 3-kinases are capable of phosphorylating the D3 position of all PIs *in vitro*, they are the only isoforms demonstrated to use PtdIns(4,5)P_2 *in vivo* to produce PtdIns(3,4,5)P_3. The subclass IA enzymes are activated/recruited by receptor and non-receptor tyrosine kinases and are dimers consisting of a p50α/55α/p55γ/p85α/p85β regulatory domain and a p110α/β/δ catalytic subunit [38]. The subclass IB comprise of only one member which is activated/recruited by GPCRs, predominantly via the βγ subunit of the

G_i–coupled GPCRs [58,59] and is a dimer consisting of the p110γ catalytic subunit and either a p101 or p84 regulatory subunit.

The class II PI 3-kinases, unlike either the class I or III enzymes, are monomeric, possessing no regulatory domain, although the catalytic core of each class II enzyme shares structural homology with the class I proteins [50]. The class II enzymes consist of three isoforms, PI3KC2α, PI3KC2β and PI3KC2γ. Originally it was proposed that the class II enzyme activity might phosphorylate PtdIns4P to produce PtdIns(3,4)P_2 *in vivo* as it does *in vitro*. Whilst this mechanism of PtdIns(3,4)P_2 production cannot be ruled out, it is now widely accepted that this lipid is predominantly synthesised by the action of 5-phosphatases on PtdIns(3,4,5)P_3. It is now well documented that Class II PI 3-kinases similar to class III, produce PtdIns3P *in vivo*, but act predominantly at the plasma membrane rather than other intracellular endosomal membranes [51].

Class III PI 3-kinase is the human orthologue of the only representative of PI 3-kinases in *Saccharomyces cerivisiae* (Vps34) and was first reported in 1995 [60]. The class III enzyme has a regulatory binding domain of 150kDa and is only capable of phosphorylating PtdIns so can be more accurately described as a PtdIns 3-kinase. Class III enzymes are predominantly involved in endosome fusion and intracellular trafficking and as such are located mainly on intracellular membranes [50,61].

Two inhibitors in particular have been widely used to determine the biological functions of PI 3-kinases, namely wortmannin and LY294002 [23].

Wortmannin, a cell permeable, fungal metabolite, was originally isolated from *Penicillium wortmannii* [62] and reported to inhibit phagocytocis induced respiratory burst [63]. It was later shown to be a potent competitor of ATP, binding to and irreversibly inhibiting PI 3-kinases with a low nM IC_{50} [64]. Also LY294002, a reversible, ATP-competitive inhibitor, selective for PI 3-kinases was synthesized from the flavenoid quercetin [65] and has an IC_{50} in the μM range. Much early work in elucidating the roles of PI 3-kinases in cell signalling was made possible by the use of these inhibitors.

1.3.2 Phosphatase and Tensin Homolog Deleted on Chromosome Ten (PTEN).

The removal of PtdIns(3,4,5)P_3 generated by class I PI 3-kinases is necessarily tightly regulated. Loss of this control either through excessive synthesis or lack of catabolism often results in cell transformation (uncontrolled cell growth and/or proliferation) [66]. One of the key phosphatases required for the removal of PtdIns(3,4,5)P_3 concentrations is PTEN, a 3-phosphatase which acts directly to oppose the activity of class I PI 3-kinases by returning PtdIns(3,4,5)P_3 to PtdIns(4,5)P_2 [67]. The role of PTEN as a tumour suppressor is well established, due in part to its constitutive activity and the lack of redundancy offered by other 3-phosphatases.

PTEN belongs to a family of protein tyrosine phosphatase (PTP)-like enzymes whose characteristic active site depends on a critical, cysteine-containing sequence of amino acids [68]. This active site is highly sensitive to oxidation and mechanisms of PTEN regulation whereby reactive oxygen species (ROS),

liberated as a consequence of RTK activation, inhibit PTEN activity are beginning to be understood [69]. Despite the significance of PTEN in normal cells, it is absent in the 1321N1 astrocytoma cell line employed for this study, so these cells are heavily dependent on the metabolism of PtdIns(3,4,5)P_3 to PtdIns(3,4)P_2 via the 5-phosphatases Src Homology 2 domain containing Inositol polyphosphate 5-phosphatase 2 (SHIP2).

1.3.3 Src Homology 2 domain containing Inositol polyphosphate 5-phosphatase 2 (SHIP2).

An alternative means of metabolism of PtdIns(3,4,5)P_3 is via the 5-phosphatases. These enzymes remove the 5-phosphate group from PtdIns(3,4,5)P_3, generating PtdIns(3,4)P_2 which is widely considered as a second messenger in its own right [38]. Although several 5-phosphatases are thought to contribute to the metabolism of PtdIns(3,4,5)P_3, including SKIP (skeletal muscle and kidney enriched inositol 5-phosphatase) and PIPP (proline rich inositol polyphosphate 5-phosphatase) [70-74], SHIP1 and SHIP2 are thought to be the prominent 5-phosphatases involved in the production of PtdIns(3,4)P_2. The two enzymes do however differ in both structure and expression. SHIP1 contains an N-terminal SH2 domain, two NPXY motifs and a C-terminal proline rich region and its expression is limited mainly to haemopoeitic cells. SHIP2 only contains a single NPXY motif, a SH2 domain and C-terminal proline rich and sterile alpha motif (SAM) domains which mediate protein-protein interactions [73,75,76]. SHIP2 is ubiquitous in its expression but is particularly highly expressed in cells which lack SHIP1 (liver, heart, muscle, brain and adipocytes) [70].

1.3.4 4-phosphatases.

The degradation of PtdIns(3,4)P_2 [generated as a consequence of 5-phosphatase activity on PtdIns(3,4,5)P_3] is controlled by the 4-phosphatases which exist as two main isoforms; type I and type II, sharing a 37% amino acid identity. Similar to PTEN, they are members of the PTP family, containing a catalytic cysteine motif which is sensitive to oxidation [77-79], a key feature which is exploited within this study. The type I (INPP4A) and II (INPP4B) 4-phosphatases differ in their levels of expression and tissue distribution and both can exist as two splice variants, α and β. The C-terminal region of the α isoforms is hydrophilic while the β isoforms have a hydrophobic tail which may contain a transmembrane sequence [80]. The literature reports that both type I and type II isoforms show strong preference for metabolising PtdIns(3,4)P_2 to PtdIns3P *in vitro* [77,78,81]. However, the enzymes preference for PtdIns(3,4)P_2 over the water soluble Ins(1,3,4)P_3 and Ins(3,4)P_2 generated during the re-cycling of Ins(1,4,5)P_3 to inositol [82], is not supported by any cellular observations. It has been suggested that the 4-phosphatases exist not only to remove PtdIns(3,4)P_2 but also contribute to the functional pools of PtdIns3P [79]. The cellular location of these pools of PtdIns3P at either the endosomal or plasma membranes is however, not clear.

1.4 PtdIns(3,4,5)P_3/PtdIns(3,4)P_2 as Second Messengers.

The enzymes which contribute to the synthesis and degradation of PtdIns(3,4,5)P_3/PtdIns(3,4)P_2 from PtdIns(4,5)P_2 have been introduced. In contrast to the PLC/PtdIns(4,5)P_2 "arm" of the PI signalling pathway, the PI 3-kinase-dependent "arm" is capable of directly recruiting and/or activating a wide variety of effectors [38]. In fact, this feature is unique amongst second messenger

systems, including cAMP and Ins(1,4,5)P_3 which tend to target a limited number or solitary, immediate effectors such as; protein kinase A (PKA), cAMP-regulated ion channels and exchange protein directly activated by cAMP (Epac) or the Ins(1,4,5)P_3 receptor respectively, which then regulates multiple downstream events. The wide variety of effectors capable of responding directly to PtdIns(3,4,5)P_3 and/or PtdIns(3,4)P_2 do so through protein modules or domains which are capable of selectively recognising these lipid products. The concept of modular domains will be introduced later.

The list of effector proteins capable of interacting with PtdIns(3,4,5)P_3 and/or PtdIns(3,4)P_2 include Grp-1 [83], Btk [84], protein kinase B (PKB)/Akt [29,85], PDK1 [86,87], DAPP-1 [88], SWAP-70 [89], GAP1 [90], DOCK180 [91], ARNO [92,93], cytohesin-1 [94], centaurin-α [95,96], Gab1 [97], ARAP3 [98], lamellipodin [99], ARAP1 [100,101] and TAPP-1 [102]. Currently TAPP-1 is the only protein established to show selective binding for PtdIns(3,4)P_2, with the remainder reported as either selective PtdIns(3,4,5)P_3 binding proteins or showing dual specificity to PtdIns(3,4,5)P_3/ PtdIns(3,4)P_2. Each of the above effectors, recruited and/or activated by PtdIns(3,4,5)P_3/PtdIns(3,4)P_2 have been shown or assumed, to serve different or overlapping cellular processes and their functions range from scaffolding proteins to small G-protein regulators and protein kinases.

The best known and most widely studied of these is PKB/Akt, its mode of recruitment and activation following PtdIns(3,4,5)P_3 synthesis defining a paradigm for a wider class of PtdIns(3,4,5)P_3 binding proteins. PKB is a serine/threonine kinase and is one of the most influential protein kinases in human

physiology [103,104]. Following activation of class I PI 3-kinases and the production of PtdIns(3,4,5)P_3, PKB recruitment to the plasma membrane is mediated via a selective interaction of PtdIns(3,4,5)P_3 with the PH domain of PKB [29,85]. The activities of two other serine/threonine (S/T) kinases (PDK1 and mTORC2) are then responsible for modulating the activity of PKB by phosphorylating it at T308 and S473 respectively [103,105,106]. Once activated PKB is, in turn, capable of phosphorylating its many substrates. Its varied substrates are responsible for mediating a wide range of cellular processes, critically including cell survival by inhibition of apoptosis or cell death. However, aberrations in the mechanism of PKB activity or the processes which regulate it, resulting in overactive or constitutive activation of PKB, are intrinsically linked to disease states such as diabetes and cancer, and as such, it is an example of an oncogene.

PKB has, however, also been shown to demonstrate the facility to bind PtdIns(3,4)P_2 [107,108]. However, the widely recognised activation of PKB under conditions of elevated PtdIns(3,4,5)P3 concentrations, achieved either following receptor activation or by mutations in PtdIns(3,4,5)P_3 metabolising enzymes, has questioned the significance of its PtdIns(3,4)P_2 binding capability. Furthermore, due to the importance of the tumour suppressor PTEN in metabolising PtdIns(3,4,5)P_3 and of course the primary consequence of PI 3-kinase activation being PtdIns(3,4,5)P_3, perhaps it is of little surprise that much attention has been directed towards PtdIns(3,4,5)P_3 and its effectors.

1.5 Protein Domains.

Protein domains are structurally conserved modules, very often displayed by multiple proteins and are often characterised by a three dimensional structure or scaffold. Many different proteins domains exist for the selective recognition of key molecular targets or ligands which include complementary protein/peptide modules or motifs as well as phospholipids, most pertinently 3-PI. The concept of protein domains was introduced courtesy of the first observed oncogene – that of the viral Rous Sarcoma gene (Src) [109,110]- and now nearly all proteins have been shown to present at least one functional module or domain. Some examples of widely expressed domains crucial in cell signal propagation and their ligands include, SH2 (phospho-Y), SH3 (P-rich peptides), FYVE (PtdIns3P), PH (predominantly 3-PIs), PX (predominantly PtdIns3P), IQ (calmodulin), PDZ (predominantly peptides), CH (actin), WW (P-rich peptides), 14-3-3 (phospho-S) and UIM (ubiquitin) [111-114]. The SH2 and PH domains are introduced below as exemplary domains, however, the structure and ligand specificity of the established lipid binding domains (LBDs), PH, PX and FYVE are addressed more thoroughly in Chapter 5.

1.5.1 The Src Homology 2 Domain (SH2).

The Src homology 2 (SH2) domain fulfils a prominent role within cellular signalling and is present within many proteins and comprises approximately 100 amino acids [114]. SH2 domains employ a characteristic structure of a β-sheet with two α-helices either side. They have been observed in proteins with wide ranging functions from adaptors, kinases, phosphatases to cytoskeletal regulators [115]. The SH2 domain characteristically bind phosphorylated tyrosine residues

but shows varying preference towards the adjacent amino acids (~5 residues C-terminal to the phospho-tyrosine), providing a mechanism for differential selectivity [115]. An example of a functional ligand or consensus sequence for the SH2 domain is provided by the RTK autophosphorylation sites, as previously introduced. The recruitment to autophosphorylated RTKs of the parent protein by its SH2 domain can provide a mechanism by which to consequently activate the recruited proteins and to build signalling complexes at sites of receptor activation. SH2 domains are found within 110 human proteins (SMART database Aug. 2010 [116,117]) and a relevant example is the prominent 5-phosphatase SHIP2, whose name is derived from its SH2 domain. Indeed SHIP2's SH2 domain may provide a mechanism for its membrane recruitment following RTK activation.

1.5.2 The Pleckstrin Homology Domain (PH).

PH domains were first observed in pleckstrin (Pleckstrin Homology) and later the PH domain of PLCδ1 was the first motif to show specific recognition of a phosphoinositide [118], although at least ten more domains have subsequently been identified which are capable of lipid binding [25,119,120]. PH domains are ~125 amino acids in length and they characteristically have little sequence similarity between one example and another but possess a highly conserved secondary structure. This structure is often referred to as a β-barrel (Figure 5.1) and creates a pocket for ligand binding, which with subtle variation can change its selectivity between different PIs [25,119,120]. PH domain containing proteins are integral components of a multitude of effectors and are capable of recognising several PIs. The function of these PH domain containing proteins include kinases, small G-protein regulating proteins (guanosine nucleotide exchange factors

[GEFs], GTP-ase activating proteins [GAPs]) and phospholipases to name but a few [38,120]. Furthermore, parent protein recruitment to cell membranes via these domains has been shown to mediate a wide range of processes such as growth, survival, membrane trafficking and cytoskeletal dynamics [25,121-123]. Examples of some of the better characterised and widely known PH domain proteins include PLC-δ which shows selectivity for PtdIns(4,5)P_2, Btk and Grp-1 which show selectivity for PtdIns(3,4,5)P_3, PDK1 and PKB which show dual selectivity for PtdIns(3,4,5)P_3 and PtdIns(3,4)P_2 and TAPP-1 which shows selectivity for PtdIns(3,4)P_2.

1.6 The Aims of this Study.

In contrast to PtdIns(3,4,5)P_3, few selective binding proteins for PtdIns(3,4)P_2 have been identified. This study aims to address this lack of currently established PtdIns(3,4)P_2 binding proteins by optimising a screen to isolate novel 3-PI effectors, and specifically those for PtdIns(3,4)P_2. It is intended that uncovering PtdIns(3,4)P_2 specific effector proteins will allow conclusions to be drawn on the role of PtdIns(3,4)P_2 as an independent second messenger. The described screen utilises a unique pharmacological approach to manipulate the actions of 3-PI metabolising enzymes; dramatically increasing the cellular concentrations of Ptdins(3,4)P_2. Subsequently, those proteins which are recruited to these membranes are recovered, and their identities determined by mass spectrometry. Positive candidates are cloned and expressed and their lipid binding characteristics are determined by *in vitro* assays. The results of this study advance the understanding of the PI 3-kinase-dependent signalling network.

Chapter 2.

Materials and Methods.

2. Materials and Methods

2.1 Materials

1321N1 astrocytoma cells and HeLa cells were from the European Collection of Cell Cultures. Foetal bovine serum (FBS) and dialysed FBS were a reserve order from Gibco. Antibodies against SHIP2, TAPP-1, as described previously [124], and PARIS-1 (raised in sheep against an N-terminal sequence [amino acid residues 17-29]) were obtained from the Division of Signal Transduction Therapy (DSTT), University of Dundee. GST-tagged PH domains of Grp-1, TAPP-1, lamellipodin, PKB and PLC-δ were also obtained from the DSTT. Potassium bisperoxo(1,10-phenanthroline)oxovanadate (V) (bpV[phen]) was from Merck, PDGF and EGF were from Sigma. Neutravidin beads were from Pierce and VectaSpin spin-filters were from Whatman. All synthetic lipids and inositol derivatives were from Cell Signals (Lexington, KY, USA). Ultrapure water for mass spectrometer sample preparation, used where indicated, was from J.T. Baker and Trypsin Gold was from Promega. Heavy isotope substituted (^{13}C) amino acids were from C.K. Gas Products (Cambridge U.K) and normal or "light" amino acids were from Sigma. Testis, brain and liver cDNA libraries were Matchmaker GAL4 Two-Hybrid Systems obtained from Clontech. KOD Hot Start polymerase and TOPO II blunt vector were from Roche and Invitrogen respectively. All expressed sequence tag (EST) and cDNA plasmids were from I.M.A.G.E. consortium (Cambridge U.K.) and primers were from MWG Eurofins. Streptavidin-dextrose (SA) sensor chips for surface plasmon resonance together with Q-Sepharose and S-Sepharose fast flow chromatography media were obtained from G.E.Healthcare, as were polyvinylidine fluoride (PVDF) and nitrocellulose supported Hybond-C

Extra membranes. Fatty acid free BSA was from Sigma. SDS polyacrylamide gels were from Invitrogen.

2.2 Methods.

2.2.1 Cell Culture.

1321N1 astrocytoma cells from European Collection of Cell Cultures were maintained in Dulbecco's Modified Eagles Medium (DMEM) supplemented with 5% (v/v) FBS. Cells were routinely seeded at ~20,000 cells/cm^2 in a 75cm^2 flask and allowed to achieve confluence (~250,000-300,000 cells/cm^2) at 37°C in a 5% (v/v) CO_2 atmosphere prior to tryptic digestion with Tryple Express (Gibco) and re-plating approximately once a week or as required. Where necessary HeLa cells were maintained identically except FBS was supplemented to 10% (v/v).

Stable Isotope Labelling with Amino acids in Cell Culture (SILAC) medium comprised DMEM which lacked arginine (R), lysine (K) and methionine. Medium was freshly supplemented with 0.2mM methionine, additional glutamine (2mM), 5% (v/v) dialysed FBS and penicillin/streptomycin (Gibco - 100units/ml penicillin [1 unit = potency in 0.6µg of supplier's standard] and 100µg/ml streptomycin). Medium was then differentiated by addition of "heavy" amino acids (0.4mM arginine 6 [R6], 0.8mM lysine 6 [K6]) or equivalent concentrations of "light" amino acids (R0, K0). Cells were initially seeded at 20,000 cells/cm^2 and allowed at least seven cell doublings, splitting where necessary, in their respective medium prior to preparation of lysates. All dishes received a medium change with appropriate DMEM 18 hrs before stimulation.

2.2.2 Preparation of Cell Extracts.

2.2.2.1 Crude Cell Fractionation.

The preparation of crude cytosolic (liberated by digitonin permeabilisation) and subsequent membrane fractions (Triton X-100 [TX-100] soluble material) for the purpose of tracking the re-localisation of cellular components in response to stimuli was achieved from individual wells of cells up to multiple 15cm dishes (10-176cm^2), depending on the experimental requirement. Confluent 1321N1 cells were washed twice in 2-10ml of serum-free DMEM (maintained in 5% (v/v) CO_2 atmosphere) or modified Krebs-Henseleit buffer (25mM Hepes pH 7.6, 118.4mM NaCl, 1.3mM $CaCl_2$, 1.2mM $MgSO_4$, 4.7mM KCl, 1.2mM KH_2PO_4, 11.6mM D(+) glucose) (subsequently maintained without additional CO_2) and allowed to equilibrate in a similar volume of the same medium at 37°C for 60 min. Where required, inhibitor or vehicle alone was added for the final portion of this time. Cells were then incubated in the presence or absence of PI 3-kinase stimuli as indicated to promote the translocation of 3-PI effector proteins to the cell membranes. The plates were then transferred onto ice and the medium was aspirated rapidly and replaced, between 1-4 times consecutively, with 2-10ml of ice-cold, digitonin permeabilisation buffer (25mM Hepes, pH 7.2, 100µg/ml digitonin, 75mM NaCl, 50mM NaF, 100µM EDTA, 100µM EGTA supplemented freshly with 0.1% (v/v) 2-mercaptoethanol, 100µM phenylmethylsulfonyl fluoride (PMSF) 100µM benzamidine and 1mM sodium vanadate) and the cells maintained on a rocking platform at 4°C for 10 min before collection of the resulting supernatant as the soluble protein (cytosol) fraction. The remaining adherent layer of insoluble cell debris was washed briefly with permeabilisation buffer to remove any residual, soluble material prior to recovery

of the membrane fraction by scraping in 1-4ml of ice-cold lysis buffer buffer (50mM Tris, pH 7.5, 50mM NaF, 1mM EDTA, 1mM EGTA, 5mM sodium pyrophosphate, 10mM glycerol 2-phosphate, 0.5% (w/v) TX-100, supplemented freshly with 0.1% (v/v) 2-mercaptoethanol, 100µM PMSF, 100µM benzamidine and 1mM sodium vanadate). These fractions were centrifuged at 10,000g for 10 min at 4°C prior to discarding the insoluble pellet and snap freezing the supernatant in N_2 and storage at -80° for later analysis by SDS-PAGE.

2.2.2.2 Triton X-100 Cell Lysates.

Cell lysates for preliminary experiments to optimise Neutravidin-biotin PtdIns(3,4)P_2 depletion of TAPP-1 (indicated where relevant) were generated similarly, although the digitonin solution was omitted and samples simply scraped into lysis buffer after the 60 min equilibration and subsequent treatment/inhibition period(s) as required.

2.2.2.3 Selective Elution from Membranes.

Proteins recruited to membranes enriched in PtdIns(3,4)P_2 as a consequence of bpV(phen) treatment could be recovered selectively by elution of digitonin permeabilised cells with Ins(1,3,4)P_3 washes. Sample preparation was as detailed for crude cell fractionation with the incorporation of an additional selective elution step prior to final TX-100 recovery of the insoluble fraction. Experimental scale was varied (typically 1-10ml of permeabilisation and elution buffer required for dishes ranging between 6-15cm respectively) according to requirement. Proteins bound to 3-PI as a consequence of elevated PtdIns(3,4)P_2 concentrations were recovered selectively from permeabilised cells by washing in

the appropriate volume of buffer A (10mM Hepes, pH 7.2, 100µM EDTA, 100µM EGTA supplemented freshly with 0.1% (v/v) 2-mercaptoethanol, 100µM PMSF, 100µM benzamidine and 1mM sodium vanadate) supplemented with or without 100µM Ins(1,3,4)P_3 or Ins(1,4,5)P_3 for 10-60 mins at 4°C. The eluted proteins were then analysed by SDS-PAGE.

2.2.3 Affinity and Ion Exchange Chromatography.

Inositol phosphate specific membrane eluates or for the purposes of optimisation, triton extracts, were purified further by affinity chromatography using Neutravidin beads pre-coupled to biotinylated PtdIns(3,4)P_2 (120-240nmol lipid/1ml packed matrix) for a minimum of 30 mins at 4°C in either lysis buffer or buffer. Extracts were pre-cleared with Neutravidin beads alone for a minimum of 30 mins at 4°C except in the case of SILAC experiments. Samples were then incubated with Neutravidin-biotin PtdIns(3,4)P_2 complex for 60 mins at 4°C. The recovery of target proteins from the Neutravidin-biotin PtdIns(3,4)P_2 complex was achieved by collection in 10µm polypropylene filter tubes (VectaSpin Micro, Whatman) coupled to an aspirator manifold modified via a 2ml syringe to support the filter tube. Each sample was washed through rapidly with 2-10 bead volumes of either ice cold lysis buffer or buffer A, according to experimental format, with eluate discarded to waste. Final sample recovery was achieved by elution with one bead volume of buffer B (2.2% (w/v) sodium dodecyl sulphate (SDS) in 70mM Tris pH 6.8) at 70°C. For larger scale experiments, notably SILAC, buffer B was diluted (by a maximum of 4 fold) to allow for subsequent vacuum concentration by a similar factor. Alternatively, where TX-100 extracts were used for experimental optimisation, Neutravidin-biotin PtdIns(3,4)P_2 complexes were

washed by a brief centrifugation step in an appropriate volume of lysis buffer which was discarded prior to direct suspension of the beads into SDS-sample buffer.

Where indicated, but routinely for SILAC experiments, final sample complexity was reduced by application of ion exchange chromatography prior to affinity chromatography with the Neutravidin-biotin PtdIns(3,4)P_2 complex. Single or multiple steps of ion-exchange chromatography consisted of loading samples onto Q-sepharose and S-sepharose columns (anion and cation exchangers respectively) and eluting with 150-600mM NaCl. Additionally, where indicated the column flow-through was also recovered for analysis. Elution volumes of NaCl were limited to 2-5 column bed volumes (0.3-0.5ml) to minimise the amount of biotinylated lipid required to achieve optimum concentration at the subsequent step. Although primarily ensuring a reduction of sample complexity, chromatographic fractionation in this manner also limited the carry-over of Ins(1,3,4)P_3.

2.2.4 SDS-PAGE.

Each cell extract for analysis was either supplemented with the appropriate volume of NuPAGE 4xLDS (lithium dodecyl sulphate) sample buffer (Invitrogen) and 14.5mM 2-mercaptoethanol or the remaining constituents were added separately where SDS had been included during sample preparation, ensuring that final concentrations in each instance were 62.5mM Tris pH 6.8, 0.01% (w/v) bromophenol blue, 10% (v/v) glycerol and SDS to a maximum of 5% (v/v). Alternatively, notably for SILAC experiments, prior to the addition of sample

buffer constituents, samples were first reduced (using 10mM dithiothreitol at 70^{o}C for 5 min) and alkylated (using 50mM iodoacetamide at room temperature for 30 min). Samples (~25µg for routine analysis and 25-100µg for samples intended for analysis by mass spectrometry) were loaded on Novex, pre-cast, bis-tris gels, typically 4-12% (w/v) and were run according to the manufacturer's instructions. Exceptionally, SILAC samples were developed to only 1/3-1/2 the gel length, ~25-35 mins at 150V. Developed gels were then stained immediately with Colloidal Coomassie (Invitrogen) or Silver Snap (Pierce) according to the respective manufacturer's protocol. Alternatively, gels were processed further by Western blotting.

2.2.5 Western Blotting.

PVDF membrane, pre-wetted in methanol and allowed to equilibrate for 10 mins in transfer buffer (Invitrogen) and 15% (v/v) methanol was assembled into a cassette and transferred using the Bio-Rad mini Trans-Blot PROTEAN wet transfer system. Transfer was achieved, typically with a ~60cm^2 membrane, either at 60V for 2.5 hrs or at 16V overnight. The membranes were then blocked for 30 mins in Tris-buffered saline with Tween-20 (TBST) (50mM Tris pH 7.6, 150mM NaCl, 0.1% [v/v] Tween-20) supplemented routinely with 5% (w/v) Marvel or alternatively with 3% (v/v) BSA for anti-phospho blots. Following blocking, membranes were incubated with primary antibody (typically 0.1-1µg/ml) for 1 hr at RT or overnight at 4°C in appropriate TBST blocking buffer supplemented with 0.05% (w/v) NaN_3 as a preservative. Several subsequent rounds of washes in TBST, typically 3 x 10 mins preceded incubation for 1 hr at RT with appropriate horseradish peroxidase-coupled secondary antibody (0.1µg/ml) in appropriate

TBST blocking buffer. Following an additional cycle of washes in TBST (3 x 10 mins), protein-antibody complexes were visualised by exposure to Immobilon Western ECL (Millipore) chemiluminescent substrate and the output recorded on a CCD camera under conditions of linear light accumulation. Images were quantified using AIDA (Advanced Image Data Analysis) software.

2.2.6 Agarose Gel Electrophoresis.

For the purposes of gel purification or qualitative analysis of fragment size, DNA samples were supplemented with DNA sample buffer (0.25% (v/v) xylene cyanol FF, 0.25% (v/v) bromophenol blue, 50% (v/v) glycerol, 1X TAE [40mM Tris-HCl pH 7.6 with acetic acid, 1mM EDTA]) and stored at 4°C**.** Separation of DNA fragments was achieved on a 1% (w/v) agarose gel (1g agrose/100ml TAE per gel required), prepared by heating until the agarose dissolved and then supplemented freshly with 0.02% (v/v) SYBR safe DNA gel stain (Invitrogen) before allowing to cool and pouring into a gel platform prior to solidifying. Following cooling to room temperature, the agarose gel was submerged in 1X TAE buffer and 10-20µl of sample was loaded accordingly into each well. Gels were developed for 1 hr at 140V prior to exposure on a CCD camera to visualise the bands and quantitation, where required, was by AIDA. Subsequent DNA purification from gel slices was carried out using QIAquick Gel Extraction Kits (Qiagen) according to the manufacturer's instructions.

2.2.7 Primer Design.

Primer design was achieved using pDRAW (AcaClone software) ensuring the selection of appropriate vectors and strategy based on the presence/absence of restriction sites within the cDNA of interest. Having selected suitable sequences (~15-35 nucleotides) from within the cDNA both 5'-3' and 3'-5', this was checked using NetPrimer (Premier Biosoft International) to ensure the absence of any significant primer dimers, hairpins and cross dimers. An approximate score of between 0-100 is provided on this basis, and no primer was selected that fell below a score of 65. All oligonucleotides (including sequencing primers) were ordered from MWG Eurofins (sequence submitted on the basis of 5'-3' regardless of sense/antisense), using either their HPSF (high purity salt free) standard unmodified oligonucleotide service or the unmodified oligonucleotide à la carte service for those where incorporation of additional restriction sites was required due to cloning strategy. The primers used are listed in Table 2.1.

Table 2.1 Primer Sequences.

Construct	Sense (5'-3')	Anti (5'-3')
PDIA5	GCTGCTGGGATGGCGC	CTGAGGCAGGAATTATAACTCTTCC
CIQGAP 718-1657	GTCTATGTCGACCTATGCAGCTTTCTCGGGAGG	TATGCGGCCGCTTACTTCCCGTAGAACTTTTTGTTGAG
NIQGAP 1-721	GTCTATGTCGACCCATGTCCGCCGCAGAC	GGATCTCCTCCCGAGAAAGC
CLIC1	TCAACGGATCCAAGCTTATGGCTGAAGAACAACCG	AGATGAGATCTGCGGCCGCTTATTTGAGGGCCTTTGC
RACK1	TCTTGGTCGACGGATCCATGACTGAGCAGATGACC	AGTACGGGCCCGCGGCCGCCTAGCGTGTGCCAATGGT
VCL	GTCCAGTCGACGGATCCATGCCAGTGTTTCATACGCGC	CTACTGTCGACGCGGCCGCCTACTGGTACCAGGGAGTC
PKM2	TCAACGGATCCAAGCTTATGTCGAAGCCCCATAGTGA	AACCAAGATCTGCGGCCGCTCACGGCACAGGAACAACA
ANKFY1	ACATGTCTGTGCCAGATGAGAAG	CTAAGAAACCCCACCCAGAGTC
YES1	GTCTATGTCGACATGGGCTGCATTAAAAGTAAAG	GCTGCGGCCGCTTATAAATTTTCTCCTGGCTGG
SOLO C-term	GTCTATGTCGACCTATGCCTGGGGACACCTTG	GCTGCGGCCGCTCACAGAGGCGTGGTGGG
CRTAP	TCTATGTCGACATGGAGCCGGGGCGC	GCTGCGGCCGCCTAGCTGGTCTCCTCCAGTTCCA
OSBPL11	TGGACTTTGGCGTTAAGATGC	GTGTCACTCTGCTGGTTGTGTTG
FOXK2	CTGGATCCATGGCGGCGGCCG	CTGTCGACCTAGTTCTGGACACCCTTTTCCC
PICALM	CAGAGATGTCCGGCCAGAG	CCATCAAGTTACATAAACTGTATCTGTG
PFN	ATGGCCGGGTGGAACG	GTCAGTACTGGGAACGCCG
PXK	ATGGCCTTCATGGAGAAGC	CCTCAGATCAATGGTGGGAC
SPARC	GCACCATGAGGGCCTGG	GGAGTGGATTTAGATCACAAGATCC
FERMT2	ATGGCTCTGGACGGGATA	TTCACACCCAACCACTGG
EPSIN1	ATGGGTGATCAGAGCTGG	CCCTTCCTCCTATAA
KDELC2	GACCATGCGCCGCCTC	GACTCAAAGTTCTTCTCTTGAAGGC
FKBP9	CTCGCCGCCCCGATG	TGCCAGGTTTAGAGTTCATCGTG
EIF4E	ATGGCGACTGTCGAACCG	GAAGGTGTCTTCTTAAACAACAAACC
SERPINH1	GCCATGCGCTCCCTCC	GGCCCTATAACTCGTCTCGC
ANXA6	ACTCAGTCGACGGAGACCATGGCCAAACC	CGGAGACCATGGCCAAACC
SWAP70	GCCATGGGGAGCTTGAAGG	GCAAGCTCAGTCACTCCGTGG
PARIS-1-Short PH	GTCCCTCCGCAGATCTCCGGCTGGCAGCGATGGAGGGCG	CAGCCCGCCGTGACCTCCTGCCA
PARIS-1-Long PH	GTCCCTCCGCAGATCTCCGGCTGGCAGCGATGGAGGGCG	GCCTTGCAGCCCTAACCTGCCCTTC

2.2.8 Polymerase Chain Reactions (PCRs).

All PCR reactions were carried out using a PTC-200 Peltier Thermal Cycler and KOD Hot Start DNA Polymerase (Calbiochem) with all reactions initially attempted using 100-500ng template DNA from human brain, liver and testis cDNA libraries. If PCR from the libraries failed, cDNAs or ESTs obtained from the I.M.A.G.E. consortium were used as an alternative, and template DNA in these PCR reactions was reduced to 10ng. As standard, primer concentrations were 300nM although this was decreased incrementally to a minimum of 50nM in conjunction with increasing template, where necessary. All reactions were carried out according to the manufacturer's instructions, and additionally both with and without 1% (v/v) DMSO. PCR cycling conditions were as described in the manufacturer's instructions for KOD Hot Start DNA Polymerase. Briefly, these were: 1. Activate; 95°C for 2 min, 2. Denature; 95°C for 20 sec, 3. Anneal; Primer Tm°C (as provided by NetPrimer analysis) for 10 sec, 4. Extension; 70°C ~20 sec/kb target DNA, with steps 2-4 repeated for 30-35 cycles.

2.2.9 Sub-Cloning and Transformations.

Following agarose gel purification, the PCR products were ligated either directly into pGex-6P-x (where x = 1, 2 or 3) or, more commonly, intermediately into pCR-Blunt II TOPO prior to insertion into pGex-6P-x. The Zero Blunt TOPO PCR Cloning Kit (Invitrogen) was used according to the manufacturer's instructions. Briefly, approximately 2µl of PCR product was incubated for 10 min at room temperature with 1µl of pCR-Blunt II TOPO in the presence of 200mM NaCl and 10mM $MgSO_4$ made up to a total volume of 6µl with PCR grade water**.** The resulting ligation product was added, with gentle mixing, to a freshly thawed

(on ice) aliquot of chemically competent TOP10 *E.Coli* and allowed to rest on ice for 30 mins. The TOP10 cells were then heat shocked at 40°C for 30 secs and then transferred immediately back on to ice**.** To this, 200µl of SOC (2% [w/v] Tryptone, 0.5% [w/v] yeast extract, 10mM NaCl, 2.5mM KCl, 10mM $MgCl_2$, 10mM $MgSO_4$, 20mM glucose) medium at room temperature was added and the samples transferred to a shaker for gentle horizontal agitation at 37°C for 1 hr before plating on LB (Luria Bertani) plates containing 50µg/ml kanamycin and incubating at 37°C for 16+ hrs. Eight colonies were selected, cultured for 12 hrs at 37°C in 5ml LB freshly supplemented with 100µM kanamycin and the DNA was isolated. Following qualitative confirmation of the insert size by restriction digest and agarose gel analysis, the insert was sequenced with either M13 forward and reverse primers or with appropriately designed sequencing primers. Upon sequence confirmation both target vector (pGex-6P-x) and PCR product were digested with appropriate restriction enzymes and compatible buffer (Roche), typically for 1-2 hrs at 37°C. The target vector was then subsequently treated with shrimp alkaline phosphatase (Roche) according to the manufacturer's instructions for 30 mins at 37°C in order to ensure that vector alone could not re-ligate. Following an agarose gel purification to eliminate undesirable DNA fragments, the cDNA and vector were ligated overnight at room temperature using T4 DNA ligase (Roche), typically in the following insert : vector ratios, 0:1, 1:1 and 1:3. The ligation mix was added to an aliquot of chemically competent BL21 *E.Coli* and cells transformed as described previously for TOP10s with the exception that resulting bacterial S.O.C. cultures were plated on 50µg/ml ampicillin LB plates. The resulting colonies were cultured for 12 hrs at 37°C in 5ml of LB supplemented freshly with 100µM ampicillin. An aliquot (100µl) of these cultures

was adjusted to 20% (v/v) with respect to glycerol and stored at -80°C as a starter culture for larger scale protein expression, following DNA purification and qualitative confirmation of insert size by agarose gel analysis of restriction digest.

2.2.10 Protein Expression.

The pGex-6P-x constructs incorporating sequence verified inserts were expressed by seeding 100ml of ampicillin supplemented (100μM) LB broth with transformed BL21 *E.coli* starter cultures generated as described in 2.2.9. Cultures were grown overnight at 37°C prior to dilution of the initial culture to 500ml with appropriate medium. Protein expression was promoted by addition of isopropyl β-D-thiogalactoside (IPTG) at 50-400μM for 1-16 hrs at 30°C or 37°C as indicated. After centrifugation at 4000g for 10 min, cell pellets were lysed by a single round of freeze-thawing in 25ml of ice-cold lysis buffer as previously described followed by sonication. Samples were centrifuged at 6000g and 4°C for 30 mins and the supernatant loaded onto a 1ml glutathione-sepharose column pre-equlibrated with lysis buffer and maintained at 4°C. The column was washed with 10ml buffer C (50mM Tris/HCl, pH 7.2) supplemented with 500mM NaCl and then with a further 10ml of buffer C supplemented with 150mM NaCl. The protein was eluted with 5ml buffer C supplemented with 150mM NaCl and 15mM glutathione. The eluate was dialysed against 5 litres of buffer B supplemented with 150mM NaCl, 1mM dithriothreitol and 20% (v/v) glycerol in a Slide-A-Lyser cassette (Pierce) for 12 hrs prior to aliquotting, snap freezing in liquid nitrogen and storage at -80°C.

2.2.11 Protein Lipid Overlay Assay.

All lipids were purchased in a lyophilised state and as the free acids of their dipalmitoyl forms: PtdIns, PtdIns3P, PtdIns4P, PtdIns5P, PtdIns(3,4)P_2, PtdIns(4,5)P_2, PtdIns(3,4,5)P_3 and were reconstituted into 1mM stocks in 1 : 2 : 0.8 by volume of chloroform : methanol : water. Stock lipid solutions were immediately stored at -80°C and for a maximum of 2 weeks preventing diminished protein binding capacity owing to the acid labile nature of phosphate bonds around the inositol ring. These stock solutions were then serially diluted so as to ensure that 1µl spotted onto Hybond-C extra membrane resulted in amounts ranging from 1-500pmol. After allowing 30 mins at room temperature to dry, the membranes were then blocked at room temperature for 1 hr with TBST supplemented freshly with 3% (w/v) fatty acid free BSA (Sigma). Following blocking, the membranes were incubated overnight at 4°C with 0.2µg/ml of the GST-fusion proteins of interest presented in the previously described blocking buffer. The membranes were then washed 10 x 5 mins in TBST prior to, and after the addition of the primary anti-GST antibody at 0.5µg/ml for 1 hr at room temperature. The secondary HRP-conjugated antibody, at 0.1µg/ml, was incubated for 1 hr at room temperature before washing the membrane as previously. Finally, the membrane was exposed to Immobilon Western ECL (Millipore) chemiluminescent substrate and the output recorded by a CCD camera under conditions of linear light accumulation as for Western blotting.

2.2.12 Surface Plasmon Resonance (SPR).

Lyophilised, dioctanoyl, biotinylated PtdIns(4,5)P_2, PtdIns(3,4)P_2 and PtdIns(3,4,5)P_3 were reconstituted to 10mM in 10mM Hepes pH 7.2 and stored at -20°C. As required, lipids were diluted to their working concentration of 100µM in SPR buffer (100mM Hepes pH 7.2, 100µM EGTA and 100µM EDTA). Streptavidin (SA) chips were loaded into a Biacore 3000 and all four flow cells were flushed through with SPR buffer prior to independent loading of each flow cell with a distict lipid (including a blank, control lane). Lipids were loaded at a flow rate of 5µl/min until response units (RU) of approximately 400-600 were achieved above with the control baseline. SPR buffer was then supplemented with 0.2mg/ml fatty acid free BSA and allowed to flow over each of the four lanes at 100µl/min for a minimum of 15 mins in an attempt to block non-specific binding to the chip surface. When present, 0.2mg/ml BSA was maintained throughout all subsequent steps. Test proteins were then diluted to working concentrations in the BSA containing SPR buffer. Proteins were presented to the lipid surface in increasing concentrations (ranging ~1-1000nM), usually including at least one duplicate and analysed with a flow rate of 100µl/min. Protein injection and dissociation times were set arbitrarily at first (1-3 min and 1-5 min respectively) with subsequent runs advised by initial data. Owing to diminishing responses over time, presumably either because of hydrolysis of the lipid or increasing non-specific binding to the dextran matrix the lipid-bound chips were used for no more than 12 hrs and limited to a maximum of 4-5 test proteins (each run with 5-6 concentrations). Where off-rates were sufficiently low to require regeneration, this was achieved (maximum twice per chip) with 30sec pulses of 5mM NaOH followed by appropriate washing buffer until a stable baseline signal was attained.

2.2.13 Preparation of Mass Spectrometry (MS) Samples.

Samples requiring MS analysis were first reduced by supplementing with 10mM DTT and incubated for 5 mins at 70°C. Alkylation was then carried out by adding 50mM iodoacetamide and incubating in the dark, at room temperature for 30 mins. The remaining constituents of sample buffer were then added. The three samples were then run out partially, on a pre-cast, bis-tris Novex gels (as previously described). After staining with collioidal coomassie, subsequent steps were carried out in a laminar flow hood, wherever possible. Each sample lane was then cut into 8-10 slices and these then diced to approximately $1mm^3$ pieces. Gel pieces were then transferred to lowbind Eppendorf tubes, washed with; ultrapure water, 50mM ammonium bicarbonate and 50% (v/v) acetonitrile / 25mM ammonium bicarbonate, using 0.5ml of each reagent and allowing 10 min at RT on a shaking platform per step. The gel pieces were then treated with 0.3ml acetonitrile for 10-15 min at room temperature before removing the solvent to waste and drying in a vacuum concentrator. The gel pieces were then swolled in 50mM ammonium bicarbonate containing 5µg/ml trypsin gold (Promega), in sufficient volume to cover the gel pieces, for 30 mins at 30°C on a shaker. After 30 mins additional ultrapure water was added, as required, in order to maintain the sample volume. The gel pieces were then incubated overnight at 30°C with gentle agitation. One volume of acetonitrile was then added to the digests which were shaken for 10-15 min before collecting the supernatant in newly labelled low bind Eppendorfs and evaporating to dryness in a vacuum concentrator. Meanwhile, the gel pieces were re-extracted with 100µl acetonitrile / 2.5% (v/v) formic acid, shaking for a minimum of 10 mins at RT. The resulting supernatant (100µl acetonitrile / 2.5% (v/v) formic acid) was collected and combined with the now

dried, first extract, and re-dried in a vacuum concentrator. Samples were stored at -20°C and immediately prior to MS run, reconstituted to 1% formic acid.

2.2.14 Stable Isotope Labelling by Amino Acids in Cell Culture (SILAC) Analysis.

Following re-constitution, samples prepared previously for MS were centrifuged at 13,000g to remove any debris and then analysed on an LTQ-Orbitrap XL mass spectrometer system (Thermo Scientific) coupled to a U3000 nano-LC system (Dionex). The samples were loaded at 20µl/min onto an LC-Packings PepMap C18 trap column (0.3 x 5mm) equilibrated in 2% (v/v) acetonitrile and 0.1% (v/v) formic acid then washed for a further 3 min following sample load. The trap column was then switched in-line with an LC-Packings PepMap C18 column (0.075 x 150mm) equilibrated similarly. The peptides were separated by a 100 min discontinuous gradient from 2% to 45% (v/v) acetonitrile in 0.1% (v/v) formic acid (2-45% acetonitrile over 65 min) at a flow rate of 300nl/min. The HPLC was interfaced to the mass spectrometer with an FS360-50-15-N-20 PicoTip (New Objectives) fitted to a nanospray interface (Proxeon) with a voltage of 1.1kV applied to the liquid junction. The Orbitrap XL was set to analyse the survey scans at 60,000 resolution with the top five ions in each duty cycle selected for MS/MS in the LTQ linear ion trap. The Raw files were processed with MaxQuant (Version 1.0.13.13) as described previously [125,126]. Peak lists generated by Quant.exe were searched against the International Protein Index human database version 3.37 run on an in-house server using the Mascot search engine v.2.2 (Matrix Science). Peptide tolerance was set to 7 ppm and 0.5Da allowing a maximum of three missed cleavages with trypsin.

Carboxyamido-methylation of cysteine was set as a fixed modification, oxidation and acetylation of methionine as variable modifications and heavy SILAC labels were (^{13}C)6 arginine (R) and (^{13}C)6 lysine (K).

Identification was performed using MaxQuant with protein ratios compiled from the contribution of individual peptide ratios, with a false discovery rate of 1%. Site quantification was by least modified peptides allowing variable modifications, requiring at least one unique peptide of minimum 6 amino acids in length for positive identification. However, analysis did allow contribution from razor peptides, with retention of low scoring version of peptides and filter labelled amino acids options deselected.

Chapter 3.

Development of a Screen for Novel PtdIns(3,4)P_2 Binding Proteins.

3.1 Introduction.

In the previous introductory Chapter the concept of lipids and particularly phosphatidylinositol as second messengers was introduced. This concept is developed further in the current Chapter which focuses on the development of a protocol to isolate and enrich novel interacting partners of the little studied second messenger, PtdIns(3,4)P_2.

3.1.1 PtdIns(3,4)P_2 as a Potential Second Messenger.

Following the identification of 3-phosphoinositides as minor components of cellular membranes, a period of intense interest focussed on PtdIns(3,4,5)P_3 due to its emerging role as a second messenger within diverse cellular processes [39,46-57]. Moreover, the recognition of PTEN as a tumour suppressor further highlighted the significance of aberrant PtdIns(3,4,5)P_3 regulation in disease states such as diabetes and cancer [127-129]. Subsequently, it was shown that class IA PI 3-kinase stimulation commonly causes an acute temporal elevation of PtdIns(3,4,5)P_3 concentrations synthesised from PtdIns(4,5)P_2 followed by a lag and more sustained (up to 60 min) [130-132] accumulation of PtdIns(3,4)P_2, although surprisingly few studies have measured the lipids directly. This model of synthesis coupled to the significance of PTEN largely consigned PtdIns(3,4)P_2 and the 5-phosphatases, to a role as a degradation product and a redundant mechanism for the removal of excess PtdIns(3,4,5)P_3 respectively. Alternative mechanisms were presented for the regulated and independent synthesis of PtdIns(3,4)P_2 via a PtdIns3P 4-kinase, or by PI 3-kinase activity towards PtdIns4P [130-132] (later suggested to be class II PI 3-kinases as a consequence of *in vitro* assays [51]), but these views were not widely accepted.

Interest in the role of PtdIns(3,4)P_2 as a second messenger was, however, renewed with the proposal that PKB and PDK1 were able to bind PtdIns(3,4)P_2 [86,133,134]. Mounting evidence which now implicates PtdIns(3,4)P_2 as a potentially important signal includes; PtdIns(3,4)P_2 requirement for complete PKB activation [135]; the identification of a small group of established PtdIns(3,4)P_2 binding molecules (dual adaptor of phosphotyrosine and 3-phosphoinositides [DAPP1], TAPP1 and lamellipodin) [99,124,136-140]; the suppression of growth in megakaryocytes and fibroblasts by attenuation of PtdIns(3,4)P_2 accumulation; the PtdIns(3,4)P_2–dependent regulation of cell growth downstream of the GATA-1 transcription factor [141] and a potential role for the 4-phosphatases as tumour suppressors [142]. Furthermore, a mutation in type I 4-phosphatase has been reported in mice, leading to the *weeble* phenotype, which is manifest in neuronal loss [79,143]. Although this phenotype is still viable it underlines the significance of PtdIns(3,4)P_2 synthesis and is not incompatible with the notion that it may act as a second messenger within its own right. Recent data supporting this conclusion shows the type I 4-phosphatase (INPP4A) acting as a suppressor of glutamate excitotoxicity in the CNS of mice and that targeted disruption of the INPP4A gene results in neurodegeneration in the striatum [144]. Despite these data, little work has been done to reveal the downstream effectors of PtdIns(3,4)P_2. Given the large number of known PtdIns(3,4,5)P_3 binding partners including PKB/Akt, PDK1, Bruton's tyrosine kinase (Btk), dual adapter for phosphotyrosine and 3-phosphoinositides (DAPP-1), centaurin-α, Gab1, growth factor receptor bound protein 2-associated protein 1 (GAP1), switch-associated protein 70 (SWAP-70) and general receptor of phosphoinositides 1/cytohesin-3

(Grp-1) [89,95,105,138,145-153] it seems unlikely that the above list of PtdIns(3,4)P_2 binder partners represents the complete repertoire. Thus, the predominant aim of this study was to expand the current list of known PtdIns(3,4)P_2 interacting proteins.

3.1.2 The Determination of Conditions to Drive the Selective Accumulation of PtdIns(3,4)P_2 in Cell Membranes.

In order to investigate the possibility of novel PtdIns(3,4)P_2 binding proteins this study took advantage of the pharmacological inhibition of PTPs (protein tyrosine phosphatases). The PTP family are phosphatases whose activities are characteristically dependent on a reactive cysteine residue. These enzymes are generally constitutively active but capable of inhibition by oxidation of the cysteine residue, notably via endogenously generated ROS (reactive oxygen species) [154,155]. ROS are commonly produced by the membrane bound enzyme complex NADPH oxidase (nicotinamide adenine dinucleotide phosphate-oxidase), crucial in the immune system's respiratory burst. They are however, also produced following growth factor mediated stimulation of RTK allowing the initiation of intracellular redox sensitive signalling cascades [155,156].

Vanadate analogues, similar to ROS, can also act as potent PTP inhibitors by their action on the PTP family of enzymes [157]. Two related phosphatases include the lipid metabolising enzymes PTEN and the 4-phosphatases described in Chapter 1, which possess the characteristic reactive cysteine residues [69,158-160]. Thus, vanadate analogues can be used to manipulate cellular 3-

phosphoinositide levels, via their ability to inhibit the action of PTEN and 4-phosphatases on PtdIns(3,4,5)P_3 and PtdIns(3,4)P_2 respectively [41,132].

Existing data from the laboratory, shown in Table 3.1, demonstrate the effects of sodium vanadate and the cell permeable vanadate analogue, potassium bisperoxo[1,10-phenanthroline]oxovanadate [V] (bpV[phen]) on cellular PI concentrations within PTEN null 1321N1 astrocytoma cells [41]. Despite subtle differences in the output of several PI species both reagents cause a dramatic change in the levels of PtdIns(3,4)P_2 with the coincident loss of PtdIns(4,5)P_2 suggesting that the 2500-5000 fold increase in the former is primarily at the expense of the latter. Subsequent work detailed the mechanism by which the role of bpV(phen) as a generic PTP inhibitor has a threefold effect on the P I3-kinase signalling pathway [41]. Firstly class IA PI 3-kinases become constitutively active as a consequence of inhibition of the PTPs which regulate the activity of RTKs. Indeed, following bpV(phen) treatment, the PI 3-kinase activity associated with anti-phosphotyrosine immunoprecipitates can be seen to increase substantially. Secondly, the activity of the 4-phosphatases which metabolise PtdIns(3,4)P_2 is inhibited and thirdly, the specific activity of SHIP2 is increased.

The extent to which the specific activity of SHIP2 can be increased is underlined by the constitutive activation of class IA PI 3-kinases which occurs with little or no observed increase in the concentration of PtdIns(3,4,5)P_3. This presents a convincing argument that the capacity for activation of the 5-phosphatases, specifically SHIP2, is equal to or greater than that of the class IA PI 3-kinases. Indeed, bpV(phen) is able to ablate the platelet derived growth factor

(PDGF) dependent accumulation of PtdIns(3,4,5)P_3 when given concomitantly [41].

Table 3.1 The effects of vanadate analogues on cellular PI concentrations.

Lipid		Stimulus	
	Control	Sodium Vanadate (1mM)	bpV(phen) (0.1mM)
	(% Total PI)	(Fold control)	(Fold control)
PtdIns	80.615 ± 1.556	0.89 ± 0.01	0.95 ± 0.03
PtdIns3P	0.425 ± 0.039	1.73 ± 0.01	3.95 ± 1.86
PtdIns4/5P*	7.511 ± 0.586	2.30 ± 0.26	0.77 ± 0.06
PtdIns(3,5)P2	0.022 ± 0.003	1.96 ± 0.22	8.63 ± 4.77
PtdIns(3,4)P2	0.004 ± 0.001	13.68 ± 4.59	5164.00 ± 2243
PtdIns(4,5)P2	11.407 ± 1.026	1.09 ± 0.02	0.27 ± 0.11
PtdInsP3	0.011 ± 0.001	1.15 ± 0.015	2.17 ± 1.25

1321N1 astrocytoma cells were pre-labelled with [^{3}H] inositol and incubated for 30mins with and without 1mM sodium vanadate or 100μM bpV(phen) prior to 0.5M TCA extraction. Each PI species as a proportion of total [^{3}H]PI is represented by control, with values equating to means ± S.E.M. of ten experiments. The fold change following treatment with either sodium vanadate and bpV(phen) treatment is shown and is representatitive of at least 3 experiments. Data reproduced from [41] and experiments carried out by I. Batty.

3.1.3 The Phosphorylation of SHIP2 Increases its 5-Phosphatase Activity.

The mechanism in which SHIP2, a prominent 5-phosphatase, is capable of mediating such acute changes in PtdIns(3,4,5)P_3 concentrations following pharmacological inhibition of PTPs was recently investigated. SHIP2 had previously been reported to possess basal levels of activity, with regulation principally determined by its localisation as either cytosolic or at the cell periphery, a mode of action similar to PTEN. Several studies underlined that SHIP2 activity was unaffected by phosphorylation following treatment with a variety of stimuli such as PDGF, epidermal growth factor (EGF), nerve growth factor (NGF) and insulin-like growth factor (IGF) [161-165]. This conclusion was widely disseminated in the literature as a consequence of subsequent review articles [166,167].

However, in order to explain the observed disparity between the PtdIns(3,4,5)P_3 concentrations following treatment with PDGF alone or with PDGF together with bpV(phen), the activity of the 5-phosphatases must possess a capacity for increased activation, an effect unlikely simply due to membrane recruitment alone. In contrast to the prevailing view in the literature, Batty *et al.* demonstrated that the specific activity of SHIP2 can be increased 8-10 fold with EGF or bpV(phen) treatment, an effect which is mediated by tyrosine phosphorylation [41,168]. Thus, SHIP2 immunoprecipitates from bpV(phen) or EGF treated samples showed an increase in activity of SHIP2 towards Ins(1,3,4,5)P_4, the water-soluble inositol headgroup of PtdIns(3,4,5)P_3, in conjunction with tyrosine phosphorylation. Moreover, the increased activity and

phosphorylation of these immunoprecipitates could be eliminated by incubation with the tyrosine phosphatase SHP1. These estimates of 8-10 fold increases in specific activity were later confirmed by intracellular assays measuring the rate of PtdIns(3,4,5)P_3 hydrolysis in PTEN null 1321N1 cells following treatment with and without sodium vanadate [41].

This capacity for the activity of SHIP2 to be regulated, and under certain conditions be coupled to the activity of class IA PI 3-kinases and the inhibition of the 4-phosphatases, presents a mechanism to effectively switch the signalling output of class IA PI 3-kinases from PtdIns(3,4,5)P_3 to PtdIns(3,4)P_2. The existence of such a route of synthesis provides strong evidence that PtdIns(3,4)P_2 is not merely a breakdown product of PtdIns(3,4,5)P_3 but that their cellular concentrations can be independently controlled.

3.1.4 TAPP-1/2: The definitive PtdIns(3,4)P_2 Binding Proteins.

Of all the evidence introduced in 3.1.1 and the capacity for an increase in the specific activity of SHIP2, discussed previously, arguably the most convincing indication that PtdIns(3,4)P_2 can elicit a response independently of PtdIns(3,4,5)P_3 was provided by the identification of TAPP-1 and TAPP-2 [102,169]. TAPP-1/2 were identified by homology using a bioinformatics approach based on the observation that six conserved residues within the N-terminal region of PH domains, called the PPBM (putative PtdIns(3,4,5)P_3 binding motif) appear to confer high affinity PtdIns(3,4,5)P_3 binding [102]. However, the subsequent discovery of the novel selectivity and high affinity of TAPP-1/2 for PtdIns(3,4)P_2

questions the reliance on such bioinformatics tools for assigning lipid selectivity, an issue addressed in Chapter 5.

Although the function of TAPP1/2 is still unclear, it is likely a scaffold protein and has been postulated to be responsible for shuttling the multi-PDZ domain protein MUPP1 and the protein tyrosine phosphatase PTPL1 to the plasma membrane following PtdIns(3,4,)P_2 synthesis [124,170]. The fact that TAPP-1 is highly conserved between humans and mice [169] suggests it has a critical, but as yet not fully understood role, a conclusion further supported by the presence of an additional, conserved, N-terminal PH domain with, to date, no reported lipid binding affinity. Regardless, the reported selectivity of the C-terminal TAPP-1 PH domain has led to its widespread use as a marker for PtdIns(3,4)P_2 in immunohistological and *in vitro* assays [171,172], and in this study provides a model protein by which to track and optimise the isolation of similarly recruited binding proteins.

3.1.5 Other Proposed PtdIns(3,4)P_2 Binding Proteins.

In addition to TAPP-1/2 several proteins have been reported to present affinity for PtdIns(3,4)P_2, although none seem to show similar levels of selectivity or affinity to those demonstrated by TAPP-1/2. The potential candidates identified include, but are not limited to; PKB, PDK1, DAPP-1, SWAP-70, lamellipodin, peroxiredoxin 1 (PRDX-1), vinculin and Igrm-1 [88,89,98,104,131,135,138,145,173-176]. With the exception of PKB and PDK1, which have been studied more thoroughly, the majority of these proposed binding proteins have had their affinity and/or selectivity for 3-PIs assumed via affinity

precipitation from cell extracts or estimated based on their observed binding in protein lipid overlay assays. In cases of identification from affinity precipitations, samples are often complex protein mixtures, containing both specific and non-specific proteins and significance may be erroneously attached to proteins purely on the basis of possessing an established LBD. Moreover, protein lipid overlay assays, more commonly known as fat blots, have significant caveats but their advantages and disadvantages in contributing understanding to lipid selectivity will be discussed in Chapter 5.

3.2 Results.

3.2.1 The Physiological Recruitment of TAPP-1.

It is widely accepted that signalling downstream of class IA PI 3-kinases is mediated by PtdIns(3,4,5)P_3 and PtdIns(3,4)P_2 [177,178]. Whilst much research has been focussed on PtdIns(3,4,5)P_3 and its effectors, little effort has been directed towards PtdIns(3,4)P_2. By optimising a screen for the selective recruitment and subsequent isolation of the model PtdIns(3,4)P_2 binding protein, TAPP-1, it was intended that similarly recruited, potentially novel PtdIns(3,4)P_2 proteins could be identified.

In order to achieve this recruitment of novel binding proteins, the previously observed phenomenon of dramatically elevated PtdIns(3,4)P_2 concentrations in response to treatment with the cell permeable vanadate analogue bpV(phen) (Table 3.1) would be exploited [41]. However, having established a mechanism for the recruitment of potential binding proteins, the techniques for subsequent isolation were considered.

To make this isolation of TAPP-1 and novel PtdIns(3,4)P_2 proteins applicable for maximal recovery and to allow subsequent identification of these proteins, any approach would require rapid and selective fractionation of the cell. To achieve rapid cell lysis and to allow free cytosolic proteins to be removed/eliminated from subsequent processing, this study utilises digitonin permeabilisation which has several advantages over other possible approaches. Fixation approaches, whilst allowing instantaneous cross linking of cell proteins and maximising the yield of even low affinity binding proteins at the membrane, are incompatible with

identification of novel candidates, particularly via mass spectrometry. Crude, whole-cell fractionation with detergents such as Triton X-100 (TX-100) would liberate intracellular proteases destabilising potential interactions as well as complicating the final sample with proteins from multiple cell compartments. This is a feature shared, although to a more limited extent, with homogenising or osmotically lysing the cells, approaches which in our hands were also commonly incomplete (data not shown and I. Batty, unpublished data).

Digitonin however, is a detergent which selectively targets cholesterol, which is present at high concentrations in the plasma membrane but essentially absent in other membranes [179-182]. The pores generated by digitonin, achieved in a method similar to that of the innate immune response of compliment to non-self cells and bacterial pore forming complex streptolysin-O, would allow rapid, *in situ* permeabilisation of cells without disrupting cell compartmentalisation and crucially without liberating intracellular stores of proteases.

The use of digitonin to achieve this goal was tested experimentally and within 2 mins, following permeabilisation with digitonin, cytosolic proteins such as SHIP2, TAPP-1, PKB, and GAPDH amongst others (data not shown), could be detected by immunoblotting the soluble eluate of unstimulated 1321N1 cells. The presence of SHIP2 in the cytosolic extract confirmed that pore size was not prohibitive to elution of proteins ≤150kDa in size. Indeed, later experiments to more comprehensively characterise the protein constituents of this eluate, would result in identification of proteins upwards of 300kDa.

Figure 3.1 shows the results of an experiment using 1321N1 astrocytoma cells, treated as indicated before transferring the culture dishes to ice and permeabilising with digitonin, retaining the eluate. Finally, residual membrane fractions were recovered by TX-100. This allowed crude fractionation into cytosolic and membrane (membrane, membrane bound and residual proteins) fractions. The majority (~90%) of cellular TAPP-1 was isolated in the cytosolic fraction of control cell populations. The residual, apparently membrane bound fraction of TAPP-1 perhaps represented a proportion trapped in either un-permeabilised cells, within internal cellular compartments or bound to the cytoskeleton, as this value was not diminished by prior treatment with the generic PI 3-kinase inhibitor wortmannin (data not shown). This localisation of TAPP-1 was reversed with bpV(phen) treatment, and to a more limited degree with PDGF treatment, with the majority of TAPP-1 bound to cell membranes, an effect which can be, for TAPP-1 at least, maintained for ≥60 mins. The small proportion of TAPP-1 recruited to cell membranes upon PDGF treatment corroborates previous data showing limited accumulation of PtdIns(3,4)P_2 following PDGF treatment in 1321N1 cells [41]. Bearing in mind the phenomena of downstream signal amplification; this noticeable recruitment of TAPP-1 to cell membranes achieved by PDGF treatment may be sufficient to maximally activate a downstream effector whose activity is directly or indirectly regulated by TAPP-1. It may therefore be possible that the supramaximal concentrations of PtdIns(3,4)P_2 achieved by bpV(phen) treatment are not necessarily required to elicit a physiological response.

Figure 3.1 TAPP-1 recruitment to cell membranes.

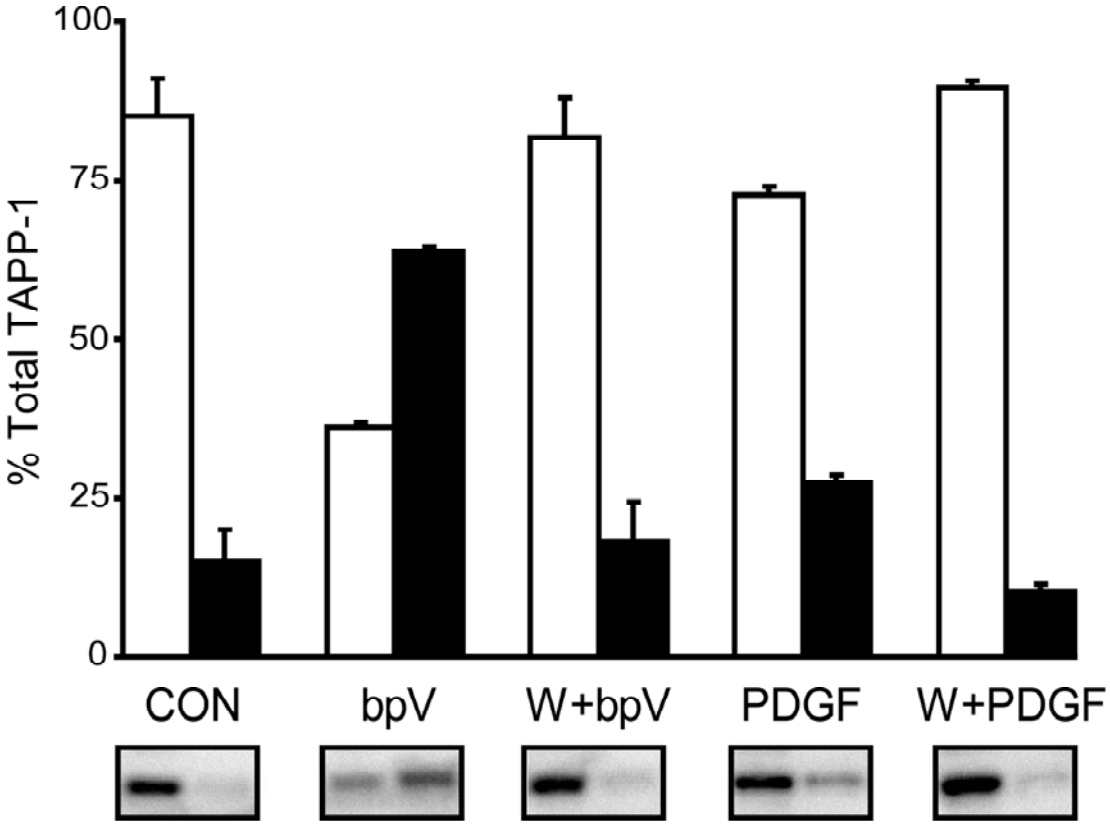

1321N1 cells were pre-treated with vehicle alone (0.1% [v/v] DMSO) or vehicle plus 1μM wortmannin (indicated by W) for 30 mins prior to incubation as control (CON) or stimulated; PDGF (5min, 50ng/ml) or bpV(phen) (30min, 100μM). Cells were then permeabilised by digitonin, yielding a soluble, cytosolic fraction (open bars) and residual membrane fractions (closed bars) and these were immunoblotted for TAPP-1. The data are presented as the proportion of total TAPP-1 proteins associated with each fraction (representative immunoblot shown in lower panels). Results are mean ± the range of duplicates, and represent similar data obtained on three further occasions.

This recruitment of TAPP-1 to cell membranes, seen in Figure 3.1 for bpV(phen) and PDGF treatment, was shown to be PI 3-kinase dependent by its complete inhibition with wortmannin. Although, unusually high concentrations of wortmannin were used in these instances (1μM), this is a necessity in order to overcome the ~2500 fold increase in cellular PtdIns(3,4)P_2 concentrations (Table 3.1) achieved by bpV(phen) treatment (assuming an IC_{50} for class IA PI 3-kinases of 10nM, 1μM should achieve ~99% inhibition). Most importantly, however, these results highlight the potential of this approach to locate TAPP-1 and other similarly recruited 3-phosphoinositide (3-PI) binding proteins to cellular membranes.

3.2.2 The Isomer Selective Elution of TAPP-1.

The above experiments effectively utilised cellular membranes enriched with PtdIns(3,4)P_2 after stimulation with bpV(phen) as an affinity matrix to recruit TAPP-1 and other 3-PI responsive proteins. These cells were then permeabilised with digitonin which released, conservatively, 90% of unbound cytosolic proteins (Figure 3.1). Subsequent, consecutive washes of these permeabilised cells further diminished the unbound cytosolic contaminants with little effect on the TAPP-1 recruited to membranes. The possibility of selectively recovering these recruited proteins with a competing concentration of the water soluble head-group of PtdIns(3,4)P_2, Ins(1,3,4)P_3, was investigated. If successful this would provide a second tier of affinity purification and do so without damaging currently uncompromised cellular membranes.

Figure 3.2A demonstrates that following stimulated recruitment TAPP-1 is retained on PtdIns(3,4)P_2 enriched cellular membranes for prolonged periods despite repeated washing. Thus, after 60 mins and several washes, TAPP-1 and presumably similar PtdIns(3,4)P_2 binding proteins, remained tightly membrane associated. In stark contrast to this, TAPP-1 could be readily eluted from PtdIns(3,4)P_2 enriched cellular membranes by supplementing the washing buffer with Ins(1,3,4)P_3. The concentrations of the eluting Ins(1,3,4)P_3 were selected based on the following estimates of lipid levels within 1321N1 astrocytoma cells. Under resting conditions PtdIns concentrations in these cells have been measured at ~10nmol/mg of total cell protein and PtdIns(4,5)P_2 represents ~5% of this value. Consequently, under conditions of bpV(phen) treatment where approximately half of the cellular PtdIns(4,5)P_2 is fluxed via PtdIns(3,4,5)P_3 (no change) in ~30 mins and accumulates as PtdIns(3,4)P_2, the latter lipid is present at concentrations of ~250pmol/mg [183].

Figure 3.2A and the associated quantitation in Figure 3.2B illustrates the optimisation of this Ins(1,3,4)P_3-dependent elution by the incremental sampling of 60 min washes supplemented with varying, competing concentrations of Ins(1,3,4)P_3. Accordingly, TAPP-1 was recovered from the PtdIns(3,4)P_2 enriched membranes in a time- and Ins(1,3,4)P_3 concentration-dependent manner, corresponding with diminished recovery of TAPP-1 in the associated membrane fractions. The maximal elution of TAPP-1 shown in Figure 3.2, of approximately 50-60% is recovered with 100μM Ins(1,3,4)P_3, representing a molar excess over cellular PtdIns(3,4)P_2 in the region of 100-1000 fold. Similar results, although not shown, were obtained by eluting with short chain (dibutyryl) PtdIns(3,4)P_2.

Figure 3.2 The concentration dependent elution of TAPP-1 with Ins(1,3,4)P_3.

(A) Following treatment with 100μM bpV(phen) for 30mins, 1321N1 cells were permeabilised with digitonin to remove unbound cytosolic proteins. The remaining residual membrane fraction was incubated for 60mins at 4°C in the absence (0μM) or presence of increasing concentrations of Ins(1,3,4)P_3 as indicated. The eluate was sampled at intervals, as indicated, and the resulting samples immunoblotted for TAPP-1 (upper band). **(B)** The quantification of samples blotted in A as a percentage of total TAPP-1 recruited to membranes following bpV(phen) treatment. Closed circles (●) indicate 0μM; open circles (○), 1μM; closed triangles (▲), 10μM and open triangles (Δ) 100μM Ins(1,3,4)P_3. Similar data was obtained on two further occasions.

Figure 3.2A

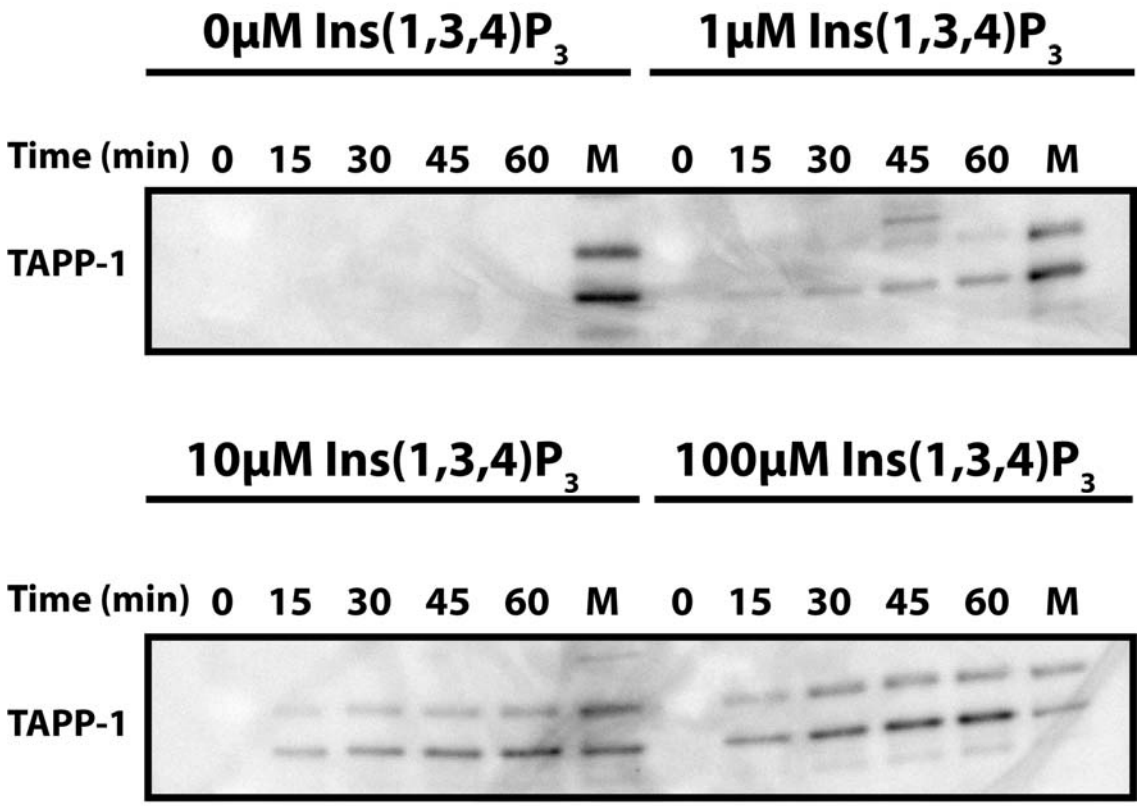
0μM Ins(1,3,4)P3
1μM Ins(1,3,4)P3
Time (min) 0 15 30 45 60 M 0 15 30 45 60 M
TAPP-1
10μM Ins(1,3,4)P3
100μM Ins(1,3,4)P3
Time (min) 0 15 30 45 60 M 0 15 30 45 60 M
TAPP-1

Figure 3.2B

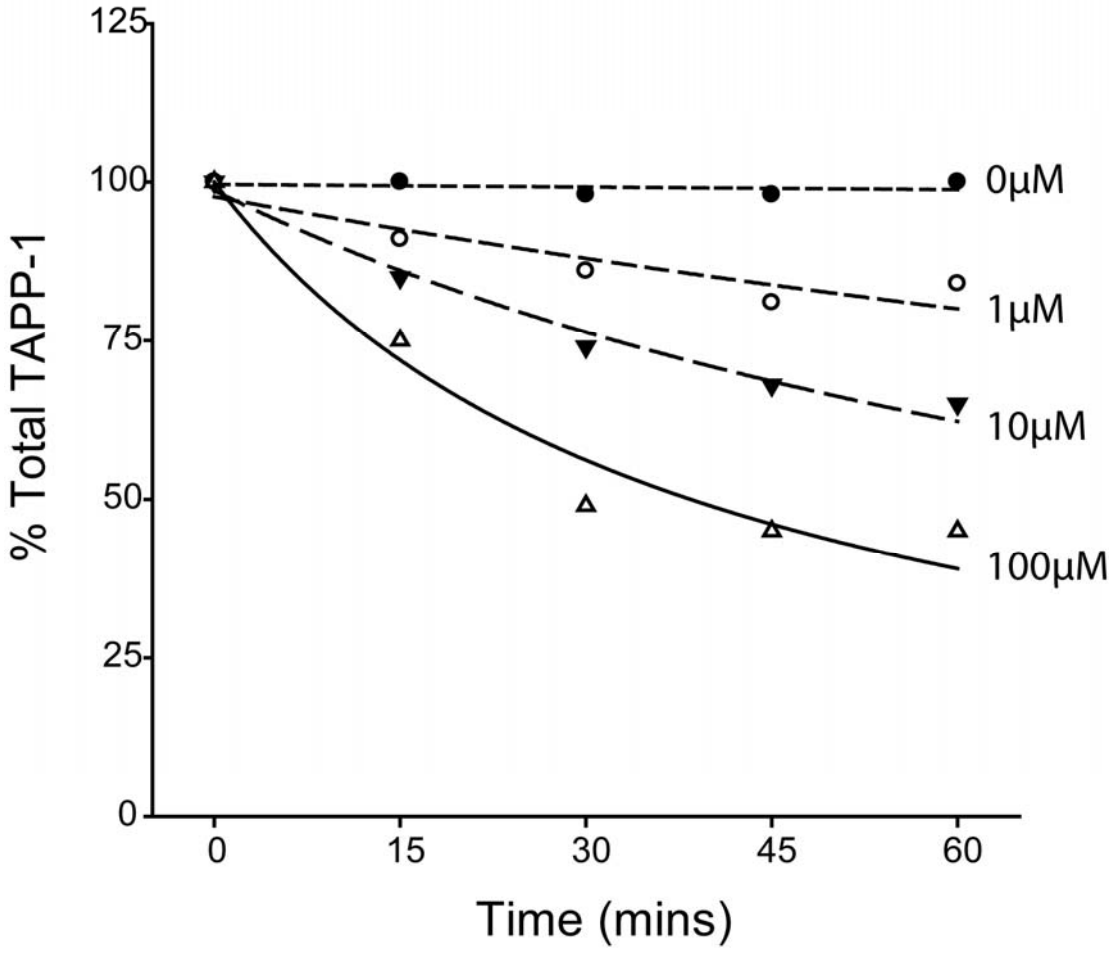
125
100
75
50
25
0
% Total TAPP-1
0
15
30
45
60
Time (mins)
0μM
1μM
10μM
100μM

Figure 3.3 addresses the isomer selectivity of the elution of TAPP-1 from PtdIns(3,4)P_2 enriched membranes. Digitonin permeabilised 1321N1 cells, pre-treated with bpV(phen), were washed with buffer supplemented with identical concentrations of Ins(1,3,4)P_3 or Ins(1,4,5)P_3 (the inositol head-group of PtdIns(4,5)P_2), before analysing the distribution of TAPP-1 as above. As shown previously, washing of PtdIns(3,4)P_2 enriched membranes in buffer alone resulted in little elution of TAPP-1 over 60 mins. However, supplementing the wash buffer with 100μM Ins(1,3,4)P_3 resulted in recovery of 50-60% of total TAPP-1. In contrast, supplementing the wash buffer with 100μM Ins(1,4,5)P_3 resulted in little or no elution of TAPP-1 from cellular membranes - comparable to that seen for buffer alone. These data demonstrate that TAPP-1 can be selectively eluted with Ins(1,3,4)P_3 and suggests that its association with membranes is directed by features compatible with the known selectivity of its C-terminal PH domain.

Having established that TAPP-1 can be recruited to PtdIns(3,4)P_2 enriched membranes and that it can be selectively eluted, the utility of a two step affinity purification to reveal novel candidate proteins was investigated. Figure 3.4 illustrates the protein content associated with samples obtained over the course of such a two step affinity purification. Following bpV(phen) stimulation, 1321N1 cells were permeabilised by consecutive digitonin washes to remove unbound cytosolic proteins. Permeabilised cells were then eluted with wash buffer supplemented with or without Ins(1,3,4)P_3 and finally, residual membrane bound fractions were recovered with TX-100 buffer. A proportion of each of the digitonin washes, the Ins(1,3,4)P_3 eluate and the residual membrane fractions were retained for analysis of protein content, as revealed by the silver staining of SDS-

PAGE gels. Sequential washes with digitonin (D1-D4), as expected, showed a coordinate loss in the protein content with the final wash essentially devoid of protein despite silver stain sensitivity to sub-nano gram amounts [184,185]. Analysis of the protein content from the subsequent elution buffer [+/-100μM $Ins(1,3,4)P_3$] revealed a number of candidate bands which were eluted in a $Ins(1,3,4)P_3$ dependent manner from membranes enriched in $PtdIns(3,4)P_2$. Examples of these enriched candidate bands are highlighted within Figure 3.4 as bands A-G.

Following isolation of candidate bands which were selectively eluted in a fashion similar to TAPP-1, such as those labelled A-G in Figure 3.4, attempts to determine their identities were made by mass spectrometry (MS). Identification was, however, confounded by two factors. Firstly, the dilute (low protein) nature of the $Ins(1,3,4)P_3$ eluate, regardless of the level of enrichment of candidate bands, made processing of sufficient quantities for MS identities problematic. Secondly, the inconsistent nature of observed bands coupled to the variable pattern of background proteins folied attempts to pool multiple gel bands from repeated experiments. However, the application of this two step affinity approach clearly provides a means by which numerous candidate $PtdIns(3,4)P_2$ interacting proteins can be enriched and isolated within a fraction of considerably less complexity than cytosolic extracts.

Figure 3.3 The isomer selective $InsP_3$ elution of TAPP-1 from membranes.

(A) Following TAPP-1 recruitment to membranes with bpV(phen) (100μM, 30mins) treatment and subsequent permeabilisation/washing by digitonin, the residual membrane bound fraction was eluted for 60min at 4°C in the absence (NONE) or presence of 100μM InsP3 (either Ins(1,3,4)P_3 or Ins(1,4,5)P_3). The resulting eluate (C) and the recovered membrane fraction (M) was then immunoblotted for TAPP-1 protein. **(B)** Quantitation of A. The wash step, following cytosolic removal, supplemented with or without IP3 (Ins(1,3,4)P_3 or Ins(1,4,5)P_3 as indicated) is represented by open bars and the residual membrane bound fraction by closed bars. TAPP-1 values are a percentage of total TAPP-1 recruited to membranes following bpV(phen) treatment. The results are representative of data obtained on three further instances with respect to Ins(1,3,4)P_3 and one further instance with respect to Ins(1,4,5)P_3.

Figure 3.3A

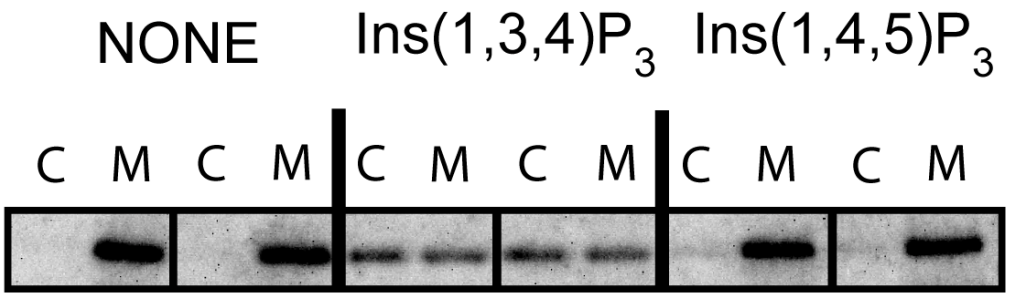

Figure 3.3B

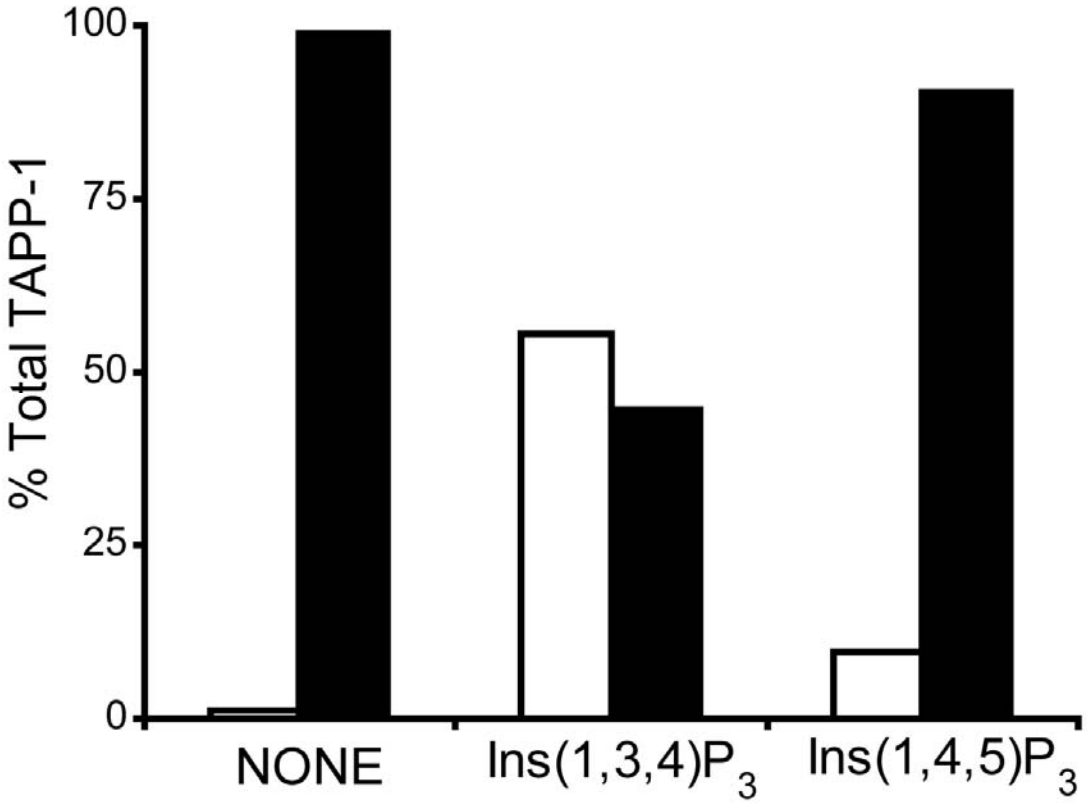

Figure 3.4 The Ins(1,3,4)P_3-dependent elution of multiple membrane recruited proteins.

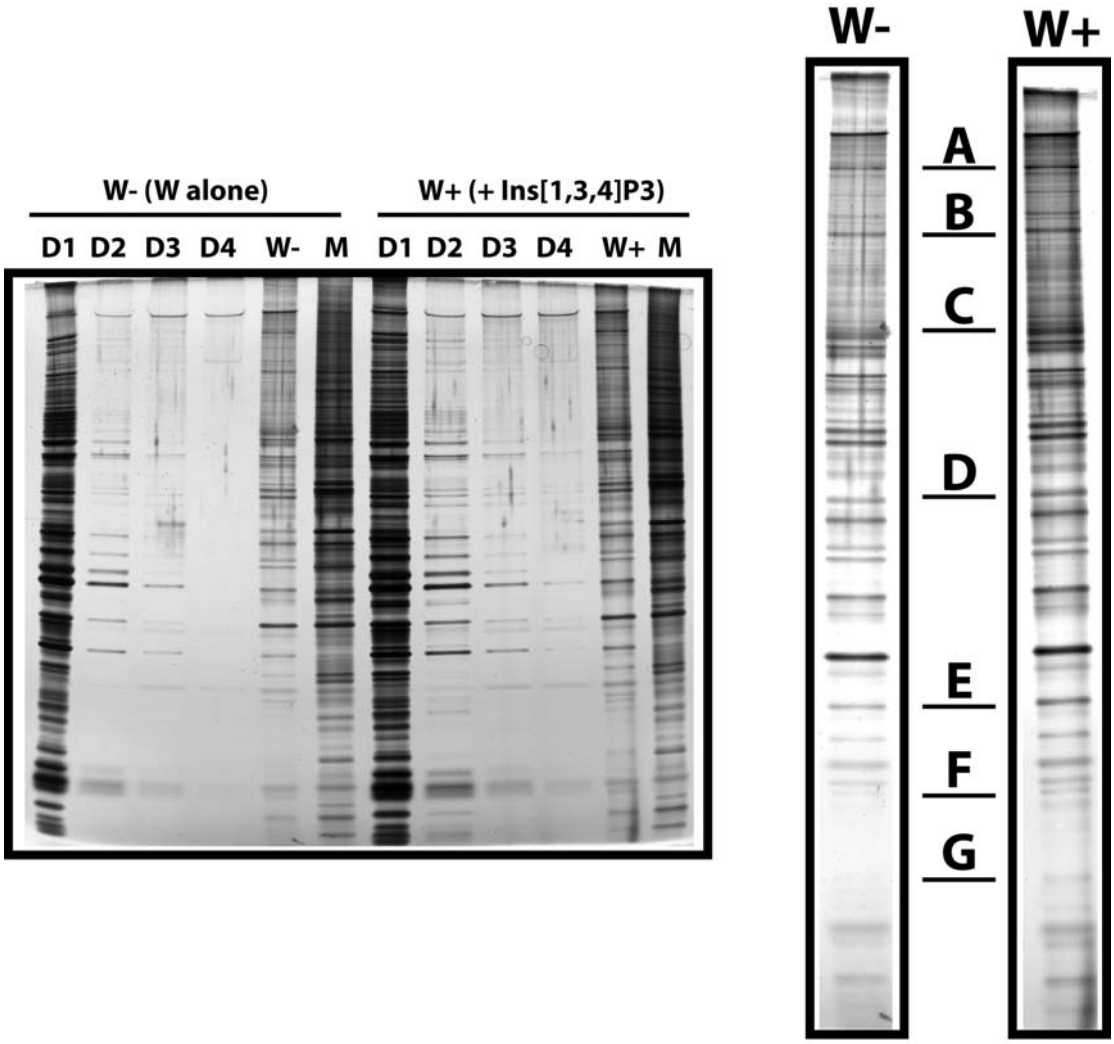

1321N1 astrocytoma cells were stimulated with bpV(phen) and permeabilised with digitonin to allow removal of unbound cytosolic proteins (D1). Consecutive 2min washes in digitonin buffer were also sampled (D2-D4) recording the efficiency of cytosolic elution. Prior to recovery of the membrane fraction (M) by LDS, residual membrane and membrane bound proteins were exposed to a 60min wash with and without 100μM Ins(1,3,4)P_3 (W+ and W- respectively) with right hand panels representing an enlargement of the silver stain gel. Bands labelled A-G are notably enriched or present as a consequence of Ins(1,3,4)P_3 elution. Data representative of at least 8 further experiments.

3.2.3 The Affinity Purification of TAPP-1.

The existing two step affinity purification recruits, to a physiological membrane in a PI 3-kinase dependent manner, proteins capable of binding PtdIns(3,4)P_2. Additionally, the protocol uses an Ins(1,3,4)P_3 elution step, providing the second tier of affinity purification whilst maintaining the integrity of internal organelles. It is evident from Figures 3.1 - 3.4 that this approach is capable of isolating and enriching TAPP-1 and equally, numerous similarly responsive candidate protein bands. Despite this enrichment of candidate proteins, their identification by MS was thwarted by a combination of low protein concentration and carry over of contaminating background proteins (Figure 3.4).

To overcome these issues, the efficacy and utility of a third affinity purification step which made use of an immobilised short chain lipid was tested. Previous studies have often used a similar approach successfully, albeit in isolation [89,98,174,186,187]. The advantages of incorporating this immobilised lipid approach would include a further reduction of non-specific proteins via a third purification step and additionally, allow dilute protein samples to be concentrated into a small volume by affinity association to an immobilised lipid matrix.

The components selected for the lipid matrix were short chain PtdIns(3,4)P_2 with an attached biotin moiety and Neutravidin (an agarose matrix coupled to a streptavidin derivative). The very high affinity interaction between biotin and avidin (K_d ~10^{-15} M) would provide the flexibility for increased incubation times and where necessary extensive washing without loss of the lipid from the matrix.

Neutravidin resin was selected as the matrix in favour of other avidin derivatives due to the reported characteristic of low non-specific binding [188], a crucial factor when considering the mass spectrometry issues encountered previously. The capacity of the Neutravidin for biotinylated-PtdIns(3,4)P_2 was assumed to be ~200nmol/ml resin, on the basis of the manufacturer's provided values of between ≥120nmol biotinylated BSA/ml resin and ≥205nmol biotinylated p-NPE/ml resin (molecular weights of 66.43KDa and 365.4 respectively). In order to determine the optimum conditions for affinity capture of TAPP-1, tests were carried out on TX-100 extracts of digitonin permeabilised cells prior to integration with the existing two tier affinity purification.

Figure 3.5 details the optimisation of TAPP-1 depletion using a Neutravidin biotinylated-PtdIns(3,4)P_2 complex. Following treatment with bpV(phen), 1321N1 cells were permeabilised and washed in digitonin as described above and the membrane bound fraction recovered by TX-100 extraction. Samples were then incubated with Neutravidin coupled to varying amounts of biotinylated-PtdIns(3,4)P_2. The TAPP-1 recovery, as a consequence of SDS elution of the lipid-matrix and in some instances its depletion from the supernatant, was subsequently measured by immunoblotting. Figure 3.5A shows the recovery of TAPP-1 into SDS eluates from the lipid-matrix and its correlated loss from the supernatant of samples following incubation with identical volumes of Neutravidin (50µl) and increasing amounts of biotinylated-PtdIns(3,4)P_2 (where 10nmol, based on the above estimation on the capacity of the Neutravidin, is a saturating amount). Maximal TAPP-1 depletion from the supernatant is shown to be achieved by ~5nmol biotinylated-PtdIns(3,4)P_2 over a pre-determined 60 mins

time period. Thus, the binding capacity of the lipid-matrix is not a factor limiting the efficiency of TAPP-1 recovery.

The small fraction of TAPP-1 recovered by non-lipid coupled Neutravidin beads (~5%) was unaffected by pre-blocking the avidin binding sites with biotin, or the matrix with BSA or lysozyme, prior to lysate depletion and increased proportionally with bead volume (data not shown). This suggests that this minority is trapped within the matrix and is not binding specifically to either the avidin component or the agarose cage. Also tested was the use of alternative buffer conditions and detergents such as cholate, CHAPS and NP-40 with each showing similar TAPP-1 depletion/recovery (data not shown).

Figure 3.5B illustrates the influence of both Neutravidin-lipid mass and concentration on the efficiency of TAPP-1 precipitation. TX-100 extracts from 1321N1 cells, of equal protein content, were generated as described above and incubated with varying volumes of Neutravidin, each saturated with lipid (10-25nmol). A range of lipid concentrations (2μM-50μM) was achieved by diluting samples prior to incubation, with additional TX-100 lysis buffer. TAPP-1 recovery was then measured as before, by immunoblotting the SDS eluates of the lipid-Neuravidin complexes. The data confirmed the observations from Figure 3.5A that maximum TAPP-1 recovery was already attained by 10nmol lipid/unit of lysate. However, Figure 3.5B and the associated quantitation in Figure 3.5C highlights that TAPP-1 recovery is dependent on the relative concentration at which the lipid is presented, with a maximally effective concentration achieved between ~25-50μM biotinylated-PtdIns(3,4)P_2. This concentration dependent but relatively

mass independent characteristic of Neutravidin biotinylated-PtdIns(3,4,)P_2 lysate recovery of TAPP-1 makes the process particularly attractive for scale up.

Figure 3.5 Optimising the affinity purification of TAPP-1 using immobilised lipid.

Panels A and B show the influence of lipid mass and concentration respectively on the recovery of TAPP-1 protein from TX-100 membrane extracts of 1321N1 cells pre-treated with bpV(phen) for 30 mins and permeabilised with digitonin. **(A)** Neutravidin-coupled to increasing amounts of biotinylated-PtdIns(3,4)P_2 (as indicated) was used to deplete cell extracts for 60mins at 4°C (lower panel) with the recovery of TAPP-1 (upper blot), following LDS elution of the Neutravidin biotinylated-PtdIns(3,4)P_2 complex, measured by immunoblots. Samples labelled blank are uncoupled to biotinylated-PtdIns(3,4)P_2. **(B)** Altered amounts of lipid and volumes of lysates were used to generate various concentrations, as indicated, showing the concentration dependent recovery of TAPP-1 to the Neutravidin biotinylated-PtdIns(3,4)P_2 complex. Control (upper panel) represents uncoupled Neutravidin and TAPP-1 control (lower panel) is positive control for TAPP-1 from lysate. A and B are representative of similar data obtained from two further experiments. **(C)** Quantification of the upper panel from B illustrating the biotinylated PtdIns(3,4)P_2 concentration dependent depletion (μM) of cell extracts as a percentage of total TAPP-1 recovered following Triton X-100 extraction of bpV(phen) treated, digitonin permeabilised cells.

Figure 3.5

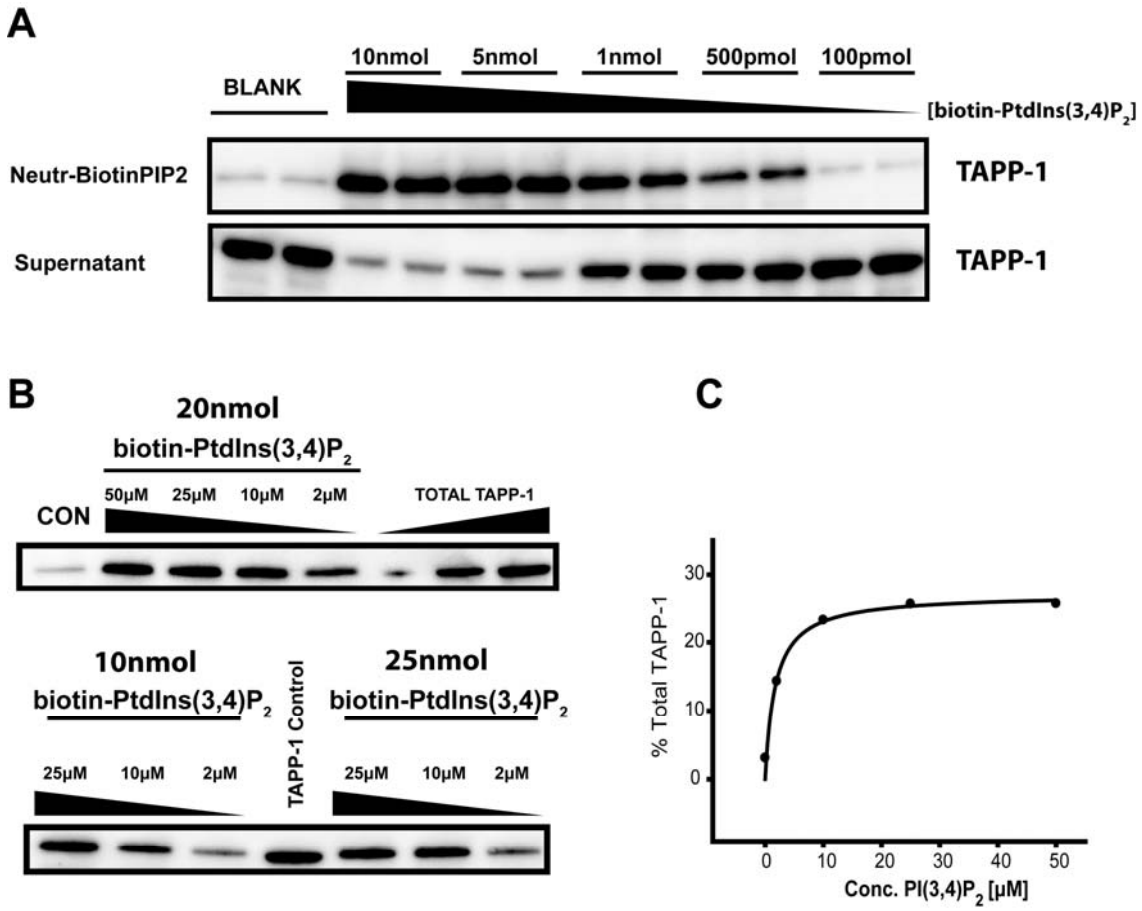
A
10nmol
5nmol
1nmol
500pmol
100pmol
BLANK
[biotin-PtdIns(3,4)P2]
Neutr-BiotinPIP2
TAPP-1
Supernatant
TAPP-1
B
20nmol
biotin-PtdIns(3,4)P2
50μM
25μM
10μM
2μM
TOTAL TAPP-1
CON
10nmol
biotin-PtdIns(3,4)P2
25nmol
biotin-PtdIns(3,4)P2
TAPP-1 Control
25μM
10μM
2μM
25μM
10μM
2μM
C
% Total TAPP-1
30
20
10
0
0
10
20
30
40
50
Conc. PI(3,4)P2 [μM]

The utility of this immobilised lipid precipitation step is further demonstrated by Figure 3.6. TX-100 extracts of 1321N1 cells, permeabilised with digitonin and following treatment as indicated were subject to a maximally effective amount and concentration of biotinylated-PtdIns(3,4)P_2 coupled to Neutravidin. The presence of TAPP-1 in the final SDS elution from the lipid matrix, as well as fractions sampled from the extracts both prior to and after depletion, were quantified by immunoblotting. Following PI 3-kinase-dependent membrane recruitment of TAPP-1, ~75% could be depleted from the resulting TX-100 extract by the lipid matrix, a value which could be further enhanced with subsequent, additional depletions (data not shown). Approximately 25% of the total cellular TAPP-1 could then be efficiently recovered by SDS elution of the matrix despite extensive washing to remove background proteins. These data highlight the capacity of this approach to recover TAPP-1 and, potentially to recover similarly responsive proteins into an enriched fraction of limited complexity and, in contrast to Ins(1,3,4)P_3 eluates, into a small volume.

Similarly generated affinity precipitated samples were further analysed by silver stained SDS-PAGE for candidate bands enriched in a PI 3-kinase dependent manner. Figure 3.7 shows an example SDS elution from an immobilised lipid depletion of 1321N1 TX-100 extracts, treated as indicated, and analysed by SDS-PAGE. Multiple, wortmannin sensitive bands are immediately apparent following washing and SDS elution of the lipid matrix. Two of the most heavily enriched of these bands, present in duplicate bpV(phen) stimulated samples at 70kDa and 105kDa, are indicated within Figure 3.7. Although this immobilised lipid precipitation is lacking in the initially intended Ins(1,3,4)P_3 selective elution, and

undoubtedly includes contaminating membrane and organelle proteins, the presence of multiple PI 3-kinase-dependently enriched bands suggest that this protocol is sufficient to isolate potentially novel PtdIns(3,4)P_2 or 3-PI interacting partners.

Figure 3.6 The affinity precipitation of TAPP-1.

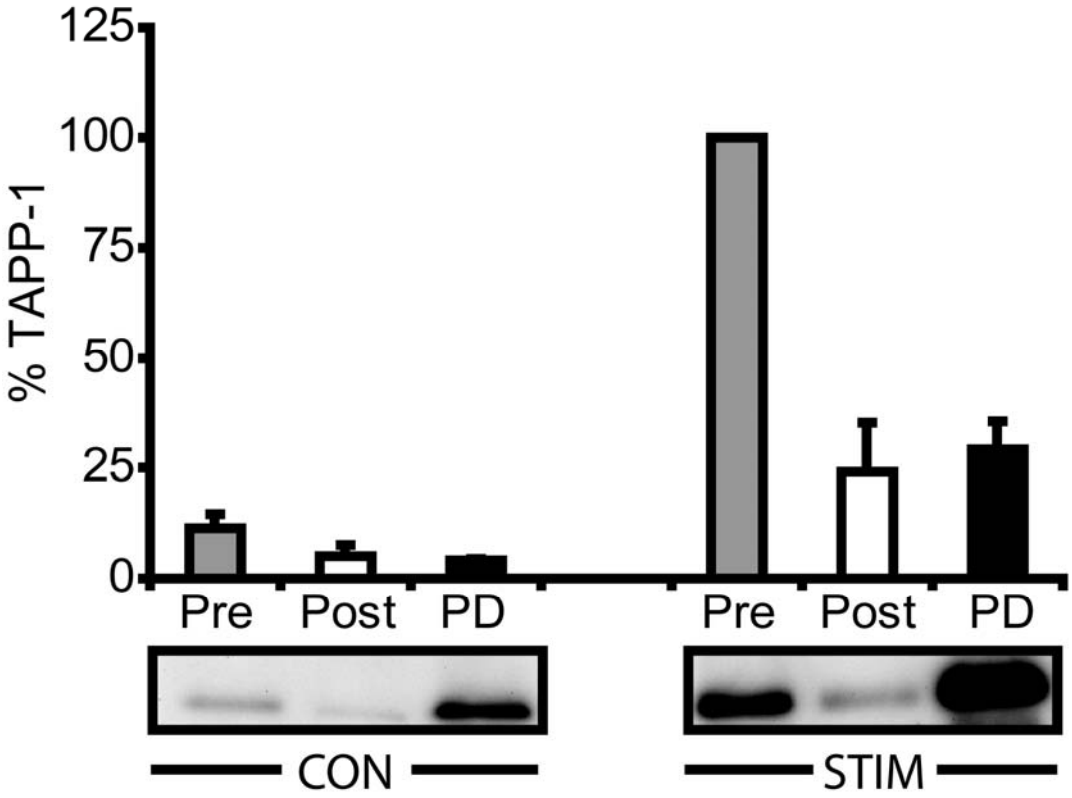

The cellular recruitment and affinity capture approaches, in combination, allow efficient recovery and concentration of TAPP-1. TX-100 soluble fractions generated from control (CON) and bpV(phen) (STIM) (100µM, 30mins) treated, digitonin permeabilised 1321N1 cells were sampled before (Pre) and after (Post) depletion by a maximally effective concentration (25µM) of immobilised PtdIns(3,4)P_2 prior to recovery by LDS elution of the complex (PD). The lower panels are representative immunoblots of TAPP-1 recovery in each fraction. The results indicate the proportion of TAPP-1 recovered, as a percentage of the total TAPP-1 recruited to cell membranes. The lower panels show example blots which contribute to the quantification. Values represent the mean ± S.D of three experiments.

Figure 3.7 Affinity capture with immobilised PtdIns(3,4)P_2 reveals PI 3-kinase responsive proteins.

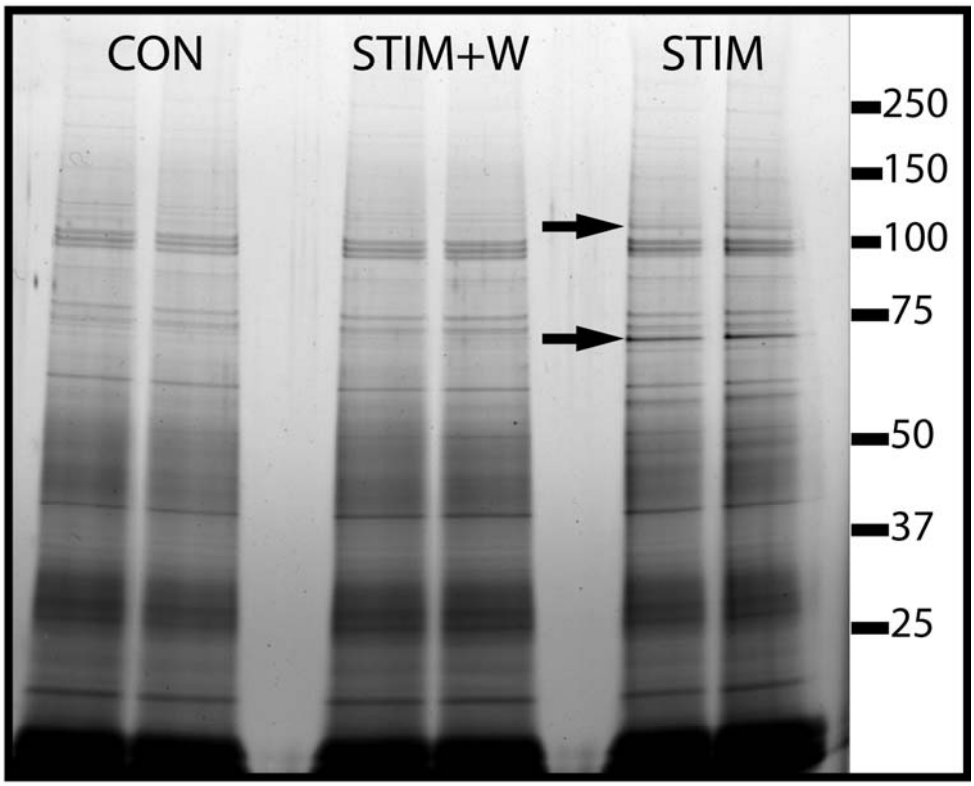

1321N1 astrocytoma cells were pre-treated for 30mins with 0.1% (v/v) DMSO alone or DMSO plus 1μM wortmannin (W) followed by treatment with (STIM) or without (CON) 100μM bpV(phen) for 30 mins. Unbound cytosolic proteins were eluted by digitonin permeabilisation prior to TX-100 solubilisation of residual membrane fraction. Extracts were depleted by Neutravidin biotinylated-PtdIns(3,4)P_2 prior to LDS elution from the complex and analysis by SDS-PAGE and silver staining. The arrows indicate bands (105kDa and 70kDa) recruited in a PI 3-kinase-dependent manner. The results are representative of similar data obtained in several further experiments.

Consistently enriched bands, such as those indicated at 70kDa and 105kDa within Figure 3.7 were processed for identity by MS, the results of which will be addressed in Chapter 4. Further identities, albeit from less enriched bands, proved too complex to confidently identify candidate proteins by MS, similar to the Ins(1,3,4)P_3 eluates previously. However, the capacity of this approach to provide a third affinity purification step and to precipitate large sample volumes should, in conjunction with the advantages offered by the Ins(1,3,4)P_3 elution step, yield samples of sufficient protein concentration and limited background, so as to achieve multiple candidate identities.

3.3 Discussion.

As a consequence of the central role that PtdIns(3,4,5)P_3 plays in normal and aberrant cell signalling, much attention has been focussed on the downstream effectors regulated and recruited by it. In contrast, little attention has been directed towards PtdIns(3,4)P_2, due in part to the lack of an established independent function attributed to this lipid. Recent studies are however beginning to implicate PtdIns(3,4)P_2 with varied roles; from its requirement for complete PKB activation to neurodegeneration. Furthermore, SHIP2, the enzyme predominantly thought responsible for its synthesis, has been implicated in type II diabetes and proposed as a viable therapeutic target.

This study attempts to redress the imbalance of previous wide ranging protein-lipid binding screens by focussing on identifying novel PtdIns(3,4)P_2 effector proteins. This Chapter is concerned with the optimisation of three affinity steps which are intended for integration into a combined three tier approach which benefits from the advantages of multiple affinity purifications.

Previous studies to identify novel lipid interacting proteins have predominantly used immobilised lipid depletions from cell lysates/extracts with a variety of synthetic lipids [89,98,174,186,187], an affinity approach similarly developed for PtdIns(3,4)P_2 in 3.2.3. However, these approaches in isolation present a number of caveats. Foremost is the identification of candidate proteins by their ability to bind non-physiologically presented lipids in a single affinity step, providing little basis on which to distinguish authentic candidates from contaminating proteins. Furthermore, the quantity of background proteins is

undoubtedly increased by the application of a complex, un-purified lysate directly to the matrix. Additionally, studies have often used indiscriminate lysis of whole cells or tissues with mixed cell extracts [89,98,174]. Whilst the latter readily lends itself to large scale sample generation, the increasing need to understand cell type specific PI 3-kinase expression and signalling networks requires the use of homogeneous cell populations [189-192]. Equally, lysis of whole cells with little regard to compartmentalisation can complicate the subsequent fractionation, analysis and interpretation. Moreover, through mass spectrometric analysis, existing studies are often data rich but the affinity and selectivity of resulting candidate binding proteins *in vitro*, or their *in vivo* functional relevance, are rarely tested. In developing the protocols described in this Chapter, for generation of a three-tier affinity purification, this study aims to improve the likelihood of identifying PtdIns(3,4)P_2 specific binding proteins and minimise the proportion of non-specific binding proteins present during analysis.

The foundation of this approach utilises the previously observed effect of the PTP inhibitor, bpV(phen) to switch the output of class IA PI 3-kinases from PtdIns(3,4,5)P_3 to PtdIns(3,4)P_2. This allows a primary step of enrichment based on the recruitment of binding proteins, alongside TAPP-1, to dramatically elevated concentrations of PtdIns(3,4)P_2, presented in the physicochemical context of an authentic membrane bilayer. Membrane features, such as lipid composition, curvature and additional protein components are notoriously difficult to replicate *in vitro* but can be crucial factors in the binding between lipids and proteins. An obvious advantage of utilising such dramatic increases in the cellular concentration of PtdIns(3,4)P_2 is to encourage membrane recruitment and

retention, prior to recovery, of even relatively low affinity PtdIns(3,4)P_2 binding proteins. However, it is possible that this approach will lead to the recruitment of proteins that are not physiologically regulated by PtdIns(3,4)P_2 and/or that have much higher affinity for a similar physiological regulator, such as PtdIns(3,4,5)P_3 [193].

This primary recruitment to the cell membrane of PtdIns(3,4)P_2 interacting proteins was coupled to digitonin permeabilisation which allows selective targeting of the plasma membrane. Such an approach offers distinct advantages over other less discriminating detergents. Firstly, digitonin allows the removal of unbound cytosolic proteins, considerably reducing the complexity of subsequent samples. Secondly, the integrity of internal membranes is maintained, limiting the release of proteases and other enzymes which may destabilise protein-lipid and protein-protein interactions, allowing for retention of binding proteins at the membrane. The utility of this combined novel approach of membrane recruitment and crude cell fractionation was demonstrated by the ability to recruit and retain the majority of TAPP-1 to cell membranes in a PI 3-kinase dependent manner.

The optimisation of a second affinity purification step, utilising Ins(1,3,4)P_3, allowed recovery of TAPP-1 and presumably of other similarly recruited proteins, from membranes enriched in PtdIns(3,4)P_2. For TAPP-1 at least, the selectivity of this approach was demonstrated by the lack of elution from identically treated membranes when incubated with Ins(1,4,5)P_3. Whilst this selectivity is consistent with the reported characteristics of the C-terminal TAPP-1 PH domain, the requirement for Ins(1,3,4)P_3 concentrations giving a molar excess of ~100-1000

fold that of the cellular PtdIns(3,4)P_2 to yield ~60% elution, suggest additional interactions between TAPP-1 and the membrane, perhaps via membrane insertion. Alternatively, this may be due to localised PtdIns(3,4)P_2 concentrations within regions of the cell membrane achieving concentrations similar to that of the competing Ins(1,3,4)P_3. Regardless, any potential limitation in the recovery of TAPP-1 at this stage is significantly outweighed by the enrichment, relative to cytosolic proteins, gained at the previous step. Furthermore, TAPP-1 with its characteristically high affinity PH domain is likely to represent the higher affinity end of the spectrum and additional PtdIns(3,4)P_2 interacting proteins could be expected to be more readily eluted with Ins(1,3,4)P_3. This conclusion is supported by the recovery of numerous bands enriched in an Ins(1,3,4)P_3 dependent manner from bpV(phen) treated and digitonin permeabilised 132N1 cells.

In order to take advantage of the novel aspects of the protocols described above, the optimisation of an immobilised lipid affinity step provided the ability to precipitate protein samples into small volumes. In this Chapter, the approach was optimised as a stand alone technique on TX-100 extracts of bpV(phen) treated, digitonin permeabilised 1321N1 cells. The integration to this, of the Ins(1,3,4)P_3 elution step will be addressed in Chapter 4. The determination that the capacity of the Neutravidin for the biotinylated-PtdIns(3,4)P_2 was not limiting, made the approach particularly attractive for large scale sample preparation. Indeed, assuming that the concentration can be maintained at the maximally effective ~25-50μM value, by limiting sample volume, then even large scale experiments should only require sparing use of biotinylated-PtdIns(3,4)P_2. To put this binding capacity into context, if the 5nmol lipid used in Figure 3.5A is capable, conservatively, of a

lipid-candidate protein interaction ratio of 10:1, then 5nmol PtdIns(3,4)P_2 interacts with 0.5nmol of candidate proteins. If these candidate proteins are then assumed to be represented by a homogeneous population of 75kDa in size, then 0.5nmol relates to 37.5µg of candidate protein. Even if these candidate PtdIns(3,4)P_2 binding proteins were present in lysates in the range 1:10,000-100,000 of the total cellular proteins, 5nmol lipid would still be sufficient to deplete 0.375 -3.75g of cellular protein. This feature will limit the volume of Neutravidin required to bind sufficient lipid for lysate depletion and similarly the volume of elution buffer needed to efficiently elute from the matrix, even for large scale experiments. Thus, the protein concentration of final samples and consequently the protein quantity processed for MS identification can be maximised.

Despite such apparent capacity for binding, TAPP-1 recovery from the lipid-matrix depletions appears to be limited to ~25-30% of total cellular TAPP-1. In contrast, the data indicate that ~75% of TAPP-1 can be depleted by first pass immobilised lipid depletions from lysates. This disparity in the retained/depleted TAPP-1 was shown to be as a consequence of the extensive washing used to minimise the non-specific protein binding to the matrix. However, when coupled to the already enriched Ins(1,3,4)P_3 fraction - considerably reduced in complexity from the lysates presented to the lipid-matrix in this Chapter - such extensive washing could be dispensed with, if necessary, in order to achieve greater recovery of TAPP-1 and other candidate proteins.

This Chapter establishes the first essential phases in isolation of potential PtdIns(3,4)P_2 binding proteins by optimising each step of a three tier affinity

purification. However, each step is clearly capable individually of identifying numerous PI 3-kinase responsive candidates which co-purify with TAPP-1. This is perhaps, most elegantly demonstrated by the isolation of two bands of sufficient purity and protein content to be identifiable by MS, a feature dealt with in Chapter 4.

Chapter 4.

Mass Spectrometric Analysis and the Application of SILAC.

4.1 Introduction.

In the previous Chapter data were presented which demonstrate that separate and combined affinity steps can be used to concentrate TAPP-1 into an enriched fraction. The protocols were optimised individually under the assumption that additional, as yet unknown PtdIns(3,4)P_2 binding proteins would be co-purified. This Chapter develops this concept; firstly, by identifying two such candidate proteins using peptide mass fingerprinting. Secondly, the Chapter describes the integration of the individual enrichment approaches into a superior, three-tier affinity isolation scheme, expected to dramatically reduce non-specific protein carry through into the subsequent MS analysis. Thirdly, to address the inherently non-quantitative nature of MS analysis, the multi-step affinity purification is also coupled to SILAC or Stable Isotope Labelling Assisted Cell culture. The differential isotope labelling of cells achieved by this technique provides a ratio-metric readout to distinguish authentically responsive components from co-purifying background proteins. The results of this powerful combined approach identify a number of existing and candidate lipid binding proteins which represent the most complete set of potential PtdIns(3,4)P_2 binding proteins reported to date.

4.1.1 An Introduction to Mass Spectrometry (MS).

Prior to the application of mass spectrometry to protein identification, the existing technique relied upon was that of sequencing by Edman degradation [194,195]. This approach requires sequential chemical removal and identification by chromatography of individual amino acids starting from the amino terminus. The limitations of this approach include the extended time frame necessary to complete a sequencing project and the development of secondary metabolites

which interfere with and limit reactions to sequences of approximately 50 amino acids in length. Furthermore, the procedure fails entirely if the protein is acetylated or otherwise modified at its amino terminus. Mass spectrometry became widely applicable to protein identification upon the introduction of suitable means to ionize peptides [196-199]. This, coupled to the availability of sequence (and recently whole genome) databases, meant that for the first time samples did not need to be purified to homogeneity for identification [200-202]. Moreover, ionization allowed fragmentation and subsequent identification in seconds as opposed to hours and days for the Edman degradation technique. Lastly, mass fingerprinting techniques are capable of identities despite protein modifications.

Mass spectrometers achieve identification of peptides by accurate measurement of mass to charge ratios (m/z) derived from the ionised sample. The measurement of m/z requires three basic components within a mass spectrometer; the ion source, a mass analyser and a detector [203,204]. Beyond these three components the growing list of variations, additions and resulting permutations can make MS platforms considerably more complex. Ion sources operate via two common methods of ionisation; presenting samples in the gas phase, either by sublimation of a crystalline matrix using laser pulses or rapid evaporation from a liquid sample. These are known as MALDI (matrix-assisted laser desorption/ionization) and ESI (electrospray ionization), respectively [197,198]. The detector component simply consists of a metal plate(s) which records the charge induced or current produced when positive ions pass by or are neutralised upon contact with a surface [205,206].

The mass analysers available all share a common function, to isolate the peptides on the basis of their m/z value. Typically peptide ions are isolated by accelerating via charge repulsion, away from the ion source, through a vacuum. The path of each ion is then deflected as a consequence of an electromagnetic field applied across the vacuum. Obviously both factors are affected by the size and charge associated with the ion (m/z value) and the temporal features of the variable electromagnetic field determine those which can reach the detector. The four basic types of mass analyser are; ion trap [207-209], time-of-flight (TOF) [210], Fourier transform ion cyclotron resonance (FTICR) [211,212] and quadrupole (Q) [208,213,214], and are selected on the basis of experimental requirement and cost. Multiples of these within a single instrument (i.e. quadrupole - time of flight [QTOF]) are referred to as tandem mass spectrometers (MS/MS) and they typically have a collision cell between the two analyser components [213,215]. This cell allows collision induced dissociation (CID) where the isolated precursor ion, measured in the first analyser, is sub-fractionated into product ions which are measured in the second analyser [216]. This process contributes considerably to the probability of identification of the precursor ion as well as providing primary sequence data.

Traditional three dimensional ion traps, whilst sensitive, robust and relatively inexpensive have a limited capacity for mass accuracy due to charged ions being stored at a point-like centre of the trap [203]. The increased charge density associated with this centre then distorts their, and those of subsequent ions, localisation. The development of “two dimensional” or linear ion traps considerably increased the capacity for ion storage and consequently increased

resolution and mass accuracy [207,209]. Furthermore, coupling such an ion trap in-line with an orbitrap analyser, developed by Alexander Makarov, further improves resolution, sensitivity and accuracy [217,218]. The orbitrap design consists of a barrel shaped trap with an inner spindle offering considerably more potential for ion distribution. High mass accuracy is intrinsic to an orbitrap due to the capacity for ions of identical m/z ratios to be isolated by synchronous rotation around the central spindle (Figure 4.1). Furthermore, these orbiting rings of m/z values have an axial motion along the central spindle, the oscillation frequencies of which are inversely proportional to the square root of their m/z ratios [217].

The development of the commercially available orbitrap platform was completed with the additional front end application of a C-trap (essentially a "curved" linear ion trap) to the existing design (Figure 4.1). The primary function of this was to match the curvature of the orbitrap entrance, squeezing ions into a condensed cloud for efficient injection. An additional benefit however, was to provide a second ion trap for storage prior to injection [219-221]. This C-trap allowed ions of lock mass, otherwise known as background airborne ions, to be injected directly, providing an internal control for real time calibration [220,222]. Furthermore, the not inconsiderable contamination of low yield protein samples by airborne keratins derived from human skin is a particular problem for MS analyses. This can be limited to an extent within an orbitrap by filtering out known identities of lock mass contaminants. The culmination of this novel design of the orbitrap is to achieve accuracy of m/z ratios in the parts per billion range – a significant increase on that previously available [219,222,223].

Figure 4.1 The schematic layout of an LTQ Orbitrap XL.

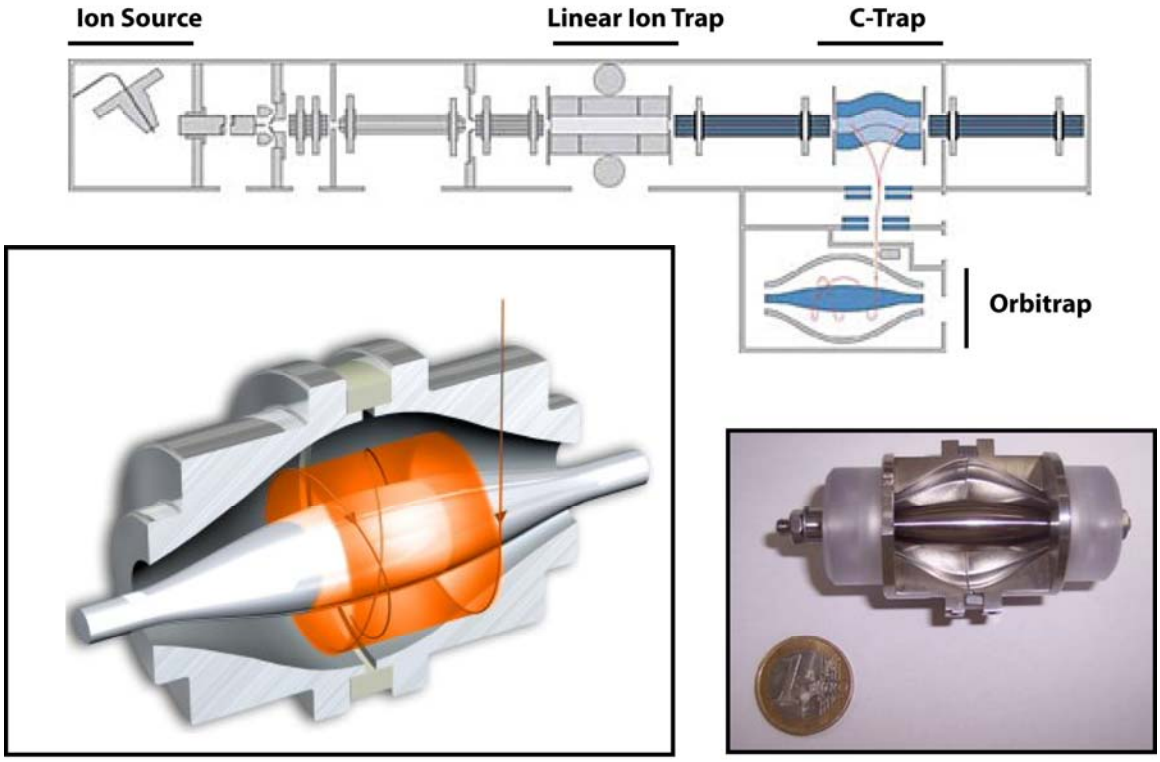

The upper image shows a schematic representation of an LTQ Orbitrap XL including the ion source, linear ion trap, C-trap and Orbitrap. The lower images detail a cross section of the orbitrap and how following injection, ions orbit the central spindle. Images reproduced from [224-226].

4.1.2 The Application of SILAC and the Associated Software for Analysis.

An established shortcoming of traditional MS analyses, despite the unparalleled sensitivity for protein identification, is its non-quantitative nature; a caveat pertinent to this and similar studies. An elegant solution to the requirement for comparative quantitation between two cell populations was provided by SILAC. This approach employs the differential metabolic labelling of control- and test-cell populations, for example with normal (^{12}C) and heavy (^{13}C) isotope substituted amino acids respectively. The specific amino acids labelled with stable isotopes can be selected to suit the intended means of enzymatic digestion for MS analysis. Typically for tryptic digestions, lysine and arginine are used – as trypsin cleaves peptides C-terminal to both - ensuring that each peptide fragment retains at least one, but usually two, substituted amino acids. The isotopes are added to the medium and allowed to be incorporated into cellular proteins via turnover [125,126] and can be assumed to be fully and equally incorporated within the proteome (>99% proteome coverage) after 7 cell doublings [227,228]. There appear to be no adverse effects or altered cellular growth rates as a result of incorporation of one isotope over another. The advantage to metabolically labelling two separate populations of cells for MS analysis is that although functionally the proteins remain identical, their peptide fragments are distinguishable due to a shift in mass [229]. By identifying two identical patterns of product ions or peptides differing only by the shift associated with the increased mass of a heavy isotope, the relative contribution of each can be quantified by the comparison of peak intensities. In this way the notoriously non-quantitative single-sample analysis traditionally achieved by MS can be quantified [203,204,229].

From the perspective of this study a significant advantage of this is that SILAC allows signal and noise to be distinguished as a consequence of the ratio between normal (^{12}C) and heavy (^{13}C) isotope labelled proteins. Furthermore, SILAC has a distinct advantage over MS-compatible chemical labelling techniques such as isobaric tagging which, unlike SILAC, are often incomplete and modify peptides, reducing the compatibility between observed and expected m/z ratios [229].

Traditionally the analysis of complex MS data was highly esoteric and mining of vast data sets by existing methods was laborious. The development of the quantitative software "MaxQuant", made the advantages of SILAC more accessible to non-specialists [223,230,231]. Furthermore, it had the added effect of maximising the data output and accuracy achieved, essentially by taking advantage of greater data resolution, when compared to existing software. This increase in accuracy was possible due to the nature of the analysis, where MaxQuant fits Gaussian distribution peaks to the three most central raw data points for each observed m/z ratio (Figure 4.2). Each of these 2D Gaussian distribution peak determinations are then further assembled on the z plane - the liquid chromatography (LC) column retention times. The generation of such 3D profiles or centroids, allow many m/z values to contribute towards identification and mean values are weighted according to their intensities. The result of this is to smooth outlying data points due to the increased intensity of the most prevalent ions [223,230]. This feature increases the accuracy of observed m/z values, offering greater data resolution and allowing partially overlapping data points to be confidently assigned separate m/z values. Moreover, observed values for ions can also be matched with more confidence to the equivalent peaks derived from

the heavy/light isotope. Such pairing of data points provides another advantage of SILAC labelling, in that the duplicate isotope patterns acts as a potent noise filter for eliminating false positives [223,230]. Further still, in some experimental designs the application of two isotopic variations, for instance (^{12}C), (^{13}C) and (^{14}N), (^{15}N) where heavy isotopes could be limited to specific amino acids such as (^{15}N) to lysine and (^{13}C) to arginine allows for pooling or binning of data sets at the analysis stage. The result of the latter is to speed up processing and increase the number of identities assigned due to the "handle" or confirmed amino acid(s) each peptide possesses prior to mining databases such as MASCOT.

This elegant process of metabolic labelling offered by SILAC and the resulting quantitation achieved by analysis with the MaxQuant software complements our approach to identify novel PtdIns(3,4)P_2 binding proteins. The ability to differently label control and test cell populations allows candidate proteins isolated in a PI 3-kinase dependent manner to be readily distinguishable from the background, non-specific proteins.

Figure 4.2 How MaxQuant achieves increased accuracy and resolution for m/z values (Figure reproduced with permission from [223]).

(A) A two dimensional (2D) peak derived from multiple fragment ion m/z values. Shown is an example of a 2D peak whose intensity drops to zero on both sides. The determined centroid mass (green line) is calculated as a fit of a Gaussian distribution to the three central raw data points.

(B) The resolution of overlapping 2D peaks. Where peaks overlap they are broken up (red lines) at points of local intensity minima of the Gaussian distribution peaks.

(C) Assembling 3D peak hills. The m/z values are assembled in the z-plane (indicated as t); the m/z retention time. Peaks whose centroid m/z positions are sufficiently close are connected.

(D and E) An example 3D peak connecting multiple centroid m/z values. Shown is an example of a 3D peak eluting over 1.5min with colour coded intensity, increasing from yellow to green, in the mass-retention time plane. Forty nine centroids (central red line) are connected to form a 3D peak. Note, weakest intensity is related to apparent mass deviations.

(F) Multiple 3D peaks forming isotope patterns. Eleven 3D peaks can clearly be seen contributing to two isotope patterns although masses of upper and lower patterns are near identical. The resolution of these pairs is possible due to the intensity profiles incorporated by the 3D peaks.

Figure 4.2

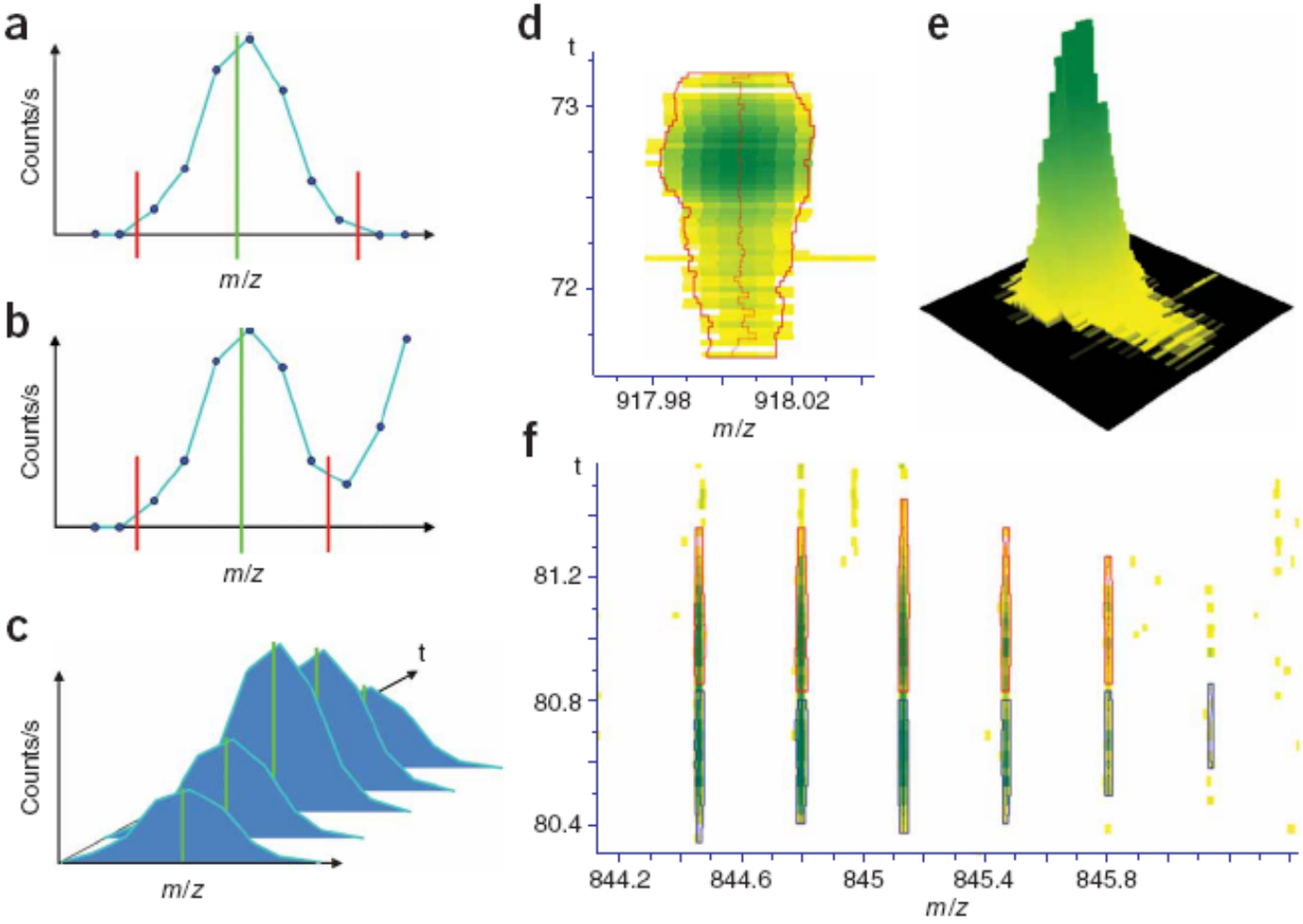
a
Counts/s
m/z
b
Counts/s
m/z
c
Counts/s
t
m/z
d
t
73
72
917.98
918.02
m/z
e
f
t
81.2
80.8
80.4
844.2
844.6
845
845.4
845.8
m/z

4.2 Results.

4.2.1 The Identification of PARIS-1 and SWAP-70 as Candidate 3-PI Binding Proteins.

The results presented in the preceding Chapter established that single step affinity purifications of TAPP-1 could be achieved (Figure 3.1 and 3.7). Although a primary purpose of this Chapter was to improve upon this purification of TAPP-1, it should be re-emphasised that single affinity purification was already sufficient to show several candidate bands visible above background on staining of SDS-PAGE gels (Figure 3.7). Many such bands however, were too low in abundance to enable identification by MS. Whilst attempts to isolate these bands by pooling multiple samples was thwarted by their variable occurrence between experiments or their low ratio of enrichment, two bands at 70kDa and 105kDa could be reproducibly obtained and in sufficient quantity to facilitate identification. Thus, the bands at 70kDa and 105kDa were isolated and processed for identification by MS.

Figure 4.3 shows the prominent protein identities associated with the 105kDa band following analysis with the identification program MASCOT, on data generated by LC MS/MS (ESI in a LTQ Orbitrap XL). Figure 4.3A details the ten most significant protein identities for the 105kDa band. Only six of these matched correctly to proteins present within the human proteome. However, the non-human protein identities were consistent with reagents used for sample isolation and processing such as trypsin and avidin. Of the remaining six potential protein contributors to the 105kDa band, four are keratins, known and common contaminants of mass spectrometry samples due to their ease of ionisation and

abundance in laboratory environments. The remaining two candidates were then assessed on the basis of their molecular weight and known cellular localisation. The 92kDa HNRNPU (heterogeneous nuclear ribo-nuclear protein U) could not be dismissed purely by its improbable presence in a band excised at ~105kDa. However, in combination with its reported nuclear localisation, bearing in mind the primary step of cytosolic fractionation by digitonin, this identity could be discounted as less feasible and/or non-specific. The only remaining credible candidate therefore, was the PH domain containing, 105kDa cytosolic protein, PARIS-1 (prostate antigen recognised and identified by SEREX 1 [232]), identified with a high MASCOT Protein Score of 1035 (published protein identities start some 20-50 fold below this value).

Figure 4.3B lists the 98 peptide queries which were identified and their individual Ion Scores which contributed to the total Protein Score of 1035 for the identification of PARIS-1 (TBC1D2) [232], detailed in Figure 4.3A. The multiplicity of some peptides (additional query numbers listed in blue following peptide sequence), the Ion Score and Expect values indicate the confidence with which PARIS-1 was identified. The Ion Score and Expect values were determined by MASCOT and are based on the probability that an observed match between experimentally derived data and the database records are a random event [233]. The Ion Score is determined by the significance threshold selected for peptide inclusion (i.e. P=0.05 or 0.01) and the number of candidate peptides within the database which fall within the mass tolerance window of the experimentally isolated precursor ion [234]. Essentially however, irrespective of the threshold selected, significance can be thought of the extent to which the protein/ion score

differs from that of background scores. Alternatively, the Expect value can be used as a marker of the confidence of the Ion Score, with, typically, values <0.1 representing a confident match.

Figure 4.3C shows the protein coverage that the 98 successfully matched peptides achieved within PARIS-1. Sequence coverage demonstrates that of the 105kDa PARIS-1, 47% of the protein was identified by one or more peptides with, in places, considerable redundancy in unique peptide identities contributing to the high certainty of identification (multiple query numbers for individual peptides in Figure 4.3B).

Figure 4.3 Mass spectrometric analysis of the protein constituents of the 105kDa band.

(A) The ten most significant identities derived from excised band at 105kDa.

Tryptic digestions of this band were analysed on an LTQ Orbitrap XL and the ten most significant identities as determined by MASCOT with their associated scores (database search parameters as indicated) are shown. Following exclusion of known contaminants PARIS-1 is identified as the constituent protein responsible for the increased intensity of this band in response to PI 3-kinase activation.

(B) Peptide matches to PARIS-1.

The individual peptides matched by MASCOT, their associated observed and expected mass values (Observed and Mr [expt]) and the resulting MASCOT scores are detailed for PARIS-1 (identity N° 5 – TBC1D2). The results are representative of one sample from a duplicate with similar results obtained on one further occasion.

(C) PARIS-1 sequence coverage.

The 47% sequence coverage of PARIS-1 achieved by the peptides identified in (B) are shown in red.

Figure 4.3A

Mascot Search Results

Database : Sprot 20100425 (516603 sequences; 181919312 residues)
Timestamp : 26 Apr 2010 at 13:00:39 GMT
Fixed modifications : Carbamidomethyl (C)
Variable modifications : Dioxidation (M),Oxidation (M),Phospho (ST),Phospho (Y)
Peptide Mass Tolerance : ± 20 ppm
Fragment Mass Tolerance: ± 0.8 Da
Max Missed Cleavages : 2
Number of queries : 3217

1.	sp|P04264|K2C1_HUMAN	**Mass:** 66170	**Score:** 1528	**Queries matched:** 81
	Keratin, type II cytoskeletal 1 OS=Homo sapiens GN=KRT1			
2.	sp|A5A6M6|K2C1_PANTR	**Mass:** 65621	**Score:** 1419	**Queries matched:** 72
	Keratin, type II cytoskeletal 1 OS=Pan troglodytes GN=KRT1			
3.	sp|Q00839|HNRPU_HUMAN	**Mass:** 91269	**Score:** 1310	**Queries matched:** 112
	Heterogeneous nuclear ribonucleoprotein U OS=Homo sapiens GN=HNRNPU			
4.	sp|P35527|K1C9_HUMAN	**Mass:** 62255	**Score:** 1046	**Queries matched:** 51
	Keratin, type I cytoskeletal 9 OS=Homo sapiens GN=KRT9			
5.	sp|Q9BYX2|TBD2A_HUMAN	**Mass:** 104953	**Score:** 1035	**Queries matched:** 98
	TBC1 domain family member 2A OS=Homo sapiens GN=TBC1D2			
6.	sp|P13645|K1C10_HUMAN	**Mass:** 59020	**Score:** 684	**Queries matched:** 29
	Keratin, type I cytoskeletal 10 OS=Homo sapiens GN=KRT10			
7.	sp|P02701|AVID_CHICK	**Mass:** 16872	**Score:** 632	**Queries matched:** 30
	Avidin OS=Gallus gallus GN=AVD			
8.	sp|Q14532|K1H2_HUMAN	**Mass:** 51769	**Score:** 583	**Queries matched:** 40
	Keratin, type I cuticular Ha2 OS=Homo sapiens GN=KRT32			
9.	sp|Q6EIZ0|K1C10_CANFA	**Mass:** 57847	**Score:** 502	**Queries matched:** 21
	Keratin, type I cytoskeletal 10 OS=Canis familiaris GN=KRT10			
10.	sp|P00761|TRYP_PIG	**Mass:** 25078	**Score:** 432	**Queries matched:** 49
	Trypsin OS=Sus scrofa			

Figure 4.3B

5. sp|Q9BYX2|TBD2A_HUMAN **Mass:** 104953 **Score:** 1035 **Queries matched:** 98 **emPAI:** 1.27

TBC1 domain family member 2A OS=Homo sapiens GN=TBC1D2 PE=1 SV=2

Query	Observed	Mr(expt)	Mr(calc)	ppm	Miss	Score	Expect	Rank	Peptide
570	393.727256	785.439960	785.439529	0.55	0	12	30	3	R.QIAELGR.R
666	408.732457	815.450362	815.450089	0.33	0	42	0.038	1	K.IQALESR.S 665
685	412.250269	822.485986	822.486435	-0.55	0	12	11	4	R.WLVHLR.V
856	441.218620	880.422688	880.422501	0.21	0	24	2.3	2	K.CAYLQAR.N
975	461.734685	921.454818	921.455597	-0.85	0	30	0.58	3	R.DFLSQQGK.I 974
1052	494.258299	986.502046	986.503235	-1.21	0	44	0.026	1	K.ALEAAQQEK.R 1051
1076	500.774343	999.534134	999.534882	-0.75	0	31	0.35	1	R.QIELDLNR.T 1075
1087	508.279777	1014.545002	1014.545761	-0.75	1	24	2.3	3	R.ERLEAELR.E
1129	522.799776	1043.585000	1043.586258	-1.21	0	48	0.0079	1	R.VLQDLLSEK.L 1128
1201	542.791203	1083.567854	1083.567245	0.56	0	54	0.0017	1	R.ESLAHTASLR.E 1202
1228	546.308040	1090.601528	1090.602249	-0.66	0	26	1.5	1	K.PSLTISFAQK.A
1297	565.301358	1128.588164	1128.588699	-0.47	1	47	0.01	1	R.RVEALEQER.E 1296 1298
1401	611.303673	1220.592794	1220.592453	0.28	0	74	2.9e-05	1	K.ADAEEGIFEIK.T 1400 1402
1515	664.828554	1327.642556	1327.644852	-1.73	0	53	0.0047	1	R.VWDAFLYEGTK.Y 1514
1615	712.318868	1422.623184	1422.623825	-0.45	0	30	0.77	1	K.HFTCPTSSFPDK.L
1633	722.415713	1442.816874	1442.816666	0.14	0	99	4e-08	1	K.VAALEQQVLMLTK.E 1631 1632
1661	730.412061	1458.809570	1458.811584	-1.38	0	(65)	0.00011	1	K.VAALEQQVLMLTK.E 1662
1670	735.402961	1468.791370	1468.792557	-0.81	0	56	0.0012	1	R.WAALGDLVPSAELK.Q 1671
1720	755.406544	1508.798536	1508.798691	-0.10	0	64	0.00026	1	R.LQNGLEIYQYLR.F 1719 1721
1728	507.244243	1518.710901	1518.713638	-1.80	1	41	0.079	1	K.IEHLKDDMEAYR.T 1729 1730 1731
1912	819.827945	1637.641338	1637.636261	3.10	0	(15)	19	1	R.AVSEGCASEDEVEGEA.- 1914
1991	829.403980	1656.793408	1656.789627	2.28	0	42	0.075	1	R.QNNTFPFFSEGITR.N 1990 1992 1993
2012	832.422523	1662.830494	1662.826004	2.70	0	49	0.012	1	K.HLGTEIQNTMHNIR.G 2009 2010 2011 2013 2014
2112	571.656475	1711.947597	1711.948166	-0.33	1	29	0.43	1	R.SHHLLGLEAVDRPLR.E 2113 2114 2115 2116 2117 2118
2153	859.811160	1717.607768	1717.602585	3.02	0	15	11	1	R.AVSEGCASEDEVEGEA.-
2154	859.811160	1717.607768	1717.602585	3.02	0	(12)	23	5	R.AVSEGCASEDEVEGEA.-
2230	891.886092	1781.757632	1781.752640	2.80	0	9	1.2e+02	9	R.DPQVPPPEEESGDCAR.S 2231
2360	907.454503	1812.894454	1812.890732	2.05	1	36	0.27	1	K.RQNNTFPFFSEGITR.N 2361
2366	909.946349	1817.878146	1817.873032	2.81	0	42	0.073	1	R.TQNCFLNSEIHQVTK.I 2363 2364 2365 2367
2465	937.862008	1873.709464	1873.703690	3.08	1	19	7.7	1	R.RAVSEGCASEDEVEGEA.-
2503	960.457108	1918.899664	1918.894180	2.86	0	108	1.9e-08	1	R.LQEALGDEASECSELLR.Q 2504 2505 2506
2524	646.659905	1936.957887	1936.957764	0.06	0	39	0.15	1	R.VQHLHTPGCYQELLSR.G 2523 2525
2644	693.367556	2077.080840	2077.080322	0.25	2	44	0.033	1	R.ASSAYLAAAEDKDRLELVR.H 2645 2646 2647
2660	1047.539144	2093.063736	2093.057526	2.97	0	61	0.00069	1	R.EQQVQELQQHVQLLMDK.N 2657 2658 2659 2661 2662
2669	704.026053	2109.056331	2109.052444	1.84	0	(27)	1.9	1	R.EQQVQELQQHVQLLMDK.N 2668 2670
2794	1134.031757	2266.048962	2266.042343	2.92	0	72	9.6e-05	1	R.TAQDANPLDSIDLSSAVFDCK.A
2812	763.676523	2288.007741	2288.005386	1.03	0	11	1.1e+02	2	K.QAQGTGHEPPGEDSPQSGEPQR.E
2841	788.058559	2361.153849	2361.146179	3.25	1	29	1.8	1	K.VTQDFTHPPDQSPLRPDAANR.D 2842 2843
2961	878.429243	2632.265901	2632.261612	1.63	2	27	3	1	R.EEQPLASDASTPGREPEDSPKPAPK.P 2960

Figure 4.3C

Mascot Search Results

Match to: **sp|Q9BYX2|TBD2A_HUMAN** Score: **1035**
TBC1 domain family member 2A OS=Homo sapiens GN=TBC1D2 PE=1 SV=2
Nominal mass (M_r): **104953**; Calculated pI value: **6.05**
Taxonomy: Homo sapiens

Fixed modifications: Carbamidomethyl (C)
Variable modifications: Dioxidation (M),Oxidation (M),Phospho (ST),Phospho (Y)
Cleavage by Trypsin/P: cuts C-term side of KR
Sequence Coverage: **47%**

Matched peptides shown in **Bold Red**

```
    1 MEGAGENAPE SSSSAPGSEE SARDPQVPPP EEESGDCARS LEAVPKKLCG
   51 YLSKFGGKGP IRGWKSRWFF YDERKCQLYY SRTAQDANPL DSIDLSSAVF
  101 DCKADAEEGI FEIKTPSRVI TLKAATKQAM LYWLQQLQMK RWEFHNSPPA
  151 PPATPDAALA GNGPVLHLEL GQEEAELEEF LCPVKTPPGL VGVAAALQPF
  201 PALQNISLKH LGTEIQNTMH NIRGNKQAQG TGHEPPGEDS PQSGEPQREE
  251 QPLASDASTP GREPEDSPKP APKPSLTISF AQKAKRQNNT FPFFSEGITR
  301 NRTAQEKVAA LEQQVLMLTK ELKSQKELVK ILHKALEAAQ QEKRASSAYL
  351 AAAEDKDRLE LVRHKVRQIA ELGRRVEALE QERESLAHTA SLREQQVQEL
  401 QQHVQLLMDK NHAKQQVICK LSEKVTQDFT HPPDQSPLRP DAANRDFLSQ
  451 QGKIEHLKDD MEAYRTQNCF LNSEIHQVTK IWRKVAEKEK ALLTKCAYLQ
  501 ARNCQVESKY LAGLRRLQEA LGDEASECSE LLRQLVQEAL QWEAGEASSD
  551 SIELSPISKY DEYGFLTVPD YEVEDLKLLA KIQALESRSH HLLGLEAVDR
  601 PLRERWAALG DLVPSAELKQ LLRAGVPREH RPRVWRWLVH LRVQHLHTPG
  651 CYQELLSRGQ AREHPAARQI ELDLNRTFPN NKHFTCPTSS FPDKLRRVLL
  701 AFSWQNPTIG YCQGLNRLAA IALLVLEEEE SAFWCLVAIV ETIMPADYYC
  751 NTLTASQVDQ RVLQDLLSEK LPRLMAHLGQ HHVDLSLVTF NWFLVVFADS
  801 LISNILLRVW DAFLYEGTKY NEKEILRLQN GLEIYQYLRF FTKTISNSRK
  851 LMNIAFNDMN PFRMKQLRQL RMVHRERLEA ELRELEQLKA EYLERRASRR
  901 RAVSEGCASE DEVEGEA
```

Similarly, Tables 4.1 and 4.2 present the MS data generated from the 70kDa band, where the samples were analysed using the less sensitive MALDI Q4700 TOF/TOF due to the comparative abundance of the 70kDa band over the 105kDa band. Table 4.1 highlights the certainty by which SWAP-70 (switch associated protein-70) was identified as the prominent protein constituent within the 70kDa band. Non-specific background proteins achieved MASCOT protein scores of 20-30 whilst SWAP-70 was the only candidate achieving a score markedly above this. The highly significant MASCOT score of 207 for SWAP-70 (70kDa, Accession number: IPI00307200) is in conjunction with a confidence interval of 100% (confidence interval is similar to the Expect value but presented as percentage, C.I. % = [1-P]x100; where P represents significance i.e. a P value of 0.05 equals C.I. of 95%). As expected for background proteins, all other identities were deemed non-significant, as represented by zero values for C.I. %.

Table 4.2 shows the features of the ~25 contributing peptides successfully matched from the MS/MS peak list to SWAP-70. The amino acid sequence for each of these peptides is listed together with their position within SWAP-70 (start sequence and end sequence position of the peptide) and the accuracy with which the observed peptide m/z ratios were matched to the calculated masses of hypothetical peptides generated by tryptic digestion of SWAP-70. From these, and repeat analysis on separately produced samples, we could unequivocally conclude that SWAP-70 is the prominent protein identity associated with the 70kDa band enriched as a consequence of cellular PI 3-kinase activation in Figure 3.7.

Thus, the identification of two PH domain containing proteins, PARIS-1 and SWAP-70, of which the latter has an established interaction with 3-PIs, demonstrates proof of principle for the described protocol designed for isolating and enriching novel 3-PI interacting proteins via single affinity purifications.

Table 4.1. The ten most significant identities derived from the excised band at 70kDa.

Following tryptic digestion, the sample derived from the band at 70kDa was analysed on an ABI MALDI Q4700 mass spectrometer. The ten most significant protein identities are shown with their accession number, molecular weight (Mw Wt.), protein score (as determined by MASCOT) and the confidence interval – a measure of the probability associated with the identity. SWAP-70 was identified with a confidence interval of 100%. A description of ion score significance values can be found at [234]. Precursor ion scores and their confidence interval are also included. Database search parameters are identical to those detailed in figure 13A. ND = not determined. The results are representative of one sample from a duplicate. Similarly conclusive data were obtained from analysis on LTQ Orbitrap XL on two further occasions.

Table 4.1

Peptide-Peptide summary by spot – MALDI Q4700
Database: IPI Human

Sample ID	Rank	Protein Name	Acc. Number	Mw Wt.	Protein P.I.	Protein Score	C.I. %	Total Ion Score	Total Ion C.I.%
071018_H01	1	Gene_Symbol=SWAP70	IPI00307200	69353.6	5.66	207	100	70	100
071018_H01	2	Gene_Symbol=SWAP70	IPI00514279	17946.2	5.17	87	99.987	39	99.124
071018_H01	3	Gene_Symbol=NIF3L1	IPI00451429	28668.5	8.55	34	0	ND	ND
071018_H01	4	Gene_Symbol=LOC339742	IPI00736604	53915.9	8.43	33	0	27	85.022
071018_H01	5	Gene_Symbol=ZFYVE19	IPI00386862	52610.7	5.57	33	0	ND	ND
071018_H01	6	Gene_Symbol=LOC651987	IPI00747409	9276.6	9.84	31	0	ND	ND
071018_H01	7	Gene_Symbol=FLJ39660	IPI00783185	129535.9	6.58	29	0	14	0
071018_H01	8	Gene_Symbol=SUHW4	IPI00792669	35113.8	8.68	28	0	ND	ND
071018_H01	9	Gene_Symbol=LOC727874	IPI00786905	20868	5.01	28	0	ND	ND
071018_H01	10	Gene_Symbol=ZFYVE19	IPI00386862	52610.7	5.57	26	0	ND	ND

Table 4.2 The identified peptides contributing to the identity of SWAP-70.

Listed are the peptides identified with the 70kDa band which are attributed to SWAP-70. Included for each peptide is the ion score, confidence interval, any modifications, expected masses (Calc. Mass), the observed masses (Observ. Mass) and the deviation between these values (±da). An alternative measure for the agreement between Observ Mass and Calc Mass values, taking into account fragment ion size is shown by ±ppm ([observed – exact]/exact x 1000000). Also detailed are the individual sequences attributed to each peptide and their relative position within SWAP-70.

Table 4.2

Calc. Mass	Obsrv. Mass	± da	± ppm	Start Seq.	End Seq.	Sequence	Ion Score	C.I. %	Modification
876.4057	876.4142	0.0085	10	441	447	QDEETVR			
881.4363	881.4378	0.0015	2	387	393	FSTELER			
903.4894	903.507	0.0176	19	361	368	KLEEAASR			
916.4482	916.4505	0.0023	3	483	489	QELENQR			
972.5109	972.5142	0.0033	3	352	359	QQELEAVR			
1031.5746	1031.5751	0.0005	0	538	546	VAHHEGLIR			
1102.5375	1102.5377	0.0002	0	429	437	LQEALEDER			
1185.6587	1185.6587	0	0	377	386	LQTQVELQAR	17	0	
1185.6587	1185.6587	0	0	377	386	LQTQVELQAR			
1244.6117	1244.6116	-0.0001	0	330	339	QLAEQEELER			
1252.6168	1252.6179	0.0011	1	409	418	SSELEQYLQR	22	54.974	
1252.6168	1252.6179	0.0011	1	409	418	SSELEQYLQR			
1295.6664	1295.6719	0.0055	4	419	428	VRELEDMYLK			
1311.6614	1311.6749	0.0135	10	419	428	VRELEDMYLK			Oxidation (M)[7]
1389.7261	1389.7285	0.0024	2	106	117	NPLLITEEDAFK			
1524.7441	1524.7451	0.001	1	81	92	VQDNFDKIEFNR	31	94.132	
1524.7441	1524.7451	0.001	1	81	92	VQDNFDKIEFNR			
1796.8715	1796.8566	-0.0149	-8	11	26	AIWHAFTALDQDHSGK			
1796.8715	1796.8566	-0.0149	-8	11	26	AIWHAFTALDQDHSGK			
1817.0068	1816.9893	-0.0175	-10	295	309	QEWIQAIHSTIHLLK			
1939.9508	1939.9741	0.0233	12	467	482	WHLEQQQAIQTTEAEK			
1945.1018	1945.0957	-0.0061	-3	294	309	KQEWIQAIHSTIHLLK			
2395.1677	2395.1492	-0.0185	-8	554	574	NPHLITNWGPAAFTEAELEER			
2395.1677	2395.1492	-0.0185	-8	554	574	NPHLITNWGPAAFTEAELEER			
2652.3052	2652.259	-0.0462	-17	554	576	NPHLITNWGPAAFTEAELEEREK			
2837.3813	2837.364	-0.0173	-6	467	489	WHLEQQQAIQTTEAEKQELENQR			

4.2.2 Coupling a Three-Tier Affinity Purification Approach to SILAC Gives an Effective Screen for 3-PI Effector Proteins.

Although a single step affinity purification step had resulted in the successful identification of SWAP-70 and PARIS-1, and indicated clearly that other PI 3-kinase responsive proteins were present in purified extracts, it was evident that to succeed in identifying a wider group, a modified strategy would be required. To this end, the value of merging three affinity purification steps to achieve greater enrichment of candidate proteins and reduce contaminants was assessed. The three tier affinity enrichment scheme comprised; (i) the cellular recruitment of proteins to PtdIns(3,4)P_2 enriched membranes (Table 3.1), (ii) cell permeabilisation by digitonin (Figure 3.1) to allow Ins(1,3,4)P_3 displacement of 3-PI bound candidates (Figures 3.2-3.4) and (iii) immobilised PtdIns(3,4)P_2 affinity purification (Figures 3.5-3.7). The scheme was tested with a pilot, comparative analysis using this multi-step approach prior to attempting integration with SILAC.

Figure 4.4 illustrates the results of this pilot experiment and shows the advantages offered by this combined affinity approach. Digitonin permeabilised 1321N1 cells, pre-treated with bpV(phen) with and without wortmannin (control and test cell populations respectively), were eluted with Ins(1,3,4)P_3 and finally depleted with immobilised PtdIns(3,4)P_2, prior to SDS recovery from the lipid matrix. The subsequent SDS-PAGE staining pattern is presented in Figure 4.4 and the numerous bands enriched in a wortmannin dependent manner between control and test samples are highlighted by the associated densitometry. Figure 4.4 reveals >10 bands enriched in a wortmannin-dependent manner, emphasising the number and range of proteins that can be isolated by this combined approach. Also,

lending further credibility to those enriched bands is the agreement of intensity associated with background non-specific bands, again shown by the densitometry traces. These data extend the limited number of proteins previously isolated using Ins(1,3,4)P_3 elution (Figure 3.4) and similarly for immobilised lipid precipitation alone (Figure 3.7). This pilot, three-tier purification scheme underlined the potential of integrating multiple affinity steps for identification of novel binding proteins and suggested that the application of SILAC would allow a quantitative proteomic analysis of numerous proteins enriched in a PI 3-kinase responsive manner.

Figure 4.4 A three-tier affinity purification approach reveals multiple co-purifying PI 3-kinase responsive proteins.

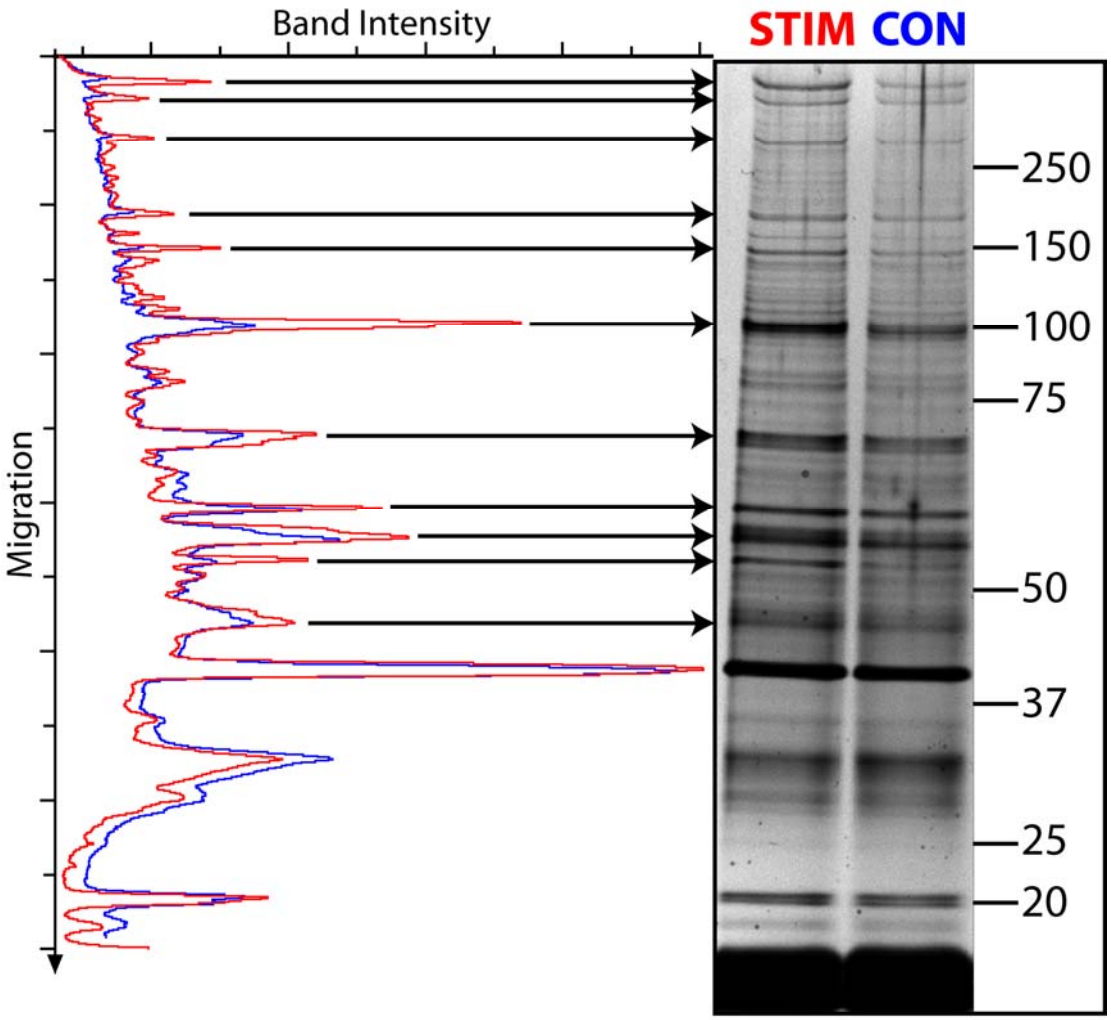

Following pre-treatment with wortmannin (CON – blue) or vehicle alone (STIM – red) 1321N1 cells were treated with 100μM bpV(phen) for 30mins. Cells were then permeabilised by digitonin and residual membrane fractions eluted with 100μM Ins(1,3,4)P_3 prior to concentration of this eluate by anion exchange and affinity chromatography. The samples were analysed by SDS-PAGE and silver stained. Molecular weight markers are indicated on the right hand panel (kDa). The left panel highlights via a densitometric scan the PI 3-kinase responsive elements enriched in STIM (red trace) over CON (blue trace) sample. Similar data were obtained on at least 3 further occasions.

Having confirmed the utility of the approach with a pilot scale experiment (Figure 4.4), the experimental design was coupled to SILAC and scaled up considerably in order to maximise the protein content processed for MS identification. Figure 4.5 details how SILAC was integrated into the existing protocol for a three-step affinity purification. Following the differentiation of control- and test-cell populations by growth in appropriate SILAC medium, and stimulation as indicated, samples were successively affinity purified, as detailed previously.

Furthermore, Figure 4.5 illustrates a feature provided by the application of SILAC – the immediate post-challenge merging of experimental workflows. As the sample of origin can be ascertained at the analysis stage courtesy of the metabolic labelling, there is no requirement to process samples independently. A considerable advantage to pooling control and test samples in this manner is to eliminate variability commonly introduced as a result of independent sample handling. A further advantage; in contrast to the preceding protocol which permeabilised cells *in situ* on tissue culture plates, requiring relatively large volumes of buffer; was that pooling samples presented an opportunity to dramatically reduce this volume of buffer per unit of cellular material processed. This was achieved by scraping all cellular material, regardless of sample origin into a single volume of digitonin permeabilisation buffer and extracting unbound cytosolic proteins by repeated cycles of centrifugation and re-suspension in fresh buffer. Crucially, this reduction in volume also decreased the amount of Ins(1,3,4)P_3 required to achieve an effective concentration for protein elution from the cellular membranes (Figure 3.2). The limited use of Ins(1,3,4)P_3 at this stage

coordinately reduced the amount of biotinylated-PtdIns(3,4)P_2 required to achieve a ratio compatible with the effective affinity precipitation of TAPP-1 at the following step (data not shown). Moreover, a reduction in the biotinylated-PtdIns(3,4)P_2 proportionally lessened the Neutravidin required and hence the volume of SDS needed to efficiently elute from the matrix, thus increasing the relative amount of sample which could be loaded onto a single SDS-PAGE gel for MS analysis.

Figure 4.5 The protocol for incorporation of SILAC into the three-tier affinity purification approach.

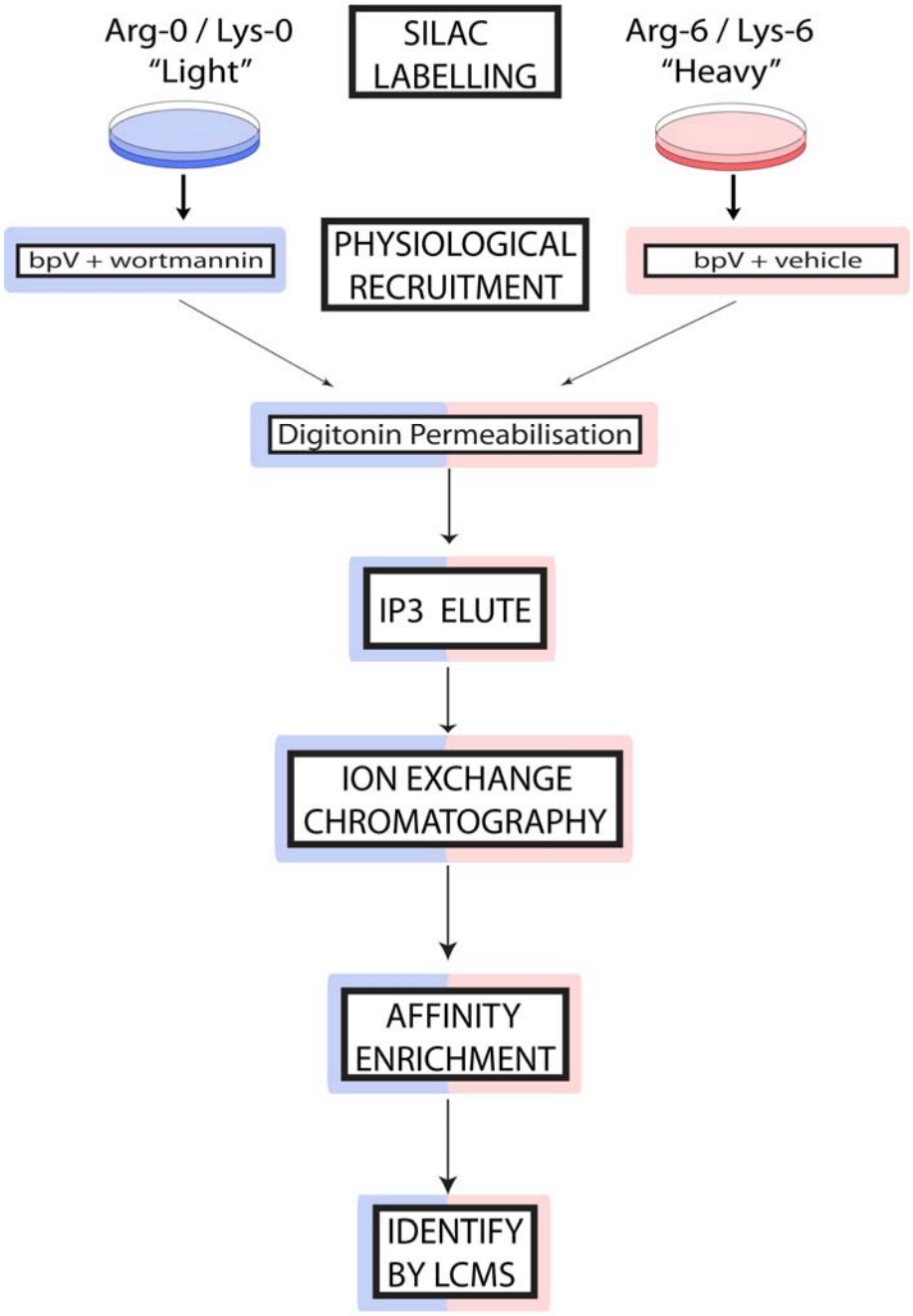

A stepwise process to label control cells (blue scheme, pre-treated with wortmannin) with "light" amino acids and stimulated cells (pink scheme, treated with vehicle) with "heavy" amino acids. Workflows were then combined following bpV(phen) treatment and subsequent purification as indicated.

4.2.3 The Reduction of Sample Complexity Achieved by Ion Exchange Chromatography.

Having established the utility of the combined affinity purification approach and the method in which SILAC would be integrated into the existing scheme, an additional chromatography step was included between the Ins(1,3,4)P_3 elution and the immobilised lipid precipitation (Figure 4.5). The purpose of including anion/cation exchange chromatography (and residual flow through fractions), as indicated, was to reduce sample complexity, reduce carry over into later affinity purifications of potentially competing concentrations of Ins(1,3,4)P_3 and thereby enhance the outcome of SILAC analysis. This method of dividing samples according to their ion exchange characteristics allowed greater depth of MS analysis into the final tryptic digestions without sacrificing overall sample content.

Figure 4.6 demonstrates the purpose of including additional chromatography steps to reduce sample complexity by showing the elution profile of TAPP-1 from one such ion exchange column in comparison to the total protein elution. Extracts from 1321N1 cells, pre-treated with bpV(phen) with and without wortmannin and permeabilised with digitonin were recovered by TX-100 and applied to an anion exchange column. Prior to recovery with increasing concentrations of NaCl, as indicated, columns were washed extensively (a minimum of 10x bed volume). The total protein content of the NaCl eluates is reflected by colloidal coomassie staining of samples on SDS-PAGE gels and the TAPP-1 elution profile was measured by immunoblotting. Figure 4.6 indicates that TAPP-1 was quantitatively recovered into a specific fraction (100-200mM NaCl). This elution profile of TAPP-1 is in contrast to that of the general protein profile and suggests that the

application of an additional chromatography step can result in a final sample significantly enriched in TAPP-1 with respect to background proteins. Although Figure 4.6 shows a limited NaCl elution profile of TAPP-1 from a single ion exchange column, it is intended to demonstrate the principle of reducing sample complexity according to varying ion exchange elution/binding characteristics. The full scale SILAC protocol used higher NaCl concentrations, to recover as wide a range of proteins from the column as possible and yet reduce sample complexity by sub-dividing samples by their retention, or not, on both anion and cation exchange columns. These data suggest that ion exchange chromatography will provide an effective way to sub-divide sample complexity, subsequently providing greater depth of analysis achieved by the parallel processing of sample fractionated through one or more ion exchange steps.

As alluded to previously, an additional benefit of including ion exchange chromatography steps was to limit the amount of the Ins(1,3,4)P_3 carried through from the preceding step into subsequent fractions for lipid depletion (data not shown). Although earlier experiments had suggested that a ten fold excess of Ins(1,3,4)P_3 over PtdIns(3,4)P_2 had only limited effect on TAPP-1 recovery from TX-100 lysates (data not shown), the possibility that any as yet unidentified PtdIns(3,4)P_2 binding protein might be similarly unaffected could not be assumed.

Figure 4.6 The elution profile of TAPP-1 in comparison to bulk, background proteins from an ion exchange column.

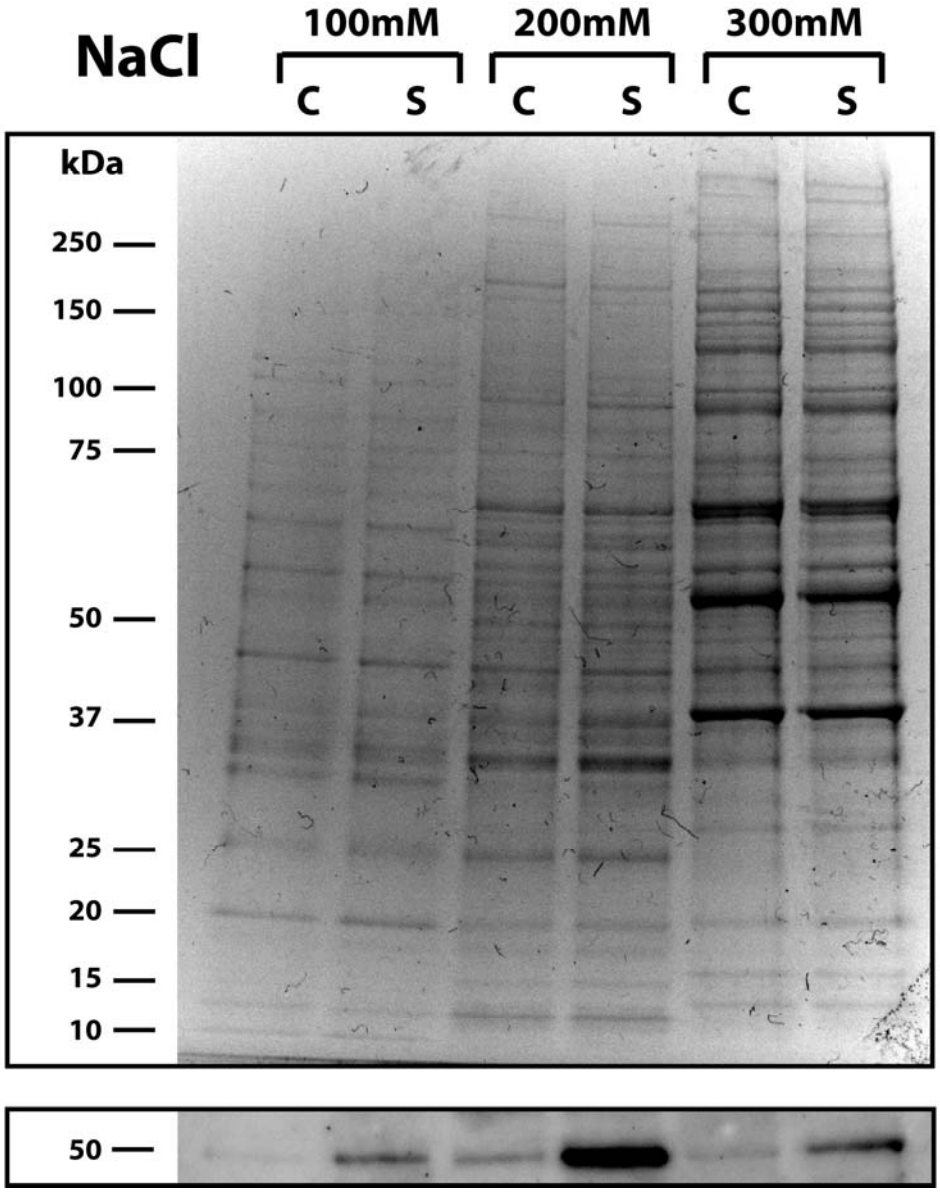

Control (C) and stimulated (S) samples were prepared by pre-treatment with wortmannin or vehicle alone respectively before treatment with 100μM bpV(phen) for 30mins. Cytosol removal by digitonin permeabilisation was followed by TX-100 extraction of the resulting membrane fraction and samples were applied to an anion exchange (Q-sepharose) column. 100mM incremental NaCl washes as indicated were collected and analysed by both colloidal coomassie staining for protein content (upper panel) and immuno-blotting, specifically for TAPP-1 (lower panel). Similar data for protein elution obtained on at least 3 further occasions.

4.2.4 SILAC Analysis I.

Having optimised each step required for a SILAC labelled three-tier affinity purification, sub-fractionated by ion exchange chromatography, as set out in the scheme shown in Figure 4.5, an initial attempt was made to quantitatively identify candidate 3-PI interacting proteins, enriched in a PI 3-kinase dependent manner. The experiment yielding the results illustrated in Figures 4.7 and 4.8 were derived from 24 x 15cm^2 dishes of confluent 1321N1 cells split between the two SILAC conditions (cultured as detailed in Materials and Methods, and treated as indicated in Figure 4.5). Calculations suggested that this should generate 400-800mg of total cell protein for subsequent processing. Following post challenge merging of the control and test samples and the ensuing cytosol elution by repeated suspension/centrifugation in digitonin buffer the residual membrane bound fraction was eluted with 200μM Ins(1,3,4)P_3. This value was chosen in order to maximise the elution of Ins(1,3,4)P_3-sensitive proteins, whilst ensuring that even total carry through into any one ion exchange eluate-fraction would not adversely affect subsequent immobilised lipid depletions. Thus, 200μM Ins(1,3,4)P_3 (500nmol in 2.5ml) did not exceed the maximally determined concentration ratio of 10:1 [Ins(1,3,4)P_3 to biotin-PtdIns(3,4)P_2], previously observed to have a negligible effect on TAPP-1 recovery from cell extracts enriched in the former.

This initial SILAC experiment utilised both anion and cation (henceforth referred to as AQ and CS respectively) exchange chromatography steps, with the Ins(1,3,4)P_3 eluate successively flowed first through AQ and then CS columns. The column flow through and subsequent washes, however, were not retained for experimental processing. Both AQ and CS columns were then eluted with 350mM

NaCl, recovering the fractions for depletion by the Neutravidin biotinlylated-PtdIns(3,4)P_2 complex (50nmol/20μM lipid). This somewhat conservative starting point for NaCl eluate concentration was selected on the basis of the binding characteristics of TAPP-1. Whilst undoubtedly limiting the total protein recovery from the columns, this allowed TAPP-1 to be quantitatively recovered and yet maintained buffer conditions for affinity precipitation of TAPP-1 that were compatible with those optimised previously. Although increasing NaCl concentrations would have recovered a broader spectrum of proteins, it was considered that these conditions might also adversely influence subsequent protein-lipid binding. Thus, since these factors cannot be tested for potential unknown proteins it seemed prudent, to at first, validate the approach with conditions established for TAPP-1.

Figure 4.7 specifically detail the ~650 protein identities established from the MS analysis of the AQ exchange eluate for the SILAC I experiment. The data are presented showing the relative enrichment of heavy to normal (or "light") isotope labelled peptides contributing to a given proteins identity along the y-axis, with randomly assigned identification numbers on the x-axis. A ratio >1 indicates enrichment as a consequence of PI 3-kinase dependent recruitment to cell membranes. Identified proteins of particular interest or those with established lipid binding characteristics are indicated, such as PKB/Akt, TAPP-1 and SWAP-70. For inclusion into the data set represented by Figure 4.7, each protein required identification of at least two peptides. In order to eliminate any potential skew introduced, for example, by unequal control and stimulated cell populations, these

ratios are adjusted so as to achieve a normal distribution, with the median value designated as 1.

Table 4.3 details the features of a limited subset of the most heavily enriched candidate proteins identified within the AQ eluate, illustrated in Figure 4.7. Amongst these are a number of established or proposed lipid binding proteins, including TAPP-1, SWAP-70 and all three isoforms of PKB, highlighted in yellow. For each identity, Table 4.3 shows the relative ratio of enrichment (heavy v.s light peptides), the posterior error probability (P.E.P, the probability of wrong assignment of peptide spectra) and the number of peptides associated with the particular identities. For inclusion into Table 4.3, each protein identity required ≥2 unique peptides. However, complete data sets for all protein identities (~650), regardless of the ratio of enrichment and number of peptides, can be found in Supplementary Table 1. The capability of the SILAC software to distinguish non-specific, background proteins from those genuinely enriched is further provided by the prevalence of keratins, common contaminants in MS analyses, identified with the lowest ratio of heavy to light peptides (Supplementary Table 1, enrichment <0.1-0.01).

Figure 4.7 SILAC I – Anion exchange eluate.

After three tiers of purification following pooling of control and test sample, the anion exchange eluate reveals ~650 proteins identified with at least one unique peptide. These proteins are represented as an arbitrary identification number on the x-axis plotted against the enrichment ratio of heavy:light peptides. A blue line marks the normalised distribution value of 1 and a red line the arbitrary enrichment value of 1.5 – isolating ~5% of the most heavily enriched proteins. Proteins of interest or those with established lipid binding characteristics are indicated. Prominent peaks derived from single peptide identities are, however, ignored.

Figure 4.7

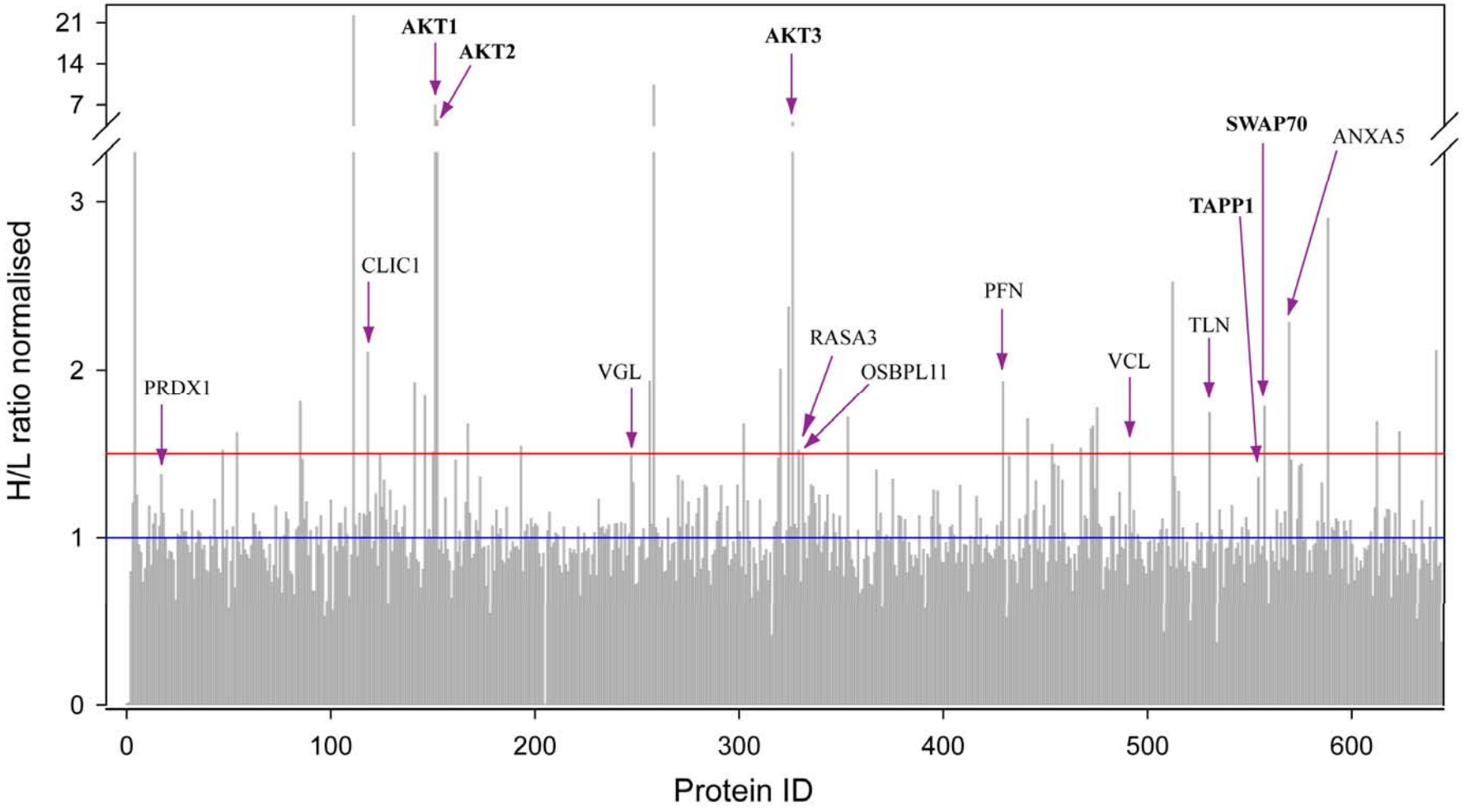
AKT1
AKT2
AKT3
SWAP70
ANXA5
TAPP1
CLIC1
PFN
RASA3
TLN
VGL
OSBPL11
VCL
PRDX1
H/L ratio normalised
Protein ID
21
14
7
3
2
1
0
0
100
200
300
400
500
600

Table 4.3 SILAC I – The candidate list of potential PtdIns(3,4)P_2 binding proteins from the anion exchange fraction.

A detailed list is shown of the most heavily enriched candidate proteins following quantification of MS data from a SILAC labelled, triple purified anion exchange column eluate. Proteins required at least two unique peptides for inclusion. For each protein, shown is the arbitrary I.D. number assigned as indicated in figure 17, the number of peptides identified, the molecular weight, the ratio of enrichment and the P.E.P. value (an indication of the certainty of identity as P.E.P. 0). Those proteins of interest or with established lipid binding characteristics are highlighted in yellow and CLIC1; a target selected for further analysis in Chapter 5, is indicated in red.

Table 4.3

I.D.	Protein Names	Gene Names	Peptides	Mw [kDa]	PEP	Ratio H/L
151	**Protein kinase B alpha; AKT1**	**AKT1**	**6**	**55.7**	**7.58E-10**	**7.0529**
152	**Protein kinase B beta; AKT2**	**AKT2**	**5**	**55.8**	**1.46E-05**	**4.3807**
326	**Protein kinase B gamma; AKT3**	**AKT3**	**4**	**58.7**	**0.0035098**	**4.045**
512	Ran GTPase-activating protein 1	RANGAP1	3	63.5	1.30E-22	2.5223
324	Protein NOXP20	NOXP20	2	60.8	0.0036731	2.3754
569	**Annexin A5**	**ANXA5**	**7**	**35.9**	**4.86E-11**	**2.2843**
651	Pyruvate kinase isozymes M1/M2	PKM2	3	57.9	2.08E-11	2.1978
641	Fructose-bisphosphate aldolase A	ALDOA	2	45.3	0.005534	2.1177
118	**Chloride intracellular channel protein 1**	**CLIC1**	**3**	**26.9**	**0.0030696**	**2.1071**
320	Rab GDP dissociation inhibitor beta	GDI2	2	50.7	2.10E-05	2.007
256	Creatine kinase B-type	CKB	2	42.6	0.19407	1.9374
429	**Profilin-1**	**PFN1**	**3**	**15.1**	**2.31E-15**	**1.9327**
85	40S ribosomal protein S5	RPS5	2	22.9	1.80E-20	1.8127
557	**Switch-associated protein 70**	**SWAP70**	**28**	**69.0**	**5.75E-54**	**1.7819**
475	ribosomal protein S17	RPS17	5	15.9	1.45E-05	1.7746
530	**Talin-1**	**TLN1**	**13**	**271.2**	**2.13E-50**	**1.7456**
441	L-lactate dehydrogenase A chain	LDHA	6	36.7	2.79E-49	1.7079
659	Ferritin heavy chain	FTH1	5	21.2	4.51E-14	1.6971
612	40S ribosomal protein SA	RPSA	21	33.3	2.23E-96	1.6917
302	Protein FAM69A	FAM69A	2	49.0	0.42523	1.6775
167	ABCF1 protein	ABCF1	2	96.1	4.24E-06	1.6773
662	Exportin-5	XPO5	2	136.3	0.0003771	1.669
473	40S ribosomal protein S15a	RPS15A	3	14.8	0.0024912	1.6641
472	40S ribosomal protein S9	RPS9	11	22.6	9.28E-15	1.6485
623	40S ribosomal protein S3a	RPS3A	21	29.9	1.91E-27	1.6317
54	Actin-related protein 2/3 complex subunit 2	ARPC2	2	34.3	0.22373	1.6262
664	Guanine nucleotide-binding protein subunit beta-2-like 1	GNB2L1	15	37.9	1.54E-50	1.5613
453	Glyceraldehyde-3-phosphate dehydrogenase	GAPDH	5	38.8	4.29E-17	1.5578
193	L-lactate dehydrogenase A-like 6B	LDHAL6B	2	41.9	3.25E-36	1.5442
467	Microtubule-associated protein 4	MAP4	2	128.1	3.07E-05	1.5323
329	**Ras GTPase-activating protein 3 (Ins P4-binding protein)**	**RASA3**	**2**	**96.5**	**0.27509**	**1.5189**
47	Glycogen phosphorylase, brain form	PYGB	9	96.7	3.34E-12	1.5185
491	**Vinculin**	**VCL**	**33**	**123.8**	**5.80E-85**	**1.512**
150	Kinesin-1 heavy chain	KIF5B	4	109.7	2.39E-16	1.5106
331	**Oxysterol-binding protein-related protein 11**	**OSBPL11**	**3**	**83.6**	**1.06E-07**	**1.5016**
124	40S ribosomal protein S3	RPS3	26	26.7	8.16E-35	1.4986
247	**Vigilin**	**VGL**	**50**	**141.4**	**9.04E-151**	**1.4867**
432	40S ribosomal protein S4	RPS4X	14	29.6	1.25E-11	1.4858
86	Ribosomal protein S10	RPS10	3	19.9	0.006951	1.4653
161	40S ribosomal protein S7	RPS7	6	22.1	4.29E-09	1.461
570	Carboxylesterase 2	CES2	3	68.9	8.78E-08	1.4601
575	Myosin light polypeptide 6	MYL6	3	18.5	2.97E-10	1.4399
456	L-lactate dehydrogenase B chain	LDHB	7	36.6	1.07E-55	1.4272
574	**Putative annexin A2-like protein**	**ANXA2P2**	**4**	**40.4**	**1.05E-11**	**1.4262**
17	**Peroxiredoxin-1**	**PRDX1**	**4**	**22.1**	**1.68E-06**	**1.3765**
270	Ubiquitin carboxyl-terminal hydrolase 5	USP5	2	95.8	3.16E-11	1.3706
713	Low-density lipoprotein receptor-related protein 1B	LRP1B	2	519.3	0.34928	1.3685
708	A-kinase anchor protein 11	AKAP11	2	210.5	0.065669	1.3662
513	Heat shock 70 kDa protein 4-like protein	HSPA4L	7	94.5	6.89E-55	1.3646
554	**TAPP-1**	**TAPP1**	**2**	**45.6**	**2.57E-06**	**1.3585**

Figure 4.8 reveals the ~275 identities assigned to the CS eluate from the SILAC I experiment. As previously, the data are presented with ratio of isotopic enrichment against arbitrary peptide number. Proteins of interest or with established lipid binding characteristics, identified with more than one unique peptide are indicated. Table 4.4 lists the P.E.P., ratio of enrichment and peptide number associated with only those proteins which achieved a ratio of ≥1.5 and, highlighted in yellow, are those marked in Figure 4.8. Similar data for all of the identified proteins is available in Supplementary Table 3. It is, however, noticeable that significantly more proteins emerged from the AQ column than the CS column. This may be a consequence of the experimental design where the Ins(1,3,4)P_3 eluate passed first through the former and then the later. Alternatively, a precedent does exist where a previous study observed a considerable predominance of potential PtdIns(3,4,5)P_3-responsive proteins in an anion- as opposed to a cation-fraction [98]. Similarly, amongst the data set presented here, established lipid binding proteins are almost exclusively identified within the AQ (anion) exchange fraction.

Figure 4.8 SILAC I – Cation exchange eluate.

The proteins identified in the corresponding cation exchange eluate from the sample derived for Figure 4.7. The bar chart shows the ~250 proteins identified with at least one unique peptide. These proteins are also presented with an arbitrary identification number on the x-axis plotted against the ratio of enrichment of heavy:light peptides. Blue and red lines are as previously described. Proteins of interest or those with established lipid binding characteristics are indicated, whilst those with only a single peptide identity are ignored.

Figure 4.8

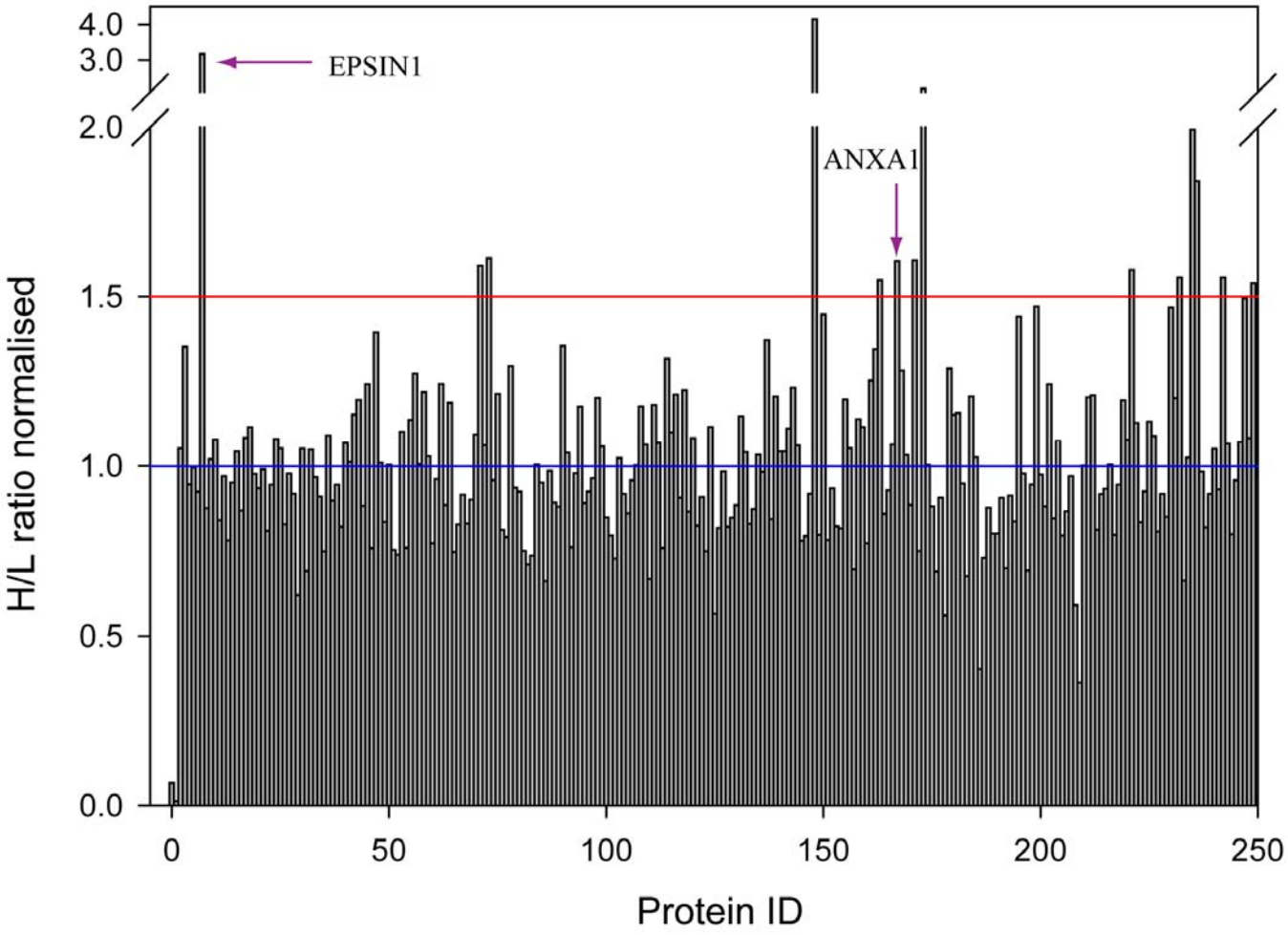
EPSIN1
ANXA1
H/L ratio normalised
Protein ID
4.0
3.0
2.0
1.5
1.0
0.5
0.0
0
50
100
150
200
250

Table 4.4 SILAC I – The candidate list of PtdIns(3,4)P_2 binding proteins from the cation exchange fraction.

I.D.	Protein Names	Gene Names	Peptides	Mw [kDa]	PEP	Ratio H/L
148	Nexilin	NEXN	1	80.657	0.43048	4.1401
7	**Epsin-1**	**EPN1**	**4**	**69.039**	**4.70E-10**	**3.1701**
173	Eukaryotic translation initiation factor 4 gamma 1	EIF4G1	3	175.53	0.0020655	2.1978
235	Fructose-bisphosphate aldolase A	ALDOA	4	45.26	3.54E-19	1.9927
236	Pyruvate kinase isozymes M1/M2ase	PKM2	38	57.936	7.40E-249	1.8424
267	Ubiquitin carboxyl-terminal hydrolase 51	USP51	2	79.755	0.38507	1.613
73	Four and a half LIM domains protein 1	FHL1	2	36.263	8.48E-10	1.6125
171	Ribose-phosphate pyrophosphokinase 2	PRPS2	3	35.054	0.057	1.6067
167	**Annexin A1**	**ANXA1**	**7**	**38.714**	**3.73E-28**	**1.6046**
71	40S ribosomal protein S12	RPS12	2	14.526	3.79E-45	1.5904
221	40S ribosomal protein SA	RPSA	1	33.313	0.067772	1.579
232	Alpha-enolase	ENO1	3	47.168	3.65E-05	1.5558
242	Guanine nucleotide-binding protein subunit beta-2-like 1	GNB2L1	19	37.889	2.48E-148	1.5557
163	L-lactate dehydrogenase A chain	LDHA	1	36.688	0.25196	1.5483
249	Collagen alpha-2(V) chain	COL5A2	2	144.91	0.0031243	1.5398

A detailed list is shown of those proteins identified with a ratio of enrichment greater than 1.5 following quantification of MS data of the SILAC labelled, triple purified cation exchange eluate. Proteins required at least one unique peptide for inclusion. The results are presented as described in the legend to Table 4.3.

Regardless of the chromatographic fractions in which they are found, the identification amongst the list of most heavily enriched proteins of PKB/Akt and of TAPP-1 is of particular importance. Their identification provides convincing proof of principle in the developed protocol to isolate, enrich and allow identification of 3-PI-responsive proteins. Moreover, each isoform of PKB/Akt was identified with multiple unique peptides and marked enrichment ratios ranging from 4-7, whilst the identification of TAPP-1 was more modest with an enrichment of 1.36 and 2 unique peptides. Pertinently, other proteins identified with a high ratio of enrichment within this data set include SWAP-70, vinculin and PRDX-1. Each of these have been reported as potential PtdIns(3,4)P_2 binding proteins either as a consequence of their ability to associate with an immobilised lipid matrix or by their binding in protein-lipid overlay assays [89,98,174]. Also, within Tables 4.3 and 4.4 there are listed a number of further established or putative lipid binding proteins, with the proposed capacity to bind ligands including PtdIns(4,5)P_2, PtdSer and inositol. These include, but are not limited to; profillin, talin, RASA3/GAP1 (IP_4 binding protein), oxysterol binding protein, vigilin, epsin, and several annexins.

4.2.5 SILAC Analysis II.

Despite considerable success in identifying established lipid binding proteins such as PKB, TAPP-1 and SWAP-70, and novel candidates alike, the experimental protocol from SILAC I was revisited for two reasons. Firstly, to expand the repertoire of proteins recovered from the ion exchange columns by increasing the NaCl elution concentration from 350mM to 600mM. And secondly, to address the relatively meagre identification of TAPP-1 peptides, possibly a contributing factor to its relatively limited ratio of enrichment.

Figure 4.9 illustrates the spectrum of proteins identified in the more comprehensive SILAC II experiment. This experiment incorporated 32 x 15cm^2 dishes of confluent 1321N1 cells, resulting in 600mg – 1.2g of total cell protein. Cell extracts were generated as described previously (Figures 4.5 - 4.8), but eluted from residual cell membranes with 100μM Ins(1,3,4)P_3 (500nmol in 5ml). Beyond increasing the input of total cell protein, SILAC II addressed the deficits of SILAC I by increasing the NaCl concentration for column elution (from 350mM to 600mM), with final adjustment to 150mM for efficient recovery by immobilised lipid. This resulted in a more comprehensive array of proteins being recovered from the chromatography columns (data not shown). Furthermore, in addition to the retention of the AQ and CS column eluates for analysis, this experiment also retained the combined flow-through fraction, from both columns for analysis (subsequently referred to as F0 fraction), in contrast to SILAC I. Conceivably however, the most pertinent alteration from SILAC I was to decrease the ratio of Ins(1,3,4)P_3 to biotinylated-PtdIns(3,4)P_2 (100nmol per affinity precipitation at 25μM) used for membrane elution and affinity precipitation, respectively. This

should enhance the recovery of lower affinity PtdIns(3,4)P_2 binding proteins, as well as those which have limited selectivity between the lipid and the soluble head-group, whose precipitation by immobilised lipid may have previously been adversely affected by the carry through of Ins(1,3,4)P_3.

Figures 4.9 illustrates the spectrum of proteins identified in this second, more comprehensive SILAC analysis of PtdIns(3,4)P_2 interacting proteins. Column fractions QA, CS and F0 underwent separate immobilised lipid depletion steps but in the MaxQuant analysis the data sets were combined to maximise the number of protein identities ultimately obtained. The normalised data are presented with the heavy to light ratio of isotope-labelled peptides, identified within candidate proteins, on the y-axis and randomly assigned identification numbers on the x-axis. Figure 4.9 reveals that ~1500 proteins were identified, each with a minimum of two peptides. A ratio of enrichment above the median value of 1.0, as before, reflects PI 3-kinase-dependent membrane recruitment. A subset of some of the most enriched candidate proteins are indicated (arrows A-Ω), selected on the basis of ratio of enrichment and number of peptides identified.

Figure 4.9 SILAC II – Three-tier affinity purification coupled to comprehensive ion exchange chromatography identifies multiple 3-PI-responsive proteins.

After labelling and purification the pooled samples yielded ~1500 protein identities each requiring a minimum of two unique peptides for inclusion at the analysis step. These proteins are presented with arbitrary identification numbers plotted against the corresponding heavy:light isotope ratio. Details of those indicated (A-Ω), with the most heavily enriched ratios or those with defined signalling roles, are provided in table 4.5.

Figure 4.9

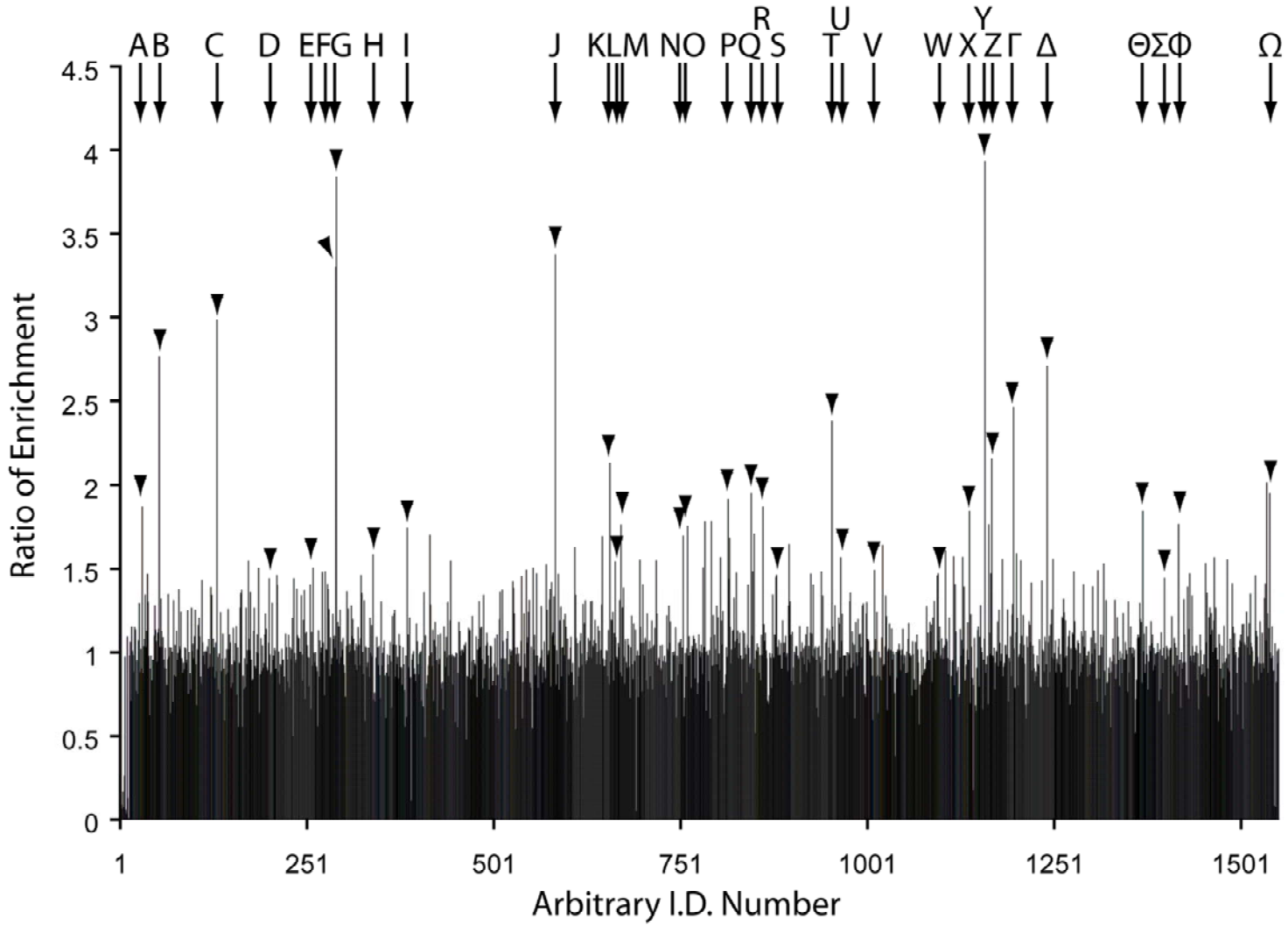
A B C D E F G H I J K L M N O P Q R S T U V W X Y Z Γ Δ Θ Σ Φ Ω
Ratio of Enrichment
0
0.5
1
1.5
2
2.5
3
3.5
4
4.5
1
251
501
751
1001
1251
1501
Arbitrary I.D. Number

The identities of the indicated proteins from Figure 4.9 (arrows A-Ω) are listed in Table 4.5 with additional details relating to each candidate protein. These details include the number of peptides identified for each protein, the P.E.P., and the presence of any established domain structure where this is not inherent in the protein's name. Similar data for all other identified proteins not indicated within Figure 4.9 is available in Supplementary Table 3. Immediately apparent amongst the 32 candidates presented within Table 4.5 is the prominence of those proteins possessing domains with established lipid binding characteristics such as PH, ANTH, ENTH, FYVE, FERM and PX domains, consistent with their purification through multiple lipid/head-group-dependent steps. The identification of TAPP-1 (arrow Y) as the most enriched protein, showing a ratio of enrichment of ~4, underlines the success of this modified, more comprehensive SILAC approach. Furthermore, the identification of all three isoforms of PKB (arrows F, G and K respectively) with significantly enriched ratios (between ~2-4) suggests that any proteins which co-purify with similarly enriched ratios represent plausible candidates for 3-PI-mediated membrane recruitment. Confirmation of the reproducibility of the approach was further provided by the identification; once again of SWAP-70 (arrow z), now identified as a candidate 3-PI interacting protein on three separate occasions. Significantly, the success of manipulating the variables discussed, to increase peptide recovery in the second SILAC experiment is highlighted in Table 4.5, most pertinently by SWAP-70, increasing peptide number by ~7 fold from SILAC I to achieve more than 200 peptides in this SILAC experiment; a sequence coverage of ~80%.

Table 4.5 SILAC II – The candidate list of putative PtdIns(3,4)P_2 and other 3-PI effector proteins.

The proteins described are those indicated in Figure 4.9 (A-Ω) whose ratio of enrichment discriminate them from background proteins. The complete data set can be found within Supplementary Table 3. Table headings are as described previously but in addition, included here are any relevant protein domains within each candidate other than those apparent from the proteins name.

Table 4.5

I.D.	Protein Name	Gene Name	UniProt.	Domains	Mw [kDa]	Peptides	PEP	Ratio H/L
A	Fermitin family homolog 2	FERMT2	A8K6S3	FERM ,PH	78.7	8	5.09E-14	1.8707
B	Epsin-1	EPN1	Q9Y6I3	ENTH	69.0	3	1.37E-27	2.7683
C	Forkhead box protein K2	FOXK2	Q01167	FHA, Fork head	69.1	3	2.58E-34	2.9826
D	Ras GTPase-activating-like protein IQGAP1	IQGAP1	P46940	CH, IQ, WW	189.3	163	0	1.4395
E	Peroxiredoxin-4	PRDX4	Q13162		30.5	16	9.06E-130	1.5059
F	Akt-1;Protein kinase B	AKT1	P31749	PH	55.7	55	2.41E-294	3.304
G	Akt-2;Protein kinase B beta	AKT2	P31751	PH	55.8	36	5.96E-147	3.8407
H	SPARC	SPARC	P09486		34.6	6	9.65E-15	1.5831
I	Protein SOLO	SOLO	Q8TER5	PH	164.6	9	5.15E-46	1.7442
J	Eukaryotic translation initiation factor 4E	EIF4E	P06730		28.8	13	5.84E-29	3.3752
K	Akt-3;Protein kinase B gamma	AKT3	Q9Y243	PH	58.7	25	4.41E-226	2.1323
L	Serpin H1	SERPINH1	P50454		46.4	104	0	1.5438
M	Oxysterol-binding protein-related protein 11	OSBPL11	Q9BXB4	PH	83.6	6	9.71E-45	1.764
N	KDEL motif-containing protein 2	KDELC2	Q7Z4H8		58.6	33	1.47E-251	1.6955
O	Rho GTPase-activating protein 29	ARHGAP29	Q52LW3	C1	142.1	2	1.13E-08	1.756
P	ELKS/RAB6-interacting/CAST family member 1	ERC1	Q8IUD2	FIP	128.1	3	3.03E-09	1.9156
Q	FK506-binding protein 9	FKBP9	O95302	EF hand	63.1	12	3.05E-55	1.9494
R	La-related protein 1	LARP1	Q6PKG0	La	123.5	14	1.01E-21	1.8714
S	PICALM	PICALM	A8K5U9	ANTH	71.7	77	0	1.4611
T	ARAP1 (Centaurin-delta-2)	ARAP1	Q96P48	PH, SAM	162.2	9	1.99E-12	2.3786
U	Annexin A6	ANXA6	P08133		75.9	46	7.83E-197	1.5655
V	Vinculin	VCL	P18206		123.8	63	0	1.4908
W	Talin-1	TLN1	Q9Y490	FERM	269.8	103	0	1.4691
X	FK506-binding protein 10	FKBP10	Q96AY3		64.2	30	3.95E-138	1.8424
Y	TAPP-1	PLEKHA1	Q9HB21	PH	45.6	4	1.09E-16	3.9363
Z	Switch-associated protein 70	SWAP70	Q9UH65	PH	69.0	209	0	2.1576
Γ	Early endosome antigen 1	EEA1	Q15075	FYVE	162.5	14	1.27E-69	2.4651
Δ	Eukaryotic translation initiation factor 4 gamma 1	EIF4G1	Q04637		175.53	50	1.55E-139	2.7079
Θ	Endoplasmic reticulum aminopeptidase 2	ERAP2	Q6P179		110.5	6	2.45E-19	1.8428
Σ	PX domain-containing protein kinase-like protein	PXK	Q7Z7A4	PX	64.9	15	9.49E-86	1.4428
Φ	Protein canopy homolog 3	CNPY3	Q9BT09		30.7	5	1.51E-51	1.7681
Ω	Ankyrin repeat and FYVE domain-containing protein 1	ANKFY1	Q9P2R3	Ankyrin repeat, FYVE	128.5	29	1.80E-139	1.9502

These data therefore represent the most comprehensive list of candidate PtdIns(3,4)P_2 binding proteins identified to date. Furthermore, this approach is the first to include within its data sets so many established lipid binding proteins isolated under the same enrichment conditions. This predominance of known 3-PI interacting proteins lends credibility to the notion that other proteins identified by the screen, without previously recognised lipid binding capability, are genuine candidates for 3-PI mediated recruitment/regulation, either directly or indirectly.

4.3 Discussion.

Whilst many informatics based, mining approaches or affinity chromatography studies have focussed their attention on identifying novel PI binding proteins [89,98,174,186,235], little effort has been directed specifically towards uncovering novel PtdIns(3,4)P_2 effectors. This study aimed to redress this by taking a unique approach to enrich and isolate candidate PtdIns(3,4)P_2 binding proteins. Using the methods described, proteins present at physiologically appropriate concentrations were recruited to authentic lipid bilayers and subsequently recovered by a combination of selective membrane permeabilisation and inositol phosphate effected elution followed by affinity precipitation. This approach alone represented a significant advance from the prior use of single step affinity purification of proteins from indiscriminate cell or tissue lysates [89,174,186,187,235,236]. Furthermore, the coupling of this refined approach to sample preparation to SILAC yielded the most sophisticated screen for PI binding proteins yet attempted.

In common with previous screens, the preliminary attempts to identify novel PtdIns(3,4)P_2 binding proteins with a single affinity purifications, described in Chapter 3, relied on traditional MS analysis. The difficulty encountered in identifying all but the most prominent proteins (SWAP-70 and PARIS-1), highlights a significant shortcoming of existing screens. Accepting that traditional MS approaches are inherently non-quantitative [203,204,229] then, despite complex proteomics and in many cases elegant chemistry, the selection of candidate bands, is essentially dependent on rudimentary visual selection according to differential SDS-PAGE gel staining patterns [237]. This process is

widely open to experimental bias, especially for cases of marginal enrichment and in highly complex samples where many proteins may contribute to a single band. Furthermore, the selection of stain is also critical, as the relative enrichment in test over control samples may be obscured by the linear response range of the chosen stain. For instance, a particular caveat with silver staining is that whilst it is particularly sensitive to sub-nano gram quantities of protein, within an order of magnitude it rapidly loses stain density/protein concentration linearity [237,238]. This allows two relatively abundant proteins differing by a factor of 5 fold between control and test samples, to appear equivalent. Conversely, in my hands at least, colloidal coomassie possess a much greater range of stain linearity from approximately 100ug (presumably only limited by the chromatography and capacity of the polyacrylamide gel matrix) down to 50ng [239,240]. However, despite this range the comparative lack of sensitivity renders it of little use in small scale experiments or those limited in size by the cost of reagents.

The quantitative nature of SILAC, however, renders staining redundant as a means of comparative selection of potentially enriched bands. Moreover, removing the dependence on visual selection may reveal, in analysis, many enriched candidate proteins, otherwise obscured by staining patterns or sensitivity [241,242]. SILAC does however, benefit from protein staining as a means of visualising sample boundaries on polyacrylamide gels. Defining the sample boundaries in this manner minimises excess polyacrylamide excised for each gel band, increasing the efficiency of subsequent tryptic digestions and reducing sample preparation times, and volumes. Furthermore, slicing gel lanes into multiple bands according to protein staining allows division for roughly equal

protein distribution, maximising the depth of subsequent MS analysis. An additional caveat to requiring stain in any format is the chemical modifications made by these to peptides under certain conditions [237]. For instance, the colloidal coomassie stain used here contains methanol and acid, components that can cause methylation or esterification of carboxylic acids [243]. Undoubtedly, these modifications will adversely affect the identification of peptides, resulting in m/z values unmatched to the peptide database and possibly mismatches or a reduction in fragment identity scores. The use of recently available MS-compatible, methanol-free stains would limit these problems.

Another feature, pertinent to this study, which affects the number of peptides successfully matched to the observed m/z values in the SILAC analysis, is the use of particular isotopes, with the advantages of mixed isotopes recently becoming clear. The SILAC method employed here took the commonly used approach of substituting (^{13}C) arginine and (^{13}C) lysine into the "heavy" medium which results in a 6Da or 12Da shift in peptide masses if one or both isotopes are incorporated respectively. The drawback to this experimental design is that it is not possible to distinguish whether incorporation of lysine and/or arginine is responsible for the increased mass of peptides, confounding the software where m/z ratios are not unique. If however, (^{15}N) arginine (4Da shift) and (^{13}C) lysine (6Da shift) are used for labelling the "heavy" sample it is easy to imagine how data analysis is considerably easier with at least one or multiple residues immediately identifiable according to the recorded mass shift. By applying this dual labelling format the rapid, first pass binning of SILAC pairs into discrete data sets at the analysis stage should significantly increase the m/z values attributable

to peptides and subsequently increase the certainty associated with SILAC enrichment ratios.

Irrespective of these minor issues associated with increasing peptide numbers, the existing strategy provided unequivocal identification of a multitude of proteins shown to be enriched in a PI 3-kinase-dependent manner. The identification of TAPP-1 as one of the most heavily enriched proteins within the second analysis reflects that not only are PI 3-kinase-responsive proteins recovered but they include those which selectively bind PtdIns(3,4)P_2. The identification of all three isoforms of PKB/Akt which have been widely demonstrated to interact with both PtdIns(3,4)P_2 and PtdIns(3,4,5)P_3 also supports this conclusion. Furthermore, the pervasiveness of additional proteins also reported to interact with PtdIns(3,4)P_2 such as SWAP-70, vinculin, OSBP and ARAP1, similarly emphasises this view [89,100,101,244]. The occurrence of these, together with the wealth of other proteins expressing established lipid binding domains such as PH, FYVE, ENTH, and FERM, lend further credibility to the view that other proteins listed with currently unreported lipid binding characteristics may be potential 3-PI binding/regulated elements.

Whilst a distinct advantage of this screen over its predecessors is the quantitative, non-biased output achieved, it is clearly not a practical prospect to determine the potential for interaction with 3-PIs for each protein identified with an enriched ratio. Thus, there was next a need to focus on a few select candidates in more detail. In attempting to reflect the unbiased nature of the screen, whilst maximising the possibility of revealing novel and directly recruited/regulated 3-PI

interacting proteins, the selection criteria were prioritised as follows; the protein's prominence within each SILAC MS identity list (high ratio and high number of peptides isolated), proteins with defined roles in PI 3-kinase-sensitive or related pathways, and those with structural/sequence similarities to established lipid binding domains. Determining the parameters for structural/sequence homology, the third selection criteria, will be dealt with in Chapter 5. However, to qualify for inclusion to a limited subset of proteins for cloning, expression and binding analysis, candidate proteins required at least two of these features. Proteins which fulfilled these criteria include, but are not limited to: EPSIN1, thought to bind PtdIns(4,5)P_2 and regulate receptor mediated endocytosis; FERMT2, involved in connecting the the actin cytoskeleton to the extracellular matrix; PKM2, an enzyme which generates ATP from ADP and phosphoenolpyruvate; SOLO (ARHGEF40), a little known PH domain containing GEF which may act on Rho family of GTPases; FOXK2, a fork-head transcription factor; OSBPL11, a PH domain containing protein implicated in lipid transport; YES1, a proto-oncogenic protein-tyrosine kinase; ANKFY1, a FYVE domain containing membrane anchoring protein; PFN1, thought to mediate the polymerisation of actin and purported to be capable of PtdIns(4,5)P_2 interaction; PXK, a PX domain containing serine/threonine kinase (possibly inactive) which may participate in the regulation of synaptic transmission; VCL, an actin binding protein involved in cell-cell and cell-matrix adhesion; EIF4G1, a component of the eIF4F complex which is involved in regulation of translation; and finally SWAP-70, CLIC1 and IQGAP1 (all of which are discussed more thoroughly below). Amongst this limited subset, SWAP-70, CLIC1 and IQGAP-1 were selected as primary candidates due to their structural features (Chapter 5); in addition to PARIS-1,

identified as a consequence of the earlier single affinity purification, and each is introduced specifically.

SWAP-70 is a widely studied guanine nucleotide exchange factor (GEF) for Rac [245-247], containing a PH domain and has previously been isolated on the basis of immobilised 3-PI affinity chromatography [89]. Initially the relationship between the interaction of SWAP-70 and 3-PIs, for the activation of GEF activity was shown to be selective for PtdIns(3,4,5)P_3. In contrast however, a subsequent article reported that binding of SWAP-70 can also be achieved by PtdIns(3,4)P_2 [146]. Thus, SWAP-70 like PKB may bind both lipids, though not necessarily with the same functional consequences. As the purpose of this study is to identify novel PtdIns(3,4)P_2 binding proteins, SWAP-70 will not be considered further although its isolation and identification provides good proof of principle for the enrichment by this screen of 3-PI interacting proteins beyond TAPP-1 and PKB. Therefore, it is a reasonable assumption, that the identification of the PH domain containing PARIS-1, enriched within the same samples might indeed represent a novel 3-PI interacting protein. PARIS-1 is a little studied Rab guanosine triphosphatase (GTP)-activating protein (GAP) whose reduced expression has been implicated as a marker for prostate cancer [248]. The association of PARIS-1 with, or the regulation of its activity by, 3-PI interaction has not previously been determined, despite PARIS-1 (TBC1D2A) and its homologue TBC1D2B being the only recognised TBC domain containing proteins (35+ in the human proteome) which also have a C-terminal PH domain.

CLIC1 (chloride intracellular channel 1) identified within SILAC I, is proposed to act as an intracellular chloride channel, although it expression and tissue distribution remains uncertain [249]. CLIC1 has been proposed to participate in the control of salt secretion/absorption, cell volume homeostasis, the regulation of membrane potentials, organellar acidification, apoptosis and the cell cycle [250-252]. The biochemical properties of CLIC1 are highly unusual for ion channels in that CLIC1 appears capable of existence as a soluble, monomeric, cytoplasmic protein or equally as an integral membrane dimer, a morphometric change which is proposed to be dependent on pH and/or oxidation [252-254]. The protein is similar, structurally, to the GST superfamily with the exception that all established GSTs are known to be dimeric [255,256]. However, ITC (isothermal calorimetry) data also indicate little or no binding of CLIC1 to glutathione (Kd ≥10mM) [257]. Although CLIC1 does not possess an established lipid binding domain, in keeping with other GST superfamily proteins, it does possess a redox-sensitive cysteine (Cys 24). This may suggest that CLIC1 can be regulated by reactive oxygen species (ROS), which may act to modulate CLIC1 morphology and/or cellular localisation. ROS have also been implicated in the regulation of PI 3-kinase signalling via the oxidation-mediated inhibition of PTP family members such as PTEN and 4-phosphatases, a mechanism likely to favour PtdIns(3,4)P_2 accumulation [258,259]. Thus, a scenario could be conceived in which CLIC1 could be recruited for insertion into particular membranes in a 3-PI dependent manner. The characteristics of CLIC1 are considered further in Chapter 5.

Prominent amongst the candidates from the second SILAC experiment but also identified within the first (Supplementary Table 1) was the much studied

protein IQGAP1, identified with ~160 peptides, a P.E.P. value of zero and a ratio of enrichment of ~1.5. IQGAP1 is a large, 190kDa protein which is associated with many signalling pathways as a consequence of its numerous protein-protein interaction domains [260-264]. It has been suggested that IQGAP1 is responsible for regulating pathways required for cytoskeletal organisation such as adhesion and migration [261,263,265]. Moreover, IQGAP1 has been proposed as an oncogene [264,266] and presents an interesting candidate if it is indeed recruited and/or regulated by 3-PIs. Despite the presence of a GAP domain, IQGAP1 appears to act paradoxically to increase the GTP loading of Rho family GTPases such as Cdc42 and Rac1 [267]. The possibility that this enzyme activity of IQGAP1 may be modified by 3-PI interaction, such as reverting to classical GAP activity, presents an intriguing hypothesis. Furthermore, in support of its inclusion for subsequent analysis, although it does not possess a recognised lipid binding domain, IQGAP1 has been observed associated with the leading edge of polarised cells, a characteristic shared by PI 3-kinase and PtdIns(3,4,5)P_3 [263,268].

The selection of these candidate proteins for further analysis is strongly supported by their similar co-purification under conditions shown to selectively enrich a number of known 3-PI effector proteins. Indeed, the prominence of IQGAP1 and CLIC1 within the SILAC lists, representing the most comprehensive and the only quantitative attempts to uncover PtdIns(3,4)P_2 effector proteins, argues persuasively their potential role as PtdIns(3,4)P_2-mediated effector proteins. This is not, however, to suggest that these lists are all inclusive or that an enriched ratio represents proof of lipid binding selectivity or even of direct lipid-protein interaction. Certainly, the absence of other reported PtdIns(3,4)P_2 binding

proteins such as lamellipodin and DAPP-1 is of significance [99,269]. This may be explained by their lack of expression in our system or their failure to ionise/yield unique peptides in MS analysis. Equally however, the absence of DAPP-1 and lamellipodin may be explained by other experimental factors such as the Ins(1,3,4)P_3/biotinylated-PtdIns(3,4)P_2 concentration ratios or NaCl column elution concentration either of which might limit the recovery or enrichment of these proteins. Furthermore, despite the optimisation of each step for the recovery of TAPP-1, the determining factor for an enriched SILAC ratio is the activation of PI 3-kinase, which under the conditions described, favours the selective but not exclusive accumulation of PtdIns(3,4)P_2. Thus, proteins with a preference other than for PtdIns(3,4)P_2 can be expected to emerge from this approach. A specific example of this may be the increase in PtdIns(3)P following bpV(phen) treatment and the subsequent isolation of EEA1 (Table 4.5), a known PtdIns(3)P binding protein [270].

Moreover, the presence of a protein with a positive ratio of enrichment does not necessarily indicate direct binding to 3-PI, as recruitment and enrichment may be a consequence of interaction with a 3-PI-responsive adaptor protein. It is however, worth noting the absence of PTPL1 and MUPP-1 from these lists, both considered established partners for the scaffold protein TAPP-1 [124,170]. This may be due to factors previously considered such as expression or inability to ionise, equally however; their lack of identification may be due to losses of weak protein-protein interactions through the multi-step affinity purification.

In conclusion this Chapter extends previous studies focussing on 3-PI binding partners and presents the first quantitative analysis of proteins capable of binding lipids within an intracellular environment. Furthermore, this represents the most comprehensive study of proteins capable of interacting with PtdIns(3,4)P_2. The utility of this approach is exemplified by the definitive identification of established PtdIns(3,4)P_2 interacting proteins such as TAPP-1, PKB/Akt, SWAP-70, and ARAP1. A number of novel candidate proteins whose enrichment is a consequence of PI 3-kinase activation are identified and determination of the binding characteristics of a limited subset including PARIS-1, CLIC1 and IQGAP1 will be addressed Chapter 5.

Chapter 5.

The Validation of Candidate 3-PI Effector Proteins.

5.1 Introduction.

The previous Chapters have described a screen for 3-PI binding proteins and the candidates emerging from it. This Chapter will focus on a subset of these proteins selected on the basis of three primary criteria, (i) the protein's enrichment ratio and the number of peptides identified (ii) the potential association of candidates with PI 3-kinase signalling pathways and (iii) the potential structural and/or sequence homology of candidates to established lipid binding domains. This last criterion is further developed; firstly by illustrating how a limited number of candidates from the subset, highlighted previously, might fulfil this feature. Later, the lipid binding characteristics of those deemed to fulfil this criterion as well as other candidates from the wider subset of ~20+ candidate proteins are examined. The data presented reveal a novel 3-PI interacting PH domain in one candidate protein and propose a new lipid binding motif in another.

5.1.1 Established Lipid Binding Domains (LBDs).

In order to address the possibility that some of the identified candidate proteins, may possess a novel motif for lipid binding, the general features conferring lipid binding capability on several established LBDs are considered. Some examples of the currently accepted LBDs include PH, PX, FYVE, ENTH, FERM, ANTH/CALM, TUBBY, C1/2, PHD, BEACH, GRAM, BAR, Gla and Annexin. These domains can be broadly divided into two distinct classes; those capable of high selectivity and/or affinity, and those exhibiting low affinity with little or no specificity [25]. In the latter instance binding tends to be as a consequence of general, physical membrane properties of the membrane such as charge, amphiphilicity and/or curvature [271]. This study aims to identify novel,

selective PtdIns(3,4)P_2 interacting partners and will ignore this latter category of non-specific binding domains but focus on examples of the former, notably FYVE, PX and PH domains. Whilst this analysis of the properties of LBDs is not exhaustive, it is intended to demonstrate that spatial presentation of a minimum number of specific residues, rather than the domain superstructure, is crucial to lipid binding selectivity and affinity.

5.1.1.1 The FYVE Domain.

FYVE domains (named for Fab1p, YOTB, Vac1 and EEA1 [272,273]) are ~60-70 amino acids in size and expressed in 26 human proteins [25]. They are almost exclusively involved in binding to PtdIns3P, prevalent in early endosomes [270]. Consequently, the majority of FYVE domain proteins are involved in endocytic trafficking, endosomal membrane fusion, vesicular transport and vacuolar sorting [274].

FYVE domains have several long loops at the N-terminus, two short double stranded antiparallel β sheets and a C-terminal α helix. An exception to this structure is the homodimeric EEA1, which possesses two additional α helices, one at the N-terminus and one connecting the β3-β4 strands (Figure 5.1) [275]. All FYVE domains are, however, distinguished by three highly conserved sequences, WxxD, RR/KHHCR and RVC. The conserved basic motif (RR/KHHCR) forms a relatively shallow but highly basic binding site for PtdIns3P which is stabilised by two Zn^{2+} ions [120].

Figure 5.1 Structural features of phospholipid specific binding domains (reproduced with permission from [25]).

The C1 domain of protein kinase Cδ (PKCδ) was solved in complex with phorbol-1,3-acetate (PDB: 1PTR [276]). The binding pocket, two stabilising Zn^{2+} ions and the hydrophobic loop thought to penetrate the lipid bilayer (represented by the shaded blue bar) are labelled. An EEA1 FYVE (Fab1, YOTB, Vac1, EEA1) domain dimer is shown, bound to Ins(1,3)P_2 (PDBsum; 1JOC [277]) with structural Zn^{2+} ions marked. The central two molecules show two pleckstrin homology (PH) domains, one from phospholipase Cδ1 (PLCδ1, upper panel, PDBsum: 1MAI [278]) and the other from ARHGAP9 (lower panel, PDBsum: 2P0D [279]), both bound to Ins(1,3,4)P_3 but showing standard and non-standard binding respectively. Similarly the two PX domains shown are from $p40^{phox}$ (upper panel, PDB; 1H6H [280]) and $p47^{phox}$ (lower panel, PDBsum: 1O7K [281]) bound to PtdIns3P, the latter with reported selectivity towards PtdIns(3,4)P_2 and additionally presenting a secondary binding site for anionic lipids [282]. Indicated yellow side chains are those likely to penetrate the membrane.

Figure 5.1

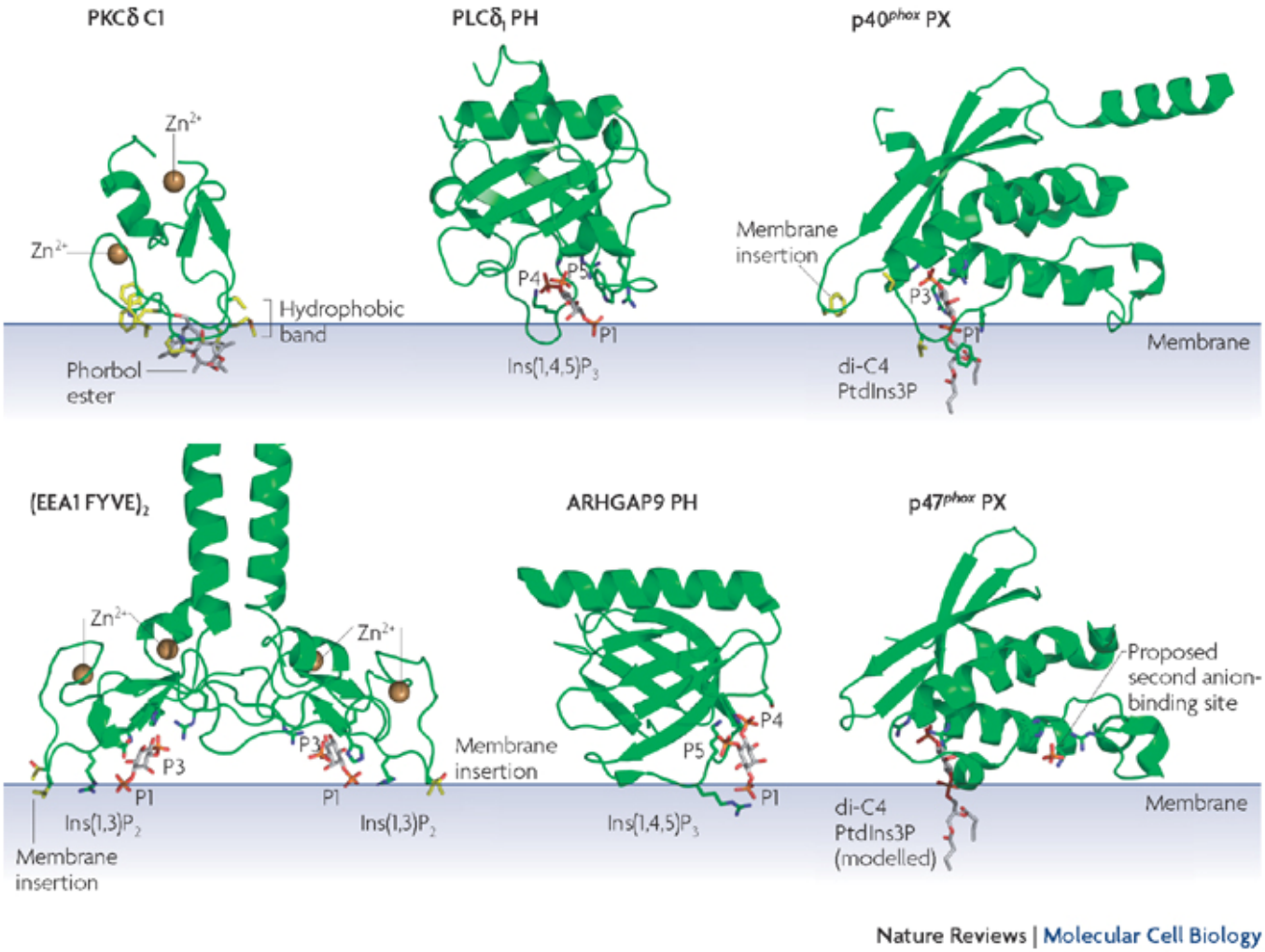

Nature Reviews | Molecular Cell Biology

Figure 5.2 highlights the residues from the RR/KHHCR and RVC motifs in EEA1 which form critical hydrogen bonds to the 1- (diester phosphate) and 3-phosphate of PtdIns3P. Also shown are the hydrogen bonds from the second histidine and the WxxD motif which tightly bind the hydroxyl groups of the inositol moiety at the 4-, 5- and 6- positions, creating high ligand selectivity [119]. An additional characteristic of the FYVE domain is the membrane insertion loop (MIL). This protrusion of hydrophobic residues allows the domain to significantly penetrate the lipid bilayer [120,270,283] (Figure 5.1). Adjacent to the MIL, at the level of the lipid headgroups are basic polar residues capable of non-specific electrostatic interactions with PtdSer, PtdOH or PtdIns [26]. In fact it is the strong positive potential around the MIL and binding pocket which facilitate initial membrane docking [119,270].

These three types of interaction dramatically increase the binding affinity of FYVE domains towards target rich membranes compared with short-chain PtdIns3P [26,275,284]. The secondary electrostatic and hydrophobic interactions [284,285] allow the FYVE domains to achieve low nM affinities despite the limited number of phosphate groups for primary, specific recognition [119]. Furthermore, the ability of FYVE domains to dimerise (i.e. homodimer formed by EEA1) maintains membrane interaction still further by increased avidity [275,286]. Lastly, FYVE domain-membrane association has been demonstrated to be pH dependent. It has been shown that the neighbouring histidines within the RR/KHHCR motif confer greater affinity when positively charged and drive membrane release upon deprotonation, sometimes referred to as the histidine switch [287].

Figure 5.2 Critical interactions conferring ligand selectivity within established LBDs (The Figure is amended from [119]).

The charged residues which, via hydrogen bonds, confer selectivity towards their respective ligands within the indicated binding pockets are illustrated. Examples from left to right are EEA1 FYVE domain (PDB; 1JOC [277]), $p40^{phox}$ PX domain (PDB; 1H6H [280]) and Grp1 PH domain PDB: 1FGY [288]. In each instance the inositol ring is highlighted in blue.

Figure 5.2

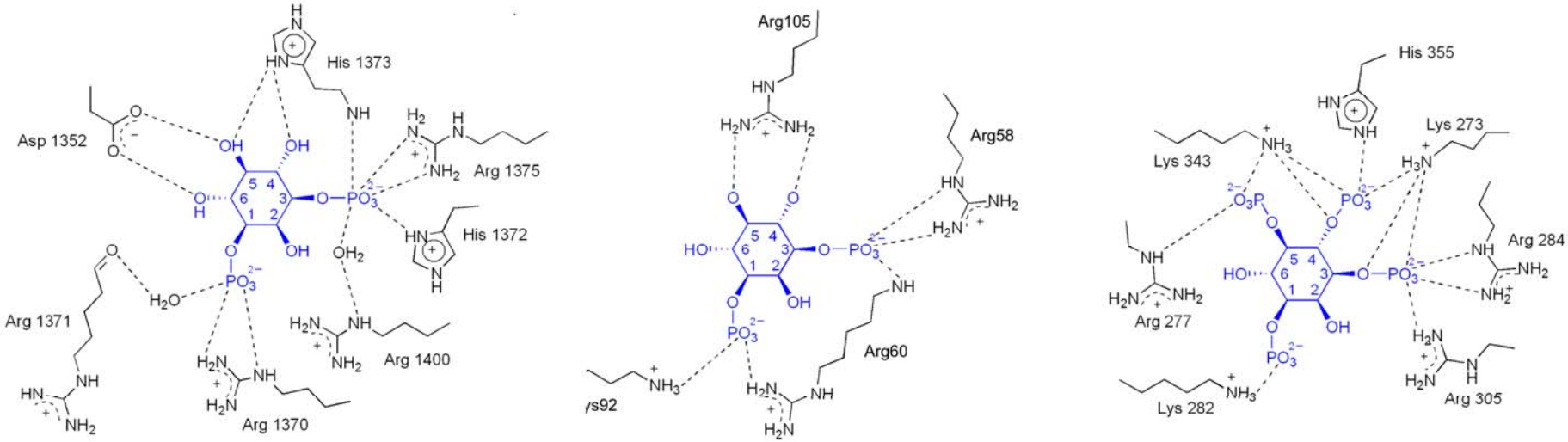
His 1373
Asp 1352
Arg 1375
His 1372
Arg 1371
Arg 1400
Arg 1370
Arg105
Arg58
Arg60
His 355
Lys 273
Lys 343
Arg 284
Arg 277
Lys 282
Arg 305

5.1.1.2 The PX Domain.

The PX domain of ~130 amino acids is present in 35 human proteins [25] and named following its identification in two proteins from the NADPH oxidase complex (phagocyte oxidase [PhoX]), $p40^{phox}$ and $p47^{phox}$ [289] but is most common in sorting nexins (SNX). PX domains are generally selective for PtdIns3P [290,291]. A notable exception is the PX domain of $p47^{phox}$, which is selective for PtdIns(3,4)P_2 and in addition, is proposed to possess a secondary binding site for anionic lipids (Figure 5.1) [292-294]. Most PX domain containing proteins are involved in endosomal or protein sorting although other functions include cell signalling, and phagocytic defence [293].

PX domains are typically based on three N-terminal β-strands comprising a β-sheet, which is followed by a helical domain of three or four α-helices (Figure 5.1) [295]. Two of these helices are linked by a polyproline loop which in conjunction with the β1-β2 loop forms the basic binding pocket. Additional interactions once again include a basic surround to the binding pocket for non-specific, electrostatic interactions and a loop capable of membrane insertion [296].

The three motifs required for binding, and which commonly identify PX domains, are $RRYx_2Fx_2Lx_3L$ of the β3-α1 loop, Px_2PxK of the MIL and RR/Kx_2L of the α2 helix. Figure 5.2 shows the bonding which confers selectivity for PtdIns3P in the PX domain from $p40^{phox}$ with the 1- and 3-phosphate interacting with the $RRYx_2Fx_2Lx_3L$ motif. Additional 1-phosphate interaction is provided by the MIL Px_2PxK motif and hydrogen bonding of the 4- and 5-hydroxyls by RR/Kx_2L [119,270].

5.1.1.3 The PH domain.

PH domains were first observed in Pleckstrin (Pleckstrin Homology) and later the PH domain of PLCδ1 was the first motif to show specific recognition of a phosphoinositide, in this case, PtdIns(4,5)P_2 [297-300]. PH domains have now been shown to be the most widely expressed domain capable of lipid interaction, occurring within 258 human proteins [25]. With the solitary exception of the PX domain from $p47^{phox}$, PtdIns(3,4)P_2 and/or PtdIns(3,4,5)P_3 appear to be uniquely recognised by a subset of PH domains. Examples of such include Btk and Grp-1 which show selectivity for PtdIns(3,4,5)P_3 and, PDK1 and PKB which show dual selectivity for PtdIns(3,4,5)P_3 and PtdIns(3,4)P_2 [83-85,87,134,301-304].

PH domains are ~125 amino acids in length and characteristically have little sequence similarity but possess a highly conserved secondary structure. Each contains two opposing β-sheets comprised of three and four strands, and capped at one end by an α-helix, often termed a "β-barrel" (Figure 5.1) [119]. The loops connecting the β-sheets at the open end create a deep binding pocket with ligand specificity determined by the basic residues in these loops. The inositide binding site within this sequence is almost always the β1-β2 and β3-β4 loop within the domain, the former most critical for binding and characterised by a conserved Kxn(K/R)xR motif [305-307].

Many PH domains are weak and promiscuous binding domains, however 10-20% exhibit high selectivity with affinities ranging from low nM to low μM [305,306]. This is exemplified by a genome wide study of yeast PH domains where, of the 33 cloned and expressed, 26 showed little or no PI binding and only

one demonstrated high specificity and affinity [308]. An example of a high affinity PH domain is provided by Grp-1 and the interactions involved in stabilising the inositol headgroup of PtdIns(3,4,5)P_3 are shown in Figure 5.2**.**

In contrast to the other LBDs described here which achieve binding via multiple interactions, PH domains rely primarily on head-group recognition [119,178,306,309]. The lack of significance of secondary binding features may explain the relatively low proportion of high affinity PH domains [305,306,308]. Equally this lack of secondary membrane interactions may explain how PH domains often show little selectivity between soluble and membrane bound ligands. The PH domain of PLC-δ1 is an exemplary case as this binds more strongly to Ins(1,4,5)P_3 than PtdIns(4,5)P_2, generating a negative feedback loop upon synthesis of Ins(1,4,5)P_3 following PLC-δ1 activation [310,311].

5.1.1.4 Structural Motifs Present Key Residues.

The established binding motifs listed above share little sequence or structural homology to each other but yet achieve, in many instances, highly selective and high affinity binding. In each case the strength and specificity of ligand binding are determined by a combination of three types of interaction, (i) head-group recognition by basic residues, (ii) membrane insertion of hydrophobic residues and (iii) additional electrostatic interactions. These features are essentially determined by the special presentation of only a dozen, or less, residues.

The importance of such a minority of residues within domains up to ~150 amino acids in size is perhaps most elegantly demonstrated by the mutation of a

critical arginine residue within the binding pocket of PH domains, which abolishes lipid binding capability [134,145]. Furthermore, the functional effect of another mutation can be seen in the E17K mutation within the PKB/Akt1 PH domain, apparently contributing to tumour development. This amino acid substitution by a single nucleotide polymorphism shifts the selectivity of the PH domain in favour of PtdIns(4,5)P_2 whose higher resting cellular concentration results in the constitutive membrane localisation and activation of PKB [312,313]. Moreover, an alanine to glycine mutation in the variable loop (β1-β2) region of the C-terminal TAPP-1 PH domain removes the normal occlusion of the 5-position and increases selectivity towards PtdIns(3,4,5)P_3. Correspondingly in DAPP-1, the reverse substitution increases affinity for PtdIns(3,4)P_2 [314]. Indeed, the crystal structure of the PKB/Akt PH domain reveals that the 5-phosphate sits in an aqueous environment, not influencing binding, perhaps explaining the apparent lack of preference demonstrated by PKB/Akt between PtdIns(3,4)P_2 and PtdIns(3,4,5)P_3 [315].

These studies highlight that mutational analysis and crystal structure comparisons can determine residues which confer selectivity within established LBDs. Nevertheless, the natural variation in sequence, within PH domains at least, means that these observations rarely translate into a predictive tool for ligand selectivity [102]. Conversely, they do support the hypothesis that the majority of the sequence contributing to the structure of a PH domain is purely scaffold, merely presenting key residues in a suitable manner, to create a binding pocket.

PH domains, however, are identified by bioinformatics tools according to their structural homology to the β-barrel scaffold, and not according to a minimum number of key residues or their lipid binding characteristics. Despite only a minority of these PH domains, identified by their scaffold, presenting key residues in the correct spatial orientation to yield high affinity lipid binding capability; a notion that PH domains are generic lipid binding modules persists. This perception is compounded further by the inherently biased approach of bioinformatics studies which often report selectivity/affinity of putative LBD proteins by using unreliable or incomplete binding assays. Conversely, affinity based screens which identify candidates by non-quantitative MS, by necessity, tend to focus on those proteins containing domains of proven ability to bind lipids. The predisposition of these approaches toward existing LBDs suggest that it may be plausible, within an unbiased approach, to identify domains which present the required residues for lipid binding but utilise a different scaffold; akin to the variation in scaffolds for known LBDs. The possibility that two candidate proteins (CLIC1 and IQGAP1) amongst the wider subset of 20+ proteins that fulfilled the previously described criteria, may present residues conferring lipid binding capability, without homology to the scaffold of established LBDs will be considered.

5.1.2 The Determination of Lipid Binding Selectivity.

The unbiased, ratio-metric identification of proteins by SILAC coupled to a three-tier affinity purification yielded a multitude of candidate 3-PI binding proteins (Chapter 4). It was, however, beyond the scope of this study to characterise the lipid binding capability of each. A limited subset of the most heavily enriched proteins was therefore selected, on the basis of association with

PI 3-kinase-dependent pathways and/or the possession of motifs which share general properties with other LBD. Whilst it was the intention that definitive experiments to determine lipid binding would be carried out by monitoring cellular recruitment/activity, preliminary *in vitro* binding studies were used initially, to qualify any lipid binding characteristics of the expressed recombinant proteins and thus minimise time-consuming *in vivo* analysis of all selected candidates.

In selecting an *in vitro* approach for determining the lipid binding selectivity of expressed candidate proteins the caveats associated with working with lipids were considered. The principal problem and arguably the source of much conflicting data is the method of lipid presentation to the target protein. Accepting that it is not possible to reliably replicate authentic lipid bilayers with all of their associated physicochemical features such as, lipid composition (PtdIns, PtdSer, PtdOH, PtdCho, cholesterol etc.), membrane curvature, protein constituents and ionic environment, *in vitro* assays tend to employ one of two approaches. These involve either the use of immobilised lipid/protein approaches or of vesicle based assays. Broadly the former can be relatively inexpensive, requiring minimum input of reagents and allows high throughput, although very often lipid presentation is unknown. The latter has a tendency to require significantly more reagents, both lipid and analyte, and demands significant optimisation but can provide a more realistic lipid presentation [316-318].

Isothermal titration calorimetry (ITC) is commonly used to assess binding to lipid vesicles. Whilst this approach is considered one of the most accurate and the

lipid presentation more closely mimics physiological membranes, it requires significant development [318]. Also the approach is not conducive to high throughput with each reaction only allowing direct comparison to a control cell, with one ligand. Thus, when coupled to the comparatively large reaction chamber, this approach is very profligate with both lipids and candidate proteins [318]. An alternative approach to ITC for determining binding to vesicles is by using a vesicle sedimentation assay. This essentially sediments, via centrifugation, vesicles of increased density from a protein-lipid mix. Following centrifugation, the proportion of the protein which partitions into the vesicle pellet is determined by protein assays. A significant caveat of this approach is the inclusion of any precipitated protein within the vesicle pellet. To overcome this, sucrose gradients can be used but this introduces additional problems with protein determination of dilute fractions within a gradient [318]. Both of these approaches, however, also suffer from the stability of the generated vesicles which notoriously have short lifetimes, leading to inconsistencies between batches [317].

Two of the more commonly used immobilised lipid/protein approaches include protein-lipid overlay assays (fat blotting) and surface plasmon resonance (SPR). These approaches, more amenable to higher throughput, are both used within this study to determine the lipid binding selectivity of the candidate proteins identified in Chapter 4. The advantages and disadvantages of each technique will be introduced below.

5.1.2.1 Protein Lipid Overlay Assay.

One of the most widely used assays to determine lipid binding selectivity is the protein-lipid overlay assay or fat blot [316]. This technique involves drying varying amounts of potential lipid ligands onto nitrocellulose membranes before incubation with a solution of the protein of interest. In the case of the typical GST tagged target, protein quantitation is provided by indirect measurement of chemiluminescence following anti-GST immunoblotting. Alternatively, the assay can be reversed by immobilising the protein and detecting binding to radio-labelled short chain lipid/head-group but with the intrinsic disadvantages of handling radioactive reagents [318].

The protein-lipid overlay assay is attractive for three reasons, firstly it demands little optimisation, with commercial equivalents (PIP strips – Echelon) also available. Secondly, it is considerably cheaper than alternative approaches, which either extensively use synthetic lipids or require access to expensive equipment. Finally, despite its relative simplicity it remains very sensitive to even very low affinity binding. However, the approach epitomises the problems associated with lipid presentation. The unknown nature of how the lipid molecules physically orientate themselves on the nitrocellulose makes determination of the effective concentration available for binding difficult to determine. Moreover, the varying aqueous solubility of phosphorylated PI derivatives (PtdIns(3,4,5)P_3 > PtdIns(3,4)P_2 / PtdIns(3,5)P_2 / PtdIns(4,5)P_2 > PtdIns(3)P / PtdIns(4)P / PtdIns(5)P) means that following extensive washing, lipid spots of equal starting masses can differ significantly [318]. Thus, since monophosphorylated phosphoinositides tend to be less hydrophilic and are retained better by the

hydrophobic membrane, they often demonstrate disproportionately high protein interaction. Furthermore, in my experience at least, approximate affinities derived for commonly used probes to their respective ligands appear considerably greater than literature values achieved via more sophisticated techniques, implying protein denaturation onto the nitrocellulose membrane. These caveats may explain why many examples of fat blot-derived binding are reported in the literature but yet, these remain unconfirmed by other techniques.

5.1.2.2 Surface Plasmon Resonance.

Surface plasmon resonance (SPR) is based around an optical sensor which measures the changing refractive index of a solution [319]. One application of this sensitive technique takes advantage of immobilising tagged lipid onto a surface (chip) to measure mass dependent analyte- or protein-binding, reported as response units or RU. Another variation allows layering lipid vesicles onto hydrophobic chips, prior to measuring analyte binding but this requires greater optimisation than the immobilisation approach. The SPR platform allows automation and the real time measurements of analyte association and dissociation. This measurement of real time interactions is of significant advantage in measuring low affinity binding between ligand and analyte. In contrast, other approaches which require separation of bound and free ligand/analyte are adversely affected by high dissociation rates, making them inappropriate for measurement of all but the highest affinity interactions. Furthermore, the quantitative nature of the SPR platform allows measurement of ligand association and retention between assays, eliminating the varying lipid solubility issues associated with fat blots. This study utilises the pseudo-irreversible immobilisation

of biotinylated lipid with streptavidin chips resulting in negligible loss of tethered lipid to solutions, even over extended periods of washing [320]. Moreover, this biotin-avidin presentation of lipid, identically used for the third affinity purification step of the three-tier scheme, provided a proven means of lipid presentation to the candidate proteins.

Another advantage to this technique is the option, on some platforms such as the Biacore 3000, to use the built in micro-fluidics system, to test protein binding to several different lipids, in real time, simultaneously [318]. Crucially this includes a blank reference cell allowing subtraction of non-specific binding. Also, due to the requirement for binding to be within 300nm of the SPR chip surface, flow cell volumes are extremely small (≤100nl) allowing sparing use of reagents [319]. Disadvantages of the technique include the requirement for expensive equipment and disposable reagents, depending on the experimental format. Also the assay is not as high throughput as fat blots although it is more reproducible.

5.1.3 Cellular Translocation Studies.

Following the identification of numerous, candidate 3-PI interacting protein from the three-tier affinity-coupled SILAC screens; a limited subset was selected on the basis of association with PI 3-kinase dependent signalling pathways and/or possession of features consistent with other, established LBDs. However, these criteria still yielded 20+ proteins of interest (Table 5.1) which are unlikely to all show direct lipid binding. The application of *in vitro* binding assays, discussed previously and exemplified later in this Chapter with the primary candidates identified in Chapter 4.3 (PARIS-1, CLIC1 and IQGAP1), is intended to

determine those with direct lipid binding potential prior to undertaking cellular translocation studies. Although preliminary data is discussed for these *in vivo* binding assays, more comprehensive analysis was limited by the time constraints of this study.

However, where *in vitro* binding studies indicated lipid binding capability, one of two approaches was used to ascertain the physiological relevance of such lipid binding. Preliminary *in vivo* approaches included digitonin permeabilisation of 1321N1 astrocytoma cells to allow the localisation of candidate proteins to be tracked by immunoblotting cytosolic and membrane fractions as described for TAPP-1 in Chapter 3. Alternatively, EGFP constructs of the candidate binding domain were expressed in mammalian cell lines and their localisation under both unstimulated and a variety of stimulated conditions was determined by microscopy.

5.2 Results

The possibility that a limited number of the candidates identified in Chapter 4 possessed novel or established structural motifs capable of lipid interaction was investigated. Where spatial presentation of key residues, as determined by comparative analysis of established LBDs, could be ascertained; candidate proteins were cloned and expressed, along with other candidates from the wider subset of the most heavily enriched proteins. The lipid binding selectivity of each was then determined by *in vitro* assays. Proteins which demonstrated *in vitro* lipid binding, from either the wider subset or the limited number which showed features similar to LBD, were analysed further by preliminary *in vivo* studies, where time allowed.

5.2.1 The Viability of Candidate Proteins**:** *In Silico* Data.

5.2.1.1 Sequence Alignment of Candidate Proteins to Established LBDs.

The sequence of candidate proteins that emerged from the screen described previously was compared with that of PH domains of known lipid binding selectivity for 3-PIs. Any similarity of candidate proteins to these PH domains, currently the only identified domain consistently capable of PtdIns(3,4)P_2 and PtdIns(3,4,5)P_3 interaction, could propose a potential binding mechanism. However, the lack of sequence alignment to PH domains does not necessarily preclude lipid binding, as discussed in 5.1.1.3.

The sequences of each of the limited subset of candidate proteins identified by SILAC analysis (Chapter 4), were obtained from the Ensembl database (October 2009) and imported into the ClustalW alignment software, alongside the

sequences for domains whose 3-PI binding selectivity is well established [202,321]. Figure 5.3A thus shows a comparative sequence alignment of the KxGxn(K/R)xR motifs (highlighted in red) from the β1-β2 loops of the PH domains of TAPP1 (C-terminal), TAPP2 (C-terminal), PKB, Grp-1, DAPP1, Centaurin-α, and SWAP-70, shown to possess high affinity 3-PI binding, to that of the PH domain of the candidate protein, PARIS-1. This comparison is useful as, in many PH domains, it is the KxGxn(K/R)xR motif which is responsible for forming the majority of phosphate interactions within the binding pocket. The critical nature of these residues within a domain otherwise known for sequence variability is shown by the high level of conservation between these and other PH domains. From Figure 5.3A it can be clearly seen that the PARIS-1 PH domain shows remarkable homology to TAPP-1, Grp-1, PKB and SWAP-70 within this KxGxn(K/R)xR motif. Interestingly, when comparing PARIS-1 to the sequences of TAPP-1, DAPP-1, and Grp-1, and in particular the alanine/glycine residue (second amino acid of the β1-β2 variable loop, immediately following the conserved glycine), PARIS-1 shows closest homology to DAPP-1 and Grp-1. This alanine residue within TAPP-1 occludes the 5-position of inositol ring, hindering binding of PtdIns(3,4,5)P_3. Importantly, PARIS-1 has a glycine in this position which may indicate an ability to bind PtdIns(3,4,5)P_3 and/or PtdIns(3,4)P_2, similar to Grp-1 or DAPP-1, respectively.

Figure 5.3 The sequence alignment of the defining motif of PH domains to candidate proteins, PARIS-1 and CLIC1.

(A) The alignment of PARIS-1 PH domain sequence to that of the defining KxGxn(K/R)xR motif of PH domains from the proteins indicated. All sequences were obtained from Ensembl and aligned using the ClustalW software [202,321]. Highly conserved residues implicated in the conformation of binding pockets/directly form interaction with 3-PIs are highlighted in red. TAPP1 and TAPP2C both relate to their respective C-terminal PH domains.

(B) The alignment of CLIC1 to similar PH domain sequences aligned according to their β1-β2 sheet transition. Conserved residues, as previously indicated in figure 5.3A, are marked in red. The residues which contribute to the characteristic hydrophobic loop, which forms between β1 and β2 sheets within PH domains, is marked in blue. A structurally similar loop is seen within CLIC1 and these residues are similarly indicated.

Figure 5.3A


TAPP1 GYCVKQGAV--MKNWKRRYFQLDEN--TIGYF- 28
TAPP2C GYCVKQGNV--RKSWKRRFFALDDF--TICYF- 28
PKBα GWLHKRGEY--IKTWRPRYFLLKNDGTFIGYK- 30
GRP1 GWLLKLGGR--VKTWKRRWFILTDN--CLYYF- 28
DAPP1 GYLTKQGGL--VKTWKTRWFTLHRN--ELKYF- 28
CENTAURINALPHA1C GYMEKTGPK-QTEGFRKRWFTMDDR--RLMYF- 29
SWAP GYMMKKGHR--RKNWTERWFVLKPN--IISYYV 29
PARIS GYLSKFGGKGPIRGWKSRWFFYDERKCQLYYS- 32

Figure 5.3B

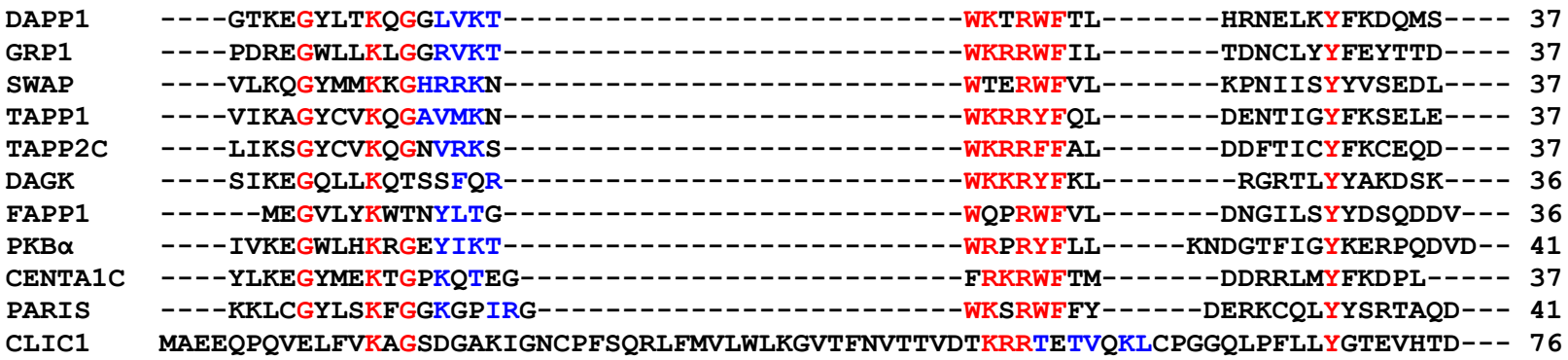
DAPP1 ----GTKEGYLTKQGGLVKT----------WKTRWFTL-------HRNELKYFKDQMS---- 37
GRP1 ----PDREGWLLKLGGRVKT----------WKRRWFIL-------TDNCLYYFEYTTD---- 37
SWAP ----VLKQGYMMKKGHRRKN----------WTERWFVL-------KPNIISYYVSEDL---- 37
TAPP1 ----VIKAGYCVKQGAVMKN----------WKRRYFQL-------DENTIGYFKSELE---- 37
TAPP2C ----LIKSGYCVKQGNVRKS----------WKRRFFAL-------DDFTICYFKCEQD---- 37
DAGK ----SIKEGQLLKQTSSFQR----------WKKRYFKL--------RGRTLYYAKDSK---- 36
FAPP1 ------MEGVLYKWTNYLTG----------WQPRWFVL-------DNGILSYYDSQDDV--- 36
PKBα ----IVKEGWLHKRGEYIKT----------WRPRYFLL-----KNDGTFIGYKERPQDVD-- 41
CENTA1C ----YLKEGYMEKTGPKQTEG----------FRKRWFTM-------DDRRLMYFKDPL----- 37
PARIS ----KKLCGYLSKFGGKGPIRG----------WKSRWFFY------DERKCQLYYSRTAQD--- 41
CLIC1 MAEEQPQVELFVKAGSDGAKIGNCPFSQRLFMVLWLKGVTFNVTTVDTKRRTETVQKLCPGGQLPFLLYGTEVHTD--- 76

Figure 5.3B shows a similar sequence alignment for the same array of PH domain KxGxn(K/R)xR motifs against the N-terminus of the candidate protein CLIC1. According to the hidden Markov model of the bioinformatic tool SMART (simple modular architecture research tool [116,117]) CLIC1 does not possess a known domain of any kind. However, the alignment, laid out according to the β1 and β2 sheet structures of the PH domains, demonstrates that CLIC1 possesses the characteristic lysine and glycine residues (KxG) conserved in the transition between the β1 strand and the variable β1-β2 loop within PH domains. Due to structural variation however, the β1-β2 loop of CLIC1 turns into an internal α-helix and is unlikely to contribute to any ligand binding. Following the internal α-helix, the secondary structure reverts to a β2 strand which doubles back to structurally position itself next to the KxG motif of the β1 strand, presenting the KRR motif. A spatially similar loop to that seen in the β1-β2 transition of PH domains is then seen in the β2-β3 loop of CLIC1 (residues highlighted in blue). This region shares characteristics with PH domain loops in that both are exposed and comprise primarily of hydrophobic and/or basic residues. These extended loops of hydrophobic and basic residues may contribute to non-specific membrane interactions or even constitute a MIL. Thus, CLIC1 may present residues in a spatially similar manner to PH domains but use an alternative scaffold, in place of the classical β-barrel seen for PH domains.

5.2.1.2 Structural Homology of Candidate Proteins to Established LBDs.

To investigate this hypothesis of alternative scaffolds presenting conserved features required for lipid binding, the tertiary structure for fragments of both CLIC1 and another candidate protein with little sequence homology to PH domains, IQGAP1, was compared to that of the C-terminal TAPP-1 PH domain.

Figure 5.4A shows the crystal structure of the C-terminal TAPP-1 PH domain, to develop the concept of spatial presentation of specific residues giving rise to a binding pocket. The structure of the C-terminal TAPP-1 PH domain was obtained from the Protein Data Bank (PDBsum: 1EAZ) and imported into PyMOL software for rendering [314,322,323]. Images were processed by removing the ordered citrate ligand that was crystallised within the binding pocket and are presented in both structural and space filling formats. The ribbon structure of TAPP-1 illustrates the β-sheets, α-helices and loops which generate the superstructure of the PH domain (coloured yellow, red and green respectively). Furthermore, the relative positions of the conserved residues, previously indicated within Figure 5.3A, which contribute to the binding pocket, are highlighted within this structure in blue (GYCV**K**Q**G**AVMKNW**KRR**YFQLDENTIG**Y**F). The cartoon ribbon model and the space filling model show how the binding pocket could accommodate the headgroup of PtdIns(3,4)P_2, positioned accordingly to allow occlusion of the 5-hydroxyl group by the alanine residues of the β1-β2 loop, described previously. The upper panel illustrates the extent to which the hydrophobic sequence of the β1-β2 loop (green) must penetrate the membrane to achieve headgroup positioning of PtdIns(3,4)P_2 within this binding pocket. This structural presentation of the C-terminal PH domain of TAPP-1 provides a model

for comparing the specific features presented by alternative scaffolds within other candidate PtdIns(3,4)P_2 binding proteins.

Figure 5.4B similarly focuses on the 27kDa candidate, CLIC1, previously identified via SILAC labelled enrichment of potential PtdIns(3,4)P_2 interacting proteins (Table 4.2). All the images are adapted from the crystal structure of a monomer (PDBsum: 1K0o [324]), several of which have been fitted speculatively with Ins(1,3,4)P_3. Immediately apparent is the departure from the established PH domain structure shown previously for TAPP-1. The only structural homology is provided by a β-sheet consisting of four β-strands which is only half of the traditional β-sandwich seen for PH domain folds. CLIC1 however, also has additional α-helices inserted between these β-strands. Despite this lack of sequence and structural homology to established LBDs, the residues which are capable of conferring lipid binding within PH domains, previously indicated for TAPP-1, are presented in a remarkably similar spatial manner. Thus, highlighted in blue within Figure 5.4B are **K**, **G**, **KRR** and **Y** to allow comparison to the TAPP-1 PH domain. The magnified section of the upper panel details how, despite differences in secondary structure, CLIC1 similarly presents these amino acids. The residues are numbered accordingly from the N-terminus to the C-terminus, revealing that following the KxG motif (13-15) the structure turns inwardly into an α-helix which then returns to the binding pocket via the β2 strand, presenting the KRR motif (amino acids 49-51) and the hydrophobic loop in a manner similar to PH domains. It is worth noting the small α-helix within the β1-β2 loop, the conformation of which may remain removed from the binding pocket or fold over to generate greater substrate selectivity. The PH domain of Grp-1 is afforded

greater selectivity towards PtdIns(3,4,5)P_3 as a consequence of additional interactions from a similarly inserted α-helix between the β6-β7 loops. Alternatively this feature may contribute to the role of CLIC1 as an ion channel – possibly required for function or membrane insertion. Regardless, these data indicate that despite significant deviation from the structure of the PH domain fold, CLIC1 presents residues deemed critical for lipid binding in a surprisingly similar spatial orientation.

Figure 5.4 A structural comparison of the C-terminal TAPP-1 PH domain to the proposed binding pocket of candidate proteins.

(A) The crystal structure of the C-terminal PH domain of TAPP-1 (PDB: 1EAZ [314]) was modelled in PyMOL and fitted with Ins(1,3,4)P_3 in the upper left ribbon and lower right space filling models [323]. The left panel ribbon models detail the residues, highlighted in blue which comprise the KxGxn(K/R)xR motif. The remaining residues are coloured according to the domains secondary structure; β-sheets (yellow), α-helices (red) and loops (green). The central space filling models give an indication to the binding pocket created by classical β-barrel of a PH domain. The orientations of all models are indicated in the upper right corner.

(B) The crystal structure of CLIC1 (PDB: 1k0o [257]) was modelled in PyMOL and fitted with Ins(1,3,4)P_3. The upper left panel and the magnified portion highlight in blue, the spatial distribution of residues similarly shown in A which are known to be critical for lipid binding within PH domains. Secondary structures are coloured as described in A. The space filling models illustrate the potential binding pocket. The orientation of each model is indicated by the central panel.

(C) The crystal structure of C-IQGAP1 (amino acids 1561-1657, PDB: 1X0H [325]) was modelled in PyMOL and fitted with PtdIns(1,3,4)P_3. The left panel shows the ribbon structure in multiple orientations including a magnified section to highlight (in blue) the similar spatial distribution of basic residues which are crucial in conferring lipid binding capability within established lipid binding domains. The ribbon structures also detail a similar structural fold to the β-sandwich seen for PH domains. The space filling models give an indication of the proposed binding pocket both with and without ligand. Secondary structures are coloured as previously described in A and orientation of each model is illustrated in the upper right panel.

Figure 5.4A

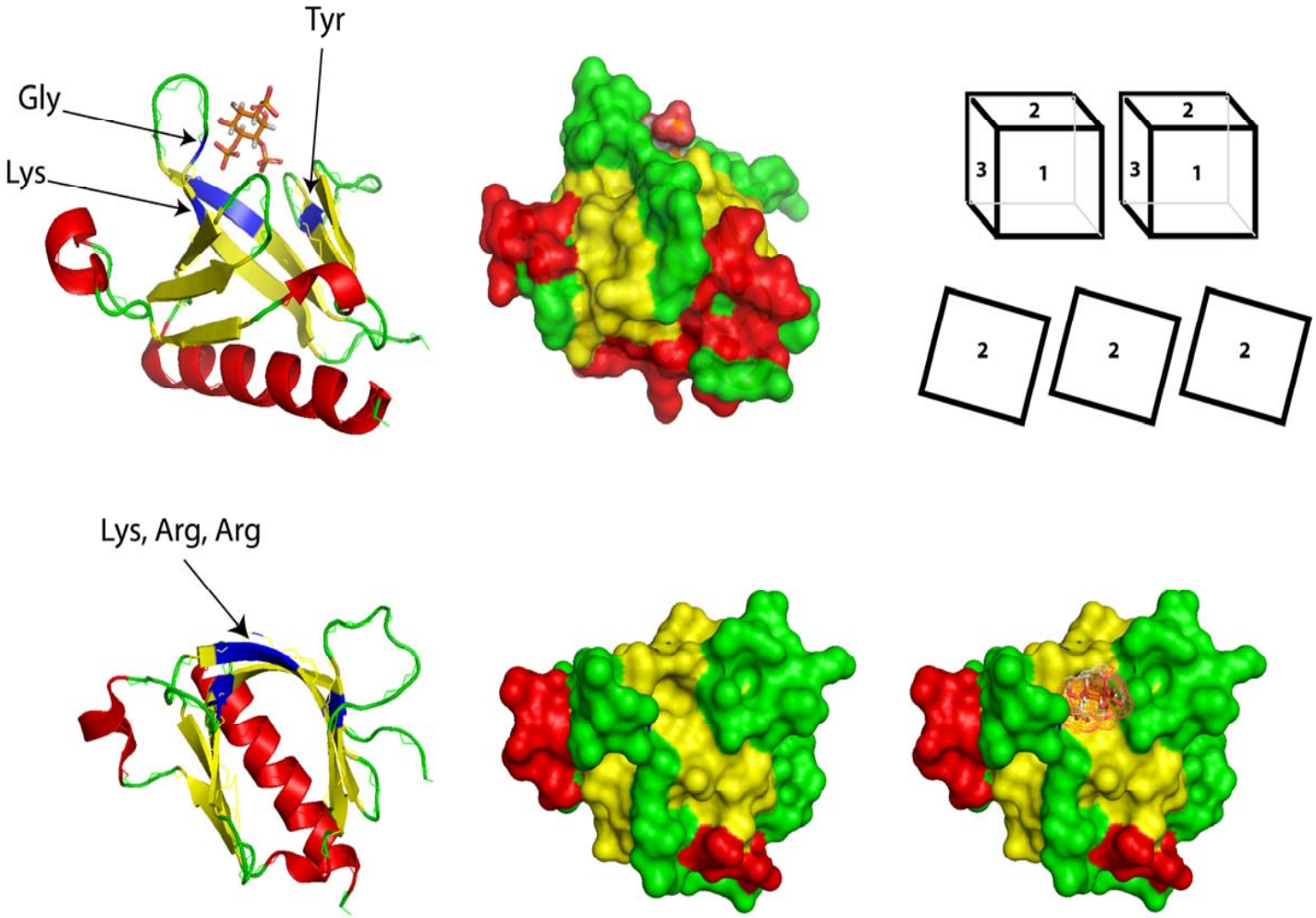

Figure 5.4B

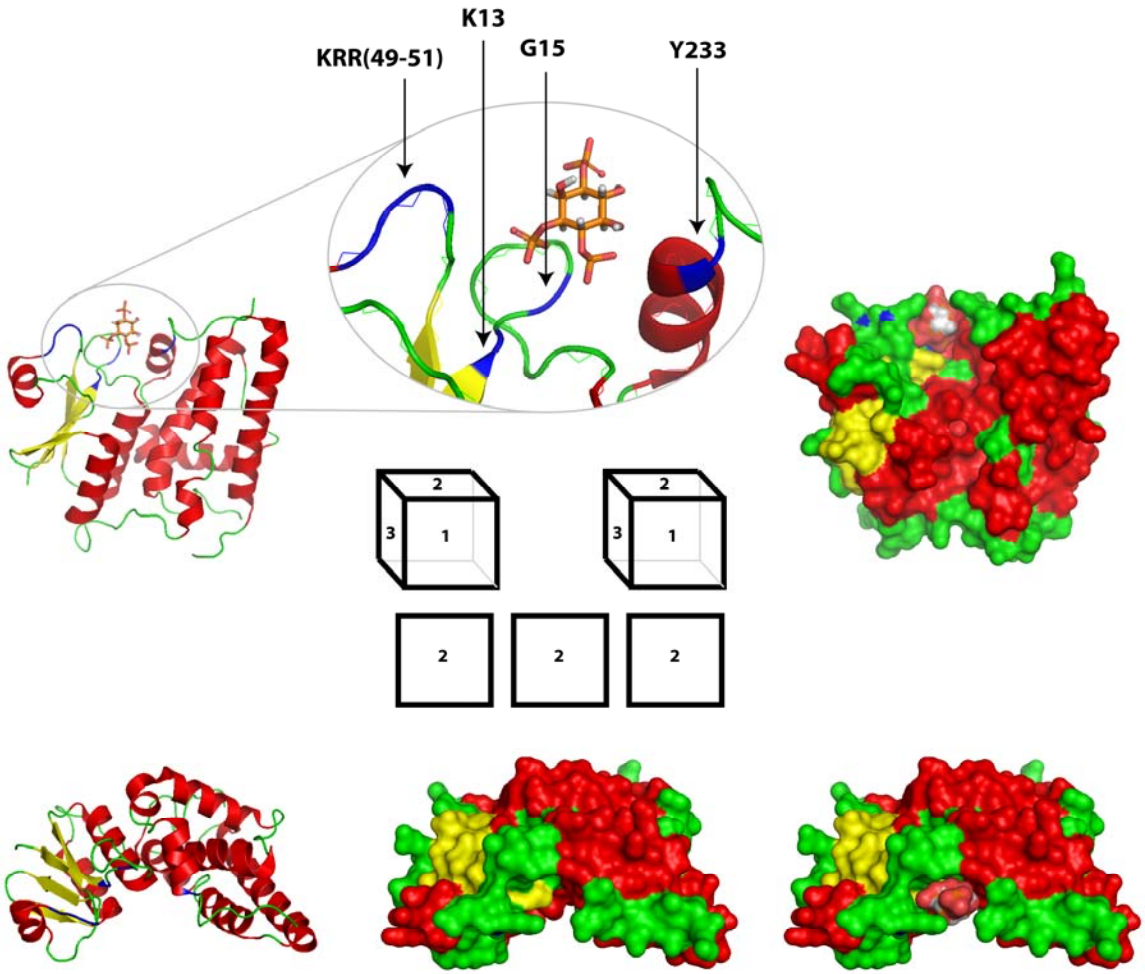

Figure 5.4C

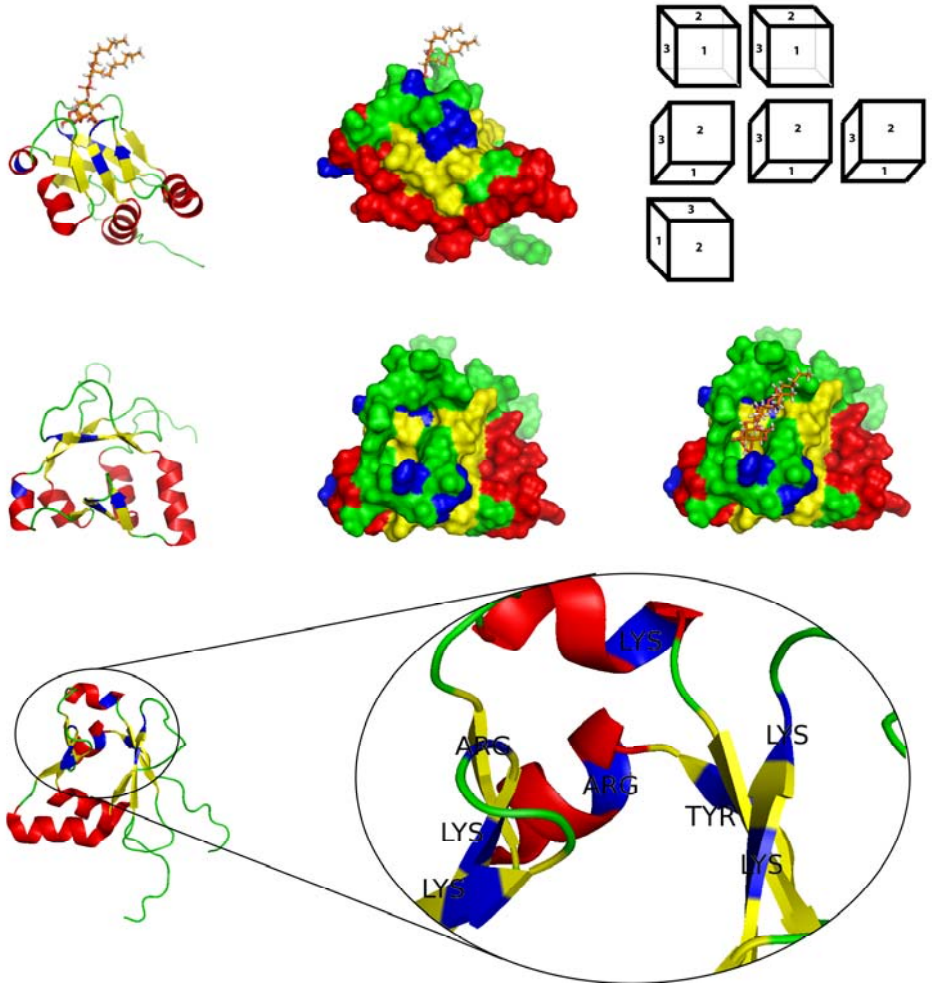

Figure 5.4C shows the structural arrangement and space filling model for a third candidate protein, IQGAP1, which yielded a positive ratio of enrichment from both SILAC studies (Table 4.4 and Supplementary Table 3). All images are adapted from a crystal structure available for the extreme C-terminus of IQGAP1 (PDBsum: 1X0H) [325]. The upper panel of Figure 5.4C shows the tertiary structure of the region which relates to amino acids 1561-1657 of IQGAP (1657 amino acids in total) and its space filling equivalent. Similarly to PH domains, the proposed binding pocket is a β-sandwich configuration formed by two opposing β-sheets of three and four β-strands. The characteristic "barrel" structure of PH domains aptly describes the capping of one open end by an α-helix in a near parallel orientation to the β-sandwich. In contrast, this structure is capped at the base by two shorter α-helices with two further short α-helices forming one side of a "modified barrel", one even contributing to the conformation of the proposed binding pocket. All four α-helices are equally spaced and are perpendicular in orientation to the β-sandwich.

The central panel of Figure 5.4C shows an alternative "top down" view which highlights the potential binding pocket of IQGAP1, hypothetically fitted with PtdIns(3,4)P_2. In each image, residues highlighted in blue are those which surround the proposed binding pocket and are responsible for conferring lipid binding capability in established LBDs. The lower inset image indicates these residues and demonstrates that the region is rich in lysine and arginine, both basic residues which are responsible for headgroup recognition by electrostatic interactions in all LBDs. These data propose a potentially novel LBD within

IQGAP1, presenting residues known to be critical for ligand binding in established LBDs by an alternative scaffold.

These sequence and structural comparisons of fragments from PARIS-1 (PH domain), CLIC1 (N-terminal and whole protein respectively) and IQGAP1 (C-terminal fragment) to PH domains of proven lipid binding compatibility, present a persuasive argument that presentation of crucial residues can be achieved by scaffolds which differ from that of established LBDs. This assumption was tested by determining the selectivity/affinity of these candidates, amongst others, by *in vitro* binding assays.

5.2.2 Cloning and Expression of Candidate proteins.

Each of the candidate proteins identified and selected on the basis of the criteria discussed previously were cloned and expressed as a GST tagged recombinant protein. The candidate proteins included: CLIC1, PARIS-1 PH domain, IQGAP1 (both N-terminal and C-terminal fragments), PFN, OSBPL11, YES1, CRT, KDEL, PKM2, RACK1, EIF4G1, FERMT2, FOXK2, ANKFY1 (N-terminal fragment), EPSIN1, VCL, SPARC, SERPIN, SOLO (PH domain), Annexin A6, PICALM, FKBP9 and PXK. Unfortunately, not all of these could be expressed in sufficient quantity/purity to facilitate analysis.

Briefly, the cloning strategy involved isolation of a PCR product and ligation into the TOPO II vector prior to sequence confirmation. The successfully sequenced constructs were then sub-cloned into pGex-6P-(X) vectors. If blunt ligation into TOPO II failed, an alternative strategy involving restriction digestion

of the PCR product and direct ligation into pGex-6P-(X) was used. All constructs were expressed within, and purified from, E.coli. The resulting GST-column purified fractions were analysed for expression level and homogeneity by SDS-PAGE analysis. Where necessary an expression matrix using 10ml LB cultures with variable conditions was used to optimise parameters including effective temperature, isopropyl β-D-1-thiogalactopyranoside (IPTG) concentration and time-dependent expression. An example of such a matrix, illustrating that for expression of two constructs of the PARIS-1 PH domain is shown in Figure 5.5. For the PARIS-1 PH domain, two constructs were expressed to reduce the possibility of deleterious effects of incomplete or unfolded secondary structure to the affinity of the PH domain. The 1-150 construct terminated immediately at the end of the reported PH domain structure, the 1-200 construct continued passed the next established unit of secondary structure prior to termination. Figure 5.5 shows the varying expression of both of these constructs induced by increasing concentrations of IPTG at a single temperature over time as indicated. For the examples presented, in order to maximise the ratio of protein expression to background contaminant proteins, 2 hrs at 37°C and 200μM IPTG were selected as the optimum expression conditions for both the PARIS-1 PH domain GST constructs. Each candidate, similarly expressed, required at least the level of sample purity/homogeneity demonstrated by the conditions for PARIS-1 expression (2 hrs at 37°C and 200μM IPTG) prior to being considered suitable for analysis of lipid binding by *in vitro* assays.

Figure 5.5 The expression of candidate proteins.

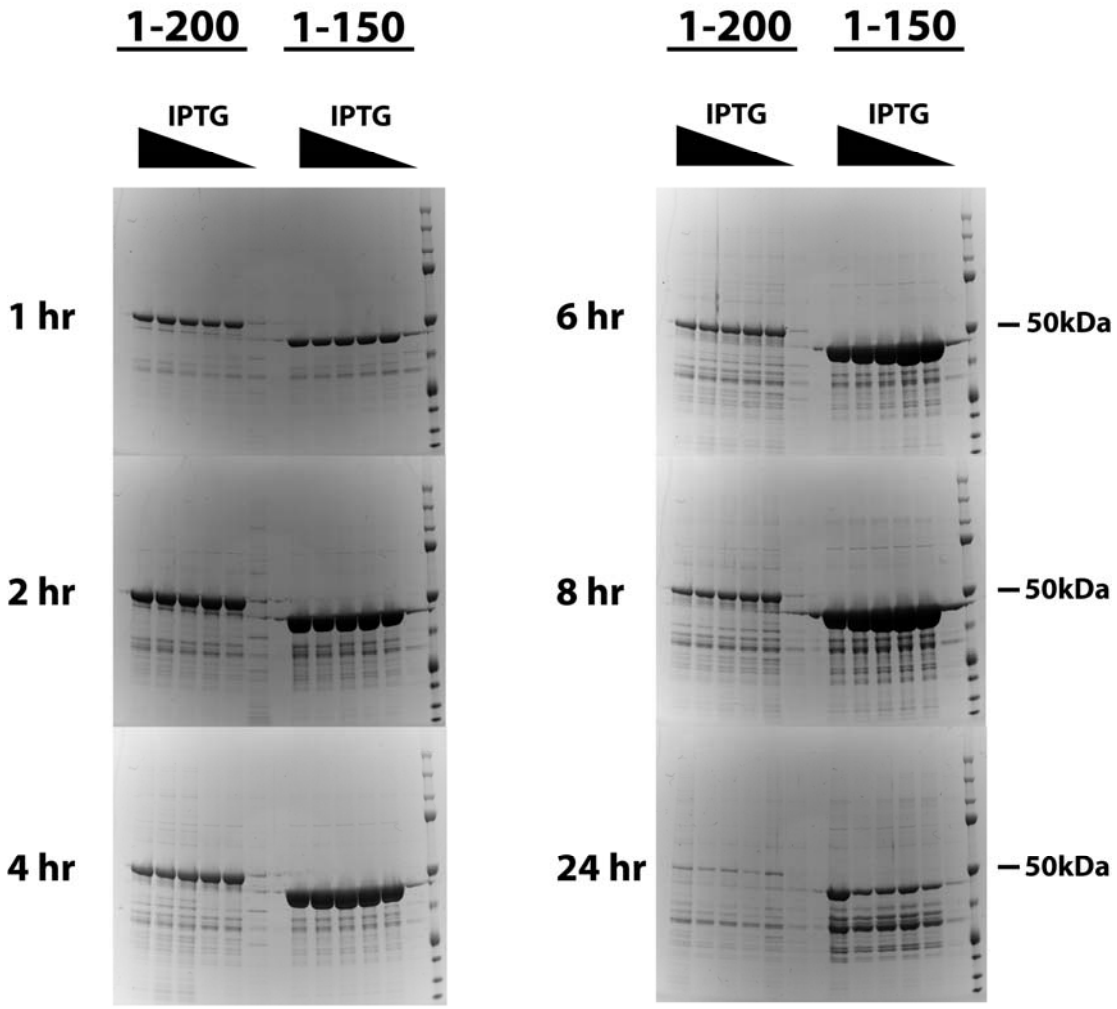

Two GST-tagged constructs for PARIS-1 were generated comprising amino acids 1-150 and 1-200. The expression profile over 24 hrs at 37°C for both constructs is shown in response to varying concentrations of IPTG induced expression (0, 50, 100, 200, 400 and 800μM – right to left for each time point). Following expression in E. Coli, proteins were recovered from bacterial lysates on GST-sepharose with extensive washing and analysed by SDS-PAGE. The Figure shows colloidal coomassie stained gels to indicate protein bands. Variations on expression conditions were similarly carried out, if required, for other candidate proteins.

5.2.3 Binding Studies.

5.2.3.1 Protein-Lipid Overlay Assay for Determining Binding Selectivity.

Preliminary efforts to determine the lipid binding characteristics of candidate proteins and positive controls alike, focussed initially on the protein lipid overlay assay or fat blot. This experimental approach involved spotting serial dilutions of dipalmitoyl PtdIns and its phosphorylated analogues onto nitrocellulose membranes, blocking with fatty acid-free BSA and then probing with the target protein [316]. Subsequently, membranes were washed extensively and any remaining bound protein was recorded by immunoblotting, in these examples, with anti-GST antibody. Whilst data for all expressed constructs is not presented, the utility of the approach is exemplified by the analysis of the PARIS-1 PH domain constructs, in comparison to the known lipid binding PH domains, TAPP-1 and Grp-1.

Figure 5.6 shows lipid overlay assays demonstrating the established lipid binding selectivity of the PH domains of Grp-1 and TAPP-1 (C-terminal) for PtdIns(3,4,5)P_3 and PtdIns(3,4)P_2 respectively, in comparison with similar assays to test the lipid binding preferences of the GST-PH domain(s) of PARIS-1. The various PI analogues were spotted on the nitrocellulose as indicated, and from left to right in a two fold serial dilution in chloroform:methanol:water (1:2:0.8) from 200 pmol to 3.1pmol. The highest affinity binding demonstrated for Grp-1 and TAPP-1 towards PtdIns(3,4,5)P_3 and PtdIns(3,4)P_2 respectively, agrees well with that reported previously [102,316]. It is noticeable, however that the PH domains of both Grp-1 and TAPP-1 show a higher than anticipated binding to PtdInsP

isomers. This may be accounted for by the recognised tendency of these lipids to adhere more persistently than higher phosphorylated PIs to nitrocellulose membranes, owing to their comparatively lower aqueous solubility [318].

The data presented in Figure 5.6 for both PARIS-1 PH domain constructs indicate that its selectivity favours bis- or tris-phosphorylated PIs, particularly PtdIns(3,4,5)P_3 and PtdIns(3,4)P_2. Although both PARIS-1 constructs present a qualitatively similar lipid binding profile, the shorter construct (1-150 amino acids) seems to show greater affinity for all PI species. This may be as a consequence of the additional sequence beyond the established PH domain motif in the larger construct (1-200 amino acids) hindering ligand binding. These data reveal the previously unreported lipid binding capability of the PARIS-1 PH domain and warrant further investigation of *in vivo* selectivity and affinity.

Figure 5.6 Lipid binding selectivities as demonstrated by protein-lipid overlay assays.

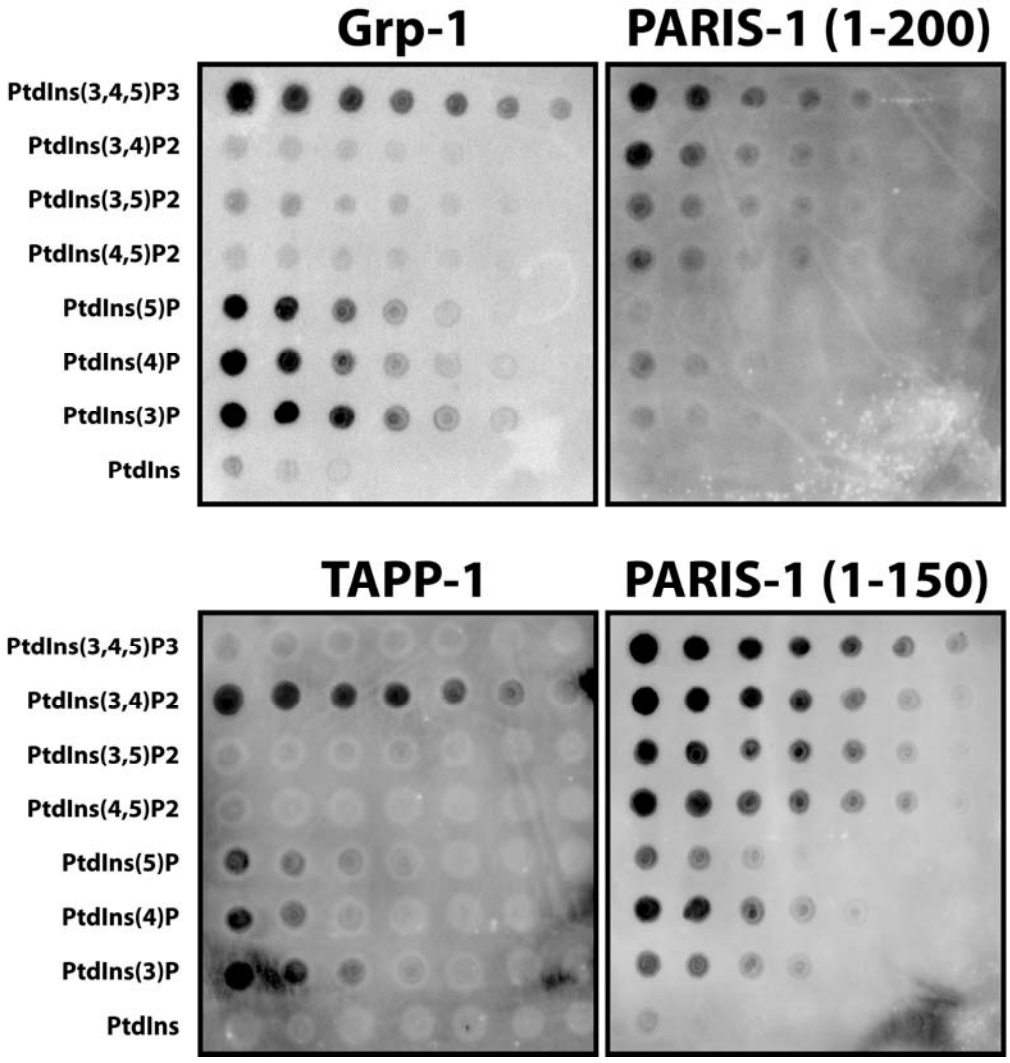

Nitrocellulose membrane were spotted from left to right with dipalmitoyl PIs diluted in 1:2:0.8; chloroform:methanol:water as indicated, to give lipid masses of 200, 100, 50, 25, 12.5, 6.3, 3.1 pmol. The membranes were then blocked with fatty acid free BSA prior to incubation with candidate/established lipid binding domains; Grp-1 PH-GST, TAPP-1 PH-GST (C-term), PARIS-1 PH(1-150)-GST and PARIS-1 PH(1-200)-GST and analysed by immunoblotting. The results are representative of at least 3 other experiments.

Although the results obtained for Grp-1 and TAPP-1 highlight the utility of this technique qualitatively to determine the selectivity of high affinity binding proteins, attempts to derive more quantitative data for these and other candidate proteins yield unrealistic affinities. This is likely to be due to denaturation of proteins onto the nitrocellulose membranes once in proximity to the lipid. For example, straightforward binding kinetics would dictate that even a high affinity binding protein with affinity constant of 10^9 M^{-1} should have a half time of dissociation ranging from ~1 min -1 hr (30°C and 0°C respectively) [326]. The fact that any binding to lipid spotted membranes is reported at all by this method, especially following extensive washing, implies largely irreversible binding of the protein - presumably to the nitrocellulose - albeit involving initial lipid recruitment.

5.2.3.2 Surface Plasmon Resonance (SPR).

To be able better to assess the lipid binding characteristics of candidate proteins, it was evident that a more reliable assay would be required. The solution to this problem was provided by the application of SPR, in this study using the Biacore 3000 platform. Furthermore, the availability of streptavidin chips presented the possibility of immobilising biotinylated lipids in a manner very similar to the third step of the affinity purification used to isolate the candidate proteins originally. Thus, the presentation of the lipids, though not physiological, would at least be consistent and in a fashion proven to be capable of interacting with established binding proteins such as TAPP-1, PKB, centaurin-δ (ARAP1) and SWAP-70.

Figure 5.7 shows some specific examples of SPR sensorgrams for the established LBDs (Grp-1, TAPP-1 and PLC-δ PH domains), and for two candidates from the subset of proteins originally identified in Chapter 4, IQGAP-1 (C-terminal fragment) and PARIS-1 PH domain (1-150). These were selected for more comprehensive analysis because of their structural homology to established LBDs as detailed in 5.2.1 and are presented as exemplary data for the SPR lipid binding assay. Panels A-C of Figure 5.7 shows the selectivity of the control proteins, Grp-1, TAPP-1 and PLC-δ. These control proteins, of established lipid binding capability, each show the expected selectivity towards PtdIns(3,4,5)P_3, PtdIns(3,4)P_2 and PtdIns(4,5)P_2 respectively. Subsequent SPR analysis on serial dilutions of the TAPP-1 PH domain indicated that the unexpectedly high affinity observed towards PtdIns(3,4,5)P_3 is not due to saturating concentrations of the protein but may genuinely reflect its selectivity under these circumstances (data not shown). This supports a previous study which suggested that the selectivity of TAPP-1 for PtdIns(3,4)P_2 over PtdIns(3,4,5)P_3 may not be as high as previously reported [327].

Figure 5.7 SPR reveals PtdIns(3,4,5)P_3-dependent binding by C-IQGAP1 and PARIS-1 PH domain.

A-D and F. The phosphoinositide binding selectivity of C-IQGAP and PARIS-1 is qualitatively similar to Grp-1. GST-tagged constructs of Grp-1 (A), TAPP-1 (B), PLC-δ (C), PARIS-1 (D) and C-IQGAP1 (F) all at 50nM except PARIS-1 (1μM) were passed over streptavidin (SA) chips without lipids or pre-loaded with equal amounts of PtdIns(3,4)P_2 (red), PtdIns(4,5)P_2 (black) and PtdIns(3,4,5)P_3 (green), asdetailed in Materials and Methods, and any interactions recorded as SPR response units. Experiments are representative of data from a range of concentrations and were observed on at least one further occasion.

E and G. The concentration dependent binding of IQGAP-1 and PARIS-1 to PtdIns(3,4,5)P3. The C-terminal construct of IQGAP1 and the PH domain of PARIS-1 (1-150) at the concentrations indicated were passed over SA chips pre-loaded with PtdIns(3,4,5)P_3 in concentrations as indicated. The protein concentrations were applied sequentially from low to high. The sensorgrams shown are representative of those obtained on at least two separate occasions.

Figure 5.7

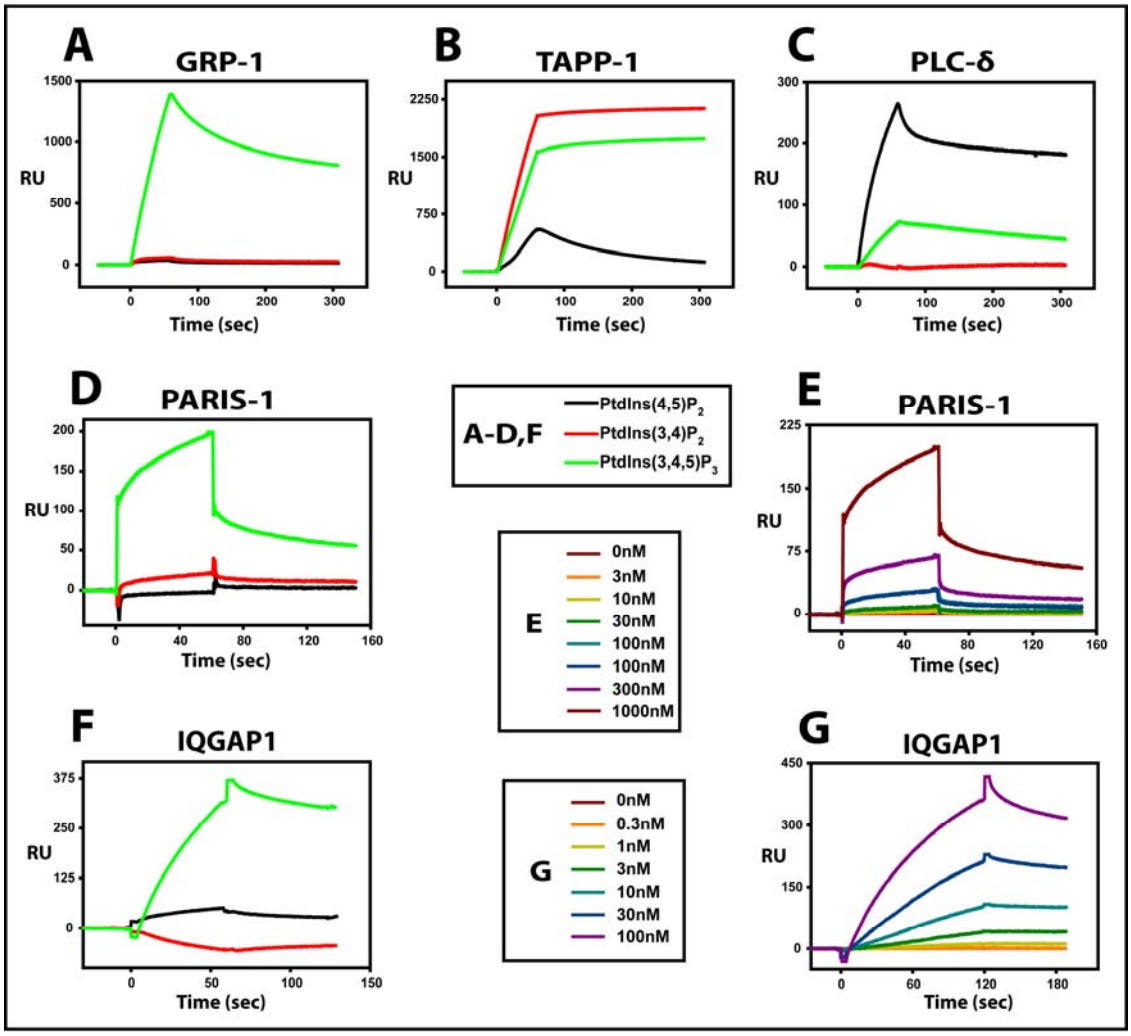
A
GRP-1
RU
Time (sec)
B
TAPP-1
RU
Time (sec)
C
PLC-δ
RU
Time (sec)
D
PARIS-1
RU
Time (sec)
A-D,F
PtdIns(4,5)P2
PtdIns(3,4)P2
PtdIns(3,4,5)P3
E
PARIS-1
RU
Time (sec)
E
0nM
3nM
10nM
30nM
100nM
100nM
300nM
1000nM
F
IQGAP1
RU
Time (sec)
G
0nM
0.3nM
1nM
3nM
10nM
30nM
100nM
G
IQGAP1
RU
Time (sec)

Panels D and F of Figure 5.7 show the selectivity of the PARIS-1 PH domain and of a C-terminal construct of IQGAP1 (amino acids 718-1657, henceforth C-IQGAP1) respectively. Both candidate proteins show selectivity towards PtdIns(3,4,5)P_3 in a manner qualitatively similar to that of Grp-1. Furthermore, panels E and G show the concentration-dependent binding of PARIS-1 and C-IQGAP to PtdIns(3,4,5)P_3, an effect not observed for PtdIns(3,4)P_2 or PtdIns(4,5)P_2 (data not shown). Importantly however, the N-terminal half of IQGAP-1 showed no binding to PtdIns(3,4,5)P_3, and analysis of a mutant R18G PARIS-1 PH domain GST construct - with a critical arginine residue mutated to glycine - abolished the observed binding to PtdIns(3,4,5)P_3 seen with the PARIS-1 PH domain (data not shown). Whilst these proteins require more definitive characterisation by *in vivo* analysis, the extrapolation of a half maximal response for C-IQGAP1 of ~50nM is consistent with a range of affinities presented by other 3-PI interacting proteins [178,318]. These data combined with the structural homology of PARIS-1 to established lipid binding PH domains and the spatial presentation of key residues within C-IQGAP1, argue that both candidate proteins represent authentic targets for either regulation or recruitment by 3-PIs, particularly PtdIns(3,4,5)P_3.

Similar SPR analyses for other recombinant GST-tagged candidate proteins from the subset selected previously, including CLIC1 and several additional control proteins of established lipid binding affinity, are qualitatively interpreted within Table 5.1. The range and magnitude of the interactions between candidate proteins and the presented lipid ligands, in conjunction with the lipid selectivity demonstrated by control proteins (Grp-1, TAPP-1, PLC-δ, lamellipodin

and PKB) presents a convincing argument that test protein interactions are genuine and not a consequence of non-specific interaction to the SPR chip surface. Interestingly, both lamellipodin and the PKB PH domain demonstrated selectivity for PtdIns(3,4,5)P_3, instead of the literature reported selectivity of PtdIns(3,4)P_2 and dual PtdIns(3,4,5)P_3/PtdIns(3,4)P_2 respectively [85,87,99]. This may be a consequence of the extended time with which these recombinant proteins have been stored and/or undergone freeze-thaw cycles; a feature carefully avoided for all candidate proteins expressed solely for the purpose of this study.

Table 5.1 also shows that CLIC1, in contrast to its initial identification through 3-PI mediated affinity purification and structural studies showing promise for lipid interaction, demonstrated little or no lipid binding capability. Whilst it is feasible that its initial enrichment was due to indirect 3-PI interaction, the possibility that expression as a tagged, recombinant protein prevented conformational changes required for CLIC1 binding, such as its dimerisation, remain. Equally, CLIC1 may depend on other physiological features of a bilayer for lipid binding, a requirement compatible with its role as a transmembrane ion channel. These issues might be addressed by cellular experiments to determine the localisation of CLIC1 under a variety of conditions.

In order for inclusion within Table 5.1 of candidate proteins, qualitative assessment of lipid binding required analysis of at least five protein concentrations across two orders of magnitude and incorporating at least one concentration duplicate (ie 3nM, 10nM, 30nM, 100nM, 100nM, 300nM). Those proteins whose lipid binding selectivity is recorded as not determined (ND) within Table 5.1

represent proteins for which the data is too limited to meet this requirement or where the expressed protein was deemed of insufficient quantity or purity. These data, although not conclusive, provide proof of principle that present within the candidates identified via the SILAC labelled triple-affinity screen are a number of genuine lipid interacting proteins.

Table 5.1 SPR reveals novel 3-PI binding proteins. The binding of candidate and positive control proteins was assessed qualitatively on the basis of SPR analysis. Interactions with PtdIns(3,4)P_2, PtdIns(4,5)P_2 and PtdIns(3,4,5)P_3 are indicated as follows: no interaction "-", limited interaction "+", concentration (analyte) dependent interaction "++", interaction comparable to Grp1/TAPP-1/PLC-δ "+++". (PARIS-1 R18G PH represents a R18G mutation which eliminates binding). Typically lipid binding was determined over at least five protein concentrations (ranging from 0.1nM to 1μM) across two orders of magnitude and incorporated at least one concentration duplicate. Those recorded as not determined (ND) represent proteins whose purity or concentration was deemed insufficient to permit adequate analysis but which were nevertheless cloned and expressed for this purpose.

Table 5.1

PROTEIN \ LIPID	PtdIns(3,4,5)P3	PtdIns(4,5)P2	PtdIns(3,4)P2
Grp-1 PH	+++	-	-
TAPP-1 PH	++	+	+++
PLC-δ PH	+	+++	-
CLIC1	-	-	-
PARIS-1 PH	++	-	+
PARIS-1 R18G PH	-	-	-
C-IQGAP1	+++	-	-
N-IQGAP1	-	-	+
PFN	+	+	+
OSBPL11	-	+	+
YES1	-	-	-
CRT	-	-	-
KDEL	-	-	+
LAMELLIPODIN	++	-	-
PKB	++	-	-
PKM2	-	-	-
RACK1	-	-	-
EIF4G1	-	-	-
FERMT2	ND	ND	ND
FOXK2	ND	ND	ND
ANKFY1	ND	ND	ND
EPSIN1	ND	ND	ND
VCL	ND	ND	ND
SPARC	ND	ND	ND
SERPIN	ND	ND	ND
SOLO	ND	ND	ND
ANNEXIN A6	ND	ND	ND
PICALM	ND	ND	ND
FBBP9	ND	ND	ND
PXK	ND	ND	ND

5.2.4 Cellular Translocation studies.

Having identified candidate proteins which demonstrated a 3-PI mediated interaction by *in vitro* analysis; the cellular lipid binding characteristics of candidate proteins were investigated, where time allowed. Preliminary experiments focussed on tracking the localisation of candidate proteins following bpV(phen) treatment of 1321N1 cells, digitonin permeabilisation and Ins(1,3,4)P_3 elution, with membrane fractions subsequently recovered by TX-100. Samples from each fraction were then immunoblotted with antibodies against the candidate protein. Examples of these immunoblots for tracking the cellular location including PARIS-1, CLIC1 and TAPP-1 are shown in Figure 5.8**.** Whilst untreated control samples confirmed that each of these proteins was predominantly cytosolic (data not shown), treatment with bpV(phen) resulted in the recovery of a proportion of each in the final membrane fraction, consistent with their initial enrichment and identification in Chapter 4. Indeed, similarly to TAPP-1, preliminary experiments showed that CLIC1 could then be in part recovered from membranes by elution with Ins(1,3,4)P_3. However, efforts to repeat these data for CLIC1 were confounded by the inability to record its localisation in any fraction, other than cytosol. Despite this, the initial identification of CLIC1 with an enriched SILAC ratio, the preliminary data within Figure 5.8 and the structural model proposing a potentially appropriate binding pocket, all indicate that further work to examine the potential binding characteristics and/or conditions of CLIC1 is warranted.

Figure 5.8 The cellular translocation of candidate proteins.

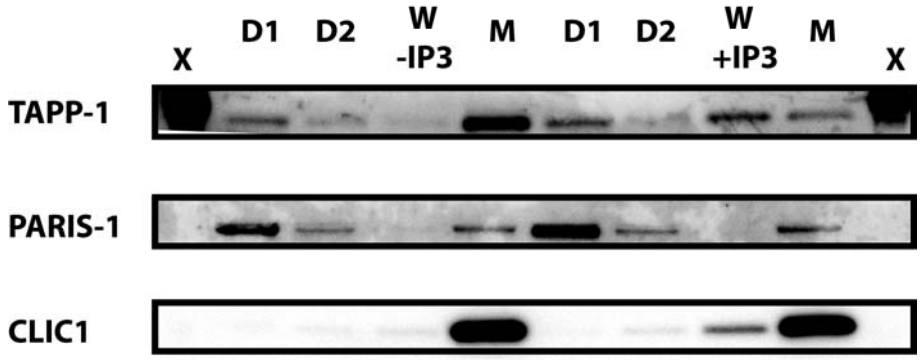

Cell fractions from bpV(phen) treated 1321N1 cells were permeabilised with consecutive 10 min digitonin washes (D1 and D2) followed by wash buffer for 30min at 4°C ±50μM Ins(1,3,4)P_3 elution (W±IP3) and finally residual membrane fractions (M) were recovered by TX-100. Fractions were then analysed by SDS-PAGE and immunoblotted for TAPP-1, PARIS-1 and CLIC1. Lanes marked X represent marker lanes. Experiments are representative of an n=1 for CLIC1 but PARIS1 and TAPP-1 data are representative of data obtained on at least two further occasions.

In contrast, PARIS-1 reproducibly demonstrated membrane translocation, to a limited extent, following treatment with bpV(phen). However, Ins(1,3,4)P_3 elution from these bpV(phen) treated, digitonin permeabilised membranes, as reflected in Figure 5.8 appeared to recover little or no PARIS-1. Despite this lack of Ins(1,3,4)P_3 elution the membrane translocation shown in Figure 5.8, coupled to the initial wortmannin dependent MS identification (Figure 4.3) is consistent with a 3-PI mediated interaction. Indeed, the demonstrated selectivity of PARIS-1 for PtdIns(3,4,5)P_3 by the *in vitro* lipid binding assays would suggest it may be prudent to repeat these translocation experiments. Ideally, these would use both; a ligand known to stimulate an increase in PtdIns(3,4,5)P_3 concentrations, such as PDGF/EGF; and an Ins(1,3,4,5)P_4 elute with which to recover PARIS-1 from the stimulated, permeabilised cells. In an attempt to address this requirement, an EGFP PARIS-1 PH domain fusion protein (amino acids 1-150 construct) was expressed in HeLa cells, to allow comparison between the effects of PDGF and bpV(phen) treatment on the translocation of this construct. Unfortunately, the subsequent analysis by immunofluorescence microscopy revealed a predominantly cytosolic localisation, regardless of stimuli (data not shown). These data may, however, be compromised by the level of over-expression of the construct, masking the ~10-20% of PARIS-1 driven to membrane following bpV(phen) treatment as reported by the biochemical data, such as that in Figure 5.8.

Similar, immunoblotting experiments to those described within Figure 5.8 but measuring the localisation of IQGAP1 in 1321N1 cells found that ~50% was membrane bound under basal conditions and this was not increased by bpV(phen) treatment (data not shown). The ability of an Ins(1,3,4)P_3 elution step to diminish

this proportion of IQGAP1 retained on the membrane remains untested, however, data presented for the *in vitro* selectivity (Figure 5.7) would suggest that, similarly to PARIS-1, this would be better undertaken with PDGF/EGF stimulation, and elution with Ins(1,3,4,5)P_4.

5.3 Discussion.

Whilst bioinformatics and affinity chromatography approaches have been successfully used previously to identify 3-PI effector proteins [89,98,102,174], both approaches have their drawbacks. Bioinformatics approaches have a bias derived from their reliance on established LBD structures to predict new, similar LBD. Affinity chromatography approaches, often rely on domain features previously identified by bioinformatics, to select proteins of interest from a large data set, thereby eliminating the possibility of identifying novel LBDs. This study aims to take advantage of one of the significant features of SILAC labelling – that of unbiased identification on the basis of quantitative enrichment – in an attempt to identify novel PtdIns(3,4)P_2 and other 3-PI interacting proteins, irrespective of modular domains. Furthermore, this chapter questions the perceived dependence on a limited number of binding domains for protein-lipid interaction and presents a sensitive, automated assay by which to reliably characterise the lipid binding selectivity of the many candidate proteins emerging from the SILAC based screen.

Despite the focus they receive, PH domains or even the structural features which define them do not have a monopoly on lipid binding. One defining feature of PH domains is their conserved secondary structure of the familiar β-sandwich comprising seven β-strands in a "barrel" formation. This scaffold is seen in many similar motifs belonging to the larger PTB/PH family of proteins include the PTB, PDZ and FERM domains, capable of interacting with a wide range of ligands [120]. The evolutionary persistence of this structure presents a compelling argument that it is merely an amenable scaffold for creating a ligand binding pocket and that the superstructure of the domain provides little indication of ligand

specificity. Equally, the existence of other structural motifs which share little or no homology but are capable of interaction with identical ligands supports the hypothesis that domains are merely a structural scaffold within which to present key residues. This is best exemplified by the FYVE and PX domains whose sequence and structure are distinct from each other but examples of which recognise an identical ligand, PtdIns3P, with high selectivity [25,119-121].

Perhaps however, the most pertinent demonstration that requirement of a conserved structural scaffold is not required for preferential lipid binding is provided by the significant number of proteins capable of highly selective lipid recognition, that possess no obviously conserved domain homology. Examples of these include; class I PI 3-kinases, capable of selective recognition of PtdIns(4,5)P_2 [328-330]; PTEN, proposed to have a PtdIns(4,5)P_2 binding site, but also capable of specifically recognising its substrate, PtdIns(3,4,5)P_3 [331-334]; the Ins(1,4,5)P_3 receptor, for selective recognition of Ins(1,4,5)P_3 [27,32]; and Ins(1,4,5)P_3 3-kinase, equally capable of substrate recognition for the synthesis of Ins(1,3,4,5)P_4 [35]. That this large number of proteins is capable of recognising PIs or their corresponding inositol phosphate head-group in the absence of a recognised LBD implies that the list of binding domains may not yet be complete, or that conserved structures are not always required. This view in conjunction with the evidence that PtdIns(3,4)P_2 may act as an independent lipid signal, prompts the need for further, unbiased studies such as this to seek additional, potential 3-PI effector proteins.

Having identified candidate 3-PI interacting proteins through a multi-tiered affinity purification approach, the lipid binding capability of these candidates was then assessed primarily by an SPR based assay. The significant advantage that this approach offers is measurement of real time association/dissociation of ligand-analyte complexes; particularly relevant when analysing low affinity binding. Whilst this is by no means the first application of SPR technology to addressing the lipid binding capability of candidate proteins, most other studies utilising SPR do so by layering lipid vesicles onto hydrophobic chips [317,318]**.** Whilst this, undoubtedly presents the lipid in a more appropriate physiological form, the avidin-biotin presentation used within this study is consistent with the initial method of candidate purification. Furthermore, the effectiveness of this manner of lipid presentation is validated by the identity of numerous proteins from the SILAC screens with established lipid binding capability, such as TAPP-1, PKB, SWAP-70, ARAP1 and EEA1. In addition, this immobilised lipid approach benefits from greater reproducibility due to the more simplistic nature of the ligand presentation. Lastly, the shorter chain, water soluble biotinylated-lipids are more amenable to buffered long term storage than the equivalent longer chain lipids used for vesicle generation.

One limitation, however, of the current SPR assay format is the need to extrapolate kinetic data based on approximations of the protein concentration at which half maximal binding is achieved. Although this is accepted as a suitable means of determining lipid-protein interaction in SPR studies [309,318], there are several factors which undoubtedly complicate any kinetic data derived from this assay. Firstly, the extent to which the GST-fusion proteins used within these

studies dimerise, which could contribute to a low off-rate, remains unclear [318,335]. Secondly, the presentation of the biotinylated lipid on the streptavidin chip, although consistent with the method of isolation, presents pure ligand in contrast to the mixed nature of lipids in a cell membrane, possibly contributing to artificially low off-rates. Finally, a feature intrinsic of the technology is limitation by the effects of mass transport, which irrespective of the analyte's affinity, limits the recorded on-rate to the flow rate and concentration by which the analyte can be delivered to the chip surface [319]. Regardless of these caveats, the SPR approach described in this study offers significant advantages over alternative *in vitro* approaches and presents a viable assay for determining lipid selectivity. This is demonstrated by the selectivity shown for domains of known lipid binding selectivity, including TAPP-1, Grp-1 and PLC-δ PH domains and candidate proteins of unknown selectivity alike.

PARIS-1, one of the primary candidates isolated in a PI 3-kinase-dependent manner, demonstrates a selective and concentration-dependent increase in the binding towards PtdIns(3,4,5)P_3. Indeed, the capacity of PARIS-1 PH domain to bind lipid was further supported by data generated from fat blots. Significantly, the observed lipid binding of PARIS-1 PH was abolished following mutation of the crucial arginine residue within the binding pocket (R18G). These binding data are consistent with the sequence alignments of PARIS-1 PH domain, suggesting homology with that of DAPP-1 and Grp-1.

In comparison to the analysis of the Grp-1 PH domain, however, PARIS-1 recorded smaller SPR response units for equivalent protein concentrations. Whilst

the magnitude of these responses does represent the mass of analyte bound to the chip surface and is suggestive of a lower affinity binding interaction than Grp-1, care must be taken when making comparative statements regarding affinity. Although protein concentrations were determined for each expressed protein, the effective concentration of protein, such as that correctly folded, may be markedly less. Furthermore, a significant component of the protein concentration may be from contaminant proteins or breakdown as a consequence of storage, giving an artificially high concentration. Alternatively, PARIS-1 may genuinely be of lesser affinity, possess distinct kinetics or require post translational modification (PTM) for full binding capability. Nonetheless, the functional relevance of PARIS-1 affinity is supported by both the initial purification of PARIS-1 from 3-PI enriched membranes and the, albeit limited, *in vivo* data which suggests that under certain conditions a proportion can be driven to cell membranes. Alternatively, the concept of PARIS-1 as a low affinity PtdIns(3,4,5)P_3 binding protein does not diminish the significance of its interaction. Whilst a low affinity, may not be sufficient to facilitate membrane recruitment in isolation, PtdIns(3,4,5)P_3 interaction may be required for regulation of enzymatic activity. Determining the effect of PtdIns(3,4,5)P_3 binding on the RabGAP activity of PARIS-1 is a current priority of continuing work on this protein.

A further primary candidate, identified with an enriched ratio in the initial SILAC experiment was CLIC1. In support of this PI 3-kinase-dependent enrichment, structural studies suggested that CLIC1 possesses a previously unrecognised motif presenting amino acids crucial for lipid binding in a remarkably similar spatial orientation to established LBDs. The role that CLIC1

seems to play as a ligand-responsive chloride channel capable of membrane insertion and the implication of its role in the oxidative damage associated with Alzheimer's disease identifies it as an intriguing candidate protein [250,252,253,255]. It has been shown that following treatment of microglial cells with β-amyloid and subsequent NADPH oxidase activation, CLIC1 translocates to and inserts into the membrane allowing flux of chloride ions [252]. Furthermore a separate study indirectly proposed a mechanism of activation via PI 3-kinases by showing PKB activation following treatment with β-amyloid peptide [336]. These data could be taken to suggest that PI 3-kinase activation may recruit and/or activate the NADPH oxidase complex via the $p47^{phox}$ PX domain whose interaction with PtdIns(3,4)P_2 is established [282]. CLIC1 may then require coincidence detection of ROS and PtdIns(3,4)P_2 for membrane insertion and ion channel activation. However, *in vitro* lipid binding analysis by SPR did not uphold this hypothesis, with little or no interaction to PtdIns(4,5)P_2, PtdIns(3,4)P_2 or PtdIns(3,4,5)P_3. Conversely, initial *in vivo* studies suggested bpV(phen)-dependent membrane recruitment and subsequent elution by Ins(1,3,4)P_3, although this result could not be reproduced. The ability of CLIC1 to bind lipids under varying conditions such as pH; increasing concentrations of divalent cations, particularly Mg^{2+}; and the presence of peroxide; which may more closely mimic conditions resulting in CLIC1 membrane insertion within glial cells, are features which can be readily addressed in the future.

The final primary candidate selected from the limited subset from Chapter 4 and highlighted within this Chapter, IQGAP-1 was similarly identified by an enriched SILAC ratio following 3-PI mediated membrane recruitment and

recovery. Structural studies revealed a C-terminal motif of unknown function that, despite fundamental differences to established LBD domains presented key residues for lipid binding in an analogous manner. Furthermore, *in vitro* lipid binding assays confirmed that an expressed C-terminal fragment of IQGAP1, of which the proposed motif is a component, demonstrated high selectivity and affinity towards PtdIns(3,4,5)P_3 comparable to that observed for the Grp-1 PH domain. Sequence homology searches of the putative, C-terminal lipid binding motif within IQGAP1 shows conservation among the other family members, IQGAP2 and IQGAP3. An assessment of any potential lipid binding associated with these proteins may determine if the motif identified within IQGAP1 represents a conserved novel lipid interacting domain or purely another example of a lipid recognition motif such as those described earlier for PTEN and the catalytic site of PI 3-kinases. Regardless, the interaction of IQGAP1 with PtdIns(3,4,5)P_3 proposes a novel mechanism of activation or regulation of the multitude of signalling pathways in which IQGAP-1 participates. Contrary to the presence of a GAP domain, IQGAP1 appears to act to maintain the active GTP bound state of Rac1 and Cdc42 [264,266,337]. This raises the intriguing question as to the effects of PtdIns(3,4,5)P_3 binding on the GAP activity of IQGAP1. Similarly to the hypothesis presented for PARIS-1, it may be that lipid binding is a mechanism for regulating IQGAP1 enzymatic activity, such as switching GAP activity on in the presence of PtdIns(3,4,5)P_3. Lastly, it may be of significance that this protein also possesses a calcium regulated calmodulin domain presenting the possibility that endogenously IQGAP1 is not regulated by PtdIns(3,4,5)P_3 but rather functions as a dual detector for calcium/Ins(1,3,4,5)P_4.

In conclusion, this Chapter assesses the lipid binding selectivity of a subset of candidates identified following a SILAC-coupled three-step affinity purification approach, and in particular focuses on PARIS-1, CLIC1 and IQGAP1. Firstly, this Chapter establishes that each possesses features consistent with lipid binding capability, despite only one of their number, PARIS-1, containing a currently recognised LBD. The identification of PARIS-1 and IQGAP1 proposes two previously unreported PtdIns(3,4,5)P_3 binding proteins and, in the case of IQGAP1, a potentially novel lipid interacting domain. The characterisation of the affinity and the functional consequences of IQGAP1 and PARIS-1 interaction with PtdIns(3,4,5)P_3 requires additional work. The possibility that both may have their GAP activity regulated by PtdIns(3,4,5)P_3 binding is an intriguing and readily testable hypothesis, assuming that a suitable small G protein, similar to Rac1 for IQGAP1, can be identified for PARIS-1- as currently this is unreported.

The identification of such a repertoire of established lipid binding protein from the three-tier affinity approach detailed in Chapter 4, including; AKT1, AKT2, AKT3, TAPP-1, SWAP-70, EEA1, OSBP, EPSIN1 and ARAP1 highlights the power and the utility of this approach. Importantly, the isolation of PARIS-1 and IQGAP1, and their identification as novel 3-PI interacting proteins strongly justifies the application of SILAC to a multi-step affinity purification technique to yield novel 3-PI interacting proteins.

Chapter 6.

General Discussion.

6. General Discussion.

6.1 Introduction

This thesis attempts to identify novel lipid interacting proteins with the aim of gaining a more comprehensive and clear view of PI 3-kinase signalling. Lipids have long been considered more than merely structural components of membranes, with their tightly regulated metabolism implicated in multifarious cell processes. Of particular significance are 3-phosphoinositides, due to the disproportionately important role they play in both normal and aberrant cell signalling pathways. Much focus has been directed at PtdIns(3,4,5)P_3, the primary product of class I PI 3-kinase activation [38,327,338,339]. However, in contrast little attention has been directed at PtdIns(3,4)P_2; a lipid whose synthesis from PtdIns(3,4,5)P_3 is tightly regulated by the 5-phosphatases and of which SHIP2, proposed as a therapeutic target for type II diabetes, is prominent [41].

Existing studies have had a tendency to focus on candidate lipid binding proteins expressing established LBDs [89,98,102,174]. This bias is either by design, as with bioinformatics screens, or applied indirectly as is the case with affinity purifications approaches, which often select from large data sets those candidates with domains of previously demonstrated lipid binding capability. This bias is undoubtedly a consequence of the combined shortcomings of single affinity precipitations and non-quantitative MS, which provide a very limited basis on which to discriminate authentically responsive proteins from non-specific, background binding proteins. This study aims to avoid these limitations and address the lack of attention received previously by PtdIns(3,4)P_2, by optimising

an unbiased, multiple-affinity based methodology founded on the primary recruitment of PtdIns(3,4)P_2 binding proteins in an authentic cellular environment.

6.2 The Optimisation of Three Affinity Purification Steps for the Identification of Novel 3-PI Interacting Proteins.

This approach utilises a unique, three-tier affinity purification approach in contrast to preceding studies which predominantly employ a single affinity step based on immobilised, synthetic lipid-coupled matrices to recover proteins from indiscriminate, mixed cell or tissue lysates. The first of the enrichment steps within this scheme takes advantage of the pharmacological inhibition of PTP-like phosphatases to constitutively activate class IA PI 3-kinases; increase the specific activity of the prominent 5-phosphatase, SHIP2; and inhibit the action of the 4-phosphatases [41]. The effect of these concerted actions is to favour the dramatic, but not exclusive, accumulation of PtdIns(3,4)P_2. The consequence of which is to allow recruitment to the membrane, of proteins capable of interacting with PtdIns(3,4)P_2. Subsequently, the digitonin permeabilisation of cells is then used to allow retention of these recruited proteins but removal of the bulk of background cytosolic contaminants. Crucially, this primary purification step offers a significant advantage over existing screens as proteins are present at physiological concentrations and are recruited to genuine lipid bilayers with all the additional physicochemical features associated with authentic cell membranes. Many of these features, such as background lipid composition, membrane curvature, protein content and the ionic environment are all important contributors to effector-protein membrane association/affinity [25,119,318], but are notoriously difficult to replicate *in vitro*. The efficiency of this membrane recruitment and of

the subsequent, additional two affinity enrichment steps, including the isomer-specific elution with a propitious concentration of the water-soluble head-group, Ins(1,3,4)P_3, was developed by monitoring the recovery of the archetypal PtdIns(3,4)P_2 binding protein TAPP-1, at each stage. Interestingly, the requirement for a 100-1000 excess mass of eluting Ins(1,3,4)P_3 over that of the estimated cellular PtdIns(3,4)P_2 to recover the majority of TAPP-1 may indicate the true selectivity of this protein for the lipid target presented in the context of a cellular membrane. The power of additional purification steps; both the Ins(1,3,4)P_3 elution and the biotinylated-PtdIns(3,4)P_2 precipitation was highlighted by the ultimate yield of multiple wortmannin-sensitive bands visible following SDS-PAGE analysis.

6.3 A SILAC-Coupled, Multi-tier Affinity Purification Scheme.

The integration of these individual strategies resulted in an approach more successful than each in isolation, revealing >10 protein bands either absent in control samples or significantly enriched in a PI 3-kinase-sensitive manner. Two of these enriched bands were isolated in sufficient quantity and purity, even in less refined samples, to be identifiable by MS. Their analysis revealed SWAP-70, an established 3-PI interacting protein [89,146], and the little studied, PH domain-containing PARIS-1 [232]. Whilst traditional MS techniques had been adequate for the identification of these relatively abundant candidates, the identities of those protein bands of more limited enrichment or of lesser abundance remained enigmatic. This difficulty in assigning candidate band identity highlights a limitation associated with non-quatitative MS analysis of complex samples – which is that this often generates a large number of protein matches, each with low

confidence. In order to facilitate the identification of a broader spectrum of the proteins that could be isolated by the three-tier affinity purification scheme, the differential metabolic labelling offered by SILAC was incorporated into the protocol. The rationale for this was that the quantitative ratio-metric output afforded by SILAC would reveal genuinely PI 3-kinase-responsive candidates with higher confidence and better discriminate these from background, contaminating proteins.

Indeed, the combined SILAC multi-step affinity purification process allowed the unequivocal MS identification of a number of proteins, recovered as a consequence of primary cellular PI 3-kinase activation, that were distinguishable from a multitude of co-purifying background proteins by their enriched isotopic profile. The identification of TAPP-1 as one of the most heavily enriched proteins confirms that this multi-affinity purification format can reveal not only PI 3-kinase-responsive proteins but also those which preferentially favour PtdIns(3,4)P_2. Equally, the identification of other proteins within these samples including all three isoforms of PKB, ARAP1 (centaurin-δ) and SWAP-70, each demonstrated to be capable of binding PtdIns(3,4)P_2 [85,87,89,100,146], further supports this view. The prominence of TAPP-1 and other known PtdIns(3,4)P_2 binding proteins within these lists therefore presents a compelling case that this experimental design can isolate novel candidates that possess similar 3-PI binding characteristics. The importance of the combined approach for purifying samples and distinguishing genuine 3-PI binding proteins is underlined by the observation that when the secondary affinity steps were omitted, markedly fewer established 3-PI interacting proteins yielded enriched SILAC ratios (data not presented).

This is not to assume that the lists of candidate proteins yielded from the three-tier affinity SILAC procedure represent the complete repertoire of PtdIns(3,4)P_2 binding proteins. Indeed, two proteins notable by their absence are lamellipodin and DAPP-1, reported to possess PtdIns(3,4)P_2 and dual PtdIns(3,4)P_2/PtdIns(3,4,5)P_3 selectivity, respectively [99,138]. Interestingly, analysis of lamellipodin by *in vitro* binding assays within this study, revealed an apparent selectivity for PtdIns(3,4,5)P_3. However, the absence of DAPP-1 and lamellipodin from the SILAC lists also may be readily explained either by their lack of expression in our system or by their inability to ionise or yield sufficient and/or unique peptides during MS/MS analysis. Furthermore, it is a distinct possibility that the SILAC lists incorporate proteins reflecting enriched ratios due to their indirect recruitment to membranes, possibly through adaptor proteins such as TAPP-1. Lastly, since the primary factor for SILAC enrichment is the activation of PI 3-kinase rather than the increased cellular accumulation of PtdIns(3,4)P_2 exclusively, enriched ratios for proteins with other 3-PI selectivities can be expected. This may explain the presence of EEA1 [25,340], ARAP1 [100] and SWAP-70 [89] within the SILAC lists, which are thought to interact preferentially with PtdIns3P and PtdIns(3,4,5)P_3 respectively .

6.4 The Validation of Candidate 3-PI Interacting Proteins.

The utility of the screen to identify novel 3-PI interacting proteins was tested by selecting a subset of some of the most promising candidates from those identified. The selection was achieved on the basis of (i) an enriched SILAC ratio, achieved in conjunction with the contribution to a given protein identity of at least

2 unique peptides, (ii) the association with PI 3-kinase related pathways or, (iii) the presentation of features compatible with lipid binding capability, although not necessarily expressed as an established LBD. The latter condition was determined by establishing conserved characteristics across a range of LBDs including C1, C2, FYVE, PX, ENTH, FERM and PH. The application of these three criteria resulted in the selection of a limited subset of candidate proteins (~20) from amongst >1500 protein identities. Furthermore, the third criterion revealed three primary candidates from within the subset of ~20 proteins, PARIS-1, CLIC1 and IQGAP-1, which were selected particularly as the focus for further study.

IQGAP1 and CLIC1 among these primary candidates appeared to possess domains of either uncharacterised or of unknown function, which exhibit remarkably similar characteristics to those crucial to binding pockets within established LBDs, yet exhibit little homology to the scaffold of these domains. IQGAP1 and CLIC1 therefore presented the opportunity to test the hypothesis that it is not the superstructure of the domain/motif which is significant, but rather the spatial presentation of key residues within this which determines the lipid selectivity/affinity. This notion is elegantly supported by the convergent evolution seen for PX and FYVE domain recognition of PtdIns3P. In addition, the PH domain-containing candidate PARIS-1, demonstrated sequence homology to PH domains of recognised 3-PI affinity and notably to that of Grp-1 and DAPP-1, particularly with respect to a glycine residue in the β1-β2 variable loop. In a analogous position, TAPP-1 has an alanine residue which occludes the 5-phosphate of the inositol head-group, a feature which has been suggested to

explain the reported selectivity of TAPP-1 for PtdIns(3,4)P_2 over PtdIns(3,4,5)P_3 [314].

The lipid binding capability of the primary candidates PARIS-1, CLIC1 and IQGAP1, as well as those from the wider subset which fulfilled the requirements previously described were determined by an *in vitro* SPR based assay. The advantages of this assay include; real-time association/dissociation; automation; ease of handling, afforded by the use of short-chain lipids as ligands and perhaps crucially, highly reproducible data sets. These features should make this approach particularly attractive to non-specialist labs that often, by necessity, use the accessible but flawed fat blotting approach, and allow for more reliable conclusions on lipid binding/selectivity to be drawn. The utility of the SPR screen was demonstrated by the selectivities observed for Grp-1 , TAPP-1 and PLC-δ PH domains towards PtdIns(3,4,5)P_3, PtdIns(3,4)P_2 and PtdIns(4,5)P_2 respectively, which are in accordance with those reported previously from multiple experimental approaches [102,193].

The primary candidates PARIS-1 PH domain and C-IQGAP1 both bound selectively and concentration dependently to PtdIns(3,4,5)P_3 but not to PtdIns(3,4)P_2 or PtdIns(4,5)P_2. Moreover, these lipid binding characteristics were not reproduced with a mutant PARIS-1 PH domain or an N-terminal fragment of IQGAP1, neither of which showed measurable binding to PtdIns(3,4,5)P_3. PARIS-1 is a little studied, 105kDa Rab GAP purported to be differently expressed between normal and cancerous prostate cells [232], and possesses a PH domain of previously unreported affinity or selectivity. IQGAP1, however, is a widely

studied 190kDa protein which is implicated in a number of roles modulating cytoskeletal architecture but does not contain a recognised LBD [263,265,266,337].

The efficiency of this unbiased three-tier affinity purification approach to identify protein(s) capable of lipid binding, regardless of reported domain features, is highlighted by the identification of IQGAP1 as a 3-PI interacting protein without an established LBD. Furthermore, the features presented by the putative LBD of IQGAP1 are consistent with the view that the lipid interaction is a consequence of the spatial presentation of key amino acids, similarly achieved by PH domains, despite little structural homology. The possibility that this spatial presentation of amino acids within a structure could be exploited by an informatics based tool to determine the characteristics of similar "orphan" crystal structures, to yield further potentially novel lipid interacting motifs is an appealing idea.

6.5 Future Work.

The utility of this screen was confirmed by the identification of numerous established 3-PI interacting proteins including TAPP-1, PKB, ARAP1 and SWAP-70. However, the identification within this screen of two novel 3-PI interacting proteins in PARIS-1 and IQGAP1 confirms the success of the approach in achieving its goal of identifying novel 3-PI interacting proteins. Moreover, the wider implication of their identification is that the candidate lists generated are likely to contain other, as yet, unrecognised proteins from PI 3-kinase signalling networks. Whilst immediate future work should centre on determining the functional consequences of lipid binding to both PARIS-1 and IQGAP1, more

long term future work should focus on characterising further candidates by applying the structural principles and anecdotal association to PI 3-kinase signalling networks,

Whilst more comprehensive *in vivo* analysis is required to ascertain the functional significance of the PARIS-1 PH domain interaction with PtdIns(3,4,5)P_3, preliminary *in vivo* data suggested that 3-PI-enriched membranes alone, may not be sufficient to result in marked translocation of PARIS-1 from the cytosol. This view is supported by the comparative SPR results which indicate that PARIS-1 PH domain may bind 3-PIs less strongly than other established target proteins such as Grp-1. However, the possibility that the PtdIns(3,4,5)P_3 selectivity demonstrated by the PARIS-1 PH domain contributes to regulation of its enzymatic activity remains, and is not without precedent. Both PKB and, perhaps more pertinently, SWAP-70 have been shown to increase their activity as a consequence of lipid binding [89,341]. The possibility that the Rab GAP activity of PARIS-1 is affected in the same manner as the PtdIns(3,4,5)P_3-dependent Rac GEF activity of SWAP-70 is eminently testable, assuming that its appropriate Rab G-protein(s) can be identified.

In contrast to PARIS-1, much is known about the proteins with which IQGAP1 interacts. It has numerous domains including a calponin homology domain, a WW domain, IQ repeats and the Ras GTPase-activating protein related domain (GRD) [266]. These have been shown to facilitate interaction and mediate inputs from a diverse group of proteins including actin, β-catenin, E-cadherin, ERK1/2, PKA, calmodulin, Cdc42 and Rac1 [261,263,265,266,337]. Indeed,

although the prominent molecular function remains unclear, IQGAP1 has been postulated as an oncogene due its involvement in the modulation of cell-cell attachments and actin polymerisation [264,266]. Decreased adhesion and increased motility, features also required for metastasis, have been reported following increased IQGAP1 expression or the translocation of endogenous IQGAP1 to cell-cell junctions [266]. Moreover, E-cadherin and calmodulin have been shown to compete for IQGAP1 binding and following deletion of a C-terminal region of IQGAP1, which includes the putative LBD suggested by this study, an increase in the calmodulin bound proportion and reduction in the cell-periphery, E-cadherin bound proportion of IQGAP1 has been observed [342]. This result is consistent with the notion that PtdIns(3,4,5)P_3 is required for its translocation or interaction at sites of cell-cell contact. The apparent selective localisation of IQGAP1 at the leading edge of migrating cells [261], a characteristic common to PI 3-kinases and PtdIns(3,4,5)P_3 further emphasises this point. It is perhaps, however, not such a surprise that the limited *in vivo* data generated indicated that acute stimulation of PI 3-kinases did not dramatically alter the cellular localisation of IQGAP1, a protein clearly so integral to formation of large cytoskeletal complexes. Alternatively, similarly to that suggested for PARIS-1, the affinity of IQGAP1 for PtdIns(3,4,5)P_3 may not be sufficient for translocation, instead providing a mechanism for coincident activation or the differential regulation of its GRD and/or that of its associated protein interacting partners. Nonetheless, the involvement of IQGAP1 in several cellular processes in which PI 3-kinase exerts an effect, the analogous localisation profiles to PtdIns(3,4,5)P_3 and the binding presented in this study, implies a close integration of these components. Lastly, the sequence analysis of IQGAP family members,

IQGAP2 and IQGAP3 confirms that both possess homologous C-terminal regions to that of the proposed LBD of IQGAP1. The analysis of the lipid binding capability of these isozymes would determine if the motif present within IQGAP1 indeed represents an example of a conserved, novel LBD.

As alluded to earlier, longer term work should focus on determining the lipid binding capability of additional candidates suggested by this screen. This could be achieved by selecting candidates in an entirely unbiased fashion or advised by structural features and/or involvement in PI 3-kinase-dependent signalling pathways. An alternative strategy, however, would be select the most prominent candidates over the course of numerous, additional experimental repeats. This strategy of gaining repeated enrichment ratios for each protein, whilst profligate in expensive reagents would provide a statistical means by which to select potential candidates for lipid binding analysis. Furthermore, advised by this present study, the opportunity to repeat these SILAC based experiments would allow for subtle modification to the approach in order to maximise both the recovery of specific PtdIns(3,4)P_2 binding proteins and, a more comprehensive set of chemically unmodified but isotopically labelled peptides. These modifications could be achieved by the complete elimination of Ins(1,3,4)P_3 carry through from the second to the third affinity purification step by more rigorous intermediate chromatography, and the use of amino acid-specific isotope labels coupled to the use of more MS compatible stains respectively.

6.6 The Broad Implications of this Study for PtdIns(3,4)P_2 as a Lipid Signal.

To date, there have been few selective binding proteins suggested for PtdIns(3,4)P_2, in stark contrast the number of molecular targets identified for PtdIns(3,4,5)P_3. However, some of the latter are limited in their capability to distinguish between PtdIns(3,4,5)P_3 and PtdIns(3,4)P_2, and several examples of these occupy key signalling nodes, such as PKB and PDK1 [85-87,104,130]. Such observations coupled to the lack of distinct PtdIns(3,4)P_2 effector proteins has contributed to the notion that these lipids fulfil a combined role. This screen, through primary PI 3-kinase activation and the manipulation of PTP-like phosphatases, attempted to identify novel PtdIns(3,4)P_2 binding proteins and hence contribute understanding to its role as an independent signal.

It is, however, apparent that both novel lipid interacting proteins identified by this screen, PARIS-1 and IQGAP-1, appear to be selective for PtdIns(3,4,5)P_3. Although several other candidates did show minimal PtdIns(3,4)P_2 binding, none showed high selectivity and affinity. Whilst the prospect remains that PtdIns(3,4)P_2 does not possess independent signalling roles and is purely a metabolite of PtdIns(3,4,5)P_3, there is now considerable evidence to the contrary. This evidence includes, principally, the existence of a mechanism for the independent synthesis of PtdIns(3,4)P_2 [41] and the existence of an established selective binding protein, TAPP-1 [102]. It is feasible that features of this screen have inadvertently undermined the ability to isolate novel PtdIns(3,4)P_2 binding proteins. Specifically, the presence of competing concentrations of Ins(1,3,4)P_3,

introduced at the second affinity purification step, which may well interfere with the binding to the immobilised lipid precipitation. However, this feature seemed to have a negligible effect on the depletion of the model PtdIns(3,4)P_2 binding protein, TAPP-1. A remaining possibility therefore, is that candidates may have simply been missed in the analysis or selection stage in the current SILAC lists and their selectivity is yet to be revealed by appropriate binding studies. In this case these candidates will benefit from the longer term further work described above and particularly, become evident following statistical analysis of multiple experiments.

Perhaps, it may simply be an attribute of the output of class I PI 3-kinase signalling that few molecular targets possess extremes of selectivity (Grp-1 and TAPP-1) whilst most demonstrate overlapping selectivities (PKB, PDK1, SWAP-70, DAPP-1 etc. etc.). This may mean that few specific PtdIns(3,4)P_2 binding proteins exist but does not necessarily detract from the signalling role this lipid may play. For instance, a range of proteins each with overlapping, but discrete selectivities would allow a highly sensitive mechanism to respond to subtle fluctuations in the balance between cellular PtdIns(3,4)P_2 and PtdIns(3,4,5)P_3 concentrations. Alternatively, the distribution of these 3-PI binding proteins may not be equal across a spectrum of lipid selectivities, ranging from those highly PtdIns(3,4)P_2-specific at one end to those highly PtdIns(3,4,5)P_3-specific at the another. In this scenario it may be possible to achieve activation of critical pathways, such as PKB/PDK1 with either ligand but further housekeeping or structural modifications through only one or the other. Speculatively, this may be demonstrated by examples isolated within this screen. For instance, PtdIns(3,4)P_2

and PtdIns(3,4,5)P_3 activate PKB, but PtdIns(3,4,5)P_3-interacting Rho/Rab G-protein regulators such as ARAP1, SWAP-70, PARIS-1 and IQGAP-1 may allude to a mechanism whereby PtdIns(3,4)P_2 is a means to activate PKB without co-incident alteration of Rho/Rab activity .

6.7 Concluding Remarks.

In conclusion, this study describes the development of an unbiased screen for the identification of novel PtdIns(3,4)P_2 and other 3-PI interacting proteins utilising a distinctive, multi-tier affinity-purification approach coupled to SILAC. This unique, quantitative approach results in the successful isolation of two novel lipid binding proteins. Firstly, PARIS-1, a little studied PH domain containing Rab GAP suggested as a marker for prostate cancer. Secondly, the much studied IQGAP1 implicated in a diverse range of cellular processes and proposed as an oncogene. Furthermore, the concentration-dependent binding of the C-terminal fragment of IQGAP1, analogous to that of Grp-1, is achieved without the expression of a recognised LBD. These data raise the exciting prospect that IQGAP1 exemplifies a novel, uncharacterised lipid binding motif. It is anticipated that the future characterisation of PARIS-1 and IQGAP1, as well as other candidates yet to be further investigated will both extend the current repertoire of 3-PI effector proteins and contribute to the wider understanding of the PI 3-kinase signalling network.

Bibliography

[1] Filmore, D. (2004). It's a GPCR world. Modern Drug Discovery. American Chemical Society, November, 24-28.

[2] Rall, T.W. and Sutherland, E.W. (1958). Formation of a cyclic adenine ribonucleotide by tissue particles. J. Biol. Chem. 232, 1065-76.

[3] Hokin, M.R. and Hokin, L.E. (1953) Enzyme secretion and the incorporation of 32P into phospholipids of pancreas slices. J. Biol. Chem. 203, 967-977.

[4] Anderson, R.J. (1930). The Chemistry of the Lipoids of Tubercle Bacilli. XIV. The Occurrence if Inosite in the Phosphatidate of Human Tubercle Bacilli. J. Am. Chem. Soc. 52, 1607-1608.

[5] Woolley, D.W. (1943) Isolation and partial determination of structure of soybean lipositol, a new inositol-containing phospholipid. J. Biol. Chem. 147, 581-591.

[6] Folch, J. (1949). Brain diphosphoninositide, a new phosphatide having inositol metadiphosphate as a constituent. J. Biol. Chem. 177, 505-19.

[7] Folch, J. (1949). Complete fractionation of brain cephalin; isolation from it of phosphatidyl serine, phosphatidyl ethanolamine, and diphosphoinositide. J. Biol. Chem. 177, 497-504.

[8] Faure, M. and Morelec-Coulon, M.J. (1954). Isolation of a crystalline phosphatide from the beef myocardium; glycero-inosito-phosphatic acid. C. R. Hebd. Seances. Acad. Sci. 238, 411-2.

[9] Dawson, R.M. (1954). The measurement of 32P labelling of individual kephalins and lecithin in a small sample of tissue. Biochim. Biophys. Acta 14, 374-9.

[10] Pizer, F.L. and Ballou, C.E. (1959). Studies on myo-Inositol Phosphates of Natural Origin. Journal of the American Chemical Society 81, 915-921.

[11] Brown, D.M., Clark, B.F. and Letters, R. (1961). Phospholipids. Part VII. The structure of a monophosphoinositide. J. Chem. Soc., 3774-3779.

[12] Hanahan, D.J. and Olley, J.N. (1958). Chemical nature of monophosphoinositides. J. Biol. Chem. 231, 813-28.

[13] Brockerhoff, H. and Ballou, C.E. (1962). On the metabolism of the brain phosphoinositide complex. J. Biol. Chem. 237, 1764-6.

[14] Brockerhoff, H. and Ballou, C.E. (1962). Phosphate incorporation in brain phosphionositides. J. Biol. Chem. 237, 49-52.

[15] Grado, C. and Ballou, C.E. (1960). Myo-inositol phosphates from beef brain phosphoinostide. J. Biol. Chem. 235, 23-24.

[16] Grado, C. and Ballou, C.E. (1961). Myo-inositol phosphates obtained by alkaline hydrolysis of beef brain phosphoinositide. J. Biol. Chem. 236, 54-60.

[17] Hendrickson, H.S. and Ballou, C.E. (1964). Ion Exchange Chromatography of Intact Brain Phosphoinositides on Diethylaminoethyl Cellulose by Gradient Salt Elution in a Mixed Solvent System. J. Biol. Chem. 239, 1369-73.

[18] Pizer, L.I. and Ballou, C.E. (1959). Specificity of phosphoglyceric acid mutase. J. Biol. Chem. 234, 1138-42.

[19] Tomlinson, R.V. and Ballou, C.E. (1961). Complete characterization of the myo-inositol polyphosphates from beef brain phosphoinositide. J. Biol. Chem. 236, 1902-6.

[20] Tomlinson, R.V. and Ballou, C.E. (1962). Myoinositol polyphosphate intermediates in the dephosphorylation of phytic acid by phytase. Biochemistry 1, 166-71.

[21] Hawthorne, J.N. and Chargaff, E. (1954). A study of inositol-containing lipides. J. Biol. Chem. 206, 27-37.

[22] Dittmer, J.C. and Dawson, R.M. (1960). The isolation of a new complex lipid: triphosphoinostide from ox brain. Biochim. Biophys. Acta 40, 379-80.

[23] Stein, R.C. (2001). Prospects for phosphoinositide 3-kinase inhibition as a cancer treatment. Endocr. Relat. Cancer 8, 237-248.

[24] Stephens, L., McGregor, A. and Hawkins, P. (2000) Biology of Phosphoinositides, Oxford University Press. Oxford.

[25] Lemmon, M.A. (2008). Membrane recognition by phospholipid-binding domains. Nat. Rev. Mol. Cell. Biol 9, 99-111.

[26] Sankaran, V.G., Klein, D.E., Sachdeva, M.M. and Lemmon, M.A. (2001). High-affinity binding of a FYVE domain to phosphatidylinositol 3-phosphate requires intact phospholipid but not FYVE domain oligomerization. Biochemistry 40, 8581-7.

[27] Berridge, M.J. and Irvine, R.F. (1984). Inositol trisphosphate, a novel second messenger in cellular signal transduction. Nature 312, 315-21.

[28] Downes, C.P. and Carter, A.N. (1991). Phosphoinositide 3-kinase: a new effector in signal transduction? Cell Signal 3, 501-13.

[29] Coffer, P.J., Jin, J. and Woodgett, J.R. (1998). Protein kinase B (c-Akt): a multifunctional mediator of phosphatidylinositol 3-kinase activation. Biochem. J. 335 (Pt 1), 1-13.

[30] Overduin, M., Cheever, M.L. and Kutateladze, T.G. (2001). Signaling with Phosphoinositides: Better than Binary. Mol. Interv. 1, 150-159.

[31] Michell, R.H. (1975). Inositol phospholipids and cell surface receptor function. Biochimica et Biophysica Acta (BBA) - Reviews on Biomembranes 415, 81-147.

[32] Streb, H., Irvine, R.F., Berridge, M.J. and Schulz, I. (1983). Release of Ca2+ from a nonmitochondrial intracellular store in pancreatic acinar cells by inositol-1,4,5-trisphosphate. Nature 306, 67-9.

[33] Berridge, M.J. and Irvine, R.F. (1989). Inositol phosphates and cell signalling. Nature 341, 197-205.

[34] Shears, S.B. (1989). Metabolism of the inositol phosphates produced upon receptor activation. Biochem. J. 260, 313-24.

[35] Irvine, R.F., Letcher, A.J., Heslop, J.P. and Berridge, M.J. (1986). The inositol tris/tetrakisphosphate pathway[mdash]demonstration of Ins(l,4,5)P3 3-kinase activity in animal tissues. Nature 320, 631-634.

[36] Batty, I.R., Nahorski, S.R. and Irvine, R.F. (1985). Rapid formation of inositol 1,3,4,5-tetrakisphosphate following muscarinic receptor stimulation of rat cerebral cortical slices. Biochem. J. 232, 211-5.

[37] Whitman, M., Downes, C.P., Keeler, M., Keller, T. and Cantley, L. (1988). Type I phosphatidylinositol kinase makes a novel inositol phospholipid, phosphatidylinositol-3-phosphate. Nature 332, 644-646.

[38] Hawkins, P.T., Anderson, K.E., Davidson, K. and Stephens, L.R. (2006). Signalling through Class I PI3Ks in mammalian cells. Biochem. Soc. Trans. 34, 647-62.

[39] Traynor-Kaplan, A.E., Thompson, B.L., Harris, A.L., Taylor, P., Omann, G.M. and Sklar, L.A. (1989). Transient increase in phosphatidylinositol 3,4-

bisphosphate and phosphatidylinositol trisphosphate during activation of human neutrophils. J. Biol. Chem. 264, 15668-73.

[40] Traynor-Kaplan, A.E., Harris, A.L., Thompson, B.L., Taylor, P. and Sklar, L.A. (1988). An inositol tetrakisphosphate-containing phospholipid in activated neutrophils. Nature 334, 353-356.

[41] Batty, I.H., van der Kaay, J., Gray, A., Telfer, J.F., Dixon, M.J. and Downes, C.P. (2007). The control of phosphatidylinositol 3,4-bisphosphate concentrations by activation of the Src homology 2 domain containing inositol polyphosphate 5-phosphatase 2, SHIP2. Biochem. J. 407, 255-66.

[42] Macara, I.G., Marinetti, G.V. and Balduzzi, P.C. (1984). Transforming Protein of Avian Sarcoma Virus UR2 is Associated with Phosphatidylinositol Kinase Activity: Possible Role in Tumorigenesis. PNAS 81, 2728-2732.

[43] Whitman, M., Kaplan, D.R., Schaffhausen, B., Cantley, L. and Roberts, T.M. (1985). Association of phosphatidylinositol kinase activity with polyoma middle-T competent for transformation. Nature 315, 239-242.

[44] Kaplan, D.R., Whitman, M., Schaffhausen, B., Pallas, D.C., White, M., Cantley, L. and Roberts, T.M. (1987). Common elements in growth factor stimulation and oncogenic transformation: 85 kd phosphoprotein and phosphatidylinositol kinase activity. Cell 50, 1021-1029.

[45] Varticovski, L., Druker, B., Morrison, D., Cantley, L. and Roberts, T. (1989). The colony stimulating factor-1 receptor associates with and activates phosphatidylinositol-3 kinase. Nature 342, 699-702.

[46] Fry, M.J. (1994). Structure, regulation and function of phosphoinositide 3-kinases. Biochimica et Biophysica Acta (BBA) - Molecular Cell Research 1226, 237-268.

[47] Rameh, L.E. and Cantley, L.C. (1999). The role of phosphoinositide 3-kinase lipid products in cell function. J. Biol. Chem., 8347-8350.

[48] Katso, R., Okkenhaug, K., Ahmadi, K., White, S., Timms, J. and Waterfield, M.D. (2001). CELLULAR FUNCTION OF PHOSPHOINOSITIDE 3-KINASES: Implications for Development, Immunity, Homeostasis, and Cancer. Annual Review of Cell and Developmental Biology 17, 615-675.

[49] Vanhaesebroeck, B. et al. (2001). Synthesis and function of 3-phosphorylated inositol lipids. Annual Review of Biochemistry 70, 535-602.

[50] Foster, F.M., Traer, C.J., Abraham, S.M. and Fry, M.J. (2003). The phosphoinositide (PI) 3-kinase family. J. Cell. Sci. 116, 3037-3040.

[51] Maffucci, T., Cooke, F.T., Foster, F.M., Traer, C.J., Fry, M.J. and Falasca, M. (2005). Class II phosphoinositide 3-kinase defines a novel signaling pathway in cell migration. J. Cell Biol. 169, 789-799.

[52] Meunier, F.A., Osborne, S.L., Hammond, G.R.V., Cooke, F.T., Parker, P.J., Domin, J. and Schiavo, G. (2005). Phosphatidylinositol 3-Kinase C2{alpha} Is Essential for ATP-dependent Priming of Neurosecretory Granule Exocytosis. Mol. Biol. Cell 16, 4841-4851.

[53] Ming, G., Song, H., Berninger, B., Inagaki, N., Tessier-Lavigne, M. and Poo, M. (1999). Phospholipase C-gamma and phosphoinositide 3-kinase mediate cytoplasmic signaling in nerve growth cone guidance. Neuron 23, 139-148.

[54] Brunet, A., Datta, S.R. and Greenberg, M.E. (2001). Transcription-dependent and -independent control of neuronal survival by the PI3K-Akt signaling pathway. Current Opinion in Neurobiology 11, 297-305.

[55] Fry, M.J. (2001). Phosphoinositide 3-kinase signalling in breast cancer: how big a role might it play? Breast Cancer Res. 3, 304 - 312.

[56] Chen, S., Yan, W., Huang, J., Ge, D., Yao, Z. and Gu, D. (2005). Association analysis of the variant in the regulatory subunit of phosphoinositide 3-kinase (p85α) with Type 2 diabetes mellitus and hypertension in the Chinese Han population. Diabetic Medicine 22, 737-743(7).

[57] Dillon, R.L., White, D.E. and Muller, W.J. (2007). The phosphatidyl inositol 3-kinase signaling network: implications for human breast cancer. Oncogene 26, 1338-1345.

[58] Stephens, L.R. et al. (1997). The G[beta][gamma] Sensitivity of a PI3K Is Dependent upon a Tightly Associated Adaptor, p101. Cell 89, 105-114.

[59] Maier, U., Babich, A. and Nurnberg, B. (1999). Roles of Non-catalytic Subunits in Gbeta gamma -induced Activation of Class I Phosphoinositide 3-Kinase Isoforms beta and gamma. J. Biol. Chem. 274, 29311-29317.

[60] Volinia, S. et al. (1995). A human phosphatidylinositol 3-kinase complex related to the yeast Vps34p-Vps15p protein sorting system. Embo J. 14, 3339-48.

[61] Wurmser, A.E., Gary, J.D. and Emr, S.D. (1999). Phosphoinositide 3-kinases and their FYVE domain-containing effectors as regulators of vacuolar/lysosomal membrane trafficking pathways. J. Biol. Chem. 274, 9129-32.

[62] Brian, P.W., Curtis, P.J., Hemming, H.G. and Norris, G.L.F. (1957). Wortmannin, an antibiotic produced by Penicillium wortmanni. Trans. Br. Mycol., 365-368.

[63] Baggiolini, M., Dewald, B., Schnyder, J., Ruch, W., Cooper, P.H. and Payne, T.G. (1987). Inhibition of the phagocytosis-induced respiratory burst by the

fungal metabolite wortmannin and some analogues. Exp. Cell Res. 169, 408-418.

[64] Arcaro, A. and Wymann, M.P. (1993). Wortmannin is a potent phosphatidylinositol 3-kinase inhibitor: the role of phosphatidylinositol 3,4,5-trisphosphate in neutrophil responses. Biochem. J. 296, 297-301.

[65] Vlahos, C.J., Matter, W.F., Hui, K.Y. and Brown, R.F. (1994). A specific inhibitor of phosphatidylinositol 3-kinase, 2-(4- morpholinyl)-8-phenyl-4H-1-benzopyran-4-one (LY294002). J. Biol. Chem. 269, 5241-5248.

[66] Besson, A., Robbins, S.M. and Wee Yong, V. (1999). PTEN/MMAC1/TEP1 in signal transduction and tumorigenesis. European Journal of Biochemistry 263, 605-611.

[67] Maehama, T. and Dixon, J.E. (1998) The Tumor Suppressor, PTEN/MMAC1, Dephosphorylates the Lipid Second Messenger, Phosphatidylinositol 3,4,5-Trisphosphate. J. Biol. Chem. 273, 13375-13378.

[68] Myers, M.P., Stolarov, J.P., Eng, C., Li, J., Wang, S.I., Wigler, M.H., Parsons, R. and Tonks, N.K. (1997) P-TEN, the tumor suppressor from human chromosome 10q23, is a dual-specificity phosphatase. PNAS 94, 9052-9057.

[69] Leslie, N.R., Bennett, D., Lindsay, Y.E., Stewart, H., Gray, A. and Downes, C.P. (2003). Redox regulation of PI 3-kinase signalling via inactivation of PTEN. Embo J. 22, 5501-10.

[70] Dyson, J.M., Kong, A.M., Wiradjaja, F., Astle, M.V., Gurung, R. and Mitchell, C.A. (2005). The SH2 domain containing inositol polyphosphate 5-phosphatase-2: SHIP2. The International Journal of Biochemistry & Cell Biology 37, 2260-2265.

[71] Sasaoka, T., Wada, T. and Tsuneki, H. (2006). Lipid phosphatases as a possible therapeutic target in cases of type 2 diabetes and obesity. Pharmacology & Therapeutics 112, 799-809.

[72] Habib, T., Hejna, J.A., Moses, R.E. and Decker, S.J. (1998). Growth Factors and Insulin Stimulate Tyrosine Phosphorylation of the 51C/SHIP2 Protein. J. Biol. Chem. 273, 18605-18609.

[73] Krystal, G. et al. (1999). Ships ahoy. The International Journal of Biochemistry & Cell Biology 31, 1007-1010.

[74] Ooms, L.M. et al. (2006). The Inositol Polyphosphate 5-Phosphatase, PIPP, Is a Novel Regulator of Phosphoinositide 3-Kinase-dependent Neurite Elongation. Mol. Biol. Cell 17, 607–622.

[75] Backers, K., Blero, D., Paternotte, N., Zhang, J. and Erneux, C. (2003). The termination of PI3K signalling by SHIP1 and SHIP2 inositol 5-phosphatases. Advances in Enzyme Regulation 43, 15-28.

[76] Raaijmakers, J.H., Deneubourg, L., Rehmann, H., de Koning, J., Zhang, Z., Krugmann, S., Erneux, C. and Bos, J.L. (2007). The PI3K effector Arap3 interacts with the PI(3,4,5)P3 phosphatase SHIP2 in a SAM domain-dependent manner. Cellular Signalling 19, 1249-1257.

[77] Norris, F.A., Auethavekiat, V. and Majerus, P.W. (1995). The Isolation and Characterization of cDNA Encoding Human and Rat Brain Inositol Polyphosphate 4-Phosphatase. J. Biol. Chem. 270, 16128-16133.

[78] Norris, F.A., Atkins, R.C. and Majerus, P.W. (1997). The cDNA Cloning and Characterization of Inositol Polyphosphate 4-Phosphatase Type II. Evidence for conserved alternative splicing in the 4-phosphatase family. Biol. Chem. 272, 23859-23864.

[79] Ivetac, I. et al. (2005). The Type I{alpha} Inositol Polyphosphate 4-Phosphatase Generates and Terminates Phosphoinositide 3-Kinase Signals on Endosomes and the Plasma Membrane. Mol. Biol. Cell 16, 2218-2233.

[80] Ferron, M. and Vacher, J. (2006). Characterization of the murine Inpp4b gene and identification of a novel isoform. Gene 376, 152-161.

[81] Norris, F.A. and Majerus, P.W. (1994). Hydrolysis of phosphatidylinositol 3,4-bisphosphate by inositol polyphosphate 4-phosphatase isolated by affinity elution chromatography. J. Biol. Chem. 269, 8716-8720.

[82] Bansal, V.S., Caldwell, K.K. and Majerus, P.W. (1990). The isolation and characterization of inositol polyphosphate 4- phosphatase. J. Biol. Chem. 265, 1806-1811.

[83] Klarlund, J.K., Guilherme, A., Holik, J.J., Virbasius, J.V., Chawla, A. and Czech, M.P. (1997) Signaling by Phosphoinositide-3,4,5-Trisphosphate Through Proteins Containing Pleckstrin and Sec7 Homology Domains. Science 275, 1927-1930.

[84] Salim, K. et al. (1996). Distinct specificity in the recognition of phosphoinositides by the pleckstrin homology domains of dynamin and Bruton's tyrosine kinase. Embo J. 15, 6241-50.

[85] Klippel, A., Kavanaugh, W.M., Pot, D. and Williams, L.T. (1997). A specific product of phosphatidylinositol 3-kinase directly activates the protein kinase Akt through its pleckstrin homology domain. Mol. Cell. Biol. 17, 338-44.

[86] Currie, R.A. et al. (1999). Role of phosphatidylinositol 3,4,5-trisphosphate in regulating the activity and localization of 3-phosphoinositide-dependent protein kinase-1. Biochem J. 337 (Pt 3), 575-83.

[87] Alessi, D.R., James, S.R., Downes, C.P., Holmes, A.B., Gaffney, P.R., Reese, C.B. and Cohen, P. (1997). Characterization of a 3-phosphoinositide-dependent protein kinase which phosphorylates and activates protein kinase Balpha. Curr. Biol. 7, 261-69.

[88] Anderson, K.E. et al. (2000). DAPP1 undergoes a PI 3-kinase-dependent cycle of plasma-membrane recruitment and endocytosis upon cell stimulation. Curr. Biol. 10, 1403-12.

[89] Shinohara, M. et al. (2002). SWAP-70 is a guanine-nucleotide-exchange factor that mediates signalling of membrane ruffling. Nature 416, 759-63.

[90] Lockyer, P.J., Wennström, S., Kupzig, S., Venkateswarlu, K., Downward, J. and Cullen, P.J. (1999). Identification of the Ras GTPase-activating protein GAP1m as a phosphatidylinositol-3,4,5-trisphosphate-binding protein in vivo. Current Biology 9, 265-269.

[91] Kobayashi, S., Shirai, T., Kiyokawa, E., Mochizuki, N., Matsuda, M. and Fukui, Y. (2001). Membrane recruitment of DOCK180 by binding to PtdIns(3,4,5)P3. Biochem J. 354, 73-8.

[92] Venkateswarlu, K., Oatey, P.B., Tavaré, J.M. and Cullen, P.J. (1998). Insulin-dependent translocation of ARNO to the plasma membrane of adipocytes requires phosphatidylinositol 3-kinase. Current Biology 8, 463-466.

[93] Chardin, P., Paris, S., Antonny, B., Robineau, S., Beraud-Dufour, S., Jackson, C.L. and Chabre, M. (1996). A human exchange factor for ARF contains Sec7- and pleckstrin-homology domains. Nature 384, 481-484.

[94] Kolanus, W., Nagel, W., Schiller, B., Zeitlmann, L., Godar, S., Stockinger, H. and Seed, B. (1996). [alpha]L[beta]2 Integrin/LFA-1 Binding to ICAM-1

Induced by Cytohesin-1, a Cytoplasmic Regulatory Molecule. Cell 86, 233-242.

[95] Venkateswarlu, K., Oatey, P.B., Tavare, J.M., Jackson, T.R. and Cullen, P.J. (1999). Identification of centaurin-alpha1 as a potential in vivo phosphatidylinositol 3,4,5-trisphosphate-binding protein that is functionally homologous to the yeast ADP-ribosylation factor (ARF) GTPase-activating protein, Gcs1. Biochem J. 340 (Pt 2), 359-63.

[96] Hammonds-Odie, L.P., Jackson, T.R., Profit, A.A., Blader, I.J., Turck, C.W., Prestwich, G.D. and Theibert, A.B. (1996). Identification and cloning of centaurin-alpha. A novel phosphatidylinositol 3,4,5-trisphosphate-binding protein from rat brain. J. Biol. Chem. 271, 18859-68.

[97] Rodrigues, G.A., Falasca, M., Zhang, Z., Ong, S.H. and Schlessinger, J. (2000) A Novel Positive Feedback Loop Mediated by the Docking Protein Gab1 and Phosphatidylinositol 3-Kinase in Epidermal Growth Factor Receptor Signaling. Mol. Cell. Biol. 20, 1448-1459.

[98] Krugmann, S. et al. (2002). Identification of ARAP3, a novel PI3K effector regulating both Arf and Rho GTPases, by selective capture on phosphoinositide affinity matrices. Mol. Cell 9, 95-108.

[99] Krause, M. et al. (2004). Lamellipodin, an Ena/VASP Ligand, Is Implicated in the Regulation of Lamellipodial Dynamics. Developmental Cell 7, 571-583.

[100] Miura, K. et al. (2002). ARAP1: A Point of Convergence for Arf and Rho Signaling. Mol. Cell 9, 109-119.

[101] Campa, F., Yoon, H.-Y., Ha, V.L., Szentpetery, Z., Balla, T. and Randazzo, P.A. (2009) A PH Domain in the Arf GTPase-activating Protein (GAP) ARAP1 Binds Phosphatidylinositol 3,4,5-Trisphosphate and Regulates Arf

GAP Activity Independently of Recruitment to the Plasma Membranes. J. Biol. Chem. 284, 28069-28083.

[102] Dowler, S., Currie, R.A., Campbell, D.G., Deak, M., Kular, G., Downes, C.P. and Alessi, D.R. (2000). Identification of pleckstrin-homology-domain-containing proteins with novel phosphoinositide-binding specificities. Biochem J. 351, 19-31.

[103] Manning, B.D. and Cantley, L.C. (2007). AKT/PKB signaling: navigating downstream. Cell 129, 1261-74.

[104] Vanhaesebroeck, B. and Alessi, D.R. (2000). The PI3K-PDK1 connection: more than just a road to PKB. Biochem. J. 346, 561-576.

[105] Alessi, D.R. (2001). Discovery of PDK1, one of the missing links in insulin signal transduction. Colworth Medal Lecture. Biochem. Soc. Trans. 29, 1-14.

[106] Sarbassov, D.D., Guertin, D.A., Ali, S.M. and Sabatini, D.M. (2005) Phosphorylation and Regulation of Akt/PKB by the Rictor-mTOR Complex. Science 307, 1098-1101.

[107] Alessi, D.R., James, S.R., Downes, C.P., Holmes, A.B., Gaffney, P.R.J., Reese, C.B. and Cohen, P. (1997). Characterization of a 3-phosphoinositide-dependent protein kinase which phosphorylates and activates protein kinase B[alpha]. Current Biology 7, 261-269.

[108] Klippel, A., Kavanaugh, W.M., Pot, D. and Williams, L.T. (1997) A specific product of phosphatidylinositol 3-kinase directly activates the protein kinase Akt through its pleckstrin homology domain. Mol. Cell. Biol. 17, 338-344.

[109] Groffen, J., Heisterkamp, N., Reynolds, F.H., Jr. and Stephenson, J.R. (1983). Homology between phosphotyrosine acceptor site of human c-abl and viral oncogene products. Nature 304, 167-9.

[110] Pawson, T., Olivier, P., Rozakis-Adcock, M., McGlade, J. and Henkemeyer, M. (1993) Proteins with SH2 and SH3 Domains Couple Receptor Tyrosine Kinases to Intracellular Signalling Pathways. Philos. Trans. R. Soc. Lond. B. Biol. Sci. 340, 279-285

[111] Pawson, T., Raina, M. and Nash, P. (2002). Interaction domains: from simple binding events to complex cellular behavior. FEBS Letters 513, 2-10.

[112] Pawson, T. and Scott, J.D. (1997) Signaling Through Scaffold, Anchoring, and Adaptor Proteins. Science 278, 2075-2080.

[113] Pawson, T. (1995). Protein modules and signalling networks. Nature 373, 573-580.

[114] Pawson, T. (2010) http://pawsonlab.mshri.on.ca/.

[115] Lab, N. (2010) http://sh2.uchicago.edu/.

[116] Schultz, J.r., Milpetz, F., Bork, P. and Ponting, C.P. (1998) SMART, a simple modular architecture research tool: Identification of signaling domains. PNAS 95, 5857-5864.

[117] Letunic, I., Doerks, T. and Bork, P. (2009). SMART 6: recent updates and new developments. Nucleic Acids Res. 37, 229-32.

[118] Harlan, J.E., Hajduk, P.J., Yoon, H.S. and Fesik, S.W. (1994). Pleckstrin homology domains bind to phosphatidylinositol-4,5-bisphosphate. Nature 371, 168-170.

[119] Kutateladze, T.G. Translation of the phosphoinositide code by PI effectors. Nat. Chem. Biol. 6, 507-513.

[120] Balla, T. (2005). Inositol-lipid binding motifs: signal integrators through protein-lipid and protein-protein interactions. J. Cell Sci. 118, 2093-104.

[121] Hurley, J.H. (2006). Membrane binding domains. Biochim. Biophys. Acta 1761, 805-11.

[122] Di Paolo, G. and De Camilli, P. (2006). Phosphoinositides in cell regulation and membrane dynamics. Nature 443, 651-7.

[123] Roth, M.G. (2004). Phosphoinositides in constitutive membrane traffic. Physiol. Rev. 84, 699-730.

[124] Kimber, W.A. et al. (2002). Evidence that the tandem-pleckstrin-homology-domain-containing protein TAPP1 interacts with Ptd(3,4)P2 and the multi-PDZ-domain-containing protein MUPP1 in vivo. Biochemical Journal 361, 525–536.

[125] Ong, S.E., Blagoev, B., Kratchmarova, I., Kristensen, D.B., Steen, H., Pandey, A. and Mann, M. (2002). Stable isotope labeling by amino acids in cell culture, SILAC, as a simple and accurate approach to expression proteomics. Mol. Cell Proteomics 1, 376-86.

[126] Ong, S.E., Foster, L.J. and Mann, M. (2003). Mass spectrometric-based approaches in quantitative proteomics. Methods 29, 124-30.

[127] Maehama, T. and Dixon, J.E. (1998). The tumor suppressor, PTEN/MMAC1, dephosphorylates the lipid second messenger, phosphatidylinositol 3,4,5-trisphosphate. J. Biol. Chem. 273, 13375-8.

[128] Myers, M.P. et al. (1998). The lipid phosphatase activity of PTEN is critical for its tumor supressor function. Proc. Natl. Acad. Sci. U S A 95, 13513-8.

[129] Myers, M.P., Stolarov, J.P., Eng, C., Li, J., Wang, S.I., Wigler, M.H., Parsons, R. and Tonks, N.K. (1997). P-TEN, the tumor suppressor from human chromosome 10q23, is a dual-specificity phosphatase. Proc. Natl. Acad. Sci. U S A 94, 9052-7.

[130] Banfic, H., Downes, C.P. and Rittenhouse, S.E. (1998). Biphasic activation of PKBalpha/Akt in platelets. Evidence for stimulation both by phosphatidylinositol 3,4-bisphosphate, produced via a novel pathway, and by phosphatidylinositol 3,4,5-trisphosphate. J. Biol. Chem. 273, 11630-7.

[131] Banfic, H., Tang, X., Batty, I.H., Downes, C.P., Chen, C. and Rittenhouse, S.E. (1998). A novel integrin-activated pathway forms PKB/Akt-stimulatory phosphatidylinositol 3,4-bisphosphate via phosphatidylinositol 3-phosphate in platelets. J. Biol. Chem. 273, 13-16.

[132] Van der Kaay, J., Beck, M., Gray, A. and Downes, C.P. (1999). Distinct phosphatidylinositol 3-kinase lipid products accumulate upon oxidative and osmotic stress and lead to different cellular responses. J. Biol. Chem. 274, 35963-8.

[133] Anderson, K.E., Coadwell, J., Stephens, L.R. and Hawkins, P.T. (1998). Translocation of PDK-1 to the plasma membrane is important in allowing PDK-1 to activate protein kinase B. Curr. Biol. 8, 684-91.

[134] Franke, T.F., Kaplan, D.R., Cantley, L.C. and Toker, A. (1997). Direct regulation of the Akt proto-oncogene product by phosphatidylinositol-3,4-bisphosphate. Science 275, 665-8.

[135] Scheid, M.P. et al. (2002). Phosphatidylinositol(3,4,5)P3 is essential but not sufficient for PKB activation: Phosphatidylinositol(3,4)P2 is required for PKB phosphorylation at Ser473. Studies using cells from SHIP knockout mice. J. Biol. Chem. 277, 9027-9035.

[136] Dowler, S., Currie, R.A., Campbell, D.G., Deak, M., Kular, G., Downes, C.P. and Alessi, D.R. (2000). Identification of pleckstrin-homology-domain-

containing proteins with novel phosphoinositide-binding specificities. Biochem. J. 351, 19-31.

[137] Watt, S.A., Kimber, W.A., Fleming, I.N., Leslie, N.R., Downes, P.C. and Lucocq, J.M. (2004). Detection of novel intracellular agonist responsive pools of phosphatidylinositol 3,4-bisphosphate using the TAPP1 pleckstrin homology domain in immunoelectron microscopy. Biochemical Journal 377, 653-663.

[138] Dowler, S., Currie, R.A., Downes, C.P. and Alessi, D.R. (1999). DAPP1: a dual adaptor for phosphotyrosine and 3-phosphoinositides. Biochem. J. 342, 7-12.

[139] Dowler, S., Montalvo, L., Cantrell, D., Morrice, N. and Alessi, D.R. (2000). Phosphoinositide 3-kinase-dependent phosphorylation of the dual adaptor for phosphotyrosine and 3-phosphoinositides by the Src family of tyrosine kinase. Biochem. J. 349, 605-610.

[140] Thomas, C.C., Dowler, S., Deak, M., Alessi, D.R. and van Aalten, D.M. (2001). Crystal structure of the phosphatidylinositol 3,4-bisphosphate-binding pleckstrin homology (PH) domain of tandem PH-domain-containing protein 1 (TAPP1): molecular basis of lipid specificity. Biochem. J. 358, 287-294.

[141] Vyas, P., Norris, F.A., Joseph, R., Majerus, P.W. and Orkin, S.H. (2000). Inositol polyphosphate 4-phosphatase type I regulates cell growth downstream of transcription factor GATA-1. PNAS 97, 13696-13701.

[142] Gewinner, C. et al. (2009). Evidence that inositol polyphosphate 4-phosphatase type II is a tumor suppressor that inhibits PI3K signaling. Cancer Cell 16, 115-25.

[143] Nystuen, A., Legare, M.E., Shultz, L.D. and Frankel, W.N. (2001). A Null Mutation in Inositol Polyphosphate 4-Phosphatase Type I Causes Selective Neuronal Loss in Weeble Mutant Mice. Neuron 32, 203-212.

[144] Sasaki, J. et al. The PtdIns(3,4)P(2) phosphatase INPP4A is a suppressor of excitotoxic neuronal death. Nature 465, 497-501.

[145] Wakamatsu, I., Ihara, S. and Fukui, Y. (2006). Mutational analysis on the function of the SWAP-70 PH domain. Mol. Cell. Biochem. 293, 137-45.

[146] Hilpela, P., Oberbanscheidt, P., Hahne, P., Hund, M., Kalhammer, G., Small, J.V. and Bahler, M. (2003). SWAP-70 identifies a transitional subset of actin filaments in motile cells. Mol. Biol. Cell 14, 3242-53.

[147] Gray, A., Van Der Kaay, J. and Downes, C.P. (1999). The pleckstrin homology domains of protein kinase B and GRP1 (general receptor for phosphoinositides-1) are sensitive and selective probes for the cellular detection of phosphatidylinositol 3,4-bisphosphate and/or phosphatidylinositol 3,4,5-trisphosphate in vivo. Biochem. J. 344 Pt 3, 929-36.

[148] Rodrigues, G.A., Falasca, M., Zhang, Z., Ong, S.H. and Schlessinger, J. (2000). A novel positive feedback loop mediated by the docking protein Gab1 and phosphatidylinositol 3-kinase in epidermal growth factor receptor signaling. Mol. Cell. Biol. 20, 1448-59.

[149] Li, Z., Wahl, M.I., Eguinoa, A., Stephens, L.R., Hawkins, P.T. and Witte, O.N. (1997). Phosphatidylinositol 3-kinase-gamma activates Bruton's tyrosine kinase in concert with Src family kinases. Proc. Natl. Acad. Sci. U S A 94, 13820-5.

[150] Vanhaesebroeck, B. and Alessi, D.R. (2000). The PI3K-PDK1 connection: more than just a road to PKB. Biochem. J. 346 Pt 3, 561-76.

[151] Burgering, B.M.T. and Coffer, P.J. (1995). Protein kinase B (c-Akt) in phosphatidylinositol-3-OH kinase signal transduction. Nature 376, 599-602.

[152] Lockyer, P.J., Wennstrom, S., Kupzig, S., Venkateswarlu, K., Downward, J. and Cullen, P.J. (1999). Identification of the ras GTPase-activating protein GAP1(m) as a phosphatidylinositol-3,4,5-trisphosphate-binding protein in vivo. Curr. Biol. 9, 265-8.

[153] Klarlund, J.K. et al. (1998). Regulation of GRP1-catalyzed ADP ribosylation factor guanine nucleotide exchange by phosphatidylinositol 3,4,5-trisphosphate. J. Biol. Chem. 273, 1859-62.

[154] Rhee, S.G. (2006). Cell signaling. H2O2, a necessary evil for cell signaling. Science 312, 1882-3.

[155] Leslie, N.R., Lindsay, Y., Ross, S.H. and Downes, C.P. (2004). Redox regulation of phosphatase function. Biochem. Soc. Trans. 32, 1018-20.

[156] Leslie, N.R. (2006). The redox regulation of PI 3-kinase-dependent signaling. Antioxid. Redox Signal 8, 1765-74.

[157] Morinville, A., Maysinger, D. and Shaver, A. (1998). From Vanadis to Atropos: vanadium compounds as pharmacological tools in cell death signalling. Trends Pharmacol. Sci. 19, 452-60.

[158] Kwon, J., Lee, S.R., Yang, K.S., Ahn, Y., Kim, Y.J., Stadtman, E.R. and Rhee, S.G. (2004). Reversible oxidation and inactivation of the tumor suppressor PTEN in cells stimulated with peptide growth factors. Proc. Natl. Acad. Sci. U S A 101, 16419-24.

[159] Lee, S.R., Yang, K.S., Kwon, J., Lee, C., Jeong, W. and Rhee, S.G. (2002). Reversible inactivation of the tumor suppressor PTEN by H2O2. J. Biol. Chem. 277, 20336-42.

[160] Norris, F.A., Atkins, R.C. and Majerus, P.W. (1997). The cDNA cloning and characterization of inositol polyphosphate 4-phosphatase type II. Evidence for conserved alternative splicing in the 4-phosphatase family. J. Biol. Chem. 272, 23859-64.

[161] Damen, J.E., Liu, L., Rosten, P., Humphries, R.K., Jefferson, A.B., Majerus, P.W. and Krystal, G. (1996). The 145-kDa protein induced to associate with Shc by multiple cytokines is an inositol tetraphosphate and phosphatidylinositol 3,4,5-triphosphate 5-phosphatase. Proc. Natl. Acad. Sci. USA 93, 1689-93.

[162] Habib, T., Hejna, J.A., Moses, R.E. and Decker, S.J. (1998). Growth factors and insulin stimulate tyrosine phosphorylation of the 51C/SHIP2 protein. J. Biol. Chem. 273, 18605-9.

[163] Artemenko, Y., Gagnon, A., Ibrahim, S. and Sorisky, A. (2007). Regulation of PDGF-stimulated SHIP2 tyrosine phosphorylation and association with Shc in 3T3-L1 preadipocytes. J. Cell. Physiol. 211, 598-607.

[164] Taylor, V., Wong, M., Brandts, C., Reilly, L., Dean, N.M., Cowsert, L.M., Moodie, S. and Stokoe, D. (2000). 5' phospholipid phosphatase SHIP-2 causes protein kinase B inactivation and cell cycle arrest in glioblastoma cells. Mol. Cell. Biol. 20, 6860-71.

[165] Phee, H., Jacob, A. and Coggeshall, K.M. (2000). Enzymatic activity of the Src homology 2 domain-containing inositol phosphatase is regulated by a plasma membrane location. J. Biol. Chem. 275, 19090-7.

[166] Backers, K., Blero, D., Paternotte, N., Zhang, J. and Erneux, C. (2003). The termination of PI3K signalling by SHIP1 and SHIP2 inositol 5-phosphatases. Adv. Enzyme Regul. 43, 15-28.

[167] Sly, L.M., Rauh, M.J., Kalesnikoff, J., Buchse, T. and Krystal, G. (2003). SHIP, SHIP2, and PTEN activities are regulated in vivo by modulation of their protein levels: SHIP is up-regulated in macrophages and mast cells by lipopolysaccharide. Exp. Hematol. 31, 1170-81.

[168] Prasad, N.K., Werner, M.E. and Decker, S.J. (2009). Specific tyrosine phosphorylations mediate signal-dependent stimulation of SHIP2 inositol phosphatase activity, while the SH2 domain confers an inhibitory effect to maintain the basal activity. Biochemistry 48, 6285-7.

[169] Marshall, A.J., Krahn, A.K., Ma, K., Duronio, V. and Hou, S. (2002). TAPP1 and TAPP2 are targets of phosphatidylinositol 3-kinase signaling in B cells: sustained plasma membrane recruitment triggered by the B-cell antigen receptor. Mol. Cell. Biol. 22, 5479-91.

[170] Kimber, W.A., Deak, M., Prescott, A.R. and Alessi, D.R. (2003). Interaction of the protein tyrosine phosphatase PTPL1 with the PtdIns(3,4)P2-binding adaptor protein TAPP1. Biochem. J. 376, 525-35.

[171] Gray, A., Olsson, H., Batty, I.H., Priganica, L. and Peter Downes, C. (2003). Nonradioactive methods for the assay of phosphoinositide 3-kinases and phosphoinositide phosphatases and selective detection of signaling lipids in cell and tissue extracts. Anal. Biochem. 313, 234-45.

[172] Smith, K., Humphreys, D., Hume, P.J. and Koronakis, V. Enteropathogenic Escherichia coli recruits the cellular inositol phosphatase SHIP2 to regulate actin-pedestal formation. Cell Host Microbe 7, 13-24.

[173] Tiwari, S., Choi, H.P., Matsuzawa, T., Pypaert, M. and MacMicking, J.D. (2009). Targeting of the GTPase Irgm1 to the phagosomal membrane via

PtdIns(3,4)P(2) and PtdIns(3,4,5)P(3) promotes immunity to mycobacteria. Nat. Immunol. 10, 907-17.

[174] Pasquali, C. et al. (2007). A chemical proteomics approach to phosphatidylinositol 3-kinase signaling in macrophages. Mol. Cell Proteomics 6, 1829-41.

[175] Krause, M. et al. (2004). Lamellipodin, an Ena/VASP ligand, is implicated in the regulation of lamellipodial dynamics. Dev. Cell 7, 571-83.

[176] Banfic, H., Tang, X.-w., Batty, I.H., Downes, C.P., Chen, C.-s. and Rittenhouse, S.E. (1998). A Novel Integrin-activated Pathway Forms PKB/Akt- stimulatory Phosphatidylinositol 3,4-Bisphosphate via Phosphatidylinositol 3-Phosphate in Platelets. J. Biol. Chem. 273, 13-16.

[177] Leevers, S.J., Vanhaesebroeck, B. and Waterfield, M.D. (1999). Signalling through phosphoinositide 3-kinases: the lipids take centre stage. Curr. Opin. Cell Biol. 11, 219-25.

[178] Lemmon, M.A. and Ferguson, K.M. (2000). Signal-dependent membrane targeting by pleckstrin homology (PH) domains. Biochem. J. 350 Pt 1, 1-18.

[179] Tenu, J.P., Etore, F. and Le Doan, T. (1997). [A simple method for the study of cytosolic content of oligonucleotides in cells]. C. R. Acad. Sci. III 320, 477-86.

[180] Eboue, D., Auger, R., Angiari, C., Le Doan, T. and Tenu, J.P. (2003). Use of a Simple Fractionation Method to Evaluate Binding, Internalization and Intracellular Distribution of Oligonucleotides in Vascular Smooth Muscle Cells. Archives of Physiology and Biochemistry 111, 265 - 272.

[181] Geelen, M.J.H. (2005). The use of digitonin-permeabilized mammalian cells for measuring enzyme activities in the course of studies on lipid metabolism. Analytical Biochemistry 347, 1-9.

[182] Liu, J., Xiao, N. and DeFranco, D.B. (1999). Use of Digitonin-Permeabilized Cells in Studies of Steroid Receptor Subnuclear Trafficking. Methods 19, 403-409.

[183] Batty, I.H. and Downes, C.P. (1994). The inhibition of phosphoinositide synthesis and muscarinic-receptor-mediated phospholipase C activity by Li+ as secondary, selective, consequences of inositol depletion in 1321N1 cells. Biochem. J. 297 (Pt 3), 529-37.

[184] Marshall, T. (1984). Detection of protein in polyacrylamide gels using an improved silver stain. Anal. Biochem. 136, 340-6.

[185] Ohsawa, K. and Ebata, N. (1983). Silver stain for detecting 10-femtogram quantities of protein after polyacrylamide gel electrophoresis. Anal. Biochem. 135, 409-15.

[186] Catimel, B. et al. (2009). PI(3,4,5)P3 Interactome. J. Proteome. Res. 8, 3712-26.

[187] Catimel, B. et al. (2008). The PI(3,5)P2 and PI(4,5)P2 interactomes. J. Proteome Res. 7, 5295-313.

[188] Hiller, Y., Gershoni, J.M., Bayer, E.A. and Wilchek, M. (1987). Biotin binding to avidin. Oligosaccharide side chain not required for ligand association. Biochem. J. 248, 167-71.

[189] Ferguson, G.J. et al. (2007). PI(3)K[gamma] has an important context-dependent role in neutrophil chemokinesis. Nat. Cell. Biol. 9, 86-91.

[190] Condliffe, A.M. et al. (2005) Sequential activation of class IB and class IA PI3K is important for the primed respiratory burst of human but not murine neutrophils. Blood 106, 1432-1440.

[191] Vanhaesebroeck, B., Guillermet-Guibert, J., Graupera, M. and Bilanges, B. The emerging mechanisms of isoform-specific PI3K signalling. Nat. Rev. Mol. Cell. Biol. 11, 329-41.

[192] Ali, K. et al. (2008) Isoform-Specific Functions of Phosphoinositide 3-Kinases: p110{delta} but Not p110{gamma} Promotes Optimal Allergic Responses In Vivo. Journal of Immunology 180, 2538-2544.

[193] Kavran, J.M., Klein, D.E., Lee, A., Falasca, M., Isakoff, S.J., Skolnik, E.Y. and Lemmon, M.A. (1998). Specificity and promiscuity in phosphoinositide binding by pleckstrin homology domains. J. Biol. Chem. 273, 30497-508.

[194] Edman, P. (1949). A method for the determination of amino acid sequence in peptides. Arch. Biochem. 22, 475.

[195] Edman, P. (1970). Sequence determination. Mol. Biol. Biochem. Biophys. 8, 211-55.

[196] Andersson, C.-O. (1958). Mass Spectrometric Studies on Amino Acid and Peptide Derivatives. Acta. Chem. Scand. 12, 1353.

[197] Koichi, T., Hiroaki, W., Yutaka, I., Satoshi, A., Yoshikazu, Y., Tamio, Y. and Matsuo, T. (1988) Protein and polymer analyses up to m/z 100 000 by laser ionization time-of-flight mass spectrometry. Rapid Comm. Mass Spec. 2 151-153.

[198] Karas, M., Bachmann, D. and Hillenkamp, F. (1985). Influence of the wavelength in high-irradiance ultraviolet laser desorption mass spectrometry of organic molecules. Analytical Chemistry 57, 2935-2939.

[199] Whitehouse, C.M., Dreyer, R.N., Yamashita, M. and Fenn, J.B. (1985). Electrospray interface for liquid chromatographs and mass spectrometers. Anal. Chem. 57, 675-9.

[200] Paul, J.K., Jorge, D., Allyson, W., Youla, K., Ewan, B. and Rolf, A. (2004) The International Protein Index: An integrated database for proteomics experiments. Proteomics 4, 1985-1988.

[201] The UniProt Consortium (2010). The Universal Protein Resource (UniProt) in 2010. Nucleic Acids Res. 38, 142-148.

[202] Hubbard, T.J.P. et al. (2009) Ensembl 2009. Nucleic Acids Res. 37, 690-697

[203] Aebersold, R. and Mann, M. (2003). Mass spectrometry-based proteomics. Nature 422, 198-207.

[204] Steen, H. and Mann, M. (2004). The ABC's (and XYZ's) of peptide sequencing. Nat. Rev. Mol. Cell. Biol. 5, 699-711.

[205] Melvin, A.P., John, H.C. and Akos, V. (1994) An inductive detector for time-of-flight mass spectrometry. Rapid Comm. Mass Spec. 8, 317-322.

[206] Dubois, F., Knochenmuss, R., Zenobi, R., Brunelle, A., Deprun, C. and Beyec, Y.L. (1999) A comparison between ion-to-photon and microchannel plate detectors. Rapid Comm. Mass Spec. 13, 786-791.

[207] Schwartz, J.C., Senko, M.W. and Syka, J.E. (2002). A two-dimensional quadrupole ion trap mass spectrometer. J. Am. Soc. Mass Spectrom. 13, 659-69.

[208] McLuckey, S.A., Van Berkel, G.J., Goeringer, D.E. and Glish, G.L. (1994). Ion trap mass spectrometry. Using high-pressure ionization. Anal. Chem. 66, 737-743.

[209] James, W.H. (2002) A new linear ion trap mass spectrometer. Rapid Comm. Mass Spec. 16, 512-526.

[210] Wollnik, H. (1993) Time-of-flight mass analyzers. Mass Spectrom. Rev. 12, 89-114.

[211] Marshall, A.G., Hendrickson, C.L. and Jackson, G.S. (1998). Fourier transform ion cyclotron resonance mass spectrometry: a primer. Mass Spectrom. Rev. 17, 1-35.

[212] Martin, S.E., Shabanowitz, J., Hunt, D.F. and Marto, J.A. (2000). Subfemtomole MS and MS/MS peptide sequence analysis using nano-HPLC micro-ESI fourier transform ion cyclotron resonance mass spectrometry. Anal. Chem. 72, 4266-74.

[213] Yost, R.A. and Boyd, R.K. (1990). Tandem mass spectrometry: quadrupole and hybrid instruments. Methods Enzymol. 193, 154-200.

[214] Jonscher, K.R. and Yates, J.R., 3rd. (1997). The quadrupole ion trap mass spectrometer--a small solution to a big challenge. Anal. Biochem. 244, 1-15.

[215] Vestal, M.L., Campbell, J.M. and Burlingame, A.L. (2005) Tandem Time-of-Flight Mass Spectrometry. Methods in Enzymology 402, 79-108.

[216] Mitchell Wells, J., McLuckey, S.A. and Burlingame, A.L. (2005) Collision-Induced Dissociation (CID) of Peptides and Proteins. Methods in Enzymology 402, 148-185.

[217] Makarov, A. (2000). Electrostatic Axially Harmonic Orbital Trapping: A High-Performance Technique of Mass Analysis. Analytical Chemistry 72, 1156-1162.

[218] Qizhi, H., Robert, J.N., Hongyan, L., Alexander, M., Mark, H. and Cooks, R.G. (2005) The Orbitrap: a new mass spectrometer. J. Mass Spectrom. 40, 430-443.

[219] Yates, J.R., Cociorva, D., Liao, L. and Zabrouskov, V. (2005). Performance of a Linear Ion Trap-Orbitrap Hybrid for Peptide Analysis. Analytical Chemistry 78, 493-500.

[220] Makarov, A., Denisov, E., Kholomeev, A., Balschun, W., Lange, O., Strupat, K. and Horning, S. (2006). Performance Evaluation of a Hybrid Linear Ion Trap/Orbitrap Mass Spectrometer. Analytical Chemistry 78, 2113-2120.

[221] Olsen, J.V. et al. (2005) Parts per Million Mass Accuracy on an Orbitrap Mass Spectrometer via Lock Mass Injection into a C-trap. Mol. Cell. Proteomics 4, 2010-2021

[222] Olsen, J.V. et al. (2005). Parts per million mass accuracy on an Orbitrap mass spectrometer via lock mass injection into a C-trap. Mol Cell Proteomics 4, 2010-2021.

[223] Cox, J. and Mann, M. (2008). MaxQuant enables high peptide identification rates, individualized p.p.b.-range mass accuracies and proteome-wide protein quantification. Nat Biotechnol 26, 1367-72.

[224] http://lpg.obs.ujf-grenoble.fr/article103.html.

[225] http://www.genome.duke.edu/cores/proteomics/instrumentation/LTQ-Orbitrap.php.

[226] http://www.unifr.ch/inph/vclab/home/Research/real-time-neurotransmitter-monitoring.

[227] Ong, S.E. and Mann, M. (2006). A practical recipe for stable isotope labeling by amino acids in cell culture (SILAC). Nat. Protoc. 1, 2650-60.

[228] Ong, S.E. and Mann, M. (2007). Stable isotope labeling by amino acids in cell culture for quantitative proteomics. Methods Mol. Biol. 359, 37-52.

[229] Ong, S.E. and Mann, M. (2005). Mass spectrometry-based proteomics turns quantitative. Nat. Chem. Biol. 1, 252-62.

[230] Cox, J. and Mann, M. (2009). Computational principles of determining and improving mass precision and accuracy for proteome measurements in an Orbitrap. J. Am. Soc. Mass. Spectrom. 20, 1477-85.

[231] Cox, J., Matic, I., Hilger, M., Nagaraj, N., Selbach, M., Olsen, J.V. and Mann, M. (2009). A practical guide to the MaxQuant computational platform for SILAC-based quantitative proteomics. Nat. Protoc. 4, 698-705.

[232] Zhou, Y., Toth, M., Hamman, M.S., Monahan, S.J., Lodge, P.A., Boynton, A.L. and Salgaller, M.L. (2002). Serological cloning of PARIS-1: a new TBC domain-containing, immunogenic tumor antigen from a prostate cancer cell line. Biochem. Biophys. Res. Commun. 290, 830-8.

[233] Perkins, D.N., Pappin, D.J., Creasy, D.M., Cottrell, J.S. (1999) Probability-based protein identification by searching sequence databases using mass spectrometry data. Electrophoresis 20, 3551-3567.

[234] http://www.matrixscience.com/help/interpretation_help.html#THRESHOLDS.

[235] Shirai, T. et al. (1998). Specific detection of phosphatidylinositol 3,4,5-trisphosphate binding proteins by the PIP3 analogue beads: an application for rapid purification of the PIP3 binding proteins. Biochim. Biophys. Acta 1402, 292-302.

[236] Kenichi, T. et al. (1997) A Target of Phosphatidylinositol 3,4,5-Trisphosphate with a Zinc Finger Motif Similar to that of the ADP-Ribosylation-Factor

GTPase-Activating Protein and Two Pleckstrin Homology Domains. Eur. J. Biochem. 245, 512-519.

[237] Galesio, M., Vieira, D.V., Rial-Otero, R., Lodeiro, C., Moura, I. and Capelo, J.L. (2008). Influence of the protein staining in the fast ultrasonic sample treatment for protein identification through peptide mass fingerprint and matrix-assisted laser desorption ionization time of flight mass spectrometry. J. Proteome Res. 7, 2097-106.

[238] Shevchenko, A., Wilm, M., Vorm, O. and Mann, M. (1996). Mass spectrometric sequencing of proteins silver-stained polyacrylamide gels. Anal. Chem. 68, 850-8.

[239] Neuhoff, V., Arold, N., Taube, D. and Ehrhardt, W. (1988). Improved staining of proteins in polyacrylamide gels including isoelectric focusing gels with clear background at nanogram sensitivity using Coomassie Brilliant Blue G-250 and R-250. Electrophoresis 9, 255-62.

[240] Candiano, G. et al. (2004). Blue silver: a very sensitive colloidal Coomassie G-250 staining for proteome analysis. Electrophoresis 25, 1327-33.

[241] Trinkle-Mulcahy, L. et al. (2008). Identifying specific protein interaction partners using quantitative mass spectrometry and bead proteomes. J. Cell. Biol. 183, 223-39.

[242] Boisvert, F-M., Lam, Y.W., Lamont, D. and Lamond, A.I. (2010). A Quantitative Proteomics Analysis of Subcellular Proteome Localization and Changes Induced by DNA Damage. Mol. Cell. Proteomics 9, 457-470.

[243] David, S. and Willy, B. (2009) Coomassie stains: are they really mass spectrometry compatible. Rapid Comm. Mass Spectro. 23, 1525-1529.

[244] Lehto, M., Hynynen, R., Karjalainen, K., Kuismanen, E., Hyvärinen, K. and Olkkonen, V.M. (2005). Targeting of OSBP-related protein 3 (ORP3) to endoplasmic reticulum and plasma membrane is controlled by multiple determinants. Experimental Cell Research 310, 445-462.

[245] Sivalenka, R.R. and Jessberger, R. (2004) SWAP-70 Regulates c-kit-Induced Mast Cell Activation, Cell-Cell Adhesion, and Migration. Mol. Cell. Biol. 24, 10277-10288.

[246] Fukui, Y., Tanaka, T., Tachikawa, H. and Ihara, S. (2007). SWAP-70 is required for oncogenic transformation by v-Src in mouse embryo fibroblasts. Biochemical and Biophysical Research Communications 356, 512-516.

[247] Ocana-Morgner, C., Wahren, C. and Jessberger, R. (2009) SWAP-70 regulates RhoA/RhoB-dependent MHCII surface localization in dendritic cells. Blood 113, 1474-1482.

[248] Zhou, Y., Toth, M., Hamman, M.S., Monahan, S.J., Lodge, P.A., Boynton, A.L. and Salgaller, M.L. (2002). Serological Cloning of PARIS-1: A New TBC Domain-Containing, Immunogenic Tumor Antigen from a Prostate Cancer Cell Line. Biochemical and Biophysical Research Communications 290, 830-838.

[249] Ulmasov, B., Bruno, J., Woost, P.G. and Edwards, J.C. (2007). Tissue and subcellular distribution of CLIC1. BMC Cell Biol. 8, 8.

[250] Littler, D.R. et al. (2004). The intracellular chloride ion channel protein CLIC1 undergoes a redox-controlled structural transition. J. Biol. Chem. 279, 9298-305.

[251] Tulk, B.M., Schlesinger, P.H., Kapadia, S.A. and Edwards, J.C. (2000). CLIC-1 functions as a chloride channel when expressed and purified from bacteria. J. Biol. Chem. 275, 26986-93.

[252] Goodchild, S.C., Howell, M.W., Cordina, N.M., Littler, D.R., Breit, S.N., Curmi, P.M. and Brown, L.J. (2009). Oxidation promotes insertion of the CLIC1 chloride intracellular channel into the membrane. Eur. Biophys. J. 39, 129-38.

[253] Milton, R.H. et al. (2008). CLIC1 function is required for beta-amyloid-induced generation of reactive oxygen species by microglia. J. Neurosci. 28, 11488-99.

[254] Warton, K. et al. (2002). Recombinant CLIC1 (NCC27) assembles in lipid bilayers via a pH-dependent two-state process to form chloride ion channels with identical characteristics to those observed in Chinese hamster ovary cells expressing CLIC1. J. Biol.Chem. 277, 26003-11.

[255] Fanucchi, S., Adamson, R.J. and Dirr, H.W. (2008). Formation of an unfolding intermediate state of soluble chloride intracellular channel protein CLIC1 at acidic pH. Biochemistry 47, 11674-81.

[256] Dulhunty, A., Gage, P., Curtis, S., Chelvanayagam, G. and Board, P. (2001). The glutathione transferase structural family includes a nuclear chloride channel and a ryanodine receptor calcium release channel modulator. J. Biol. Chem. 276, 3319-23.

[257] Harrop, S.J. et al. (2001). Crystal structure of a soluble form of the intracellular chloride ion channel CLIC1 (NCC27) at 1.4-A resolution. J. Biol. Chem. 276, 44993-5000.

[258] Leslie, N.R., Bennett, D., Lindsay, Y.E., Stewart, H., Gray, A. and Downes, C.P. (2003). Redox regulation of PI 3-kinase signalling via inactivation of PTEN. EMBO J. 22, 5501-5510.

[259] Xu, D., Rovira, I.I. and Finkel, T. (2002). Oxidants Painting the Cysteine Chapel: Redox Regulation of PTPs. Developmental Cell 2, 251-252.

[260] Natale, D.R. and Watson, A.J. (2002). Rac-1 and IQGAP are potential regulators of E-cadherin-catenin interactions during murine preimplantation development. Mech. Dev. 119, 21-26.

[261] Mateer, S.C., Wang, N. and Bloom, G.S. (2003). IQGAPs: integrators of the cytoskeleton, cell adhesion machinery, and signaling networks. Cell Motil. Cytoskeleton 55, 147-55.

[262] Tirnauer, J.S. (2004). A new cytoskeletal connection for APC: linked to actin through IQGAP. Dev. Cell 7, 778-80.

[263] Watanabe, T., Noritake, J. and Kaibuchi, K. (2005). Roles of IQGAP1 in cell polarization and migration. Novartis Found. Symp. 269, 92-101; discussion 101-5, 223-30.

[264] White, C.D., Brown, M.D. and Sacks, D.B. (2009). IQGAPs in cancer: a family of scaffold proteins underlying tumorigenesis. FEBS Lett. 583, 1817-24.

[265] Briggs, M.W. and Sacks, D.B. (2003). IQGAP proteins are integral components of cytoskeletal regulation. EMBO Rep. 4, 571-4.

[266] Johnson, M., Sharma, M. and Henderson, B.R. (2009). IQGAP1 regulation and roles in cancer. Cell Signal. 21, 1471-8.

[267] Kuroda, S., Fukata, M., Kobayashi, K., Nakafuku, M., Nomura, N., Iwamatsu, A. and Kaibuchi, K. (1996). Identification of IQGAP as a putative target for the small GTPases, Cdc42 and Rac1. J. Biol. Chem. 271, 23363-7.

[268] Zhou, R., Guo, Z., Watson, C., Chen, E., Kong, R., Wang, W. and Yao, X. (2003). Polarized distribution of IQGAP proteins in gastric parietal cells and their roles in regulated epithelial cell secretion. Mol. Biol. Cell. 14, 1097-108.

[269] Dowler, S., Currie, R.A., Downes, C.P. and Alessi, D.R. (1999) DAPP1: a dual adaptor for phosphotyrosine and 3-phosphoinositides. Biochem. J. 342, 7-12.

[270] Kutateladze, T.G., Ogburn, K.D., Watson, W.T., de Beer, T., Emr, S.D., Burd, C.G. and Overduin, M. (1999). Phosphatidylinositol 3-Phosphate Recognition by the FYVE Domain. Molecular Cell 3, 805-811.

[271] Stahelin, R.V. (2009). Lipid binding domains: more than simple lipid effectors. J. Lipid Res. 50, S299-304.

[272] Burd, C.G. and Emr, S.D. (1998). Phosphatidylinositol(3)-phosphate signaling mediated by specific binding to RING FYVE domains. Mol Cell 2, 157-62.

[273] Gaullier, J.M., Simonsen, A., D'Arrigo, A., Bremnes, B., Stenmark, H. and Aasland, R. (1998). FYVE fingers bind PtdIns(3)P. Nature 394, 432-3.

[274] Gillooly, D.J., Simonsen, A. and Stenmark, H. (2001). Cellular functions of phosphatidylinositol 3-phosphate and FYVE domain proteins. Biochem J. 355, 249-58.

[275] Dumas, J.J., Merithew, E., Sudharshan, E., Rajamani, D., Hayes, S., Lawe, D., Corvera, S. and Lambright, D.G. (2001). Multivalent endosome targeting by homodimeric EEA1. Mol. Cell. 8, 947-58.

[276] Zhang, G., Kazanietz, M.G., Blumberg, P.M. and Hurley, J.H. (1995). Crystal structure of the cys2 activator-binding domain of protein kinase C delta in complex with phorbol ester. Cell 81, 917-24.

[277] Dumas, J.J., Merithew, E., Sudharshan, E., Rajamani, D., Hayes, S., Lawe, D., Corvera, S. and Lambright, D.G. (2001). Multivalent Endosome Targeting by Homodimeric EEA1. Molecular Cell 8, 947-958.

[278] Ferguson, K.M., Lemmon, M.A., Schlessinger, J. and Sigler, P.B. (1995). Structure of the high affinity complex of inositol trisphosphate with a phospholipase C pleckstrin homology domain. Cell 83, 1037-1046.

[279] Ceccarelli, D.F.J., Blasutig, I.M., Goudreault, M., Li, Z., Ruston, J., Pawson, T. and Sicheri, F. (2007) Non-canonical Interaction of Phosphoinositides with Pleckstrin Homology Domains of Tiam1 and ArhGAP9. J. Biol. Chem. 282, 13864-13874.

[280] Bravo, J. et al. (2001). The Crystal Structure of the PX Domain from p40phox Bound to Phosphatidylinositol 3-Phosphate. Molecular Cell 8, 829-839.

[281] Karathanassis, D., Stahelin, R.V., Bravo, J., Perisic, O., Pacold, C.M., Cho, W. and Williams, R.L. (2002). Binding of the PX domain of p47phox to phosphatidylinositol 3,4-bisphosphate and phosphatidic acid is masked by an intramolecular interaction. EMBO J. 21, 5057-5068.

[282] Kanai, F., Liu, H., Field, S.J., Akbary, H., Matsuo, T., Brown, G.E., Cantley, L.C. and Yaffe, M.B. (2001). The PX domains of p47phox and p40phox bind to lipid products of PI(3)K. Nat. Cell Biol. 3, 675-8.

[283] Misra, S. and Hurley, J.H. (1999). Crystal structure of a phosphatidylinositol 3-phosphate-specific membrane-targeting motif, the FYVE domain of Vps27p. Cell 97, 657-66.

[284] Stahelin, R.V., Long, F., Diraviyam, K., Bruzik, K.S., Murray, D. and Cho, W. (2002). Phosphatidylinositol 3-phosphate induces the membrane penetration of the FYVE domains of Vps27p and Hrs. J. Biol. Chem. 277, 26379-88.

[285] Kutateladze, T.G., Capelluto, D.G., Ferguson, C.G., Cheever, M.L., Kutateladze, A.G., Prestwich, G.D. and Overduin, M. (2004). Multivalent mechanism of membrane insertion by the FYVE domain. J. Biol. Chem. 279, 3050-7.

[286] Callaghan, J., Simonsen, A., Gaullier, J.M., Toh, B.H. and Stenmark, H. (1999). The endosome fusion regulator early-endosomal autoantigen 1 (EEA1) is a dimer. Biochem. J. 338 (Pt 2), 539-43.

[287] Lee, S.A., Eyeson, R., Cheever, M.L., Geng, J., Verkhusha, V.V., Burd, C., Overduin, M. and Kutateladze, T.G. (2005). Targeting of the FYVE domain to endosomal membranes is regulated by a histidine switch. Proc. Natl. Acad. Sci. U S A 102, 13052-7.

[288] Lietzke, S.E., Bose, S., Cronin, T., Klarlund, J., Chawla, A., Czech, M.P. and Lambright, D.G. (2000). Structural Basis of 3-Phosphoinositide Recognition by Pleckstrin Homology Domains. Molecular Cell 6, 385-394.

[289] Ponting, C.P. (1996). Novel domains in NADPH oxidase subunits, sorting nexins, and PtdIns 3-kinases: binding partners of SH3 domains? Protein Sci. 5, 2353-7.

[290] Seet, L.-F. and Hong, W. (2006). The Phox (PX) domain proteins and membrane traffic. Biochimica et Biophysica Acta (BBA) - Molecular and Cell Biology of Lipids 1761, 878-896.

[291] Carlton, J., Bujny, M., Rutherford, A. and Cullen, P. (2005). Sorting Nexins – Unifying Trends and New Perspectives. Traffic 6, 75-82.

[292] Kanai, F., Liu, H., Field, S.J., Akbary, H., Matsuo, T., Brown, G.E., Cantley, L.C. and Yaffe, M.B. (2001). The PX domains of p47phox and p40phox bind to lipid products of PI(3)K. Nat. Cell Biol 3, 675-678.

[293] Xu, Y., Seet, L.F., Hanson, B. and Hong, W. (2001) The Phox homology (PX) domain, a new player in phosphoinositide signalling. Biochem. J. 360, 513-530.

[294] Karathanassis, D., Stahelin, R.V., Bravo, J., Perisic, O., Pacold, C.M., Cho, W. and Williams, R.L. (2002). Binding of the PX domain of p47(phox) to phosphatidylinositol 3,4-bisphosphate and phosphatidic acid is masked by an intramolecular interaction. Embo J. 21, 5057-68.

[295] Bravo, J. et al. (2001). The crystal structure of the PX domain from p40(phox) bound to phosphatidylinositol 3-phosphate. Mol. Cell 8, 829-39.

[296] Stahelin, R.V., Burian, A., Bruzik, K.S., Murray, D. and Cho, W. (2003). Membrane binding mechanisms of the PX domains of NADPH oxidase p40phox and p47phox. J. Biol. Chem. 278, 14469-79.

[297] Cifuentes, M.E., Honkanen, L. and Rebecchi, M.J. (1993). Proteolytic fragments of phosphoinositide-specific phospholipase C-delta 1. Catalytic and membrane binding properties. J. Biol. Chem. 268, 11586-93.

[298] Garcia, P. et al. (1995). The pleckstrin homology domain of phospholipase C-delta 1 binds with high affinity to phosphatidylinositol 4,5-bisphosphate in bilayer membranes. Biochemistry 34, 16228-34.

[299] Lemmon, M.A., Ferguson, K.M., O'Brien, R., Sigler, P.B. and Schlessinger, J. (1995). Specific and high-affinity binding of inositol phosphates to an isolated pleckstrin homology domain. Proc. Natl. Acad. Sci. U S A 92, 10472-6.

[300] Yagisawa, H. et al. (1994). Expression and characterization of an inositol 1,4,5-trisphosphate binding domain of phosphatidylinositol-specific phospholipase C-delta 1. J. Biol. Chem. 269, 20179-88.

[301] Stephens, L. et al. (1998) Protein Kinase B Kinases That Mediate Phosphatidylinositol 3,4,5-Trisphosphate-Dependent Activation of Protein Kinase B. Science 279, 710-714.

[302] James, S.R., Downes, C.P., Gigg, R., Grove, S.J., Holmes, A.B. and Alessi, D.R. (1996). Specific binding of the Akt-1 protein kinase to phosphatidylinositol 3,4,5-trisphosphate without subsequent activation. Biochem. J. 315 (Pt 3), 709-13.

[303] Franke, T.F., Yang, S.I., Chan, T.O., Datta, K., Kazlauskas, A., Morrison, D.K., Kaplan, D.R. and Tsichlis, P.N. (1995). The protein kinase encoded by the Akt proto-oncogene is a target of the PDGF-activated phosphatidylinositol 3-kinase. Cell 81, 727-36.

[304] Stokoe, D. et al. (1997) Dual Role of Phosphatidylinositol-3,4,5-trisphosphate in the Activation of Protein Kinase B. Science 277, 567-570.

[305] Isakoff, S.J. et al. (1998). Identification and analysis of PH domain-containing targets of phosphatidylinositol 3-kinase using a novel in vivo assay in yeast. Embo J. 17, 5374-87.

[306] DiNitto, J.P. and Lambright, D.G. (2006). Membrane and juxtamembrane targeting by PH and PTB domains. Biochim. Biophys. Acta 1761, 850-67.

[307] Cronin, T.C., DiNitto, J.P., Czech, M.P. and Lambright, D.G. (2004). Structural determinants of phosphoinositide selectivity in splice variants of Grp1 family PH domains. Embo J. 23, 3711-20.

[308] Yu, J.W. et al. (2004). Genome-wide analysis of membrane targeting by S. cerevisiae pleckstrin homology domains. Mol. Cell. 13, 677-88.

[309] Manna, D., Albanese, A., Park, W.S. and Cho, W. (2007). Mechanistic basis of differential cellular responses of phosphatidylinositol 3,4-bisphosphate- and phosphatidylinositol 3,4,5-trisphosphate-binding pleckstrin homology domains. J. Biol. Chem. 282, 32093-105.

[310] Cifuentes, M.E., Delaney, T. and Rebecchi, M.J. (1994) D-myo-inositol 1,4,5-trisphosphate inhibits binding of phospholipase C-delta 1 to bilayer membranes. J. Biol. Chem. 269, 1945-1948.

[311] Hirose, K., Kadowaki, S., Tanabe, M., Takeshima, H. and Iino, M. (1999). Spatiotemporal dynamics of inositol 1,4,5-trisphosphate that underlies complex Ca2+ mobilization patterns. Science 284, 1527-30.

[312] Carpten, J.D. et al. (2007). A transforming mutation in the pleckstrin homology domain of AKT1 in cancer. Nature 448, 439-44.

[313] Landgraf, K.E., Pilling, C. and Falke, J.J. (2008). Molecular mechanism of an oncogenic mutation that alters membrane targeting: Glu17Lys modifies the PIP lipid specificity of the AKT1 PH domain. Biochemistry 47, 12260-9.

[314] Thomas, C.C., Dowler, S., Deak, M., Alessi, D.R. and van Aalten, D.M. (2001). Crystal structure of the phosphatidylinositol 3,4-bisphosphate-binding pleckstrin homology (PH) domain of tandem PH-domain-containing protein 1 (TAPP1): molecular basis of lipid specificity. Biochem J. 358, 287-94.

[315] Thomas, C.C., Deak, M., Alessi, D.R. and van Aalten, D.M. (2002). High-resolution structure of the pleckstrin homology domain of protein kinase b/akt bound to phosphatidylinositol (3,4,5)-trisphosphate. Curr. Biol. 12, 1256-62.

[316] Dowler, S., Kular, G. and Alessi, D.R. (2002). Protein lipid overlay assay. Sci. STKE 129, l6.

[317] Ferguson, C.G., James, R.D., Bigman, C.S., Shepard, D.A., Abdiche, Y., Katsamba, P.S., Myszka, D.G. and Prestwich, G.D. (2005). Phosphoinositide-containing polymerized liposomes: stable membrane-mimetic vesicles for protein-lipid binding analysis. Bioconjug. Chem. 16, 1475-83.

[318] Narayan, K. and Lemmon, M.A. (2006). Determining selectivity of phosphoinositide-binding domains. Methods 39, 122-33.

[319] van der Merwe, P. (2001) Surface Plasmon Resonance in Protein-Ligand interactions: hydrodynamics and calorimetry, Oxford University Press.

[320] Schmidt, A., Spinke, J., Bayerl, T., Sackmann, E. and Knoll, W. (1992). Streptavidin binding to biotinylated lipid layers on solid supports. A neutron reflection and surface plasmon optical study. Biophys J. 63, 1385-92.

[321] Chenna, R., Sugawara, H., Koike, T., Lopez, R., Gibson, T.J., Higgins, D.G. and Thompson, J.D. (2003). Multiple sequence alignment with the Clustal series of programs. Nucleic Acids Res. 31, 3497-500.

[322] Laskowski, R.A., Hutchinson, E.G., Michie, A.D., Wallace, A.C., Jones, M.L. and Thornton, J.M. (1997). PDBsum: a web-based database of summaries and analyses of all PDB structures. Trends in Biochemical Sciences 22, 488-490.

[323] The PyMOL Molecular Graphics System. http://www.pymol.org/

[324] Harrop, S.J. et al. (2001) Crystal Structure of a Soluble Form of the Intracellular Chloride Ion Channel CLIC1 (NCC27) at 1.4-Ã Resolution. J. Biol. Chem. 276, 44993-45000.

[325] Saito, K., Koshiba, S., M., I., Kigawa, T. and Yokoyama, S. Solution structure of the carboxyl-terminal rgc domain in human iqgap1. (2005) http://www.ebi.ac.uk/thornton-srv/databases/cgi-bin/pdbsum/GetPage.pl

[326] Hulme, E.C. (1992) Receptor-Ligand Interactions: A Practical Approach, Oxford University Press.

[327] Lemmon, M.A. (2003). Phosphoinositide Recognition Domains. Traffic 4, 201-213.

[328] Hawkins, P.T., Jackson, T.R. and Stephens, L.R. (1992). Platelet-derived growth factor stimulates synthesis of Ptdlns(3,4,5)P3 by activating a Ptdlns(4,5)P2 3-OH kinase. Nature 358, 157-159.

[329] Foster, F.M., Traer, C.J., Abraham, S.M. and Fry, M.J. (2003) The phosphoinositide (PI) 3-kinase family. J. Cell Sci. 116, 3037-3040.

[330] Rameh, L.E. and Cantley, L.C. (1999) The Role of Phosphoinositide 3-Kinase Lipid Products in Cell Function. J. Biol. Chem. 274, 8347-8350.

[331] Leslie, N.R., Batty, I.H., Maccario, H., Davidson, L. and Downes, C.P. Understanding PTEN regulation: PIP2, polarity and protein stability. Oncogene 27, 5464-5476.

[332] Campbell, R.B., Liu, F. and Ross, A.H. (2003) Allosteric Activation of PTEN Phosphatase by Phosphatidylinositol 4,5-Bisphosphate. J. Biol. Chem. 278, 33617-33620.

[333] Walker, S.M., Leslie, N.R., Perera, N.M., Batty, I.H. and Downes, C.P. (2004) The tumour-suppressor function of PTEN requires an N-terminal lipid-binding motif. Biochem. J. 379, 301-307.

[334] Downes, C.P., Perera, N., Ross, S. and Leslie, N. (2007). Substrate specificity and acute regulation of the tumour suppressor phosphatase, PTEN Biochem. Soc. Symp., 69-80.

[335] Tudyka, T. and Skerra, A. (1997). Glutathione S-transferase can be used as a C-terminal, enzymatically active dimerization module for a recombinant protease inhibitor, and functionally secreted into the periplasm of Escherichia coli. Protein Sci. 6, 2180-7.

[336] Martin, D., Salinas, M., Lopez-Valdaliso, R., Serrano, E., Recuero, M. and Cuadrado, A. (2001). Effect of the Alzheimer amyloid fragment Abeta(25-35) on Akt/PKB kinase and survival of PC12 cells. J. Neurochem. 78, 1000-8.

[337] Brown, M.D. and Sacks, D.B. (2006). IQGAP1 in cellular signaling: bridging the GAP. Trends Cell. Biol. 16, 242-9.

[338] Cantley, L.C. (2002). The phosphoinositide 3-kinase pathway. Science 296, 1655-7.

[339] Di Paolo, G. and De Camilli, P. (2006). Phosphoinositides in cell regulation and membrane dynamics. Nature 443, 651-657.

[340] Simonsen, A. et al. (1998). EEA1 links PI(3)K function to Rab5 regulation of endosome fusion. Nature 394, 494-498.

[341] Milburn, C.C., Deak, M., Kelly, S.M., Price, N.C., Alessi, D.R. and Van Aalten, D.M.F. (2003). Binding of phosphatidylinositol 3,4,5-trisphosphate to the pleckstrin homology domain of protein kinase B induces a conformational change. Biochem. J. 375, 531-538.

[342] Li, Z., Kim, S.H., Higgins, J.M., Brenner, M.B. and Sacks, D.B. (1999). IQGAP1 and calmodulin modulate E-cadherin function. J. Biol. Chem. 274, 37885-92.

Supplementary Data